The Inclusive Radiative $B \to X_s\gamma$ Decay in the Standard Model

Ulrich Haisch

Max-Planck-Institut für Physik
(Werner-Heisenberg-Institut)
Föhringer Ring 6
D-80805 München
Email: haisch@mppmu.mpg.de

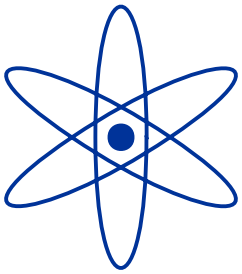

Physik-Department
Technische Universität München
Institut für Theoretische Physik
Lehrstuhl Univ.-Prof. Dr. Andrzej Buras

The Inclusive Radiative $B \to X_s\gamma$ Decay in the Standard Model

Ulrich Haisch

Vollständiger Abdruck der von der Fakultät für Physik der Technischen Universität München zur Erlangung des akademischen Grades eines

Doktors der Naturwissenschaften (Dr. rer. nat.)

genehmigten Dissertation.

Vorsitzender:		Univ.-Prof. Dr. Stephan Paul
Prüfer der Dissertation:	1.	Univ.-Prof. Dr. Andrzej Buras
	2.	Univ.-Prof. Dr. Manuel Drees

Die Dissertation wurde am 1. Oktober 2002 bei der Technischen Universität München eingereicht und durch die Fakultät für Physik am 22. Oktober 2002 angenommen.

Abstract

We discuss inclusive radiative B decays within the Standard Model of elementary particle physics. In particular, we consider the $B \to X_s\gamma$ mode, where X_s denotes an arbitrary state of total strangeness -1. At quark level, this decay is dominated by the flavor changing neutral current $b \to s\gamma$ transition, which appears at the one-loop level in the Standard Model. Such processes allow us to study CP violation and the interplay of strong and electroweak interactions, to determine the elements of the quark mixing matrix, and to search for new physics. As it is well-known the inclusive rate is of much more theoretical interest than the exclusive modes, because non-perturbative effects play a subdominant role and are well under control due to heavy quark expansion. In particular, the decay width $\Gamma(B \to X_s\gamma)$ is well approximated by the partonic decay rate $\Gamma(b \to s\gamma)$ which can be analyzed in renormalization group improved perturbation theory. Exclusive decay modes, however, are more accessible to experiments, in particular at hadronic machines.

We review the status quo of the theoretical prediction of the weak radiative B-meson decay $B \to X_s\gamma$ in the Standard Model. In particular, we point out that the charm contribution to $B \to X_s\gamma$ is numerically dominant and practically renormalization scale independent. The well-known enormous enhancement of the branching ratio by leading large logarithms is mainly due to the b-quark mass evolution in the top sector. By splitting the top and the charm contributions to the decay amplitude good control of the behavior of the perturbation series in $B \to X_s\gamma$ is achieved. Moreover, we argue that one source of perturbative uncertainty was not properly taken into account in many previous analyses. It is related to the question of the definition of m_c and m_b that should be used in the matrix element $\langle Q_2(\mu)\rangle$. This problem is numerically very important because of the strong sensitivity of $\langle Q_2(\mu)\rangle$ to the mass ratio m_c/m_b. We give arguments which renormalization scheme for m_c/m_b should be used in the calculation of the branching ratio of the inclusive $B \to X_s\gamma$ decay mode.

We compute the complete two-loop $\mathcal{O}(\alpha)$ Wilson coefficients relevant for radiative decays of the B-meson in the Standard Model. This is a necessary step in the calculation of the next-to-leading order photonic corrections and improves on previous analyses of electroweak effects in $B \to X_s\gamma$. We describe in detail several interesting technical aspects of the calculation and include all relevant $\mathcal{O}(\alpha)$ matrix elements. The final expressions for the $\mathcal{O}(\alpha)$ corrections of the Wilson coefficients, however, are very long, due to the presence of four different heavy masses. Hence, we provide only approximate formulas for the numerical implementation of our results. We also consider the heavy top expansion of our results and show that in the case at hand it converges very slowly, and that the leading term of this expansion disagrees from the result obtained in the gaugeless approximation. The origin of the discrepancy is discussed and we provide a criterion for the validity of the gaugeless approximation in general. As a byproduct of our calculation we also obtain the $\mathcal{O}(\alpha)$ correction to the Wilson coefficient of the four quark operator Q_2. In our final result, we neglect only terms originated from the unknown $\mathcal{O}(\alpha\alpha_s)$ evolution of the Wilson coefficients and the $\mathcal{O}(\alpha)$ bremsstrahlung corrections which are suspected to be negligible small. Due to the compensation among different effects, we find that non-trivial electroweak corrections decrease the branching ratio by about 3.6% for a light Higgs boson of around 100 GeV. The corresponding up-to-date Standard Model prediction for the branching ratio with $E_\gamma > 1.6\,\text{GeV}$ is $(3.58 \pm 0.30) \times 10^{-4}$ in good agreement with the present experimental results obtained at CLEO, BaBar, Belle and ALEPH.

Contents

Chapter 1

Introduction

The last century has seen in physics a dazzling expansion of the frontiers of scientific knowledge. Einstein's special and general relativity have permanently changed our view of space, time and gravitation. In an even more radical break with the past, quantum mechanics has transformed the very language we use to describe nature: In place of particles with definite positions and velocities, we have learned to speak of wave functions and probabilities. Out of the fusion of relativity and quantum mechanics there has evolved a new view of the world, one in which matter has lost its central role. This role has been usurped by principles of symmetry, some of them hidden from view in the present state of the universe. On this formulation physicists have built a successful theory of electromagnetism and the weak and strong interactions of elementary particles, which has become the Standard Model (SM) of particle physics.

The SM is a renormalizable quantum field theory which predicts or is consistent with almost all known aspects of the elementary particles and their interactions over an enormous range of probes and scales. In particular, the latest precision measurements at the Large Electron Positron Collider (LEP) at the European Organization for Nuclear Research (CERN), at the Stanford Linear Collider (SLC) at the Stanford Linear Accelerator Center (SLAC) and at the Tevatron at the Fermi National Accelerator Laboratory (FNAL), have confirmed the validity of the gauge sector of the SM to a level that we can say was unexpected at the beginning. In the present data there is no significant evidence for departures from the SM, no convincing hint of new physics. The precision tests of the standard electroweak theory have established that the couplings of quarks and leptons to the weak gauge bosons $W^{\pm}$ and Z are indeed precisely those prescribed by the gauge symmetry. The accuracy at the level of order 0.1% for these precision tests [1–3] implies that, not only the tree level, but also the structure of the electroweak quantum corrections including genuine bosonic weak contributions has been verified. To a lesser accuracy the triple gauge vertices $W^{\pm}W^{\mp}\gamma$ and $W^{\pm}W^{\mp}Z$ have also been found in agreement with the specific prediction of the electroweak theory. This means that it has been verified that the gauge symmetry is unbroken in the vertices of the theory, that is, that the currents are indeed conserved. Moreover, the impressive success of the SM poses strong limitations on the possible forms of new physics. Favored are models of the Higgs sector and of new physics that preserve the SM structure and only very delicately improve it, as is the case for fundamental Higgses and supersymmetry. Disfavored are models with a nearby strong non-perturbative regime that almost inevitably would affect the electroweak radiative corrections, as for composite Higgses or technicolor and its variants.

However, despite it tremendous successes, the SM is generally not believed to be the final answer to the question for the fundamental building blocks of nature. Even if one accepts the rather bizarre set of group representations and hypercharges that it requires, the SM contains at least 19 parameters. These consist of three gauge couplings, six quark and three charged lepton masses, three weak mixing angles and one CP violating phase, and two parameters to characterize the Higgs sector. In addition there is a further non-perturbative vacuum angle which describes potential strong CP violation. Moreover, many more parameters are required if one wishes to accommodate non-accelerator observations. For example, neutrino masses and mixing introduce at least seven parameters, namely, three masses, three mixing angles and one CP violating phase. Cosmological inflation introduces at least one new mass scale of order $M_{\rm GUT} \approx 10^{16}\,{\rm GeV}$. The cosmological baryon asymmetry is not explicable within the SM, so one or more additional parameters are needed. Finally, the cosmological constant may be non-zero. The ultimate "Theory of Everything" should explain all these as well as the parameters of the SM of strong and electroweak interactions.

It is convenient to organize the questions raised by the SM into three categories. One is the problem of mass: Do particle masses really originate from a Higgs boson, and, if so, why are these masses not much closer to the Planck scale $M_{\rm Planck} \approx 10^{19}\,{\rm GeV}$? Another one is the problem of unification: Can all the particles interactions be unified in a simple gauge group, and, if so, does it predict observable new phenomena such as baryon decay or neutrino masses, and does it predict relations between parameters of the SM such as gauge couplings or fermion masses? Then there is the problem of flavor: What is the origin of the six flavors each of the quarks and leptons, and what explains their weak charged-current mixing and CP violation? Finally, the quest of the "Theory of Everything" seems most promising in the context of string theory, particularly in its most recent incarnation of M-theory. The phenomenological richness of this speculative M-theory approach is only beginning to be explored, and it remains to be seen whether it offers a realistic phenomenological description.

Nevertheless, the SM remains the rock on which our quest for new physics must be built, and it seems worthwhile to examine whether its successes or deficits offer any hint of the direction in which to search for new physics. In this vicinity special attention should be paid to the flavor sector of the SM, which apart from the low-energy regime of the strong interactions, can be regarded as the experimentally least constrained part of the theory. This is reflected in the rather large uncertainties of several flavor parameters such as the mixing parameters at the 20% level [4,5], which has to be compared with the aforementioned errors established in the electroweak precision measurements. However, while the time of the electroweak precision physics focusing on the gauge sector of the SM has drawn to a close with the completion of the LEP and SLC experiments, the era of precision flavor physics focusing on the scalar sector of the SM has just begun with the start of the BaBar experiment [6] at SLAC and the Belle experiment [7] at the High Energy Accelerator Research Organization (KEK), which add a wealth of data to the results of the CLEO experiment [8,9] at the Cornell Electron Positron Storage Ring (CESR), the four LEP experiments ALEPH [10,11], DELPHI [12,13], L3 [14,15], and OPAL [16,17] at CERN, the two Tevatron experiments CDF [18,19] and D0 [20], and the SLD experiment [21,22] at SLAC. Although the physics potential of these experiments is very promising, it may well be that a definite answer in the search for new physics will be left to the second generation flavor experiments at hadronic machines, namely

ATLAS [23], CMS [24] and LHCb [22, 25] at CERN, and BTeV [26] and the upgraded CDF and D0 experiments at FNAL. All these fascinating experimental facilities let expect that flavor physics, in particular the physics of b-flavored mesons, will be the most active and promising areas of high-energy particle physics in the near future.

Indeed, the value of the mass of the b-quark, of around 5 GeV leads to a special role of the B-mesons in the studies of flavor physics. The most heavy quark, the t-quark, does not form hadrons, because it can decay by weak interaction into a real $W^{\pm}$ and a b-quark. This decay occurs much faster than the typical time needed to bind a quark and an antiquark into a meson by the strong interactions. Thus, mesons containing a b-quark are the heaviest mesons that can be produced at high-energy colliders. The fact that the B-mesons are heavy has two important consequences: B decays show an extremely rich phenomenology and theoretical techniques relying on the expansion in the heavy b-quark mass allow for model-independent predictions. The rich phenomenology is based on the one hand on the large available phase space allowing for a plethora of possible final states and on the other hand on the possibility for large CP violating asymmetries in B decays. For years large CP violation in the B system was considered to be one of the cornerstone predictions of the SM. Yet it took a very long time to come up with the definitive evidence [27, 28]. With the combined efforts of theorists and experimentalist, the next years will show how precisely the measurements of the direct CP asymmetry in the various B decay modes will determine ρ and η, and if the five independent constraints on ρ and η from $|V_{ub}|$, $|V_{td}|$, ϵ, α and β will establish a consistent description, or will falsify the assumption that all weak processes including CP violation are well described within the SM.

In this thesis we will focus on a particular subclass of B decays, the so-called radiative weak decays. These transitions have been the subject of a considerable number of experimental and theoretical investigations. Being rare processes mediated by loop diagrams, radiative weak decays test the detailed structure of the underlying theory at the level of quantum corrections and provide information on the couplings and masses of the heavy virtual particles appearing as intermediate states. The resulting sensitivity to nonstandard contributions, such as charged Higgs bosons, gluinos and charginos or even more exotic particles arising in some extentions of the SM, implies the possibility for an indirect observation of new physics, a strategy complementary to the direct production of the new particles. Whereas the latter option is reserved to the planned hadronic machines such as the Large Hadron Collider (LHC) at CERN, the indirect search of the B factories already implies significant restrictions for the parameter space of many new physics scenarios, and it might well be that these rare processes lead to the first evidence of new physics by a significant deviation from the SM prediction.

Among all rare weak decays the penguin induced $b \to s\gamma$ and $b \to d\gamma$ transitions play a special role. Proceeding at rates of order $G_F^2\alpha$, they are systematically enhanced over most other loop induced, non-radiative, rare decays that are proportional to $G_F^2\alpha^2$. In fact, the Cabibbo-favored $b \to s\gamma$ modes belong to the small number of rare decays that are experimentally accessible already today. Following the first observation of the exclusive electromagnetic penguin process $B \to K^*\gamma$ nearly a decade ago by the CLEO collaboration [29], these measurements have been refined [30] and confirmed by other experiments [31, 32]. However, quantitative test of the SM with rates measured for exclusive channels are severely handicapped by our inability to calculate hadronization probabilities from the first principles of the theory of strong interactions. The resulting large hadronic

uncertainties of around 40% [33–36] restrict the opportunities in those channels significantly. If new physics does not show up in B physics through large deviations from the SM expectations as recent experimental data indicates the focus on theoretically clean variables is mandatory. Fortunately, when summed over all possible final states, hadronization probabilities are not relevant and the inclusively measured rate should reflect the short distance interactions which can be accurately predicted using the full machinery of renormalization group improved perturbation theory. The general framework for such a calculation is provided by the heavy quark expansion (HQE), which predicts that up to small bound-state corrections, inclusive decay rates agree with the parton model rates of the underlying decays of the b-quark. As long as the fine structure of the photon energy spectrum is not probed locally, the theoretically analysis of $B \to X_s\gamma$ and $B \to X_d\gamma$ decays relies only on the weak assumption of global quark-hadron duality.

Of course, the power of the inclusive branching ratio of $B \to X_s\gamma$ for testing new physics crucially depends on how accurate its measurements are and how precise the theoretical prediction in the SM is. One year after the detection of the exclusive $B \to K^*\gamma$ mode, the CLEO collaboration reported the first measurement of the rate of the inclusive analogue $B \to X_s\gamma$ through the determination of the characteristic photon energy spectrum [37]. As this process is dominated by the two-body decay $b \to s\gamma$, its gamma energy spectrum is expected to be a smeared delta function centered at the kinematical endpoint, where the smearing is due to perturbative emission of gluon bremsstrahlung, and to the non-perturbative Fermi motion of the b-quark inside the B-meson. Since the first measurement of the inclusive $B \to X_s\gamma$ mode considerable progress has been made by CLEO [30, 38], BaBar [39], Belle [31] and ALEPH [40]. The current experimental results read

$$\begin{aligned}
\mathrm{BR}(B \to X_s\gamma) &= \left(3.21 \pm 0.43 \pm 0.27^{\,+0.18}_{\,-0.10}\right) \times 10^{-4}\,, \\
\mathrm{BR}(B \to X_s\gamma) &= \left(3.88 \pm 0.36 \pm 0.37^{\,+0.43}_{\,-0.23}\right) \times 10^{-4}\,, \\
\mathrm{BR}(B \to X_s\gamma) &= \left(3.36 \pm 0.53 \pm 0.42^{\,+0.50}_{\,-0.54}\right) \times 10^{-4}\,, \\
\mathrm{BR}(H_b \to X_s\gamma) &= (3.11 \pm 0.80 \pm 0.72) \times 10^{-4}\,,
\end{aligned} \tag{1.1}$$

where the first error is statistical, the second is systematic and the third error represents the theoretical model dependence. It should be noted that although the four different measurements are consistent with each other, the statistical errors in the ALEPH measurement of $H_b \to X_s\gamma$ are much larger than the expected differences among weak radiative branching ratios of the included B-hadrons, and thus the latter result should be treated with care. Including the present data from CLEO, BaBar, Belle and ALEPH the current experimental world average for the branching ratio of the $B \to X_s\gamma$ decay is

$$\mathrm{BR}(B \to X_s\gamma)_{\mathrm{exp}} = (3.39 \pm 0.40) \times 10^{-4}\,, \tag{1.2}$$

with an error of around 12%. More accurate data are expected in the near future. With the expected high luminosity of the B factories, an experimental accuracy below 10% in the inclusive $B \to X_s\gamma$ mode appears to be possible.

Since only the high-energy part of the photon spectrum is sensitive to the rare $B \to X_s\gamma$ decay, some lower cut-off in the photon energy spectrum has to be imposed in order to exclude the dominant charm background, which has a typical bremsstrahlungs spectrum that is maximal at the photon energy $E_\gamma = 0$ and falls off for larger value of E_γ. In consequence only the kinematic branching ratio of $B \to X_s\gamma$ in the range $E_\gamma = 2.0\,\mathrm{GeV}$

and the kinematical endpoint at $E_\gamma = 2.7\,\text{GeV}$ is experimentally accessible [30]. Therefore an understanding of the spectral shape is a prerequisite for extrapolating the data to the full phase space, that is, to obtain the total branching ratio. Unfortunately, the operator product expansion (OPE) breaks down near the endpoint of the photon spectrum and the fraction of the $B \to X_s\gamma$ events with $E_\gamma > 2\,\text{GeV}$ is not calculable from first principles, at least at the moment. This uncertainty spotted in the experimental measurement should definitely be regarded as a purely theoretical one. However, an important observation is that the shape of the photon spectrum is not sensitive to physics beyond the SM. This implies that we do not have to assume the correctness of the SM in the experimental analysis and, thus, a precise measurement of the photon spectrum can be used to determine the parameters of the shape function. Clearly, a lower experimental cut-off would decrease the sensitivity to the parameters of the shape function, or more generally, the model dependence. In the future, experimental effort should therefore be made to lower the cut-off on the photon energy to a value of around $E_\gamma = 1.6\,\text{GeV}$, which would allow an ideal comparison between theory and experiment.

After all this experimental exposition it is really time to discuss the theoretical prediction for the branching ratio of the inclusive $B \to X_s\gamma$ decay in the SM. This will be done in the subsequent 137 pages that we have organized as follows. In Chapter 2 we provide a self-contained introduction to the SM. After stating without proof some general results from the theory of continuous groups relevant to the construction of non-abelian gauge theories, we will introduce the classical Lagrangian of the minimal SM of strong and electroweak interactions step by step, explaining its symmetries in detail. This will be followed by a illuminating discussion of the quantization of the SM, putting special emphasize on the role played by the Becchi-Rouet-Stora-Tyutin (BRST) symmetry. Finally, we outline the on-shell renormalization of the physical and unphysical sector of the electroweak SM and provide explicit expression for the counterterms at the one-loop level.

In Chapter 3 we review the status quo of the theoretical predictions of the weak radiative B-meson decay $B \to X_s\gamma$ in the SM. In the first section we will briefly recall the general formalism on which the calculation of the branching ratio of the $B \to X_s\gamma$ mode is based, giving the effective off-shell Hamiltonian needed for the subsequent calculations of the $b \to s\gamma$ and $b \to sg$ transition in the SM. The next section deals with renormalization group techniques and illustrates how leading and next-to-leading order gluonic and photonic corrections should be taken into account in the calculation of the Wilson coefficient functions of the relevant operators. In what follows we will explain why splitting the top and charm contributions to the amplitude allows us to better understand the origin of the enormous enhancement of the $B \to X_s\gamma$ branching ratio due to leading large logarithms. Motivated by this observation we will then rewrite the known next-to-leading order corrections to the Wilson coefficients of the magnetic type operators. Furthermore, we will give a short survey of the non-perturbative corrections that have to be included in order to pass from the calculated b-quark decay rate to the final B-meson decay rate. The presentation of the explicit expressions needed for the analysis of the branching ratio of $B \to X_s\gamma$ in next-to-leading order approximation concludes this chapter.

The study of electroweak effects in the $b \to s\gamma$ and $b \to sg$ transitions within the SM is performed in Chapter 4. After a short general introduction, we outline in detail the two-loop $\mathcal{O}(\alpha)$ matching for the magnetic penguin operators. Several subtleties arise in the calculation, mostly linked to the presence of unphysical operators. We will describe them in detail and illustrate how non-physical operators effect the final result for the initial

conditions of the Wilson coefficients. Moreover, we discuss some technical details of the computation of the two-loop unrenormalized amputated Green's function, which has been the most involved part of our calculation. In renormalizing the two-loop amplitudes our aim is to attain the maximal simplicity. The actual procedure we have adopted will be illustrated in great detail, giving explicit expressions for the various counterterms. Although the final expression for the $\mathcal{O}(\alpha)$ corrections to the initial conditions of the Wilson coefficient functions can be expressed in terms of logarithms and dilogarithms, they are rather lengthy due to the presence of four different heavy masses, and thus we provide only practical formulas for the numerical implementation of our results. We also consider the heavy top expansion (HTE) and show that in the case at hand it converges very slowly, and that the leading term of this expansion disagrees from the result obtained in the gaugeless approximation. The origin of the discrepancy will be discussed and we provide a criterion for the validity of the gaugeless approximation in general. Furthermore, we deal with the evolution of the coefficient functions down to the low-energy scale and explain how next-to-leading order photonic corrections should be taken into account in the computation of the $B \to X_s\gamma$ branching ratio. Finally, we reconsider the SM prediction for this quantity using the next-to-leading order formulae collected in the preceding chapter, including all relevant $\mathcal{O}(\alpha)$ matrix elements.

Our conclusions and a short outlook are given in Chapter 5. Some more technical details are discussed in the appendices. In Appendix A we report the preliminary results of an ongoing calculation of the anomalous dimension matrices up to $\mathcal{O}(\alpha_s^2)$ and $\mathcal{O}(\alpha)$, respectively. Further details of this computation as well as a comprehensive discussion of the classification of physical and non-physical operators of dimension five and six arising in the renormalization of the effective theory at two- and three-loop level will be given in a forthcoming publication. The one-loop off-shell matching for the $b \to s\gamma$ transition will be performed in Appendix B, where we explicitly show that the gauge-invariant part of the corresponding effective vertex depends on whether the external photon is quantum or background. In Appendix C we give all the relevant functions necessary for the calculation of the $\mathcal{O}(\alpha_s)$ bremsstrahlungs corrections affecting the inclusive $B \to X_s\gamma$ mode. Moreover, we demonstrate in Appendix D how the $\mathcal{O}(\alpha)$ corrections to the Wilson coefficients of the four quark operators transform when passing from one operator basis to another. A detailed description of how to evaluate the renormalized on-shell $b \to s\gamma$ amplitude, from which the two-loop $\mathcal{O}(\alpha)$ matrix elements of the four quark operators can be determined, will be given in Appendix E and concludes this thesis.

Part I

Basics

Chapter 2

Standard Model of Elementary Particle Physics

This chapter provides a self-contained introduction to the SM of strong and electroweak interactions. The SM is a renormalizable quantum field theory and allows consistent predictions of physical processes in terms of a few parameters, such as masses and couplings, order by order in perturbation theory. The SM includes electromagnetic, weak and strong interactions and the classical model is a non-abelian gauge theory based on the non-simple gauge group $SU(3)_C \times SU(2)_L \times U(1)_Y$. The $SU(2)_L \times U(1)_Y$ gauge group is spontaneously broken to the electromagnetic subgroup $U(1)_Q$ providing masses for the charged leptons and quarks and for the vector bosons of weak interactions via the Higgs mechanism, but leaving the photon as a massless particle. Since the symmetry of the electroweak model is broken in such a way that the abelian subgroup cannot be factorized the weak interactions cannot be described consistently without the electromagnetic interactions. In contrast to this the color group $SU(3)_C$ is unbroken and its generators of global symmetry do not mix with the one of the $SU(2)_L \times U(1)_Y$ symmetry.

2.1 Lie Groups and Lie Algebras

Before discussing the classical Lagrangian of the SM in detail, it is worthwhile to consider the general properties of Lie groups on which non-abelian gauge theories are based. In the following we will state, without proof, some general results from the theory of continuous groups relevant to the construction of non-abelian gauge theories, putting special emphasis on the non-abelian subgroup factors of the $SU(3)_C \times SU(2)_L \times U(1)_Y$ symmetry underlying the SM.

The basic feature of any Lie group is that it contains a non-countable number of elements lying in a region arbitrarily close to its identity, and that the structure of this region both very largely determines the structure of the whole group and is itself determined by its corresponding Lie algebra. To ensure this, the elements close to the identity must be parameterized in such a way, that in terms of this parameterization the group multiplication operation is expressible in terms of analytic functions.

For the application to gauge theories, the local symmetry is normally a unitary transformation of a set of fields. Therefore we are primarily interested in Lie algebras that have finite-dimensional hermitian representations, leading to finite-dimensional unitary repre-

sentations of the associated Lie group. In addition we will also assume that the number of generators is finite. Such Lie algebras are called compact, because these conditions imply that the Lie group forms a finite-dimensional compact manifold.

Any element of a compact Lie group which can be obtained from the identity by continuous change of its parameters can be written as

$$g(\theta) = e^{i\theta^\alpha t^\alpha} , \tag{2.1}$$

where the summation over repeated indices should be understood as usual. The coefficients of the real group parameters θ^α are linearly independent hermitian operators t^α, $\alpha = 1, \ldots, d_G$, known as the generators of the Lie group and d_G is the dimension of the associated Lie algebra.

As the product of a pair of group elements is another group element the commutator of any two generators t^α and t^β can be written as

$$[t^\alpha, t^\beta] = ic^{\alpha\beta\gamma} t^\gamma . \tag{2.2}$$

The real numbers $c^{\alpha\beta\gamma}$ are called the structure constants of the Lie algebra. Clearly, in a particular representation the explicit values of the structure constants are completely determined by the group multiplication operation. They also determine the local properties of the associated Lie group close to its identity. In general, however, they do not determine the global properties, that is, the properties of the whole group. As the Lagrangian of a non-abelian gauge theory depends only on the Lie algebra of a local symmetry group, we will ignore these global questions from here on.

In addition, the generators obey the following equality

$$[t^\alpha, [t^\beta, t^\gamma]] + [t^\beta, [t^\gamma, t^\alpha]] + [t^\gamma, [t^\alpha, t^\beta]] = 0 , \tag{2.3}$$

known as the Jacobi identity. Notice that for the commutator (2.2) the identity (2.3) is automatically fulfilled. The reason why we nevertheless state it here is that, in the abstract theory of Lie algebras, the Jacobi identity will no longer be immediately satisfied and therefore plays a fundamental role. Accordingly, we call the vector space spanned by the generators with the additional operation of commutation which satisfies the Jacobi identity a Lie algebra. A Lie algebra is said to be abelian, if $[t^\alpha, t^\beta] = 0$ for all generators t^α and t^β. Thus in an abelian Lie algebra all the structure constants are zero.

At this point a few more definitions concerning the classification of Lie algebras seem to be appropriate. A subalgebra of a Lie algebra is defined to be a subset of elements of the whole algebra that themselves form a Lie algebra with the same commutation relations. If, in addition, the subset of generators closes among themselves under commutation with any element of the whole algebra, the subalgebra is said to be invariant. An algebra which is not abelian and does not posses a non-trivial invariant subgroup[1] is called simple. Algebras without abelian invariant subalgebras are said to be semi-simple. Consequently, a general Lie algebra can be written as a direct sum of non-abelian simple components and additional abelian generators.

Once we have specified the local symmetry group, the fields that appear in the Lagrangian most naturally transform according to a finite-dimensional unitary representation of this group. A d-dimensional unitary representation of a Lie group is a set of $d \times d$

[1] The whole algebra, and the subset of no generators at all are always trivial invariant subalgebras.

hermitian matrices t^a fulfilling the commutation relations (2.2). If there exists no subspace of the d-dimensional vector space so that the t^a transform any vector of the subspace into another member of this subspace the representation is said to be irreducible. We denote the representation matrices in the irreducible representation r by t_r^α.

It is standard practice to adopt a normalization convention for the matrices t_r^α, based on traces of their products. If the Lie algebra is semi-simple, the matrices t_r^α themselves are traceless. However, it can be shown, that for any irreducible representation a basis of generators can be chosen in such a way, that the trace of the product of two generators is proportional to the identity:

$$\mathrm{tr}[t_r^\alpha t_r^\beta] = T_r \delta^{\alpha\beta} \,, \tag{2.4}$$

where the Dynkin index T_r is a constant for each representation r. Once this is done for one irreducible representation, it is true for all irreducible representations. It is then easy to see, that the commutation relations (2.2) together with the normalization (2.4) lead to the following relation

$$c^{\alpha\beta\gamma} = -\frac{i}{T_r}\mathrm{tr}\left[[t_r^\alpha, t_r^\beta]t_r^\gamma\right] \,, \tag{2.5}$$

which implies that, due to the cyclic property of the trace, the structure constants of any irreducible representation are totally antisymmetric.

As a consequence of the antisymmetric property of the structure constants the operator $t^2 = t^\alpha t^\alpha$ commutes with all group generators for any simple Lie algebra. In other words, t^2 is an invariant of the Lie algebra. This means that in an irreducible representation, t^2 is proportional to the unit matrix:

$$t_r^\alpha t_r^\alpha = C_r \cdot 1 \,, \tag{2.6}$$

where 1 is the $d_r \times d_r$ unit matrix and C_r is a constant for each representation, known as the quadratic Casimir operator. Furthermore, it is easy to derive, that the Dynkin index and the quadratic Casimir operator are not independent of each other. If we contract Eq. (2.4) by $\delta^{\alpha\beta}$ and evaluate the left-hand side using Eq. (2.6), we find

$$d_r T_r = d_G C_r \,. \tag{2.7}$$

As we will see later on, Dynkin indices and quadratic Casimir operators appear very often in computations in non-abelian gauge theories. Therefore we will give these group invariants for the simplest representations of the non-abelian subgroup factors of the SM in what follows.

In the case of $SU(2)$, the basic irreducible representation, usually called the fundamental representation, is the two-dimensional spinor representation, which is given in terms of Pauli matrices by $\tau^i = \sigma^i/2$, $i = 1, \ldots, 3$. Accordingly, the generators are normalized in the conventional way, that is, $\mathrm{tr}\,[\tau^i\tau^j] = \delta^{ij}/2$. In the standard basis for the fundamental representation of $SU(3)$ the generators denoted by T^a are chosen so that the isospin subgroup $SU(2)$ is generated by the first three generators acting on the three-dimensional complex vector. In terms of the Gell-Mann matrices they can be written as $T^a = \lambda^a/2$, $a = 1, \ldots, 8$. In consequence, the generators obey $\mathrm{tr}\,[T^aT^b] = \delta^{ab}/2$. As any $SU(N)$ group contains an $SU(2)$ subgroup, this convention fixes the values of T_r and C_r for all irreducible representations of $SU(N)$. For the fundamental representation of

$SU(N)$ denoted by $r = F$ the Dynkin index is directly given by the normalization, and the quadratic Casimir operator follows from Eq. (2.7). We obtain

$$T_F = \frac{1}{2}\,, \qquad C_F = \frac{N^2-1}{2N}\,. \tag{2.8}$$

Another irreducible representation, present for any simple Lie algebra, is the one to which the generators of the algebra belong. This representation which has the dimension of the group is called the adjoint or regular representation and denoted by $r = A$. The representation matrices are given by the structure constants:

$$(t_A^\alpha)_{\beta\gamma} = -ic^{\alpha\beta\gamma}\,. \tag{2.9}$$

With this definition, the statement that t_A^α satisfies the Lie algebra (2.2) is just a rewriting of the Jacobi identity (2.3). For $SU(2)$, the structure constants are given by the totally antisymmetric Levi-Civita tensor ϵ^{ijk}, known from the angular momentum algebra. In the case of $SU(3)$ the totally antisymmetric structure constants will be denoted by f^{abc}. It can be proven that in the adjoint representation of $SU(N)$, the Dynkin index equals the value of the quadratic Casimir operator:

$$T_A = C_A = N\,. \tag{2.10}$$

Since the examples we have discussed in this section, combined with the basic group theoretical concepts that we have reviewed, already provide enough material to carry out the most important calculations of physical interest in the SM, we will go ahead to see how non-abelian local gauge symmetries determine the interactions of particles in nature.

2.2 Lagrangian of the Standard Model

In this section we shall assemble the ingredients of the SM of strong and electroweak interactions. The theory of strong interaction, known as Quantum Chromodynamics or QCD [41–46], is a non-abelian gauge theory with gauge group $SU(3)_C$, coupled to fermions in the fundamental representation. On the contrary, weak and electromagnetic interactions of fermions exhibit a symmetry under the gauge group $SU(2)_L \times U(1)_Y$, so that the complete SM is a $SU(3)_C \times SU(2)_L \times U(1)_Y$ gauge theory. However, in contrast to the gauge bosons of the strong and electromagnetic interaction, the electroweak gauge bosons are massive. Therefore the formulation of a gauge theory of electroweak interaction requires a new concept, known as spontaneous symmetry breaking. By applying this concept to the $SU(2)_L \times U(1)_Y$ gauge group we arrive at the only known form of renormalizable and unitary quantum field theory of the weak interaction with massive gauge bosons, often referred to as the Glashow-Weinberg-Salam (GWS) theory [47–50].

Gauge Sector

As the gauge group of the SM is non-simple, electromagnetic, weak and strong interactions are combined by three gauge coupling constants, g' for the weak-hypercharge $U(1)_Y$, g for the weak-isospin $SU(2)_L$ and g_s for the color symmetry group $SU(3)_C$. We denote the

generator of weak-hypercharge by Y, the three generators of the weak-isospin by τ^i and the eight generators of the color charges by T^a.

According to the dimension of the gauge group $SU(3)_C \times SU(2)_L \times U(1)_Y$, twelve gauge fields, which transform with respect to the adjoint representation, mediate the interactions between the matter fields. The gauge field belonging to $U(1)_Y$ is denoted by B_μ, the gauge fields belonging to $SU(2)_L$ are denoted by W^i_μ, $i = 1, \ldots, 3$, and the gauge fields belonging to $SU(3)_C$, called the gluon fields, are denoted by G^a_μ, $a = 1, \ldots, 8$.

The antisymmetric abelian and non-abelian field-strength tensors can be written as

$$\begin{aligned} B_{\mu\nu} &= \partial_\mu B_\nu - \partial_\nu B_\mu \,, \\ W^i_{\mu\nu} &= \partial_\mu W^i_\nu - \partial_\nu W^i_\mu - g\epsilon^{ijk} W^j_\mu W^k_\nu \,, \\ G^a_{\mu\nu} &= \partial_\mu G^a_\nu - \partial_\nu G^a_\mu - g_s f^{abc} G^b_\mu G^c_\nu \,. \end{aligned} \tag{2.11}$$

The gauge fields themselves become a dynamical quantity by adding a gauge field term to the Lagrangian. The most general power counting renormalizable[2] kinetic term for the gauge fields reads

$$\mathcal{L}_{\mathrm{G}} = -\frac{1}{4} B_{\mu\nu} B^{\mu\nu} - \frac{1}{4} W^i_{\mu\nu} W^{i,\mu\nu} - \frac{1}{4} G^a_{\mu\nu} G^{a,\mu\nu} \,. \tag{2.12}$$

Notice that, in contrast to the abelian field-strength tensor $B_{\mu\nu}$, the non-abelian field-strength tensors $W^i_{\mu\nu}$ and $G^a_{\mu\nu}$ contain both linear and quadratic terms in the gauge fields, so that the theory is non-trivial even in the absence of matter fields. These self-interactions are an important aspect of non-abelian gauge theories and are responsible in particular for the asymptotic freedom of QCD [51–53].

The Lagrangian (2.12) is invariant under the infinitesimal gauge transformations

$$\begin{aligned} \delta B_\mu &= -\frac{1}{g'} \partial_\mu \theta^Y \,, \\ \delta W^i_\mu &= -\frac{1}{g} \partial_\mu \theta^i + \epsilon^{ijk} W^j_\mu \theta^k \,, \\ \delta G^a_\mu &= -\frac{1}{g_s} \partial_\mu \theta^a + f^{abc} G^b_\mu \theta^c \,, \end{aligned} \tag{2.13}$$

where θ^Y, θ^i and θ^a are the infinitesimal parameters of the gauge transformations corresponding to the groups $U(1)_Y$, $SU(2)_L$ and $SU(3)_C$, respectively. Obviously, if we take an infinitesimal gauge transformation with constant parameters, the gauge fields transform according to the adjoint representation of the associated Lie group.

From Eqs. (2.13) it follows that the transformation properties of the field strengths are those of a tensor of the adjoint representation

$$\delta B_{\mu\nu} = 0 \,, \qquad \delta W^i_{\mu\nu} = \epsilon^{ijk} W^j_{\mu\nu} \theta^k \,, \qquad \delta G^a_{\mu\nu} = f^{abc} G^b_{\mu\nu} \theta^c \,. \tag{2.14}$$

Note that in the non-abelian case the field strength tensor is no longer gauge-invariant. It cannot be, since there are now several field strengths, each associated with a given direction of rotation in the abstract vector space.

[2] This means that the dimension of the terms in the Lagrangian must not exceed four.

Fermionic Sector

The gauge structure of the SM is essentially determined in the matter sector: It is seen, that the matter currents of the weak interactions, the charged current and the neutral current together with the electromagnetic current form a closed representation with respect to $SU(2)_L \times U(1)_Y$. In order to embed these currents into a gauge theory, one groups the fermions into left-handed doublets, which transform under the fundamental representation of $SU(2)_L \times U(1)_Y$, and right-handed singlets, which transform with respect to the abelian subgroup.

The fermions appear in three generations or families: Each generation consists of a neutrino ν_i', a charged lepton e_i' with electric charge $Q_e = -1$, and the up- and down-type quarks u_i' and d_i' with charge $Q_u = +2/3$ and $Q_d = -1/3$. The lepton doublets $E_L'^i$ and the quark doublets $Q_L'^i$ are given by

$$\begin{aligned} E_L'^i &= P_L \begin{pmatrix} \nu_i' \\ e_i' \end{pmatrix} = \left(\begin{pmatrix} \nu_e' \\ e' \end{pmatrix}_L , \begin{pmatrix} \nu_\mu' \\ \mu' \end{pmatrix}_L , \begin{pmatrix} \nu_\tau' \\ \tau' \end{pmatrix}_L \right) , \\ Q_L'^i &= P_L \begin{pmatrix} u_i' \\ d_i' \end{pmatrix} = \left(\begin{pmatrix} u' \\ d' \end{pmatrix}_L , \begin{pmatrix} c' \\ s' \end{pmatrix}_L , \begin{pmatrix} t' \\ b' \end{pmatrix}_L \right) . \end{aligned} \tag{2.15}$$

The singlets consist of

$$\begin{aligned} e_R'^i &= P_R e_i' = (e_R', \mu_R', \tau_R') , \\ u_R'^i &= P_R u_i' = (u_R', c_R', t_R') , \\ d_R'^i &= P_R d_i' = (d_R', s_R', b_R') , \end{aligned} \tag{2.16}$$

where $P_{L/R} = (1 \mp \gamma^5)/2$ are the projectors onto left- and right-handed chiral fields and $i = 1, \ldots, 3$ is the generation index. Here and in the following the color index of the quark fields will be suppressed for simplicity. Notice that gauge symmetry does not motivate the inclusion of right-handed neutrinos, which would be neutral under all three gauge groups. Therefore they are omitted in the minimal SM.[3]

The gauge interaction of the matter fields is determined by the covariant derivative

$$D_\mu = \partial_\mu + ig' B_\mu Y + igW_\mu^i \tau^i + ig_s G_\mu^a T^a , \tag{2.17}$$

with Y, τ^i and T^a evaluated in the particular representation to which the fermion field belongs. The prime at the fermion fields indicates eigenstates of the electroweak interaction, that is, the covariant derivatives (2.17) are diagonal with respect to the generation indices in this basis. However, these states are not necessarily mass eigenstates. In this notation the fermionic part of the Lagrangian reads

$$\mathcal{L}_{\mathrm{F}} = \sum_{i=1}^{3} \left(\bar{E}_L'^i i\not{D} E_L'^i + \bar{Q}_L'^i i\not{D} Q_L'^i + \bar{e}_R'^i i\not{D} e_R'^i + \bar{u}_R'^i i\not{D} u_R'^i + \bar{d}_R'^i i\not{D} d_R'^i \right) . \tag{2.18}$$

As far as gauge interactions are concerned, the generations are simply copies of each other and the fermionic part of the Lagrangian possesses a large global flavor symmetry. For

[3] As we will explain later on, right-handed neutrinos can be easily included in the SM without affecting its basic structure. This might become necessary in order to allow for the description of recent experimental results on neutrino oscillations [54–65].

three generations the symmetry group is $U(3)_E \times U(3)_Q \times U(3)_e \times U(3)_u \times U(3)_d$, that is, a $U(3)$ symmetry for each of the multiplets $E_L'^i$, $Q_L'^i$, $e_R'^i$, $u_R'^i$ and $d_R'^i$.

The Lagrangian given by Eq. (2.18) is invariant under the following infinitesimal gauge transformations of the weak eigenstates of the fermionic fields

$$\begin{aligned}
\delta E_L'^i &= i\left(\theta^Y Y + \theta^j \tau^j\right) E_L'^i \,, \\
\delta Q_L'^i &= i\left(\theta^Y Y + \theta^j \tau^j + \theta^a T^a\right) Q_L'^i \,, \\
\delta e_R'^i &= i\theta^Y Y e_R'^i \,, \\
\delta u_R'^i &= i\left(\theta^Y Y + \theta^a T^a\right) u_R'^i \,, \\
\delta d_R'^i &= i\left(\theta^Y Y + \theta^a T^a\right) d_R'^i \,.
\end{aligned} \tag{2.19}$$

Higgs Sector

With only gauge fields and fermions the SM is incomplete. In particular, it does not accommodate the observed non-zero masses of the charged leptons, quarks, and weak gauge bosons. However, left- and right-handed fermion fields transform according to different representations of the gauge group $SU(2)_L$. Thus simple mass terms for the fermions of the form $\bar{f}f = \bar{f}_L f_R + \bar{f}_R f_L$ are forbidden, because they would break chiral gauge invariance. Besides this, exact pure gauge symmetry demands that all gauge fields are massless, since vector field mass terms $V_\mu V^\mu$ would transform non-invariant under the corresponding gauge group and the resulting field theory will be unrenormalizable in general.

The only known way for introducing masses without violating gauge invariance is the Higgs mechanism [66–71], which is based on spontaneous symmetry breaking. Thereby, gauge fields are coupled with additional, postulated scalar fields which, owing to heir self-interactions, acquire asymmetric non-vanishing vacuum expectation values (VEVs), despite the gauge symmetry of the Lagrangian. These scalar fields are also necessary to guarantee unitarity in a theory with massive vector bosons [72, 73]. Some of these scalar fields, the so-called Higgs fields, give rise to physically observable scalar particles. However, the details of the mechanism that induces spontaneous symmetry breaking of the $SU(3)_C \times SU(2)_L \times U(1)_Y$ gauge symmetry are still unknown.

In the minimal formulation of the SM, spontaneous symmetry breaking is achieved by means of a single complex scalar field[4] ϕ that transforms as a spinor of $SU(2)_L$

$$\phi = \begin{pmatrix} \phi^+ \\ \phi^0 \end{pmatrix} \,, \tag{2.20}$$

where the superscripts denote the electric charge of the individual component. The most general renormalizable Lagrangian for the scalar doublet reads

$$\mathcal{L}_{\mathrm{H}} = \left(D_\mu \phi\right)^\dagger \left(D^\mu \phi\right) + \mu^2 \phi^\dagger \phi - \lambda \left(\phi^\dagger \phi\right)^2 \,, \tag{2.21}$$

and involves two new real parameters μ and λ. This Lagrangian is invariant under the infinitesimal local $SU(2)_L \times U(1)_Y$ transformation

$$\delta\phi = i\left(\theta^Y Y + \theta^i \tau^i\right) \phi \,. \tag{2.22}$$

[4] The particle physics vacuum is observed to be translation and Lorentz invariant, so it is clear that the internal symmetry with which we are concerned must be broken by a scalar field having a non-zero value in the vacuum.

The classical configuration with minimum energy, called the vacuum, is a uniform field, chosen to minimize the potential. Since the vacuum would be unstable, if the potential energy is unbounded from below, we have to require that the quartic coupling λ must be positive. Under this assumption there are two possibilities for the theory. If $\mu^2 > 2$, then there is a single minimum of the potential with VEV zero and the symmetry is preserved. Accordingly, the weak gauge bosons remain massless. The alternative scenario is more interesting. If $\mu^2 < 2$, the scalar field will aquire a VEV which we can calculate by asking for the stationary value of the Lagrangian (2.21). We receive

$$\left\langle \phi^\dagger \phi \right\rangle = \frac{\mu^2}{2\lambda} \,, \tag{2.23}$$

which corresponds to an infinite number of degenerate minima transforming into one another under the gauge group. All these ground states are physically equivalent. However, each of them selects a direction in representation space. Choosing one of them as the ground state of the theory, the symmetry is said to be spontaneously broken. The $SU(2)_L \times U(1)_Y$ transformation (2.22) is then an invariant of the Lagrangian, but not of the vacuum state. Without loss of generality, we can therefore make an $SU(2)_L$ rotation so that it is the lower component of ϕ which acquires a real VEV, constant over the whole Minkowski space:

$$\langle \phi \rangle = \frac{1}{\sqrt{2}} \begin{pmatrix} 0 \\ v \end{pmatrix} \,, \tag{2.24}$$

where $v = \sqrt{\mu^2/\lambda}$ at the classical level. With this particular choice, the subgroup of $SU(2)_L \times U(1)_Y$ which corresponds to the infinitesimal transformations

$$\delta\phi = i\theta \left(Y + \tau^3 \right) \phi \,, \tag{2.25}$$

leaves the vacuum state invariant, provided we assign the scalar field a charge $Y = +1/2$ under the $U(1)_Y$ gauge symmetry. Thus, the linear combination

$$Q = Y + \tau^3 \,, \tag{2.26}$$

may be identified with the generator of the unbroken residual electromagnetic $U(1)_Q$ symmetry. The three remaining linear independent generators, which span the quotient space $SU(2)_L \times U(1)_Y / U(1)_Q$, are spontaneously broken, and we will express them through the linear combinations $\tau^\pm = \tau^1 \pm i\tau^2$ and τ^3 in order to diagonalize the mass matrix of the electroweak gauge bosons.

The mass eigenstates of the vector bosons are obtained by the following orthogonal transformation

$$W_\mu^\pm = \frac{1}{\sqrt{2}} \left(W_\mu^1 \mp i W_\mu^2 \right) \,, \quad Z_\mu = c_W W_\mu^3 - s_W B_\mu \,, \quad A_\mu = s_W W_\mu^3 + c_W B_\mu \,, \tag{2.27}$$

where the weak mixing or Weinberg angle θ_W is the angle which appears in the change of basis of the neutral vector bosons:

$$s_W = \sin\theta_W = \frac{g'}{\sqrt{g^2 + g'^2}} \,, \qquad c_W = \cos\theta_W = \frac{g}{\sqrt{g^2 + g'^2}} \,. \tag{2.28}$$

In terms of the mass eigenstate fields (2.27) the $SU(2)_L \times U(1)_Y$ part of the covariant derivative (2.17) becomes

$$D_\mu = \partial_\mu + i\frac{g}{\sqrt{2}}\left(W_\mu^+\tau^+ + W_\mu^-\tau^-\right) + i\frac{g}{c_W}Z_\mu\left(\tau^3 - s_W^2 Q\right) + ieA_\mu Q\,, \tag{2.29}$$

where the last term makes explicit the fact that the neutral gauge boson A_μ, still to be identified with the massless photon field, couples to the electric charge quantum number Q, which generates precisely the symmetry operation (2.25). Consequently, we have expressed the coupling of the vector field A_μ through the electrical charge e:

$$e = \frac{gg'}{\sqrt{g^2 + g'^2}}\,. \tag{2.30}$$

In order to formulate a perturbation theory for $\mu^2 < 0$ we have to expand the Lagrangian (2.21) about the classical ground state (2.24). Let us therefore decompose the complex scalar doublet as

$$\phi = \begin{pmatrix} \phi^+ \\ \frac{1}{\sqrt{2}}(v + H + i\chi) \end{pmatrix}\,, \tag{2.31}$$

where ϕ^+ is a charged and H, χ are neutral scalar fields with vanishing VEV. It is now straightforward to rewrite the Lagrangian (2.21) in terms of mass eigenstates and physical parameters. We get

$$\begin{aligned}\mathcal{L}_{\rm H} = {} & \frac{1}{4}v\left(2t + \lambda v^3\right) + tH + (\partial_\mu\phi^+)(\partial^\mu\phi^-) + \frac{1}{2}(\partial_\mu H)(\partial^\mu H) + \frac{1}{2}(\partial_\mu\chi)(\partial^\mu\chi) \\ & + \frac{t}{v}\left(\phi^+\phi^- + \frac{1}{2}H^2 + \frac{1}{2}\chi^2\right) - \frac{1}{2}M_H^2H^2 + M_W^2W_\mu^+W^{-\mu} + \frac{1}{2}M_Z^2Z_\mu Z^\mu \\ & + iM_W\left(W_\mu^+\partial^\mu\phi^- - W_\mu^-\partial^\mu\phi^+\right) - M_Z Z_\mu\partial^\mu\chi + \dots\,,\end{aligned} \tag{2.32}$$

where $\phi^- = (\phi^+)^*$ and terms cubic and quartic in the fields have been omitted. The original $SU(2)_L \times U(1)_Y$ symmetry is no longer apparent. Its only manifestation is in the relations among the coefficients in Eq. (2.32), which depend in a special way on only two parameters.

The first term in Eq. (2.32) causes a shift of the vacuum energy, which is unobservable in elementary particle physics experiments[5] since it does not contribute to the physical scattering or S-matrix elements. The term linear in H is proportional to the tadpole t defined by

$$t = v\left(\mu^2 - \lambda v^2\right)\,, \tag{2.33}$$

which vanishes at the classical level due to the choice of v. In the GWS theory, however, no symmetry forbids the appearance of a non-vanishing one-point amplitude of the H field at the loop level. This amplitude produces a non-zero VEV of H and so shifts $\langle\phi\rangle$. Such a shift is quite acceptable, as long as it is finite after counterterms are properly added into the computation of the amplitude. However, as we will point out in Section 2.4, it will be convenient to require that the one-point amputated renormalized Green's function of H is zero to all orders in perturbation theory. Then the masses of the fields $\phi^\pm$, H and χ

[5] However, there is a way that the absolute vacuum energy could potentially be observed through the coupling of the vacuum energy to gravity.

will differ from the result of the classical equations by terms of order t/v as indicated by Eq. (2.32).

The tree level masses of the scalar particle H, called the Higgs boson, and of the electroweak vector bosons $W^\pm$ and Z are given by

$$M_H = \sqrt{\frac{\lambda}{2}}v\,, \qquad M_W = g\frac{v}{2}\,, \qquad M_Z = \sqrt{g^2+g'^2}\frac{v}{2}\,, \tag{2.34}$$

while the fourth vector boson A remains massless and thus will be identified with the photon, having the correct coupling to fermions proportional to e. The fields $\phi^\pm$ and χ, the so-called would-be Goldstone bosons, are unphysical degrees of freedom, as we will see in a moment, and remain massless at tree level. In fact, the appearance of massless particles is a general consequence of the spontaneous breaking of a continuous symmetry, known as Goldstone's theorem [74, 75]. These scalar particles have the quantum numbers of the symmetry currents, and therefore might appear as intermediate states in the vacuum polarization amplitude of the electroweak gauge bosons. To compute the contribution of the would-be Goldstone bosons to the gauge boson propagators, we need the vertices that mix the massless with the massive modes. These come from the third line of the Lagrangian given in Eq. (2.32). We see that the amplitude for a $W^\pm$ and Z boson to convert into a $\phi^\pm$ and χ is

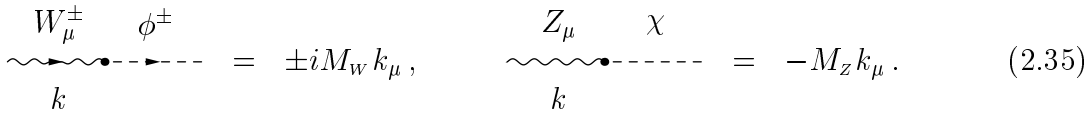

(2.35)

If we also treat the $W^\pm$ boson mass term of Eq. (2.32) as a vertex in perturbation theory, then the leading-order contributions to the vacuum polarization amplitude of the $W^\pm$ boson gives the expression

$$\begin{aligned} &= iM_W^2 g^{\mu\nu} + (iM_W k^\mu)\frac{i}{k^2}(iM_W k^\nu) \\ &= iM_W^2\left(g^{\mu\nu} - \frac{k^\mu k^\nu}{k^2}\right), \end{aligned} \tag{2.36}$$

which implies that the would-be Goldstone boson $\phi^\pm$ supplies exactly the right contribution to make the vacuum polarization amplitude of the $W^\pm$ boson properly transverse. Obviously, the same reasoning holds also in the case of the Z boson.

Although the would-be Goldstone bosons play an important formal role in the theory, they do not appear as independent physical particles. The easiest way to see this is to make a particular choice of gauge, called the unitary gauge. Using the local $SU(2)_L \times U(1)_Y$ gauge symmetry (2.13), we can choose

$$W^\pm_\mu \to W^\pm_\mu \mp \frac{i}{M_W}\partial_\mu\phi^\pm\,, \qquad Z_\mu \to Z_\mu - \frac{1}{M_Z}\partial_\mu\chi\,, \tag{2.37}$$

which corresponds to the following phase rotation of the scalar field

$$\phi \to \frac{1}{\sqrt{2}} \begin{pmatrix} 0 \\ v + H \end{pmatrix} . \tag{2.38}$$

By virtue of our choice of gauge, the would-be Goldstone degrees of freedom have been removed from the Lagrangian (2.32) and the unitarity of the physical S-matrix is manifest [76–80]. However, we might argue that the would-be Goldstone bosons have not completely disappeared. Before spontaneous symmetry breaking the theory had twelve degrees of freedom: A complex scalar field ϕ with four degrees of freedom, three massless $SU(2)_L$ gauge fields with two physical polarization states each and a massless $U(1)_Y$ vector field with two helicity states. After spontaneous symmetry breaking, we are left with a physical real scalar field H with one degree of freedom, massive $W^\pm$ and Z fields with two transversal and one longitudinal polarization state each and a massless photon field with two transversal helicity states. So the total number of physical degrees of freedom has not changed. Figuratively one says that the gauge bosons acquired their extra degree of freedom by eating the would-be Goldstone bosons. Likewise, we see that the disappearance of unwanted massless scalars and the acquisition of mass by the gauge bosons are coupled phenomena. In Section 2.3 we will clarify this picture by studying the quantization and gauge fixing of the SM.

Yukawa Sector

We began the last subsection by assuming that a scalar field ϕ acquires a VEV in order to give mass to the $W^\pm$ and Z bosons. This scalar field needed to be a spinor under $SU(2)_L$ and to have weak-hypercharge $Y = +1/2$ in order to produce the correct pattern of symmetry breaking. To allow for Yukawa interactions of both up- and down-type right-handed quark fields we need in addition a scalar doublet with weak-hypercharge $Y = -1/2$. In the minimal SM we may use the complex-conjugate of the scalar doublet given by

$$\tilde{\phi} = 2i\tau^2\phi^* = \begin{pmatrix} \frac{1}{\sqrt{2}}(v + H - i\chi) \\ -\phi^- \end{pmatrix} . \tag{2.39}$$

When we couple gauge fields to the fermions, we replace the ordinary derivatives with the covariant derivatives. In the GWS theory, we use this technique to insure that only left-handed components of the lepton and quark fields couple to the $W^\pm$ bosons. Once we have specified the third component of the weak-isospin for each fermion field, its weak-hypercharge must be chosen in such a way that the correct electric charge results from the Gell-Mann-Nishijima formula (2.26). This automatically gives all leptons and quarks of the same type the same coupling to the electroweak interactions and all of the quarks the same coupling to the strong interactions. It does not allow mixing between the various lepton and quark flavors. However, the coupling of the scalar field to the fermions does not follow from a gauge principle. Accordingly, we may write down the most general renormalizable gauge-invariant Lagrangian linking the fermionic fields with the scalar doublets:

$$\mathcal{L}_{\mathrm{Y}} = -\sum_{i,j=1}^{3} \left(y_e^{\prime ij} \bar{E}_L^{\prime i} \phi e_R^{\prime j} + y_u^{\prime ij} \bar{Q}_L^{\prime i} \tilde{\phi} u_R^{\prime j} + y_d^{\prime ij} \bar{Q}_L^{\prime i} \phi d_R^{\prime j} + \mathrm{h.c.} \right) , \tag{2.40}$$

Type	Spin	Field	Multiplet
Vector	1	B_μ	$(1,1,0)$
		W_μ	$(1,3,0)$
		G_μ	$(8,1,0)$
Spinor	1/2	$E_L'^i$	$(1,2,-1/2)$
		$Q_L'^i$	$(3,2,+1/6)$
		$e_R'^i$	$(1,1,-1)$
		$u_R'^i$	$(3,1,+2/3)$
		$d_R'^i$	$(3,1,-1/3)$
Scalar	0	ϕ	$(1,2,+1/2)$

Table 2.1: The field content of the minimal SM. Each multiplet is listed according to its color, weak-isospin and weak-hypercharge assignment.

where the Yukawa couplings y_e', y_u' and y_d' are general complex valued matrices, that neither have to be symmetric nor hermitian. Notice that, in contrast to explicit mass terms, the Yukawa interactions are invariant under $SU(2)_L$ and have zero total weak-hypercharge, as can be seen from Tab. 2.1.

As mentioned above, the fermionic part of the Lagrangian (2.18) is invariant under the global $U(3)_E \times U(3)_Q \times U(3)_e \times U(3)_u \times U(3)_d$ symmetry. In order to diagonalize the Yukawa matrices we may exploit this symmetry. Let us therefore make the following change of variables in the sector of the left-handed fermion fields

$$E_L'^i \to \sum_{j=1}^{3} U_{e,L}^{ij} E_L'^j \,, \qquad Q_L'^i \to \sum_{j=1}^{3} U_{u,L}^{ij} Q_L'^j \,. \tag{2.41}$$

The analogous transformations on the right-handed chiral fields read

$$e_R'^i \to \sum_{j=1}^{3} U_{e,R}^{ij} e_R'^j \,, \qquad u_R'^i \to \sum_{j=1}^{3} U_{u,R}^{ij} u_R'^j \,, \qquad d_R'^i \to \sum_{j=1}^{3} U_{d,R}^{ij} d_R'^j \,. \tag{2.42}$$

Here $U_{e,L}$, $U_{u,L}$, $U_{e,R}$, $U_{u,R}$ and $U_{d,R}$ are unitary matrices belonging to the associated symmetry group. In consequence, the Yukawa matrices transform according to

$$y_e = U_{e,L} y_e' U_{e,R}^\dagger \,, \qquad y_u = U_{u,L} y_u' U_{u,R}^\dagger \,, \qquad y_d = U_{u,L} y_d' U_{d,R}^\dagger \,. \tag{2.43}$$

These relations imply that it is possible to diagonalize simultaneously either y_e' and y_u' or y_e' and y_d' by a suitable choice of the chiral transformations (2.41) and (2.42). Without loss of generality, let us assume that we have performed the unitary rotations of the fermionic fields in such a way that the first possibility is realized. Then the transform of the Yukawa coupling y_d' is, in general, neither real nor diagonal. Instead we can write

$$V D_d = U_{u,L} y_d' U_{d,R}^\dagger \,, \tag{2.44}$$

where $D_d = U_{d,L} y'_d U^\dagger_{d,R}$ is diagonal, real and non-negative, and

$$V = U_{u,L} U^\dagger_{d,L} \,, \tag{2.45}$$

is the so-called Cabibbo-Kobayashi-Maskawa (CKM) mixing matrix [81, 82], which is unitary by construction.

Because of the possibility of rephasing the fermionic fields we may diagonalize the Yukawa couplings by choosing a new basis for the leptons and quarks. This basis is the physical one, since it is the basis which diagonalize the mass matrices. Therefore it is called mass eigenstate basis. From Eqs. (2.41), (2.42), (2.44) and (2.45) we read off that the weak and the mass eigenstates of the fermion fields are related by the following unitary transformations:

$$\begin{gathered} \nu^i_L = \sum_{j=1}^3 U^{ij}_{e,L} \nu'^j_L \,, \quad e^i_L = \sum_{j=1}^3 U^{ij}_{e,L} e'^j_L \,, \quad u^i_L = \sum_{j=1}^3 U^{ij}_{u,L} u'^j_L \,, \quad d^i_L = \sum_{j=1}^3 U^{ij}_{d,L} d'^j_L \,, \\ e^i_R = \sum_{j=1}^3 U^{ij}_{e,R} e'^j_R \,, \quad u^i_R = \sum_{j=1}^3 U^{ij}_{u,R} u'^j_R \,, \quad d^i_R = \sum_{j=1}^3 U^{ij}_{d,R} d'^j_R \,. \end{gathered} \tag{2.46}$$

Notice that we are making the same change of variables on the two components of the weak doublet E'^i_L. Accordingly, the resulting theory of leptons conserves the lepton number of each generation, as we will see in a moment. In contrast, u'^i_L and d'^i_L transform different under the unitary transformations (2.46) and the misalignment of the matrices $U_{u,L}$ and $U_{d,L}$ leads to flavor mixing in the quark sector.

In terms of the mass and charge eigenstates (2.46) the Lagrangian describing the Yukawa interactions (2.40) takes the form

$$\begin{aligned} \mathcal{L}_{\rm Y} = & - \sum_{f=e,u,d} \sum_{i=1}^3 m^i_f \bar{f}^i f^i - \sum_{f=\nu,e,u,d} \sum_{i=1}^3 \frac{e}{2 s_W} \frac{m^i_f}{M_W} \left(\bar{f}^i f^i H - 2 i \tau^3_f \bar{f}^i \gamma^5 f^i \chi \right) \\ & + \sum_{i,j=1}^3 \frac{e}{\sqrt{2} s_W} \left[\frac{m^i_u}{M_W} \left(V_{ij} \bar{u}^i_R d^j_L \phi^+ + V^\dagger_{ij} \bar{d}^i_L u^j_R \phi^- \right) - \frac{m^i_d}{M_W} \left(V_{ij} \bar{u}^i_L d^j_R \phi^+ + V^\dagger_{ij} \bar{d}^i_R u^j_L \phi^- \right) \right] \\ & - \sum_{i=1}^3 \frac{e}{\sqrt{2} s_W} \frac{m^i_e}{M_W} \left(\bar{\nu}^i_L e^i_R \phi^+ + \bar{e}^i_R \nu^i_L \phi^- \right) \,, \end{aligned} \tag{2.47}$$

where the masses of the charged leptons, up- and down-type quarks are related to the diagonal elements of the Yukawa couplings in the fermion mass eigenstate basis by

$$m^i_e = \frac{v}{\sqrt{2}} D^{ii}_e \,, \qquad m^i_u = \frac{v}{\sqrt{2}} D^{ii}_u \,, \qquad m^i_d = \frac{v}{\sqrt{2}} D^{ii}_d \,. \tag{2.48}$$

The matrices D_e, D_u and D_d are diagonal, by definition, and have real and non-negative eigenvalues, as indicated by Eqs. (2.43) and (2.44). It is interesting to note that in the minimal version of the SM neutrinos have zero Dirac masses due to the fact that no right-handed neutrino fields have been introduced in Eq. (2.16). Since neutrinos have zero electric charge, one could think that neutrinos can acquire Majorana mass terms of the form $\nu^{iT}_L C^{-1} \nu^i_L$ where C is the charge conjugation matrix. This however cannot happen, as such terms would transform as triplets under $SU(2)_L$. Hence, in the absence

of scalar triplets they cannot be generated by renormalizable Yukawa interactions at tree level. In addition, no Majorana neutrino masses are induced either by perturbative or non-perturbative loop corrections, because they would violate the global $B-L$ symmetry of the SM, to be discussed in the next subsection. It follows that the minimal SM predicts that neutrinos are precisely massless.

On the contrary, recent experiments of various features of the fluxes of atmospheric and solar neutrinos have provided strong evidence for neutrino oscillations [54–65], and thus for neutrino masses and mixing. That means that the minimal SM cannot be a complete description of nature. Indeed, the SM prediction of massless neutrinos is an accidental fact: Unlike photons, no profound principle protects them from having a mass and right-handed neutrino fields can be easily added to the minimal SM without affecting its basic structure. If right-handed neutrinos are introduced, then quark-lepton symmetry is reestablished, and the most general renormalizable and $SU(2)_L \times U(1)_Y$ invariant Lagrangian includes Yukawa interactions which generate neutrino masses upon spontaneous symmetry breaking. The inclusion of right-handed neutrinos, however, does not explain the smallness of neutrino masses even though it can accommodate it. Fortunately, modern elementary particle theories, the best-known examples being $SO(10)$ grand unified theory [83–85] and left-right symmetry [86,87], anticipate ways in which the neutrinos have small, but definitely non-vanishing masses. In fact, there are good theoretical reasons, to go by the name of the see-saw mechanism [83–85], to expect that neutrinos are massive but much lighter than all the charged fermions of the SM. Specifically, it is very likely that neutrino masses are inversely proportional to the scale of new physics. Consequently, if neutrino masses are measured, one can estimate the relevant new scales and gain some insight into physics beyond the SM.

In order to extract the physical content of the minimal SM in the spontaneous broken form, let us also rewrite the fermion gauge boson interactions (2.18) in terms of the physical fields (2.27) and (2.46), and parameters. We obtain

$$\begin{aligned}
\mathcal{L}_{\rm F} = & \sum_{f=\nu,e,u,d} \sum_{i=1}^{3} \left[\bar{f}^i i\partial\!\!\!/ f^i + \frac{e}{s_W c_W} \left(\tau_f^3 \bar{f}_L^i \gamma^\mu f_L^i - s_W^2 Q_f \bar{f}^i \gamma^\mu f^i \right) Z_\mu - e Q_f \bar{f}^i \gamma^\mu f^i A_\mu \right] \\
& + \sum_{f=u,d} \sum_{i=1}^{3} g_s \bar{f}^i \gamma^\mu T^a f^i G_\mu^a + \sum_{i,j=1}^{3} \frac{e}{\sqrt{2} s_W} \left(V_{ij} \bar{u}_L^i \gamma^\mu d_L^j W_\mu^+ + V_{ij}^\dagger \bar{d}_L^i \gamma^\mu u_L^j W_\mu^- \right) \\
& + \sum_{i=1}^{3} \frac{e}{\sqrt{2} s_W} \left(\bar{\nu}_L^i \gamma^\mu e_L^i W_\mu^+ + \bar{e}_L^i \gamma^\mu \nu_L^i W_\mu^- \right) , \qquad (2.49)
\end{aligned}$$

where τ_f^3 and Q_f are the third component of the weak-isospin and the charge of the fermion f^i, respectively. Owing to the their unitarity, the rotation matrices introduced in Eq. (2.46) drop out of the interaction terms between fermions and neutral gauge bosons. It follows that there are no flavor changing neutral currents (FCNCs) at the tree level in the SM. This is known as the Glashow-Iliopoulus-Maiani (GIM) mechanism [50]. Even at the loop level, where the FCNCs are induced, the GIM mechanism guarantees that such processes are suppressed by at most a factor of m_q^2/M_W^2, which is very small, expect in the case of the t-quark. GIM suppression therefore implies predictions for several physical processes very close to zero and an observation of any of these would provide a clear signal of non-standard physics.

As a result of the fact that the CKM matrix is not diagonal in general, the $W^\pm$ gauge bosons couple to the quark mass eigenstates of different generations, as can be observed by inspection of Eq. (2.49). Apart from the quark-would-be Goldstone interactions of Eq. (2.47), which can be eliminated by transition to the unitary gauge (2.37) and (2.38), this is the only source of flavor changing quark interactions within the SM. No such interactions take place in the lepton sector, since the charged current interactions preserve their form under the chiral transformations (2.46). Thus there are no flavor changing lepton interactions in the SM. However, keep in mind that if neutrinos are massive, as indicated by the recent observation of neutrino oscillations, this will no longer be the case, since then we are not allowed to transform $\nu_L'^i$ and $e_L'^i$ by using the same unitary matrix $U_{e,L}$. Correspondingly, this will give rise to a non-trivial mixing matrix for leptons, whose actual form depends on whether neutrinos are Dirac or Majorana particles [88–90].

Since we have rewritten the most important parts of the classical Lagrangian of the minimal SM in terms of physical fields, that is the mass and charge eigenstates $W_\mu^\pm$, Z_μ, A_μ, f^i, and H, the would-be Goldstone fields $\phi^\pm$ and χ, and the physical parameters e, M_W, M_Z, m_f^i, M_H, and V, it is suggestive do the same for the infinitesimal gauge transformations given in Eqs. (2.13), (2.19) and (2.22). We find

$$
\begin{aligned}
\delta W_\mu^\pm &= -\frac{1}{e}\partial_\mu\theta^\pm \pm \frac{i}{s_W}\left[W_\mu^\pm\left(c_W\theta^Z + s_W\theta^A\right) - \left(c_W Z_\mu + s_W A_\mu\right)\theta^\pm\right] ,\\
\delta Z_\mu &= -\frac{1}{e}\partial_\mu\theta^Z - 2i\frac{c_W}{s_W}\left(W_\mu^+\theta^- - W_\mu^-\theta^+\right) ,\\
\delta A_\mu &= -\frac{1}{e}\partial_\mu\theta^A - 2i\left(W_\mu^+\theta^- - W_\mu^-\theta^+\right) ,\\
\delta\nu_L^i &= \frac{i}{2s_W c_W}\theta^Z\nu_L^i + \frac{i}{s_W}\theta^+ e_L^i ,\\
\delta e_L^i &= -i\left[\frac{s_W}{c_W}\left(Q_e + \frac{1}{2s_W^2}\right)\theta^Z - Q_e\theta^A\right] e_L^i + \frac{i}{s_W}\theta^-\nu_L^i ,\\
\delta u_L^i &= -i\left[\frac{s_W}{c_W}\left(Q_u - \frac{1}{2s_W^2}\right)\theta^Z - Q_u\theta^A - T^a\theta^a\right] u_L^i + \sum_{j=1}^{3}\frac{i}{s_W}V_{ij}\theta^+ d_L^j ,\\
\delta d_L^i &= -i\left[\frac{s_W}{c_W}\left(Q_d + \frac{1}{2s_W^2}\right)\theta^Z - Q_d\theta^A - T^a\theta^a\right] d_L^i + \sum_{j=1}^{3}\frac{i}{s_W}V_{ij}^\dagger\theta^- u_L^j ,\\
\delta e_R^i &= -iQ_e\left(\frac{s_W}{c_W}\theta^Z - \theta^A\right) e_R^i ,\\
\delta u_R^i &= -i\left[Q_u\left(\frac{s_W}{c_W}\theta^Z - \theta^A\right) - T^a\theta^a\right] u_R^i ,\\
\delta d_R^i &= -i\left[Q_d\left(\frac{s_W}{c_W}\theta^Z - \theta^A\right) - T^a\theta^a\right] d_R^i ,\\
\delta\phi^\pm &= \pm\frac{i}{2s_W}\left(v + H \pm i\chi\right)\theta^\pm \mp i\phi^\pm\left(\frac{s_W^2 - c_W^2}{s_W c_W}\theta^Z + \theta^A\right) ,\\
\delta H &= \frac{1}{2s_W c_W}\chi\theta^Z + \frac{i}{2s_W}\left(\phi^+\theta^- - \phi^-\theta^+\right) ,\\
\delta\chi &= -\frac{1}{2s_W c_W}\left(v + H\right)\theta^Z + \frac{1}{2s_W}\left(\phi^+\theta^- + \phi^-\theta^+\right) ,
\end{aligned}
\tag{2.50}
$$

where

$$\theta^{\pm} = \frac{s_W}{\sqrt{2}} \left(\theta^1 \mp i\theta^2\right) , \qquad \theta^Z = s_W c_W \left(\theta^3 - \theta^Y\right) , \qquad \theta^A = s_W^2 \theta^3 + c_W^2 \theta^Y . \tag{2.51}$$

Symmetries of the Standard Model

In addition to continuous Lorentz transformations, there are two other spacetime operations that are potential symmetries of any quantum field theory: Parity and time reversal. Parity, denoted by P, sends $(t, \vec{x}) \to (t, -\vec{x})$, reversing the handedness of space. Time reversal, denoted by T, sends $(t, \vec{x}) \to (-t, \vec{x})$, interchanging the forward and backward light-cone. Recall that the full Lorentz group possesses four disconnected parts: The proper, orthochronous Lorentz group to which the continuous Lorentz transformations belong, the improper, orthochronous part which is connected with the first subset by parity transformation P, the proper, non-orthochronous group which is generated by the time reversal operation T and the improper, non-orthochronous transformations which contains the combined PT transformation. It follows that neither the P nor the T operation can be achieved by a continuous Lorentz transformation starting from the identity. At the same time that we review P and T, it will be convenient to discuss a third non-spacetime symmetry: Charge conjugation, denoted by C. Under this operation, particles and antiparticles are interchanged.

In quantum field theory the transformations P, T and C are represented by the operators $\mathcal{P}$, $\mathcal{T}$ and $\mathcal{C}$, respectively. First let us consider parity. The operator $\mathcal{P}$ should reverse the momentum of a particle without flipping its spin. Consequently, it may be implemented by an unitary operator, that is, $\mathcal{P}^\dagger = \mathcal{P}^{-1}$. In order to derive the transformation properties of the different types of quantum fields one should remember that each field may be written as a linear combination of creation and annihilation operators for particles and antiparticles. Exploiting this idea we find the following transformation rules of the various quantum fields

$$\begin{aligned} \mathcal{P} V_\mu(t, \vec{x}) \mathcal{P}^{-1} &= \eta_P V^\mu(t, -\vec{x}) , \\ \mathcal{P} f(t, \vec{x}) \mathcal{P}^{-1} &= \eta_P P f(t, -\vec{x}) , \\ \mathcal{P} S(t, \vec{x}) \mathcal{P}^{-1} &= \eta_P S(t, -\vec{x}) , \end{aligned} \tag{2.52}$$

where V_μ, f and S denotes a generic Lie algebra valued vector, spinor and complex scalar field, respectively. P denotes a non-singular matrix such that $P\gamma^\mu P^{-1} = \gamma^{\mu\dagger}$ and $P = P^\dagger = P^{-1}$. In the usual representations of the homogeneous Lorentz group, that is the Dirac-Pauli, Weyl and Majorana representation, it can be expressed as $P = \gamma^0$. The phase factor[6] η_P parameterizes the arbitrariness in the definition of $\mathcal{P}$. It is related to the internal symmetries of the Lagrangian. The simplest internal symmetry corresponds to the possibility of changing the phase of each individual quantum field. More generally, whenever there are various quantum fields with the same quantum numbers, there might be an internal symmetry which mixes those fields. However, an operator $\mathcal{P}$ which mixes some fields occupying an equivalent position in the Lagrangian is just as good a representation of parity as an operator $\mathcal{P}$ which does not mix them, and thus leads to a physical

[6]Notice that the phase factor associated with different fields need not be the same. For the sake of simplicity we have omitted this dependence in Eqs. (2.52), (2.53) and (2.54).

equivalent Lagrangian. This is the origin of the large degree of freedom in the definition of $\mathcal{P}$, and analogously also of $\mathcal{T}$ and $\mathcal{C}$.

The implementation of the time reversal symmetry in a quantum mechanical context is more subtle. This is because the relevant operator $\mathcal{T}$, is not unitary but rather antiunitary, that is, $\mathcal{T}^\dagger = \mathcal{T}^{-1}$ with $\langle\psi|\mathcal{T}^\dagger|\varphi\rangle = \langle\mathcal{T}\psi|\varphi\rangle^*$, where $|\psi\rangle$ and $|\varphi\rangle$ denote arbitrary multiparticle quantum states. A straightforward way to realize that the operator $\mathcal{T}$ must be antiunitary is to consider the behavior of the Schrödinger equation for a free particle under time reversal. In classical mechanic, a free particle has a time reversal invariant motion, and it is reasonable that we would like to retain this property in quantum mechanics as well. But the operator $\partial/\partial t$ is T-odd while $\vec{\nabla}$ is T-even. This is impossible to reconcile with the Schrödinger equation unless $\mathcal{T}$ changes $i \to -i$ and $\psi \to \psi^*$. The operator $\mathcal{T}$ therefore has to be antiunitary. Note that the antiunitarity of $\mathcal{T}$ implies that it does not have meaningful eigenvalues, contrary to what happens with $\mathcal{P}$ and $\mathcal{C}$. As there is no quantum number associated with $\mathcal{T}$, no conservation law exists when there is T invariance. Just as for parity, we define the time reversal transformation in quantum field theory by the action of $\mathcal{T}$ on the annihilation operators of particles and antiparticles. In addition to reversing the momentum of a particle, $\mathcal{T}$ should flip the spin. Applying this notion to the diverse quantum fields, we see that

$$\begin{aligned} \mathcal{T}V_\mu(t,\vec{x})\mathcal{T}^{-1} &= \eta_T V^\mu(-t,\vec{x})\,, \\ \mathcal{T}f(t,\vec{x})\mathcal{T}^{-1} &= \eta_T T f(-t,\vec{x})\,, \\ \mathcal{T}S(t,\vec{x})\mathcal{T}^{-1} &= \eta_T S(-t,\vec{x})\,. \end{aligned} \tag{2.53}$$

Here T denotes a unitary matrix satisfying $T\gamma^\mu T^{-1} = g^{\mu\mu}\gamma^{\mu *}$ and $T = T^\dagger = T^{-1}$, where $g^{\mu\nu}$ is the usual Minkowski metric tensor given by $g_{\mu\nu} = g^{\mu\nu} = \mathrm{diag}(1,-1,-1,-1)$. In the standard representations T can be written as $T = i\gamma^1\gamma^3$. In analogy to the case of parity, η_T denotes an arbitrary phase factor which codifies the freedom in the definition of $\mathcal{T}$ due to internal symmetries.

The last of the three discrete symmetries is the particle-antiparticle symmetry C. Like the parity transformation P it can be implemented as a unitary linear operator. Charge conjugation is conventionally defined to take a particle with a given spin orientation into an antiparticle with the same spin orientation. If in addition we require that the coupling of the Yang-Mills fields to the charged vector current is invariant under C, we can derive the transformation properties of the different types of quantum fields. We get

$$\begin{aligned} \mathcal{C}V_\mu(t,\vec{x})\mathcal{C}^{-1} &= -\eta_C V_\mu^T(t,\vec{x})\,, \\ \mathcal{C}f(t,\vec{x})\mathcal{C}^{-1} &= \eta_C C\bar{f}^T(t,\vec{x})\,, \\ \mathcal{C}S(t,\vec{x})\mathcal{C}^{-1} &= \eta_C S^\dagger(t,\vec{x})\,, \end{aligned} \tag{2.54}$$

where C is the charge conjugation matrix which obeys $C^{-1}\gamma^\mu C = -\gamma^{\mu T}$ and $C = -C^\dagger = -C^{-1} = -C^T$. For the simplest representations of the Dirac algebra it is given by $C = i\gamma^2\gamma^0$. Again η_C is an arbitrary phase factor.

Any of the discrete symmetries P, T, or C, or any combination thereof, may be violated in the framework of quantum field theory. There is, however, a strong theoretical believe that the combined CPT transformation, which simultaneously performs a reflection relative to all axis of spacetime, and interchanges particles and antiparticles, is a perfect symmetry of nature. This believe is based on the so-called CPT theorem [91–96] which,

starting from very general properties of quantum field theory, in particular, Poincaré invariance and local commutation and anticommutation relations obeying the spin-statistic connection, asserts that any such theory is CPT invariant. Because of this theorem, it is very difficult to conceive a realistic, sensible relativistic quantum theory in which CPT is violated. However, as CPT invariance implies that particles and antiparticles have equal masses and total decay widths, the assumption that nature is CPT invariant can be experimentally tested. Down to the present day numerous experiments have confirmed the supposition of CPT invariance [2], including in particular high-precision tests using neutral-kaon interferometry [97–99]. The simultaneous existence of a general theoretical proof of CPT invariance in particle physics and accurate experimental tests makes CPT violation, however, an attractive candidate signature for non-particle physics such as string theory.[7]

Let us now investigate the properties of the complete classical Lagrangian of the SM. The couplings of the QCD gauge bosons are invariant to each of the discrete symmetries separately. Strictly speaking, however, the prove of the invariance of the Lagrangian of QCD is not sufficient to obtain invariance of the strong interactions. This is due to the fact, that QCD has a non-trivial vacuum structure which gives rise to both P and T violation in general. For the rest of this thesis, however, we shall neglect this awkward strong CP problem [106–108], and assume that the vacuum of QCD is invariant under the discrete transformations.

The interactions of the $SU(2)_L$ gauge bosons violate P and C in the strongest possible way, since these transformations flip the chirality of the fermionic fields. For example, using Eqs. (2.52) and (2.54) it is straightforward to derive that the couplings of the $W^\pm$ to the up- and down-type quarks transform under P and C as follows

$$\begin{aligned} V_{ij}\bar{u}^i_L\gamma^\mu d^j_L W^+_\mu + V^\dagger_{ij}\bar{d}^i_L\gamma^\mu u^j_L W^-_\mu &\xrightarrow{P} V_{ij}\bar{u}^i_R\gamma^\mu d^j_R W^+_\mu + V^\dagger_{ij}\bar{d}^i_R\gamma^\mu u^j_R W^-_\mu\,, \\ V_{ij}\bar{u}^i_L\gamma^\mu d^j_L W^+_\mu + V^\dagger_{ij}\bar{d}^i_L\gamma^\mu u^j_L W^-_\mu &\xrightarrow{C} V_{ij}\bar{d}^j_R\gamma^\mu u^i_R W^-_\mu + V^\dagger_{ij}\bar{u}^j_R\gamma^\mu d^i_R W^+_\mu\,, \end{aligned} \tag{2.55}$$

where the corresponding phase factors η_P and η_C have been dropped. Clearly, each of these operations converts a left-handed current that couples to the $W^\pm$ to one that does not, and thus P and C are broken badly. However, the combination of these two operations interchanges left-handed particles with right-handed antiparticles, and naively one could guess that CP is an exact symmetry of the SM. Let us investigate this point more accurate. After diagonalization of the fermion mass matrices, the CP violating Yukawa couplings to the scalar particle (2.40) disappear. Then, apart from the quark would-be Goldstone interactions of Eq. (2.47), the only potential CP violating terms occur in the couplings of the charged current to the $W^\pm$ bosons. Combining Eqs. (2.55) we see that these interactions transform under CP as follows:

$$V_{ij}\bar{u}^i_L\gamma^\mu d^j_L W^+_\mu + V^\dagger_{ij}\bar{d}^i_L\gamma^\mu u^j_L W^-_\mu \xrightarrow{CP} V^\dagger_{ji}\bar{u}^i_L\gamma^\mu d^j_L W^+_\mu + V_{ji}\bar{d}^i_L\gamma^\mu u^j_L W^-_\mu\,. \tag{2.56}$$

For CP invariance of the charged current couplings, we require that the left-hand side of Eq. (2.56) should equal its right-hand side. Neglecting arbitrary phase factors the

[7] Since the critical string dimensionality is larger than four, it is plausible that higher dimensional Lorentz breaking would be incorporated in a realistic model. In fact, a mechanism is known in string theory that can cause spontaneous CPT violation [100,101] with accompanying partial Lorentz symmetry breaking [102–105].

condition for CP invariance therefore becomes

$$V_{ij} = V_{ij}^* \,, \tag{2.57}$$

or, in other words, the CKM mixing matrix must be real to guarantee that CP is conserved. The same condition would follow if, instead of the charged current couplings we would have imposed CP invariance on the quark would-be Goldstone interactions of Eq. (2.47). Notice that, if one considers a single matrix element of V, Eq. (2.57) can always be made to hold by adjusting the phases of the quark fields. However, if one simultaneously considers all elements of the CKM mixing matrix, one realizes that Eq. (2.57) forces all rephasing invariant functions of V to be real. We shall see later on that in general there is CP violation in the SM if and only if any of the rephasing invariant functions of the CKM mixing matrix is not real.

This illuminates why CP violation is related to complex phases in the couplings, and immediately raises the question how many CP violating parameters there are in the SM. The unitarity of the CKM mixing matrix expresses the universality of the weak interactions in the quark sector. Being a general unitary $N_G \times N_G$ matrix for N_G generations, V depends on N_G^2 parameters: $N_G(N_G-1)/2$ that are real and CP conserving, and another $N_G(N_G+1)/2$ that are imaginary and CP violating. Not all of them, however, do have physical meaning. In fact, one has the freedom to perform a change of variables on the quark fields

$$u_L^i \to e^{i\varphi_u^i} u_L^i \,, \qquad d_L^i \to e^{i\varphi_d^i} d_L^i \,, \tag{2.58}$$

with N_G arbitrary phases φ_u^i and N_G arbitrary phases φ_d^i. Under Eq. (2.58) the CKM mixing matrix transforms as

$$V_{ij} \to e^{i(\varphi_d^j - \varphi_u^i)} V_{ij} \,. \tag{2.59}$$

Since a common rephasing of all quark fields has no effect on V, one may thus eliminate the phases of $2N_G - 1$ matrix elements of the CKM mixing matrix. Therefore, out of the $(N_G-1)^2$ parameters of V

$$N_\theta = \frac{1}{2} N_G \left(N_G - 1\right) \,, \tag{2.60}$$

should be identified with Euler-type rotation angles. The remaining

$$N_\delta = \frac{1}{2} \left(N_G - 1\right) \left(N_G - 2\right) \,, \tag{2.61}$$

parameters of V are physical phases causing CP violation. Consequently, in the case of two generations there is only one rotation angle and V takes the form of the Cabibbo matrix [81]. For three fermion families, the quark mixing matrix can be parameterized by three rotation angles and one complex phase, as was first pointed out by Kobayashi and Maskawa [82]. Clearly, this phase leading to an imaginary part of the CKM matrix is a necessary ingredient to describe CP violation within the minimal SM.

We saw that CP non-conservation in the CKM formalism is associated with imaginary parts of elements of the quark mixing matrix. This condition tells us for what we should look for in order to see whether CP is conserved or not, but it does not tell us anything about the size of CP violation in the SM. In particular, it does not provide a framework to answer the question if maximal CP non-conservation is realized in nature or not. In order to answer this question one must first provide an adequate measure of CP violation.

The derivation of such a quantity starts with recalling the lesson learned from classical quantum mechanics, that observables are represented by hermitian operators and their commutators give a measure of their compatibility, that is, whether the observables can be measured simultaneously or not. Although the non-diagonal quark mass matrices m'_u and m'_d are not necessarily hermitian, they may be used to form hermitian operators, namely[8]

$$H_u = m'_u m'^{\dagger}_u \,, \qquad H_d = m'_d m'^{\dagger}_d \,. \tag{2.62}$$

They are, as usual, diagonalized by $U_{u,L}$ and $U_{d,L}$, respectively:

$$U_{u,L} H_u U^{\dagger}_{u,L} = m_u^2 \,, \qquad U_{d,L} H_d U^{\dagger}_{d,L} = m_d^2 \,, \tag{2.63}$$

where m_u and m_d denote the physical mass matrices introduced in Eq. (2.48). Notice that the hermitian and traceless matrices H_u and H_d are only partial observables. Only their eigenvalues and their relative orientation, that is, the quantity V, are measurable. Nevertheless, their commutator is a measure whether they can be diagonalized simultaneously or not. We shall see in a moment that this commutator plays an important role in testing CP invariance.

The squares of the mass matrices H_u and H_d dictate the flavor structure of the SM. However, it is important to keep in mind that these are by no means unique. The reason is that the measurable quantities are not affected if H_u and H_d are both rotated with the same unitary matrix:

$$H_u \to U^{\dagger}_L H_u U_L \,, \qquad H_d \to U^{\dagger}_L H_d U_L \,. \tag{2.64}$$

Such a rotation leaves the eigenvalues as well as the quark mixing matrix V invariant. The above unitary rotation corresponds to choosing a particular basis or frame of reference in flavor space. Since measurable quantities cannot depend on the choice of the coordinate frame they must be invariants under the symmetry transformation (2.64).

The essential point is now, that one can prove [109], that the Lagrangian of the SM is CP invariant if and only if the matrices H_u and H_d are such that a unitary matrix U_L exists which satisfies:

$$U^{\dagger}_L H_u U_L = H^*_u \,, \qquad U^{\dagger}_L H_d U_L = H^*_d \,. \tag{2.65}$$

It is clear that although Eq. (2.65) constitutes a necessary and sufficient condition for CP invariance, it is of little practical use in that form. If one attempts to evaluate invariants of both sides of Eq. (2.65), one obviously obtains trivial identities. In order to derive non-trivial conditions on H_u and H_d, we note that the trace of any product of matrices H_u and H_d is invariant under unitary transformations of the left-handed quark fields. Therefore Eq. (2.65) implies

$$\mathrm{Im}\,\mathrm{tr}\,[H_u^{p_1} H_d^{p_2} H_u^{p_3} \ldots H_d^{p_i}] = 0 \,, \tag{2.66}$$

where $p_1, \ldots, p_i$ is an arbitrary sequence of positive integers. These are the necessary and sufficient conditions for CP invariance which we were looking for. They are valid for an arbitrary number of families and the violation of any one of them guarantees the existence of CP non-conservation [110]. At this stage, it is worthwhile emphasizing that

[8] Notice that the combinations $m'^{\dagger}_u m'_u$ and $m'^{\dagger}_d m'_d$ are also hermitian. However, it is easy to show that the commutator of these operators does not provide a sensible measure of CP violation, because it is connected to the right-handed analogue of V which is unobservable in the SM.

the conditions (2.66) are independent of the particular basis which one chooses to write the matrices H_u and H_d. In other words, if one finds a solution of Eq. (2.66) in one basis, then there will be a solution in any other basis. However, in practice one is interested in finding a minimal subset of these necessary and sufficient conditions. In the case of the SM with three families for instance, it has been shown [109–111], that there is only one such condition necessary and sufficient for CP conservation:

$$\mathrm{Im}\,\mathrm{tr}\left[H_u^2 H_d H_u H_d^2\right] = -\frac{i}{6}\,\mathrm{tr}\left[H_u, H_d\right]^3 = -\frac{i}{2}\,\det\left[H_u, H_d\right] = 0\,. \tag{2.67}$$

The commutator $[H_u, H_d]$ is, by definition, hermitian and traceless. Thus its eigenvalues are real. In fact, they are measurable, even though the commutator itself is not a observable. Using the definition of the CKM mixing matrix (2.45) and the relations (2.63) we have

$$\left[H_u, H_d\right] = U_L^\dagger \left[m_u^2, V m_d^2 V^\dagger\right] U_L\,. \tag{2.68}$$

Hence, the eigenvalues of $[H_u, H_d]$ are calculable in terms of the quark masses and the elements of the quark mixing matrix. Making repeated use of the unitarity of V one finally obtains

$$\det\left[H_u, H_d\right] = -2i\Delta m_u^2 \Delta m_d^2 J\,, \tag{2.69}$$

where

$$\begin{aligned} \Delta m_u^2 &= \left(m_t^2 - m_c^2\right)\left(m_t^2 - m_u^2\right)\left(m_c^2 - m_u^2\right)\,, \\ \Delta m_d^2 &= \left(m_b^2 - m_s^2\right)\left(m_b^2 - m_d^2\right)\left(m_s^2 - m_d^2\right)\,. \end{aligned} \tag{2.70}$$

Here m_i denotes the mass of the quark of type i and the quantity J, which is often referred to as the Jarlskog invariant, can be expressed in terms of the simplest non-real rephasing invariant functions of the CKM mixing matrix [111–114]. The exact formula reads

$$J = \sum_{m,n=1}^{3} \epsilon_{ikm}\epsilon_{jln}\,\mathrm{Im}\left(V_{ij} V_{kl} V_{il}^* V_{kj}^*\right)\,, \tag{2.71}$$

for all combinations i, j, k and l. One concludes that, in order to have CP violation in the minimal SM with three generations, no two quarks with the same charge are allowed to be degenerate in mass, and in addition J must be different from zero. Thus the relation Eq. (2.67) has the remarkable feature, that it unifies six conditions on the masses of the quarks and eight conditions on the angles and the phases of the quark mixing matrix, for a total of fourteen necessary and sufficient conditions for CP conservation. Ignoring the strong CP problem, any CP violating observable in the SM with three generations is proportional to the factors introduced in Eqs. (2.70) and (2.71). Hence, the SM is very predictive in describing CP violating effects. In practice, however, strong interaction effects have to be controlled before such calculations can be performed.

We have seen that chiral phase invariance is broken in the minimal SM explicitly by the quark mass matrices. Consequently, all the fermion flavor charges are no longer generally conserved. However, within the minimal SM the following accidental global symmetry arises[9]

$$U(1)_B \times U(1)_e \times U(1)_\mu \times U(1)_\tau\,, \tag{2.72}$$

[9] It often happens that, as a consequence of the symmetries that define a model and of its particle content, all renormalizable terms in the Lagrangian obey additional symmetries, that are not a priori imposed on the model itself. These are called accidental symmetries.

Here $U(1)_B$ is the baryon number symmetry, and $U(1)_e$, $U(1)_\mu$ and $U(1)_\tau$ are the three lepton flavor symmetries, with the total lepton number given by $L = L_e + L_\mu + L_\tau$. It is easy to see that the total number of quarks minus antiquarks is conserved in the SM at tree level, due to the exact color invariance. The covariant derivative (2.17) and the colorless scalar field (2.20) must therefore connect quark fields of compensating color representations. Thus all terms in the SM Lagrangian create and annihilate equally many quarks. A priori this gives baryon number conservation, but the baryon number current has an anomaly [115–119], due to its electroweak interactions. In the vacuum sector this phenomenon is associated with instantons [120], describing tunneling transitions between topologically distinct vacua. In the weakly coupled theories the probabilities of these transitions are exponentially suppressed. In particular, the corresponding suppression factor in the standard electroweak theory is $\exp(-16\pi^2/g^2)$, as was first pointed out by 't Hooft [121, 122]. The predicted baryon number violation, at temperatures much lower than the electroweak breaking scale v, is therefore unobservable. Similarly, it is easy to see that there is a lepton conservation law for each of the fermion generation by inspecting the Yukawa couplings (2.47) and the fermion gauge boson interactions (2.49). Again, there is an anomaly in each of the lepton number currents. Due to the enormous suppression factor for $SU(2)_L$ gauge field instantons, however, there is in practice no violation of any of the lepton number conservation laws. Finally, let us note that, it is even possible to construct anomaly free conservation laws by taking differences in which the anomalies cancel out. In fact, the lepton number differences $L_\mu - L_e$ and $L_\tau - L_e$ are exactly conserved. Furthermore $B - L$ is a conserved quantity, even with anomalies taken into account.

2.3 Quantization of the Standard Model

The perturbative construction of Green's functions and finally the S-matrix starts with the specification of the free fields and their respective propagators. In the SM the scalars $\phi^\pm$ and χ are unphysical degrees of freedom being absorbed into the longitudinal polarization of the massive vector fields $W^\pm$ and Z. Eliminating them by transition to the unitary gauge according to Eqs. (2.37) and (2.38), however, leads to propagators with a bad ultraviolet (UV) behavior, and renormalizability by power counting is not evident any more. However, this special gauge can be continously transformed into a renormalizable or R_ξ gauge [76, 78] in such a way that in all intermediate gauges the theory is well-defined. Then, the gauge independence of the S-matrix ensures that the theory is unitary also in the R_ξ gauges [79]. Accordingly, a systematic treatment of higher orders can be performed most convenient in this class of gauges. If one constructs the off-shell Green's functions in the R_ξ gauges, one is then able to refer to power counting properties of renormalized perturbation theory and, especially, to the quantum action principle [123–127].

The free field propagators are calculated from the bilinear parts of the gauge-invariant classical Lagrangian and the gauge-fixing part. For the purpose of this thesis we choose the following linearized generalization of the usual R_ξ gauges:

$$\mathcal{L}_{\mathrm{GF}} = -\frac{1}{\xi_W} F^+ F^- - \frac{1}{2\xi_Z} F^Z F^Z - \frac{1}{2\xi_A} F^A F^A - \frac{1}{2\xi_s} F^a F^a \,. \tag{2.73}$$

The gauge-fixing functions of the R_ξ gauges fix the scalar part of the vector fields and

introduce mass terms for the would-be Goldstone fields $\phi^\pm$ and χ. We use

$$\begin{aligned} F^\pm &= \partial_\mu W^{\pm\mu} \mp i M_W \zeta_W \phi^\pm \,, \\ F^Z &= \partial_\mu Z^\mu - M_Z \zeta_Z \chi \,, \\ F^A &= \partial_\mu A^\mu \,, \\ F^a &= \partial_\mu G^{a\mu} \,, \end{aligned} \tag{2.74}$$

allowing two different bare gauge parameters for both $W^\pm$ and Z bosons, $\xi_{W,Z}$ and $\zeta_{W,Z}$, and also one independent gauge parameter for the photon and gluon field, ξ_A and ξ_s. Various choices of the gauge parameters have special names: The Landau gauge has $\xi_W = \xi_Z = \xi_A = \xi_s = 0$ and $\zeta_W = \zeta_Z = 0$, the 't Hooft gauges have $\xi_W = \zeta_W$ and $\xi_Z = \zeta_Z$, and the 't Hooft-Feynman gauge has in addition $\xi_W = \xi_Z = \xi_A = \xi_s = 1$. As we will see in a moment, the 't Hooft Feynman gauge is particularly simple, since at lowest order the poles of the unphysical scalar fields and the longitudinal gauge fields coincide with the poles of the corresponding transverse gauge fields. Furthermore, no tree level mixing between the gauge bosons and the corresponding unphysical scalars occurs. Notice that the latter property holds also in the 't Hooft gauges, as can easily be observed by inspection of Eqs. (2.32), (2.73) and (2.74).

All the propagators now behave such that naive power counting is possible. In the 't Hooft gauges one finds for example for the $W^\pm$ gauge boson propagator:

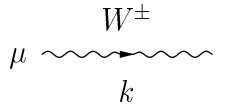

$$= \frac{-i}{k^2 - M_W^2} \left(g^{\mu\nu} - (1 - \xi_W) \frac{k^\mu k^\nu}{k^2 - \xi_W M_W^2} \right) . \tag{2.75}$$

Notice that the transverse parts, which describe the physical degrees of freedom, are independent of the gauge parameters, whereas the longitudinal parts are gauge-dependent. Similar expressions apply to the case of the Z boson, the photon and the gluon.

The terms quadratic in the would-be Goldstone fields introduced in Eq. (2.73) generate mass terms for those fields, so that the corresponding propagators in the 't Hooft gauges read:

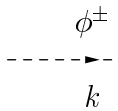

$$= \frac{i}{k^2 - \xi_W M_W^2} \,, \qquad \chi \quad = \frac{i}{k^2 - \xi_Z M_Z^2} \,. \tag{2.76}$$

k

The gauge-fixing (2.73) breaks gauge invariance and also its integrated version, the rigid $SU(2)_L \times U(1)_Y$ symmetry[10], which is obtained by taking the infinitesimal transformation parameters of the gauge transformations (2.50) as constants. Therefore the unphysical fields, the longitudinal parts of the vector and the would-be Goldstone boson fields, interact with the physical fields violating thereby the unitarity of the physical S-matrix in the tree approximation. In order to cancel these interactions in the physical S-matrix further fields, the so-called Faddeev-Popov ghosts [128] are needed. The conventional way for introducing Faddeev-Popov fields into gauge theories does not start

[10] In order not to spoil the group structure of global $SU(2)_L \times U(1)_Y$ symmetry, one has to make the following choices for the gauge-fixing parameters: $\xi_W = \xi_Z = \xi_A = \xi$ and $\zeta_W = \zeta_Z = \zeta$.

from unitarity arguments but from the path integral formulation of quantum field theory. To implement the gauge-fixing program in path integrals one needs a compensating determinant. This determinant can be rewritten in the form of a path integral over a set of anticommuting scalar fields with negative norm. These scalar fields violate the spin-statistic theorem. This is unproblematic, however, as they are unphysical degrees of freedom which occur in perturbative calculations only inside loops but never as external fields or particles.

To this end, we introduce the Faddeev-Popov fields u^α, $\alpha = \pm, Z, A, a$, with ghost charge $+1$ and the respective antighosts $\bar{u}^\alpha$, $\alpha = \pm, Z, A, a$, with ghost charge -1, and add the following ghost part to the classical Lagrangian:

$$\mathcal{L}_{\rm FP} = - \sum_{\alpha,\beta=\pm,Z,A,a} \bar{u}^\alpha \frac{\delta F^\alpha}{\delta\theta^\beta} u^\beta = - \int d^4y \sum_{\alpha,\beta=\pm,Z,A,a} \bar{u}^\alpha(x) \frac{\delta F^\alpha(x)}{\delta\theta^\beta(y)} u^\beta(y)\,, \tag{2.77}$$

where $\delta F^\alpha/\delta\theta^\beta$ is the variation of the gauge-fixing terms F^α under the infinitesimal gauge transformations of the quantum fields. Note that the fields u^α and $\bar{u}^\alpha$ are independent of each other and, in particular, not related by hermitian conjugation. Inserting the gauge-fixing terms (2.74) and using the gauge transformations (2.13) and (2.50) we find up total derivatives

$$\begin{aligned} \mathcal{L}_{\rm FP} = {} & \frac{1}{e}\bar{u}^+ \left(\partial^\mu\partial_\mu + \zeta_W M_W^2\right) u^+ + \frac{1}{e}\bar{u}^- \left(\partial^\mu\partial_\mu + \zeta_W M_W^2\right) u^- \\ & + \frac{1}{e}\bar{u}^Z \left(\partial^\mu\partial_\mu + \zeta_Z M_Z^2\right) u^Z + \frac{1}{e}\bar{u}^A \partial^\mu\partial_\mu u^A + \frac{1}{g_s}\bar{u}^a \partial^\mu\partial_\mu u^a + \dots\,, \end{aligned} \tag{2.78}$$

where the ellipsis denotes cubic terms which couple the ghost fields to the gauge boson fields and the would-be Goldstone fields. From the bilinear terms of Eq. (2.78) we obtain the Faddeev-Popov ghost propagators. In the 't Hooft gauges, one finds for example for the $u^\pm$ and u^Z propagators

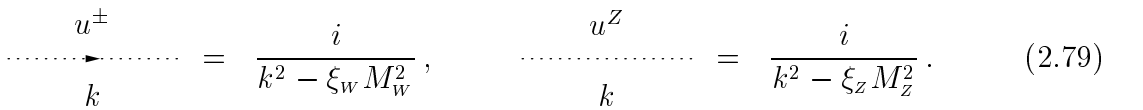

(2.79)

Notice that the Faddeev-Popov ghost fields u^A and u^a are massless. The masses of the other ghosts coincide with those of the scalar gauge bosons and the would-be Goldstone bosons. This is necessary to allow for the cancellation of the corresponding unphysical poles in the physical S-matrix elements. The gauge dependence of these masses reflects the unphysical nature of the associated fields.

For any finite value of the gauge parameters, the gauge boson, the would-be Goldstone boson and the Faddeev-Popov ghost propagators fall off as $1/k^2$ and thus obey the general power counting properties. It follows, that in any of these gauges, the perturbation theory will be renormalizable in the sense that the divergences are removed by a finite set of counterterms. Furthermore, the only counterterms required are those that are symmetric under the original global symmetry of the theory. However, we should require one further condition of our renormalization procedure. We should insist that the counterterms preserve local gauge invariance, and, in particular, preserve the property that S-matrix elements and the matrix elements of gauge-invariant operators are gauge-independent.

This result was proved to all orders in perturbation theory by 't Hooft and Veltman [129] and Lee and Zinn-Justin [130–133]. Thus in the gauge defined by any finite value of the gauge parameters, we can, in principle, straightforwardly compute a physical quantity to any order in perturbation theory.

By taking the limit $\zeta_W = \xi_W^2 \to \infty$ and $\zeta_Z = \xi_Z^2 \to \infty$ of the R_ξ gauges, we find a gauge with very different simplifying features. In this limit the unphysical degrees of freedom, which have masses proportional to $\sqrt{\xi_W}$ and $\sqrt{\xi_Z}$, tend to infinity. As a consequence, the unphysical degrees of freedom decouple and we are left with the theory in the quantum mechanical realization of the unitary gauge, introduced in Eqs. (2.37) and (2.38). It is not straightforward to prove renormalizability directly in the unitary gauge. In this gauge, the gauge boson propagators fall off more slowly than $1/k^2$ at large k. This signals trouble for the evaluation of loop diagrams. Typically, in fact, individual loop diagrams will diverge as $\ln \xi_W$ and $\ln \xi_Z$ or worse as $\zeta_W = \xi_W^2 \to \infty$ and $\zeta_Z = \xi_Z^2 \to \infty$. Still, the gauge invariance of the S-matrix implies that these divergences must cancel in the sum of all diagrams contributing to a given process, so that this sum has a smooth limit as the gauge parameters approach infinity. There is no difficulty in principle with the fact that we use one gauge to prove the renormalizability of spontaneously broken gauge theories and another to prove unitarity. In fact, this method of argumentation makes natural use of the underlying symmetries of the theory.

After gauge-fixing, the local gauge invariance of the classical Lagrangian is no longer manifest. However, a new global symmetry of the effective Lagrangian with all the consequences of gauge invariance for the physical observables can be defined by an extension of the gauge transformations to the Faddeev-Popov ghost fields. These non-linear symmetry transformations which were first found by Becchi, Rouet, Stora [134, 135] and independently by Tyutin [136] can be regarded as the quantum version of the classical local gauge transformations. The invariance of the full quantum Lagrangian under what is nowadays called BRST transformations is referred to as the BRST symmetry, which is the basic ingredient in the proof of the unitarity of the physical S-matrix and generally in the construction of gauge-invariant operators. BRST symmetry is in fact a supersymmetry, that is, its transformations involve parameters that take their values in a Grassmann algebra. Let λ be an infinitesimal constant that anticommutes with the Faddeev-Popov ghosts and all the fermionic matter fields. Then the transformations for the gauge boson, scalar and fermion fields are obtained from Eqs. (2.13) and (2.50) by the replacement $\theta^\alpha = \lambda u^\alpha$, $\alpha = \pm, Z, A, a$. Using the BRST operator s, defined as the left derivative with respect to λ of the BRST transformed fields, the BRST transformations of the quantum fields read

$$
\begin{aligned}
sW_\mu^\pm &= -\frac{1}{e}\partial_\mu u^\pm \pm \frac{i}{s_W}\left[W_\mu^\pm\left(c_W u^Z + s_W u^A\right) - \left(c_W Z_\mu + s_W A_\mu\right) u^\pm\right] , \\
sZ_\mu &= -\frac{1}{e}\partial_\mu u^Z - 2i\frac{c_W}{s_W}\left(W_\mu^+ u^- - W_\mu^- u^+\right) , \\
sA_\mu &= -\frac{1}{e}\partial_\mu u^A - 2i\left(W_\mu^+ u^- - W_\mu^- u^+\right) , \\
sG_\mu^a &= -\frac{1}{g_s}\partial_\mu u^a + f^{abc} G_\mu^b u^c , \\
s\nu_L^i &= \frac{i}{2 s_W c_W} u^Z \nu_L^i + \frac{i}{s_W} u^+ e_L^i ,
\end{aligned}
$$

$$
\begin{aligned}
se_L^i &= -i\left[\frac{s_W}{c_W}\left(Q_e+\frac{1}{2s_W^2}\right)u^Z - Q_e u^A\right]e_L^i + \frac{i}{s_W}u^-\nu_L^i\,,\\
su_L^i &= -i\left[\frac{s_W}{c_W}\left(Q_u-\frac{1}{2s_W^2}\right)u^Z - Q_u u^A - T^a u^a\right]u_L^i + \sum_{j=1}^{3}\frac{i}{s_W}V_{ij}u^+ d_L^j\,,\\
sd_L^i &= -i\left[\frac{s_W}{c_W}\left(Q_d+\frac{1}{2s_W^2}\right)u^Z - Q_d u^A - T^a u^a\right]d_L^i + \sum_{j=1}^{3}\frac{i}{s_W}V_{ij}^\dagger u^- u_L^j\,,\\
se_R^i &= -iQ_e\left(\frac{s_W}{c_W}u^Z - u^A\right)e_R^i\,,\\
su_R^i &= -i\left[Q_u\left(\frac{s_W}{c_W}u^Z - u^A\right) - T^a u^a\right]u_R^i\,,\\
sd_R^i &= -i\left[Q_d\left(\frac{s_W}{c_W}u^Z - u^A\right) - T^a u^a\right]d_R^i\,,\\
s\phi^\pm &= \pm\frac{i}{2s_W}\left(v+H\pm i\chi\right)u^\pm \mp i\phi^\pm\left(\frac{s_W^2-c_W^2}{s_W c_W}u^Z + u^A\right)\,,\\
sH &= \frac{1}{2s_W c_W}\chi u^Z + \frac{i}{2s_W}\left(\phi^+u^- - \phi^-u^+\right)\,,\\
s\chi &= -\frac{1}{2s_W c_W}\left(v+H\right)u^Z + \frac{1}{2s_W}\left(\phi^+u^- + \phi^-u^+\right)\,.
\end{aligned}
\tag{2.80}
$$

Since the classical Lagrangian is gauge-invariant, it is invariant under the BRST transformations by construction. The transformation behavior of the ghost fields in the basis of mass and charge eigenstates

$$
\begin{aligned}
su^\pm &= \mp i\frac{e}{s_W}u^\pm\left(c_W u^Z + s_W u^A\right)\,, & s\bar{u}^\pm &= -\frac{1}{\xi_W}F^\pm\,,\\
su^Z &= ie\frac{c_W}{s_W}u^+u^-\,, & s\bar{u}^Z &= -\frac{1}{\xi_Z}F^Z\,,\\
su^A &= ieu^+u^-\,, & s\bar{u}^A &= -\frac{1}{\xi_A}F^A\,,\\
su^a &= -\frac{1}{2}g_s f^{abc}u^b u^c\,, & s\bar{u}^a &= -\frac{1}{\xi_s}F^a\,,
\end{aligned}
\tag{2.81}
$$

is chosen so that the sum of the gauge-fixing and Faddeev-Popov Lagrangian is also BRST invariant, although both terms transform non-trivially under the global gauge symmetry. This once again shows the importance of the Faddeev-Popov ghost fields, which establish the BRST invariance of the full effective Lagrangian of the minimal SM destroyed by the inclusion of the gauge-fixing part.

The BRST transformation rules, as given in Eqs. (2.80) and (2.81), suffer two drawbacks. First, the rule for $s\bar{u}^\alpha$ depends on F^α, so that the algebra is not defined independently of the effective Lagrangian. Second, the algebra does not close unless the field equation for $\bar{u}^\alpha$ is imposed. To illustrate the second remark, one should verify that s^2 annihilates each of the quantum fields. This is straightforward. The algebra closes if s^2 annihilates $\bar{u}^\alpha$ as well. But, clearly

$$
s^2\bar{u}^\pm = -\frac{1}{\xi_W}sF^\mp\,,\quad s^2\bar{u}^Z = -\frac{1}{\xi_Z}sF^Z\,,\quad s^2\bar{u}^A = -\frac{1}{\xi_A}sF^A\,,\quad s^2\bar{u}^a = -\frac{1}{\xi_s}sF^a\,,
\tag{2.82}
$$

are in general all different from zero. The Euler-Lagrange equation corresponding to $\bar{u}^\alpha$ is $sF^\alpha = 0$. Thus Eqs. (2.82) vanish only when the Euler-Lagrange equation for the antighost fields $\bar{u}^\alpha$ are imposed. Under this conditions, we say that the BRST transformations are realized on-shell.

We wish to modify our effective theory so that the BRST transformations are realized off-shell. This can be accomplished by adding new non-dynamical degrees of freedom, in form of auxiliary fields, the so-called Nakanishi-Lautrup fields [137, 138], which play the role of Lagrange multipliers for the gauge conditions. Specifically, in the minimal SM we reformulate the gauge-fixing part of the effective Lagrangian (2.73) by introducing the commuting scalar fields B^α, $\alpha = \pm, Z, A, a$. Coupling the gauge-fixing operators (2.74) to these Lagrange multipliers we obtain

$$\begin{aligned}\mathcal{L}_{\rm GF} &= B^+F^- + B^-F^+ + B^ZF^Z + B^AF^A + B^aF^a \\ &\quad + \xi_W B^+B^- + \frac{\xi_Z}{2}B^ZB^Z + \frac{\xi_A}{2}B^AB^A + \frac{\xi_s}{2}B^aB^a\,.\end{aligned} \tag{2.83}$$

Because the B^α fields appear only in quadratic terms without derivatives, they are auxiliary fields without an own dynamic. Upon performing the functional integral over B^α by completing the square one recovers the original Lagrangian (2.73) and the generating functional. In other words, Eq. (2.83) can be transformed into the usual form of the R_ξ gauges (2.73) by eliminating the B^α fields via their equations of motions:

$$B^\pm = -\frac{1}{\xi_W}F^\pm\,, \qquad B^Z = -\frac{1}{\xi_Z}F^Z\,, \qquad B^A = -\frac{1}{\xi_A}F^A\,, \qquad B^a = -\frac{1}{\xi_s}F^a\,. \tag{2.84}$$

On first sight the gauge-fixing with the B^α fields seems to be less practical than the R_ξ gauges (2.73), since one introduces extra non-diagonal propagators between B^α fields and vector fields, and B^α fields and scalar fields into the theory. But, as we will discuss in a moment, in this formulation the BRST transformations are independent of the gauge-fixing terms (2.74) and strictly nilpotent on all fields. Thus both drawbacks described above are cured by retaining the auxiliary fields B^α in Eq. (2.83). Let us already note at this stage, that in the linear B^α gauges (2.83) the gauge-fixing part of the Lagrangian does not get loop corrections and remains a local field polynomial as in the classical approximation. This observation is simply deduced from the observation that there are no interaction vertices of the B^α fields with other propagating fields.

Clearly, in order to guarantee the BRST invariance of the full effective Lagrangian it is necessary to extend the BRST transformations to the auxiliary fields B^α. The modified BRST transformations are given by Eqs. (2.80) and (2.81) with the antighost transformations replaced by

$$\begin{aligned} s\bar{u}^\pm &= B^\pm\,, & s\bar{u}^Z &= B^Z\,, & s\bar{u}^A &= B^A\,, & s\bar{u}^a &= B^a\,, \\ sB^\pm &= 0\,, & sB^Z &= 0\,, & sB^A &= 0\,, & sB^a &= 0\,. \end{aligned} \tag{2.85}$$

These rules represent an improvement over the original formulation of the R_ξ gauges, since they are defined independently of the gauge-fixing operators (2.74). Furthermore, having written the gauge-fixing with the help of the auxiliary fields B^α, the modified BRST transformations (2.80) and (2.81) close, since

$$s^2 = 0\,, \tag{2.86}$$

on each of the quantum fields. This is easily verified. The condition (2.86) tells us that the BRST operator s is nilpotent. In this case the BRST transformations are said to be realized off-shell.

The ghost part of the full effective theory is likewise determined from the requirement that the sum of the gauge-fixing and the Faddeev-Popov Lagrangian has to be invariant under the modified BRST transformations (2.80) and (2.85). One easily obtains

$$\mathcal{L}_{\mathrm{FP}} = -\sum_{\alpha=\pm,Z,A,a} \bar{u}^{\alpha} s F^{\alpha} \,, \tag{2.87}$$

valid for arbitrary choices of F^{α}. In this connection, it is also very important to note that the gauge-fixing and the Faddeev-Popov Lagrangian in the B^{α} gauges (2.83) can be added up into such a remarkable form as

$$\begin{aligned} \mathcal{L}_{\mathrm{GF}} + \mathcal{L}_{\mathrm{FP}} = s\Big(& \bar{u}^{+}F^{+} + \bar{u}^{-}F^{-} + \bar{u}^{Z}F^{Z} + \bar{u}^{A}F^{A} + \bar{u}^{a}F^{a} \\ & + \frac{\xi_W}{2}\bar{u}^{+}B^{+} + \frac{\xi_W}{2}\bar{u}^{-}B^{-} + \frac{\xi_Z}{2}\bar{u}^{Z}B^{Z} + \frac{\xi_A}{2}\bar{u}^{A}B^{A} + \frac{\xi_s}{2}\bar{u}^{a}B^{a}\Big) \,. \end{aligned} \tag{2.88}$$

This shows that, in spite of the drastic changes of the theory due to the introduction of Faddeev-Popov ghosts, the difference between the original Lagrangian and the total quantum one, is just a BRST variation. Thus the BRST invariance of the full effective Lagrangian is a natural consequence of the local gauge invariance of the original Lagrangian as well as of the nilpotency of the BRST transformations (2.86).

According to the Noether theorem, the invariance of the effective Lagrangian under the global BRST transformations (2.80) and (2.85) implies the existence of a conserved current. The integral of the time component of this current will be a conserved charge Q_B which acts on a generic field ψ by the ghost number graded commutator,

$$[iQ_B, \psi\} = s\psi \,, \tag{2.89}$$

that is, by a commutator or anticommutator for fields ψ with even or odd ghost number, respectively. Thus, the transformations generated by Q_B are indeed the BRST transformations (2.80) and (2.85). Owing to the nilpotency of the BRST transformations (2.86), the BRST charge is nilpotent and, as a conserved charge, commutes with the effective Hamiltonian H and thus with the total S-matrix:

$$Q_B^2 = 0 \,, \qquad [Q_B, H] = 0 \,, \qquad [Q_B, S] = 0 \,. \tag{2.90}$$

Moreover, it is hermitian provided we assign the hermitian conjugation properties of the Faddeev-Popov ghost fields in the following way

$$\begin{aligned} u^{\pm\dagger} &= u^{\mp} \,, & u^{Z\dagger} &= u^{Z} \,, & u^{A\dagger} &= u^{A} \,, & u^{a\dagger} &= u^{a} \,, \\ \bar{u}^{\pm\dagger} &= -\bar{u}^{\mp} \,, & \bar{u}^{Z\dagger} &= -\bar{u}^{Z} \,, & \bar{u}^{A\dagger} &= -\bar{u}^{A} \,, & \bar{u}^{a\dagger} &= -\bar{u}^{a} \,, \end{aligned} \tag{2.91}$$

where the minus sign appearing in the hermitian conjugation of the antighost fields is required because of the anticommuting nature of the ghost fields. These hermiticity assignments, which were originally proposed by Kugo and Ojima [139–143], turn out to play an essential role in the construction of a manifestly covariant and local canonical operator

formalism of non-abelian gauge theories for mainly two reasons. First, they assure the consistency of the formulation: The charge Q_B is hermitian only when these assignments are adopted. This hermiticity, however, is necessary to guarantee the conservation of Q_B following from $d/dt\,\langle\psi|Q_B^\dagger|\varphi\rangle = \langle\varphi|d/dt\,Q_B|\psi\rangle^* = 0$, which should hold as far as Q_B is well-defined. Moreover, hermiticity assignments different from the above ones would also be incompatible with the BRST transformations (2.80) and (2.85) itself. Second, only when the hermitian conjugation properties of the Faddeev-Popov ghost fields (2.91) are chosen, the full Lagrangian including the gauge-fixing term (2.83) and the Faddeev-Popov ghost part (2.87) becomes hermitian and, therefore, the unitarity of the total S-matrix can reasonable hold.

As is generally known, local and covariant field operators can be introduced only in an extended Hilbert space in which the vectors corresponding to the physical states do not form a dense set. In particular, the manifestly covariant theory of massless vector fields is necessarily quantized with an indefinite metric and the appearance of unphysical states with negative norm is inevitable. On the other hand, the positivity of the metric is vital to the probabilistic interpretability of quantum mechanics. In order to formulate a physically meaningful theory of scattering processes in gauge theory, we thus first of all have to define a physical S-matrix between physical states with positive norm and secondly should verify that it satisfies the genuine unitarity without spoiling the standard probabilistic interpretation of quantum theory. Assuming the hermiticity of the Hamiltonian, these requirements can be summarized into the following two conditions, called physical state conditions:

(i) The physical subspace $\mathcal{V}_{\rm phys}$ should be invariant under the time evolution, namely, $H\mathcal{V}_{\rm phys} \subseteq \mathcal{V}_{\rm phys}$ should hold for the Hamiltonian H.

(ii) The indefinite inner product $\langle|\rangle$ in the total state vector space $\mathcal{V}$ should be positive semi-definite when restricted to the physical subspace $\mathcal{V}_{\rm phys}$, $\langle\psi|\psi\rangle \geq 0\ \forall\,|\psi\rangle \in \mathcal{V}_{\rm phys}$.

Then, according to a general theorem, the physical S-matrix can be defined consistently in the quotient space of $\mathcal{V}_{\rm phys}$ with respect to its zero-norm subspace $\mathcal{V}_0$ given by $\mathcal{H}_{\rm phys} = \mathcal{V}_{\rm phys}/\mathcal{V}_0$, which is a Hilbert space equipped with positive definite metric, and the physical S-matrix is unitary with respect to this Hilbert space structure.

Now, having argued that the physical state conditions are necessary and sufficient for the physical S-matrix to be unitary, we must look for a concise subsidiary condition specifying the physical subspace $\mathcal{V}_{\rm phys}$ in such a way that the above physicality criteria are satisfied. The key for the solution of this problem is given by the BRST charge Q_B providing, essentially, a global version of the local gauge invariance. Indeed, in general renormalizable gauges one can select the physical states $|\psi\rangle_{\rm phys}$ from the total state vector space $\mathcal{V}$ by requiring $|\psi\rangle_{\rm phys}$ to be BRST invariant [139–143]. Accordingly, despite of all the complications in non-abelian gauge theories due to the introduction of the Faddeev-Popov ghost fields, the physical subspace $\mathcal{V}_{\rm phys}$ can be specified by the elegant subsidiary condition[11]

$$Q_B\,|\psi\rangle_{\rm phys} = 0\,. \tag{2.92}$$

[11] If one prefers to specify the physical subspace as small as possible, then one can add one more subsidiary condition: $Q_u|\psi\rangle_{\rm phys} = 0$, where Q_u is the conserved Faddeev-Popov ghost charge, which generates the scale transformations $u^\alpha \to e^\theta u^\alpha$ and $\bar{u}^\alpha \to e^{-\theta}\bar{u}^\alpha$.

Now, since the charge Q_B is conserved, this, however, tells us immediately that $\mathcal{V}_{\text{phys}}$ is manifestly invariant under the time evolution as well as under Lorentz transformations, and thus the first criterion of the physical state conditions is automatically satisfied. So one only has to prove the second criterion, that is, the semi-definiteness of the inner product in $\mathcal{V}_{\text{phys}}$ which is quite a non-trivial problem. For its complete solution, detailed analysis is necessary of the metric structure of the total state vector space $\mathcal{V}$ and of the physical subspace $\mathcal{V}_{\text{phys}}$ in each concrete model. However, it is also possible to extract the essential features of the inner product structures to a considerable extent solely by inspecting the irreducible representations of the BRST algebra given by:

$$\{Q_B, Q_B\} = 2Q_B^2 = 0\,, \qquad [iQ_u, Q_B] = Q_B\,, \qquad [Q_u, Q_u] = 0\,, \tag{2.93}$$

where Q_u denotes the Faddeev-Popov ghost charge associated with ghost number conservation. Identifying the Faddeev-Popov ghost number with the eigenvalues of the operator Q_u multiplied by i, the second and third relation of Eq. (2.93) tell us that the charges Q_B and Q_u carry ghost number one and zero, respectively. On the basis of such an analysis, one will find a very general norm-cancellation mechanism, called quartet mechanism [139–143]. By this mechanism, the unphysical particles having non-positive norm are made undetectable in the physical world described by the physical Hilbert space. In the following we will present this argument at an intuitive level.[12]

Because of the fact that the non-vanishing Faddeev-Popov ghost charge is carried only by the fields u^α and $\bar{u}^\alpha$, it can be assumed that the total state vector space $\mathcal{V}$ can be decomposed into a direct sum of sectors $\mathcal{V}_N$ with definite ghost number N. This assumption together with the non-degeneracy property of the inner product in $\mathcal{V}$, that is, $\langle\psi|\varphi\rangle = 0 \;\forall\, |\psi\rangle \in \mathcal{V} \Leftrightarrow |\varphi\rangle = 0$, which can be postulated without lose of generality, necessarily implies that for any eigenstate $|\psi_N\rangle \in \mathcal{V}_N$ with non-vanishing eigenvalue N, there exists a Faddeev-Popov conjugated state $|\psi_{-N}\rangle \in \mathcal{V}_{-N}$ with the opposite Faddeev-Popov ghost number $-N$. Moreover, the hermiticity of Q_u, which is assured by the hermitian conjugate properties of the ghost fields (2.91), implies that the eigenstates $|\psi_N\rangle$ satisfy the following orthogonality relations

$$\langle\psi_N|\psi_M\rangle = \delta_{N,-M}\,, \tag{2.94}$$

where the inner product $\langle|\rangle$ has been normalized to unity by convention. Under this normalization the Faddeev-Popov conjugate states are unique and an orthogonal decomposition of $\mathcal{V}$ into the direct sum of sectors $\mathcal{V}_N$ and $\mathcal{V}_{-N}$ is realized.

Owing to the nilpotency of the BRST charge Q_B (2.90), any state can be classified into its irreducible representations with dimensions up to two, namely, singlet or doublet representation. We call a singlet representation of Q_B a BRST-singlet and a doublet one a BRST-doublet. If a state $|\psi_N\rangle$ satisfies

$$Q_B\,|\psi_N\rangle = 0\,, \tag{2.95}$$

and there exists no state $|\varphi_{N-1}\rangle$ such that $Q_B|\varphi_{N-1}\rangle = |\psi_N\rangle$, then $|\psi_N\rangle$ constitutes a BRST-singlet. Otherwise, if a state $|\psi_N\rangle$ is not annihilated by the BRST charge Q_B,

$$Q_B\,|\psi_N\rangle = |\varphi_{N+1}\rangle \neq 0\,, \tag{2.96}$$

[12] A rigorous discussion has first be given by Kugo and Ojima [139–143] to which we would like to relegate the interested reader for further reading.

then the two vectors $|\psi_N\rangle$ and $|\varphi_{N+1}\rangle$ form a BRST-doublet. For convenience, we call such a $|\psi_N\rangle$ with non-vanishing image of Q_B a parent state, and its image $|\varphi_{N+1}\rangle = Q_B|\psi_N\rangle \neq 0$ a daughter state. In the case of a BRST-doublet, the non-degeneracy of the inner product requires, however, the existence of another BRST-doublet Faddeev-Popov conjugate to the original one. Thus, the BRST-doublet representations are always realized in pairs: $|\psi_N\rangle$, $|\varphi_{N+1}\rangle = Q_B|\psi_N\rangle$ and $|\psi_{-N-1}\rangle$, $|\varphi_{-N}\rangle = Q_B|\psi_{-N-1}\rangle$. These Faddeev-Popov conjugate pairs of two BRST-doublets, which go by the name of BRST-quartets, provide the third and final type of possibility for the representations of the BRST algebra (2.93) in indefinite inner product spaces.

Due to the nilpotency itself, the definitions of a BRST-singlet and a parent state in a BRST-doublet necessarily involve the ambiguity of adding arbitrary daughter states to them. However, unambiguous description of the behavior of the BRST-singlets can be attained by switching over to the space of equivalence classes where two BRST-singlets are identified if their difference is given by a daughter state. The physical Hilbert space is then obtained as the covariant space of equivalence classes, the BRST-cohomology of states in the kernel modulo those in the image of Q_B, that is, $\mathcal{H}_{\text{phys}} = \text{Ker}\, Q_B/\text{Im}\, Q_B$ which is isomorphic to the space of BRST-singlets. It is easy to see that the image is furthermore contained in the orthogonal complement of the kernel, $\text{Ker}\, Q_B \cap (\text{Ker}\, Q_B)^{\perp}$, which is the isotropic subspace of $\text{Ker}\, Q_B$. It follows that states in $\text{Im}\, Q_B$ do not contribute to the inner product in $\text{Ker}\, Q_B$, and hence, the inner product structure of $\text{Ker}\, Q_B$ can be transferred consistently to the quotient space $\mathcal{H}_{\text{phys}} = \text{Ker}\, Q_B/\text{Im}\, Q_B$.

These considerations seem extremely abstract, but they have a direct physical correspondence. To see this, consider the single-particle states of the non-abelian gauge theory in the asymptotic regions $t \to \pm\infty$. According to our definition of physical states (2.92), the physical components of the asymptotic fields must have vanishing BRST variation

$$s\psi^{\text{as}}_{\text{phys}} = 0\,. \tag{2.97}$$

In order to determine the physical degrees of freedom of the fields we thus have to find the BRST transformations of the asymptotic fields. A careful analysis of the Fock space of asymptotic fields shows, that the BRST variations of the asymptotic fields are essentially obtained from the BRST variations of the Heisenberg fields (2.80) and (2.85) by disregarding all terms that involve composite operators [139–143]. Hence, in the present case only the following asymptotic fields transform non-trivial under the BRST symmetry:

$$\begin{aligned}
&sW^{\text{as},\pm}_\mu = -\frac{1}{e}\partial_\mu u^{\text{as},\pm}\,, \qquad sZ^{\text{as}}_\mu = -\frac{1}{e}\partial_\mu u^{\text{as},Z}\,, \qquad sA^{\text{as}}_\mu = -\frac{1}{e}\partial_\mu u^{\text{as},A}\,,\\
&sG^{\text{as},a}_\mu = -\frac{1}{g_s}\partial_\mu u^{\text{as},a}\,, \qquad s\phi^{\text{as},\pm} = \pm iM_W\, u^{\text{as},\pm}\,, \qquad s\chi^{\text{as}} = -M_Z u^{\text{as},Z}\,,\\
&s\bar{u}^{\text{as},\pm} = B^{\text{as},\pm}\,, \qquad s\bar{u}^{\text{as},Z} = B^{\text{as},Z}\,, \qquad s\bar{u}^{\text{as},A} = B^{\text{as},A}\,, \qquad s\bar{u}^{\text{as},a} = B^{\text{as},a}\,.
\end{aligned} \tag{2.98}$$

These relations allow to read off the unphysical fields of the SM. The scalar component of the massive gauge fields $W^{\text{as},\pm}$ and Z^{as}, the would-be Goldstone fields $\phi^{\text{as},\pm}$ and χ^{as}, and the antighost fields $\bar{u}^{\text{as},\pm}$ and $\bar{u}^{\text{as},Z}$ are not annihilated by s and therefore correspond to unphysical degrees of freedom. The ghost fields $u^{\text{as},\pm}$ and $u^{\text{as},Z}$ and the auxiliary fields $B^{\text{as},\pm}$ and $B^{\text{as},Z}$ are BRST transformations and consequently involve only zero-norm states, that decouple from the physical S-matrix. The unphysical degrees of freedom in the case of the massless gauge fields are the longitudinal components A^{as}_L and $G^{\text{as},a}_L$ of the

photon and gluon field, and the antighost fields $\bar{u}^{\mathrm{as},A}$ and $\bar{u}^{\mathrm{as},a}$. The ghost fields $u^{\mathrm{as},A}$ and $u^{\mathrm{as},a}$, and the Nakanishi-Lautrup fields $B^{\mathrm{as},A}$ and $B^{\mathrm{as},a}$ belong to the image of s having zero norm. From this we see that for each gauge field there are exactly four unphysical modes, the scalar or longitudinal gauge-boson mode, the antighost, the ghost and the Nakanishi-Lautrup mode. These modes constitute the elementary quartets which appear in the SM: $(\bar{u}^{\mathrm{as},\pm}, \phi^{\mathrm{as},\pm}, u^{\mathrm{as},\pm}, B^{\mathrm{as},\pm})$, $(\bar{u}^{\mathrm{as},Z}, \chi^{\mathrm{as}}, u^{\mathrm{as},Z}, B^{\mathrm{as},Z})$, $(\bar{u}^{\mathrm{as},A}, A_L^{\mathrm{as}}, u^{\mathrm{as},A}, B^{\mathrm{as},A})$ and $(\bar{u}^{\mathrm{as},a}, G_L^{\mathrm{as},a}, u^{\mathrm{as},a}, B^{\mathrm{as},a})$. These quartets can appear in the physical subspace of the total Hilbert space only in a zero-norm combination and hence cannot be observed. This is guaranteed by the physical state condition (2.92). The BRST charge Q_B thus ensures the decoupling of unphysical states from the physical Fock space, guaranteeing the unitarity of the S-matrix and the gauge independence of the physical observables.

2.4 Renormalization of the Standard Model

Once the problem of quantization is settled, perturbative calculations can be systematically performed in principle. The higher order corrections to the S-matrix elements and the Green's functions are quantum effects resulting from Feynman graphs containing loops. Since these corrections change the relation between the parameters in the Lagrangian and the observables, the original parameters of the theory, the so-called bare parameters, are no longer directly related to the physical quantities. Moreover, the bare parameters differ from the corresponding physical quantities by UV divergent contributions associated with the behavior of the loop integrals at high virtual momenta. Thus to allow for a proper treatment of UV divergent quantities, a so-called regularization procedure is needed. This amounts to a modification of the theory in such a way that the possibly UV divergent quantities become well-defined, and that in a suitable limit the original theory is recovered. Consequently, a redefinition of the basic parameters, a renormalization of the theory, is needed as well.

The requirement that the UV divergences are compensated, however, does not fix the finite parts of the renormalization constants. Indeed, these can be defined in many different ways leading to different parameterizations of the theory. If we know an exact solution of the theory, different choices of the renormalization scheme do not cause any difference in the resulting S-matrix element although its expression as a function of the renormalized parameters may differ. However, in finite order of perturbation theory different choices of the renormalization scheme differ by higher order contributions and therefore lead to different physical predictions in general. In order to define a renormalization scheme one first has to choose a set of independent parameters. One possibility is to start from the Lagrangian in its symmetric form. For practical calculations it is, however, more convenient to fix the renormalization constants by renormalization conditions on the physical parameters. Clearly, since there is an one-to-one correspondence between the parameters of the symmetric Lagrangian and the physical parameters, this approach also yields finite quantities. In this way one arrives at theoretical predictions for physical observables in terms of other physical quantities, which have to be determined from experiment.

In the electroweak sector of the SM[13] it has become customary to use the electric charge

[13]Since the gauge group $SU(3)_C$ is unbroken in the SM, the renormalization of the strong and electroweak sector of the SM can be performed independently. In this section we only consider the renormalization of the GWS theory.

e, the masses M_W and M_Z of the electroweak gauge bosons, the fermion masses m_f^i, the Higgs mass M_H and the quark mixing matrix V as renormalized parameters. In this so-called on-shell renormalization scheme, which was proposed by Ross and Taylor [144], the renormalized electric charge is defined as the strength of the electromagnetic coupling in the Thomson limit, and the masses as the position of the poles of the renormalized propagators. The advantage of the on-shell scheme is that all parameters have a clear physical meaning and can be measured directly in suitable experiments.[14] Furthermore, the Thomson cross section from which the electrical charge e is obtained is exact to all orders of perturbation theory according to Thirring's theorem [145, 146].

The renormalization of the parameters is sufficient to obtain UV finite S-matrix elements, but it leaves Green's functions divergent. This is due to the fact that radiative corrections change the normalization of the fields by an infinite amount. Consequently, in order to get UV finite two- and three-point functions the fields have to be renormalized, too. Moreover, radiative corrections provide non-diagonal corrections to the mass matrices so that the bare fields are no longer mass eigenstates. In order to rediagonalize the mass matrices one has to introduce matrix valued field renormalization constants. These allow to define the renormalized fields in such a way that they are the correct physical mass eigenstates in all orders of perturbation theory. If one does not renormalize the fields in this way, one needs a non-trivial wave function renormalization for the external particles. This is required in going from Green's functions to S-matrix elements in order to obtain a properly normalized S-matrix.

Renormalization Constants and Counterterms

In this subsection we specify the on-shell renormalization scheme for the electroweak sector of the SM quantitatively following the standard treatment in the literature [147–149]. The starting point for the calculation of S-matrix elements and Green's functions including radiative corrections is the Lagrangian written in terms of physical fields and parameters. Since symmetry arguments were important in the construction of the classical Lagrangian we perform the multiplicative renormalization of the electroweak part of the full SM Lagrangian in such a way that the gauge symmetry is respected. Therefore also the counterterm Lagrangian and the renormalized Green's functions reflect the gauge symmetry. The price for this, however, is that not all residues of the the propagators can be normalized to unity. As a consequence, any calculation with the renormalized Lagrangian will have to include finite multiplicative wave function renormalization factors for some of the external lines in the S-matrix elements.

As we have already explained radiative corrections affect the Higgs potential in such a way that its minimum is shifted. In order to correct for this shift, one has to perform a renormalization of the tadpole

$$t_0 = t + \delta t\,, \tag{2.99}$$

which, according to the definition (2.33), corresponds to a renormalization of the VEV of the complex scalar field. In addition we introduce the following renormalization constants

[14] Due to the presence of the strong interaction this is not the case for the light quark masses. Fortunately, their contributions can often be expressed through universal quantities, which can be directly determined from experiment.

for the parameters:

$$\begin{aligned} e_0 &= Z_e e = (1+\delta Z_e)\, e\,, \\ M^2_{W,0} &= M^2_W + \delta M^2_W\,, \\ M^2_{Z,0} &= M^2_Z + \delta M^2_Z\,, \\ m^i_{f,0} &= m^i_f + \delta m^i_f\,, \\ M^2_{H,0} &= M^2_H + \delta M^2_H\,, \\ V_{ij,0} &= V_{ij} + \delta V_{ij}\,, \end{aligned} \tag{2.100}$$

where quantities with subscript 0 denote bare parameters. The renormalization constants for the charge, δZ_e, the masses, δM_W, δM_Z, δm^i_f, δM_H, and the quark mixing matrix, δV_{ij}, are fixed by on-shell renormalization conditions, as will be explained below.

In order to be able to define renormalized fields which are mass eigenstates in the presence of higher order corrections we introduce field renormalization of a general form using matrix valued renormalization constants for fields with equal quantum numbers. In the on-shell renormalization scheme the bare physical fields are split as

$$\begin{aligned} W^\pm_{\mu,0} &= Z^{1/2}_W W^\pm_\mu = \left(1+\frac{1}{2}\delta Z_W\right) W^\pm_\mu\,, \\ Z_{\mu,0} &= Z^{1/2}_{ZZ} Z_\mu + Z^{1/2}_{ZA} A_\mu = \left(1+\frac{1}{2}\delta Z_{ZZ}\right) Z_\mu + \frac{1}{2}\delta Z_{ZA} A_\mu\,, \\ A_{\mu,0} &= Z^{1/2}_{AZ} Z_\mu + Z^{1/2}_{AA} A_\mu = \frac{1}{2}\delta Z_{AZ} Z_\mu + \left(1+\frac{1}{2}\delta Z_{AA}\right) A_\mu\,, \\ f^i_{L,0} &= \sum_{j=1}^{3} Z^{1/2,f,L}_{ij} f^j_L = \sum_{j=1}^{3} \left(\delta_{ij} + \frac{1}{2}\delta Z^{f,L}_{ij}\right) f^i_L\,, \\ f^i_{R,0} &= \sum_{j=1}^{3} Z^{1/2,f,R}_{ij} f^j_R = \sum_{j=1}^{3} \left(\delta_{ij} + \frac{1}{2}\delta Z^{f,R}_{ij}\right) f^i_R\,, \\ H_0 &= Z^{1/2}_H H = \left(1+\frac{1}{2}\delta Z_H\right) H\,, \end{aligned} \tag{2.101}$$

where the last expression in each line is valid in first order approximation. Notice that we have explicitly assumed that the Higgs field does neither mix with the longitudinal components of the Z boson and of the photon nor with the neutral would-be Goldstone boson. Since at least four CKM matrix elements are required to construct a CP-odd rephrasing invariant function of the quark mixing matrix, two- and three-point functions are unaffected by CP violation at the one-loop level in the minimal SM. Consequently, our discussion is general as long as one works at first-order in perturbation theory. However, even if the CP violation mixes up physical and unphysical scalar fields at high perturbative order, it is not difficult to disentangle them taking advantage of the Slavnov-Taylor identities (STIs) [77, 150], which implement the BRST symmetry at the quantum level. Considering the system formed by the longitudinal components of the Z boson and the photon, and by the Higgs and the neutral would-be Goldstone boson one can show [151] in particular, that there is no propagator for the longitudinal components of the Z boson and the photon, and that the Higgs and the neutral would-be Goldstone bosons are decoupled on the mass-shell of the unphysical states. As a consequence the complex pole of

the only physical field, the Higgs boson, is gauge-invariant to all orders in perturbation theory.

The counterterms defined above are sufficient to render physical S-matrix elements and Green's functions of physical particles UV finite. For a complete renormalization of the electroweak SM we need the renormalization of the unphysical sector as well. This consists of the field renormalization of the would-be Goldstone fields,

$$\begin{aligned} \phi_0^\pm &= Z_\phi^{1/2}\phi^\pm = \left(1+\frac{1}{2}\delta Z_\phi\right)\phi^\pm\,, \\ \chi_0 &= Z_\chi^{1/2}\chi = \left(1+\frac{1}{2}\delta Z_\chi\right)\chi\,, \end{aligned} \tag{2.102}$$

of the Faddeev-Popov ghost fields

$$\begin{aligned} u_0^\pm &= \tilde{Z}_\pm u^\pm = \left(1+\delta\tilde{Z}_\pm\right)u^\pm\,, \\ u_0^Z &= \tilde{Z}_{ZZ}u^Z + \tilde{Z}_{ZA}u^A = \left(1+\delta\tilde{Z}_{ZZ}\right)u^Z + \delta\tilde{Z}_{ZA}u^A\,, \\ u_0^A &= \tilde{Z}_{AZ}u^Z + \tilde{Z}_{AA}u^A = \delta\tilde{Z}_{AZ}u^Z + \left(1+\delta\tilde{Z}_{AA}\right)u^A\,, \end{aligned} \tag{2.103}$$

and of the renormalization of the gauge parameters

$$\xi_{W,0} = Z_{\xi_W}\xi_W\,,\quad \xi_{Z,0} = Z_{\xi_Z}\xi_Z\,,\quad \xi_{A,0} = Z_{\xi_A}\xi_A\,,\quad \zeta_{W,0} = Z_{\zeta_W}\zeta_W\,,\quad \zeta_{Z,0} = Z_{\zeta_Z}\zeta_Z\,. \tag{2.104}$$

The Faddeev-Popov antighost fields are kept unrenormalized. This is legitimate because ghost number conservation allows one to renormalize the fields with non-vanishing ghost number in any desired way. Thus the choice made above is a pure matter of convenience.

Beyond one-loop order, counterterm contributions from the Faddeev-Popov ghost sector, which are associated with the gauge-fixing part, have to be taken into account in the calculation of physical amplitudes. As is well-known, the renormalization of the unphysical sector is not independent from the way the physical sector is treated. Indeed, it is governed by the STIs. This restricts the possible counterterms and relates the renormalization constants introduced above. These relations can be derived from the requirement that the renormalized Green's functions fulfill STIs of the same form as the unrenormalized ones. According to the organization of the calculation, it is possible to use different procedures that respect the STIs and are particularly convenient in order, for example, to minimize the number of counterterms to be considered. Of course, physical amplitudes are independent of the chosen procedure, and this can be used as an additional check of the calculation.

Renormalization Conditions in the On-Shell Scheme

The renormalization constants introduced in the previous subsection are fixed by imposing renormalization conditions. Usually one distinguishes three different categories. The conditions that define the renormalized physical parameters, those that define the renormalized fields and those that fix the renormalization in the unphysical sector. While the choice of the first affects the physical predictions to finite order of perturbation theory, the second are only relevant for Green's functions and drop out when calculating S-matrix elements. Nevertheless, their use is very convenient in the on-shell renormalization scheme,

since they not only allow to eliminate the explicit wave function renormalization of the external particles, but also simplify the explicit form of the renormalization conditions for the physical parameters considerably. The choice of the third set determines the form of the renormalized STIs. This renormalization is therefore purely conventional, but it turns out that not all choices are equally convenient when one considers higher order corrections.

Renormalization of the Tadpole

At first, in order to implement the Higgs mechanism at higher orders one has to renormalize the tadpole. Since the tadpole is not a physical quantity, its definition beyond tree level is arbitrary and a matter of convenience. The standard renormalization of the tadpole consists in defining the counterterm δt such that the Higgs field one-point amputated renormalized Green's function is canceled in each order of perturbation theory

$$\hat{\Gamma}_H(0) = \Gamma_H(0) + \delta t = 0\,, \tag{2.105}$$

which corresponds to minimizing the effective potential [152]. Here and henceforth, we will use a caret to distinguish renormalized from bare quantities. In practice, we will satisfy the above condition by simply ignoring any one-particle-irreducible (1PI) one-point diagram, since any such diagram will be canceled by adjustment of δt. The removal of the tadpole diagrams is then built in here as a natural part of the formalism. Clearly, this is not the only possible choice, but its physical meaning is transparent and it is generally adopted, because it simplifies practical calculations since no Feynman graphs involving tadpoles as subdiagrams need to be considered. However, according to Eq. (2.32), a renormalization of the tadpole amplitude induces a shift proportional to δt in the mass parameters of all SM fields. In practice, this means, that the mass counterterms become gauge-independent only after the corresponding gauge-dependent parts of the tadpole graphs are included.

Notice that in the presence of CP violation, another tadpole amplitude emerges in the minimal SM, connected to the VEV of the CP-odd neutral would-be Goldstone boson. As the CP violation in the minimal SM is confined to the fermionic sector, this will happen only at higher orders. In extended models, any neutral scalar field with zero ghost number could develop a VEV trough radiative corrections. In all cases the linear terms in the fields should be removed in order to define the 1PI Green's functions as the Legendre transform of the connected generating functional [153]. For the SM, however, using the STI for the corresponding one-point Green's functions one can prove [151, 154], that the vanishing of the tadpole of the Higgs field implies the vanishing of the tadpole of the unphysical would-be Goldstone boson even in the presence of CP violation.

Renormalization of the Physical Sector

In the on-shell scheme the renormalized mass parameters of the physical particles are fixed by the requirement that they are equal to the physical masses, that is, to the real parts of the poles of the corresponding propagators.[15] These poles are equivalent to the zeros of the 1PI two-point functions. In the case of mass matrices these conditions have to

[15] It turns out that the conventional approach to the one-loop mass renormalization [147–149] adopted here leads to renormalized mass parameters for the unstable particles that are gauge-dependent beyond one-loop order [155–159]. The generalization of the on-shell renormalization scheme to higher orders thus

be fulfilled by the corresponding eigenvalues resulting in complicated expressions. These can be considerably simplified by requiring simultaneously the on-shell conditions for the field renormalization matrices. The latter conditions require that close to its pole each propagator is given by its lowest order expression with the bare mass replaced by its renormalized one. Consequently, the renormalized 1PI two-point functions are diagonal if the external particles are on their mass shell, and the residues of the renormalized propagators are equal to one, that is, the quanta of the renormalized fields are mass eigenstates. In this way, one arrives at the following set of renormalization conditions for the two-point functions for on-shell external particles[16]

$$
\begin{aligned}
&\widetilde{\mathrm{Re}}\,\hat{\Gamma}_{W_\mu^\pm W_\nu^\mp}(k)\epsilon^\nu(k)\Big|_{k^2=M_W^2} = 0\,, && \lim_{k^2\to M_W^2}\frac{1}{k^2-M_W^2}\,\widetilde{\mathrm{Re}}\,\hat{\Gamma}_{W_\mu^\pm W_\nu^\mp}(k)\epsilon^\nu(k) = -\epsilon_\mu(k)\,,\\
&\mathrm{Re}\,\hat{\Gamma}_{Z_\mu Z_\nu}(k)\epsilon^\nu(k)\Big|_{k^2=M_Z^2} = 0\,, && \lim_{k^2\to M_Z^2}\frac{1}{k^2-M_Z^2}\,\mathrm{Re}\,\hat{\Gamma}_{Z_\mu Z_\nu}(k)\epsilon^\nu(k) = -\epsilon_\mu(k)\,,\\
&\mathrm{Re}\,\hat{\Gamma}_{A_\mu A_\nu}(k)\epsilon^\nu(k)\Big|_{k^2=0} = 0\,, && \lim_{k^2\to 0}\frac{1}{k^2}\,\mathrm{Re}\,\hat{\Gamma}_{A_\mu A_\nu}(k)\epsilon^\nu(k) = -\epsilon_\mu(k)\,,\\
&\mathrm{Re}\,\hat{\Gamma}_{HH}(k)\Big|_{k^2=M_H^2} = 0\,, && \lim_{k^2\to M_H^2}\frac{1}{k^2-M_H^2}\,\mathrm{Re}\,\hat{\Gamma}_{HH}(k) = 1\,,\\
&\widetilde{\mathrm{Re}}\,\hat{\Gamma}_{f^i\bar{f}^j}(k)u_j(k)\Big|_{k^2=m_f^{j\,2}} = 0\,, && \lim_{k^2\to m_f^{i\,2}}\frac{\not{k}+m_f^i}{k^2-m_f^{i\,2}}\,\widetilde{\mathrm{Re}}\,\hat{\Gamma}_{f^i\bar{f}^i}(k)u_i(k) = u_i(k)\,,\\
&\widetilde{\mathrm{Re}}\,\bar{u}_i(k)\hat{\Gamma}_{f^i\bar{f}^j}(k)\Big|_{k^2=m_f^{i\,2}} = 0\,, && \lim_{k^2\to m_f^{i\,2}}\bar{u}_i(k)\,\widetilde{\mathrm{Re}}\,\hat{\Gamma}_{f^i\bar{f}^i}(k)\frac{\not{k}+m_f^i}{k^2-m_f^{i\,2}} = \bar{u}_i(k)\,,
\end{aligned}
\tag{2.106}
$$

where $\epsilon_\mu(k)$, $u_i(k)$ and $\bar{u}_i(k)$ are the polarization vectors and spinors of the external fields. The symbol $\widetilde{\mathrm{Re}}$ takes the real part of the logarithms that arise in the loop integrals appearing in the self-energies, and commutes with complex valued parameters such as V_{ij}. Its purpose is to remove the absorptive parts. Owing to the required hermiticity of the renormalized Lagrangian, the counterterms can only affect the non-absorptive parts. To ensure the masslessness of the photon and to avoid mixing of the gauge bosons as far as possible, we require the following normalization conditions

$$
\widetilde{\mathrm{Re}}\,\hat{\Gamma}_{Z_\mu A_\nu}(k)\epsilon^\nu(k)\Big|_{k^2=M_Z^2} = 0\,, \qquad \hat{\Gamma}_{A_\mu Z_\nu}(k)\epsilon^\nu(k)\Big|_{k^2=0} = 0\,, \tag{2.107}
$$

which are necessary to guarantee the infrared (IR) finiteness of the SM to all orders in perturbation theory [154, 160]. These normalization conditions have to be proven to be in accordance with the symmetries of the SM, and can be shown to lead to higher order corrections to the sine of the weak mixing angle.

Renormalization of the Quark Mixing Matrix

In addition to the masses and the couplings of the SM particles, the elements of the quark mixing matrix need to be renormalized as well. This was realized for the Cabibbo angle in the SM with two fermion generations in a pioneering paper by Marciano and Sirlin [161],

requires a proper definition of the mass parameters of the unstable particles which is discussed in a very clear manner in reference [151].

[16] For simplicity the on-shell renormalization conditions for antifermions are omitted here.

and for the CKM matrix of the three generation SM by Denner and Sack [162] more than a decade ago. Although the renormalization of the CKM matrix is relevant from the conceptual point of view, its phenomenological significance is damped by the fact that, as a result of GIM cancellations, the radiative one-loop corrections related to the renormalization of the CKM matrix are very small, of $\mathcal{O}(G_F m_q^2)$, where G_F denotes the Fermi or muon decay constant and m_q is the mass of a light quark. The situation might, however, be very different for lepton mixing in a non-minimal SM with massive Dirac neutrinos or in extensions of the SM involving Majorana neutrinos.

Upon renormalization, the fermionic fields are rescaled by non-diagonal complex wave function renormalization matrices $Z^{f,L}$ and $Z^{f,R}$. Consequently, the bare parameters $V_{0,ij}$ are replaced by the renormalized CKM matrix elements

$$V_{ij} = \sum_{k,l=1}^{3} \left(Z_{ik}^{-1/2,u,L} V_{0,kl} Z_{lj}^{1/2,d,L} \right) . \tag{2.108}$$

Expanding V_{ij} up to first order, we obtain for the counterterm of the quark mixing matrix

$$\delta V_{ij} = \frac{1}{2} \sum_{k=1}^{3} \left(\delta Z_{ik}^{u,L} V_{0,kj} - V_{0,ik} \delta Z_{kj}^{d,L} \right) . \tag{2.109}$$

Clearly, δV_{ij} must cancel the UV divergences that, upon mass and coupling renormalization, are left in the loop corrected amplitude of an arbitrary physical process involving quark mixing. This requirement fixes the UV divergences of δV_{ij}. Different renormalization schemes then differ in the finite parts of δV_{ij}. Apart from being finite, the parameters V_{ij} should also be gauge independent, so that they qualify as proper physical observables that can be extracted from experiment with reason. Moreover, renormalization should be arranged so that the basic structure of the theory is preserved. Since the bare CKM matrix is unitary, the same should, therefore, be true for its renormalized version. Otherwise, four real input parameters would not be sufficient to parameterize the latter, and the familiar notion of the unitary triangle would no longer be meaningful beyond tree level. At the one-loop level, this leads us to require that

$$\sum_{k=1}^{3} V_{0,ik} \left(\delta Z_{kj}^{d,L} + \delta Z_{kj}^{d,L\dagger} \right) = \sum_{k=1}^{3} \left(\delta Z_{ik}^{u,L} + \delta Z_{ik}^{u,L\dagger} \right) V_{0,kj} , \tag{2.110}$$

is valid up to higher order terms. Combining the last two equations we find

$$\delta V_{ij} = \frac{1}{4} \sum_{k=1}^{3} \left[\left(\delta Z_{ik}^{u,L} - \delta Z_{ik}^{u,L\dagger} \right) V_{0,kj} - V_{0,ik} \left(\delta Z_{kj}^{d,L} - \delta Z_{kj}^{d,L\dagger} \right) \right] , \tag{2.111}$$

where, as expected for a unitary matrix, the renormalization of V_{ij} is expressed in terms of the antihermitian parts of the wave function renormalization constants. Therefore it depends on the scheme chosen for the wave function renormalization. It should be clear, on the other hand, that once the counterterms δV_{ij} are calculated employing the above equation, it can be used independently of the scheme adopted for the wave function renormalization. For example, in practical applications at the level of S-matrix elements, it is often convenient to avoid the rescaling of the fields altogether [163] and introduce

only the Lehmann-Symanzik-Zimmermann (LSZ) factors [164] for the external fields. If mixing is present, however, one still has to renormalize the mixing parameters.

A number of different renormalization prescriptions for the quark mixing matrix are indeed possible. A first convenient option is the modified minimal subtraction ($\overline{\rm MS}$) renormalization scheme [165] in dimensional regularization [79,166], where one only retains the UV divergences of the CKM counterterms. By definition, assuming gauge invariant mass renormalization and after adjusting for the possible breaking of chiral invariance, it can be guaranteed to satisfies the three requirements enumerated above. However, it is well-known that the decoupling of heavy particles is not manifest in the $\overline{\rm MS}$ scheme. This means that if one works in the framework of an effective Lagrangian where the heavy fields are integrated out, the dimension three and four operators that mix the quark fields yield contributions to the amplitude which are not suppressed by the high mass scale. This property makes the $\overline{\rm MS}$ definition inconvenient in realistic studies.

A second physical motivated possibility is provided by the use of the on-shell renormalization conditions (2.106) to define the wave function renormalization constants by setting them equal to the LSZ factors. It has been shown in reference [162] that this condition correctly cancels all one-loop divergences. Furthermore, it leads to $V_{ij} = V_{0,ij}$ in the limit of degenerate up- and down-type quark masses. Hence, the on-shell renormalization prescription for the CKM matrix is compact and plausible, complies with the first and third criterion by construction, but at first sight surprisingly, it fails to satisfy the second criterion, because the finite terms of the proposed expressions for the CKM counterterms (2.111) are gauge-dependent, as was noticed only recently by several authors [167–174].

A convenient and natural alterative to the latter prescription, which avoids the aforementioned problem at one-loop, but maintains decoupling and enhances the symmetry among the quark generations, can be obtained by using a different set of fermion wave function renormalization constants $\bar{Z}^{f,L}$ and $\bar{Z}^{f,R}$ for the renormalization of the quark mixing matrix. These renormalization constants result from requiring the renormalization conditions (2.106) for the off-diagonal fermion two-point functions not on the mass shell, but at the common subtraction point $k^2 = 0$,

$$\widetilde{\rm Re}\,\hat{\Gamma}_{f^i\bar{f}^j}(k)\Big|_{k^2=0} = 0\,, \qquad \frac{\partial}{\partial \not{k}}\widetilde{\rm Re}\,\hat{\Gamma}_{f^i\bar{f}^j}(k)\Big|_{k^2=0} = 0\,, \qquad i \neq j\,. \tag{2.112}$$

Clearly, these conditions which were introduced by Gambino et al. [167] do not fix the diagonal parts of the two-point functions. Since the right-handed off-diagonal quark self-energies are finite and proportional to the light quark masses, one can also choose to disregard the renormalization condition for the right-handed part of $\hat{\Gamma}_{f^i\bar{f}^j}$ and set the corresponding off-diagonal renormalization constants $\bar{Z}^{f,R}$ to zero. Finally, we stress once more, that the use of the CKM counterterm based on the renormalization conditions (2.112) and consequently on the antihermitian part of $\bar{Z}^{f,L}$, is independent of the choice of the wave function renormalization adopted in the rest of the calculation, and corresponds to just one of the many gauge-invariant definition of the one-loop CKM elements. Needless to say, it is always the LSZ procedure (2.106) to dictate the treatment of the external lines.

Renormalization of the Electric Charge

In the on-shell renormalization scheme, the electric charge of the electron is defined as the coupling of an on-shell electron to a photon with zero momentum. The full electron-electron-photon coupling consists of the corresponding three-point vertex function and the wave function renormalization constants. Owing to the Z boson-photon mixing, also the electron-electron-Z boson coupling will occur in general. However, due to our choice for the field renormalization (2.106) and (2.107) the corrections on the external legs vanish and the charge renormalization condition takes the simple form[17]

$$\bar{u}_e(p)\hat{\Gamma}_{A_\mu e\bar{e}}(p,p)u_e(p)\Big|_{p^2=m_e^2} = e\,\bar{u}_e(p)\gamma_\mu u_e(p)\,, \tag{2.113}$$

for the truncated three-point vertex function

$i\hat{\Gamma}_{A_\mu e\bar{e}}(p,p') \;=\; \mu$

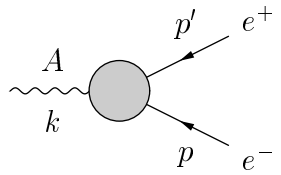

. (2.114)

Owing to charge universality, to be discussed at the end of the next section, we may, in fact, impose the above renormalization condition on any charged fermion to obtain the same renormalized electrical charge.

Renormalization of the Unphysical Sector

For proving unitarity of the physical S-matrix we have to impose normalization conditions on the unphysical fields. The poles of the propagators of the longitudinal part of the vector, of the unphysical would-be Goldstone and the Faddeev-Popov ghost fields are seen to be related by STIs [154]. The normalization conditions on the poles of unphysical particles are most easily established on the Faddeev-Popov ghost fields and read:

$$\mathrm{Re}\,\hat{\Gamma}_{u^+\bar{u}^-}(k)\Big|_{k^2=M^2_{u^\pm}} = 0\,, \quad \mathrm{Re}\,\hat{\Gamma}_{u^Z\bar{u}^Z}(k)\Big|_{k^2=M^2_{u^Z}} = 0\,, \quad \mathrm{Re}\,\hat{\Gamma}_{u^A\bar{u}^A}(k)\Big|_{k^2=0} = 0\,. \tag{2.115}$$

Furthermore, one has to require on-shell separation for the neutral ghosts

$$\begin{aligned} \mathrm{Re}\,\hat{\Gamma}_{u^Z\bar{u}^A}(k)\Big|_{k^2=M^2_{u^\pm}} &= 0\,, & \mathrm{Re}\,\hat{\Gamma}_{u^Z\bar{u}^A}(k)\Big|_{k^2=0} &= 0\,, \\ \mathrm{Re}\,\hat{\Gamma}_{u^A\bar{u}^Z}(k)\Big|_{k^2=M^2_{u^Z}} &= 0\,, & \mathrm{Re}\,\hat{\Gamma}_{u^A\bar{u}^Z}(k)\Big|_{k^2=0} &= 0\,, \end{aligned} \tag{2.116}$$

[17] This is a condition for the vector part of the electron-electron-photon vertex $\hat{\Gamma}_{A_\mu e\bar{e}}$ only. For the axial vector part no separate condition has to be imposed since it is finite and vanishes for real photons due to the STIs [148].

in order to carry out IR finite higher order calculations [154, 160]. Finally, we also impose normalization conditions on the residua of the ghost propagators:

$$\begin{aligned}
&\mathrm{Re}\,\frac{\partial}{\partial k^2}\hat{\Gamma}_{u^+\bar{u}^-}(k)\Big|_{k^2=M^2_{u^\pm}} = 1\,,\\
&\mathrm{Re}\,\frac{\partial}{\partial k^2}\hat{\Gamma}_{u^Z\bar{u}^Z}(k)\Big|_{k^2=M^2_{u^Z}} = 1\,,\\
&\mathrm{Re}\,\frac{\partial}{\partial k^2}\hat{\Gamma}_{u^A\bar{u}^A}(k)\Big|_{k^2=0} = 1\,.
\end{aligned} \tag{2.117}$$

Notice that the Faddeev-Popov ghost masses are independent parameters of the theory and their renormalization can be achieved by adjusting the independent 't Hooft parameters ζ_W and ζ_Z. For practical calculations, in order to avoid the double poles, it is advantageous to the set the Faddeev-Popov ghost masses $M_{u^\pm}$ and M_{u^Z} equal to the masses M_ϕ and M_χ of the would-be Goldstone bosons. That corresponds, at tree level, to setting all the 't Hooft parameters ζ_W and ζ_Z equal to the gauge parameters ξ_W and ξ_Z. However, at higher orders, this degeneracy cannot be maintained since the 't Hooft parameters must be used to enforce the normalization conditions (2.116).

Explicit Form of the Renormalization Constants

The renormalized vertex functions defined in the last section consist of the unrenormalized ones and the counterterms. Thus the renormalization conditions allow to the express the counterterms through the unrenormalized vertex functions at specific external momenta. In the following we will perform this task for the renormalization constants for the physical fields and parameters at the one-loop level.

From condition (2.105) we obtain for the tadpole counterterm

$$\delta t = -\Gamma_H(0)\,. \tag{2.118}$$

In order to proceed, we decompose the vertex functions into covariants. The transversal and longitudinal part of the gauge boson two-point functions is defined according to

$$\hat{\Gamma}_{V^i_\mu V^j_\mu}(k) = \left(g_{\mu\nu} - \frac{k_\mu k_\nu}{k^2}\right)\hat{\Gamma}^{V^iV^j}_T(k^2) + \frac{k_\mu k_\nu}{k^2}\hat{\Gamma}^{V^iV^j}_L(k^2)\,, \tag{2.119}$$

where $V^i, V^j = W^\pm, Z, A$ indicates vector fields and, as throughout this thesis, all momenta of the fields in the vertex functions are incoming.

The most general form of the fermionic two-point function in compliance with hermiticity [175] reads

$$\hat{\Gamma}_{f^i\bar{f}^j}(k) = \not{k}\,P_L\hat{\Gamma}^{f,L}_{ij}(k^2) + \not{k}\,P_R\hat{\Gamma}^{f,R}_{ij}(k^2) + P_L\hat{\Gamma}^{f,D}_{ij}(k^2) + P_R\hat{\Gamma}^{f,D*}_{ji}(k^2)\,, \tag{2.120}$$

supplemented by the constraints

$$\hat{\Gamma}^L_{ij}(k^2) = \hat{\Gamma}^{L*}_{ji}(k^2)\,, \qquad \hat{\Gamma}^R_{ij}(k^2) = \hat{\Gamma}^{R*}_{ji}(k^2)\,. \tag{2.121}$$

Note that since the two-point vertex functions are 1PI, they contain no tadpole contributions. These appear explicitly as Γ_H.

Now we split the two-point functions entering the renormalization conditions for the physical fields and parameters into tree level contributions, unrenormalized self-energies and counterterms. In first order approximation we have

$$\begin{aligned}
\hat{\Gamma}_T^{V^iV^j}(k^2) &= -\delta_{ij}\left(k^2 - M_{V^i}^2\right) - \Sigma_T^{V^iV^j}(k^2) \\
&\quad - \left[\frac{1}{2}\left(k^2 - M_{V^i}^2\right)\delta Z_{V^iV^j} + \frac{1}{2}\left(k^2 - M_{V^j}^2\right)\delta Z_{V^jV^i} - \delta_{ij}\delta M_{V^i}^2\right] , \\
\hat{\Gamma}_L^{V^iV^j}(k^2) &= \delta_{ij}M_{V^i}^2 - \Sigma_L^{V^iV^j}(k^2) \\
&\quad + \left[\frac{1}{2}M_{V^i}^2\delta Z_{V^iV^j} + \frac{1}{2}M_{V^j}^2\delta Z_{V^jV^i} + \delta_{ij}\delta M_{V^i}^2\right] , \\
\hat{\Gamma}^{HH}(k^2) &= \left(k^2 - M_H^2\right) + \Sigma^{HH}(k^2) + \left(k^2 - M_H^2\right)\delta Z_H - \delta M_H^2 , \\
\hat{\Gamma}_{ij}^{f,L}(k^2) &= \delta_{ij} + \Sigma_{ij}^{f,L}(k^2) + \frac{1}{2}\left(\delta Z_{ij}^{f,L} + \delta Z_{ij}^{f,L\dagger}\right) , \\
\hat{\Gamma}_{ij}^{f,R}(k^2) &= \delta_{ij} + \Sigma_{ij}^{f,R}(k^2) + \frac{1}{2}\left(\delta Z_{ij}^{f,R} + \delta Z_{ij}^{f,R\dagger}\right) , \\
\hat{\Gamma}_{ij}^{f,D}(k^2) &= -\delta_{ij}m_f^i + \Sigma_{ij}^{f,D}(k^2) - \frac{1}{2}\left(m_f^i\delta Z_{ij}^{f,L} + m_f^j\delta Z_{ij}^{f,R\dagger}\right) - \delta_{ij}\delta m_f^i ,
\end{aligned} \tag{2.122}$$

Inserting these equations into the renormalization conditions (2.106) and using the fact that in the minimal SM one can write

$$\Sigma_{ij}^{f,D}(k^2) = m_f^i\Sigma_{ij}^{f,S}(k^2) , \qquad \Sigma_{ji}^{f,D*}(k^2) = m_f^j\Sigma_{ij}^{f,S}(k^2) , \tag{2.123}$$

we find for the mass counterterms

$$\begin{aligned}
\delta M_W^2 = \widetilde{\mathrm{Re}}\,\Sigma_T^{WW}(M_W^2) , \qquad \delta M_Z^2 = \mathrm{Re}\,\Sigma_T^{ZZ}(M_Z^2) , \qquad \delta M_H^2 = \mathrm{Re}\,\Sigma_T^{HH}(M_H^2) , \\
\delta m_f^i = \frac{m_f^i}{2}\,\widetilde{\mathrm{Re}}\left(\Sigma_{ii}^{f,L}(m_f^{i\,2}) + \Sigma_{ii}^{f,R}(m_f^{i\,2}) + 2\Sigma_{ii}^{f,S}(m_f^{i\,2})\right) .
\end{aligned} \tag{2.124}$$

From the normalization conditions (2.106) and (2.107) the field renormalization constants of the boson fields are obtained as[18]

$$\begin{aligned}
\delta Z_W &= -\widetilde{\mathrm{Re}}\,\frac{\partial\Sigma_T^{WW}(k^2)}{\partial k^2}\bigg|_{k^2=M_W^2} , & \delta Z_{ZZ} &= -\mathrm{Re}\,\frac{\partial\Sigma_T^{ZZ}(k^2)}{\partial k^2}\bigg|_{k^2=M_Z^2} , \\
\delta Z_{ZA} &= 2\frac{\Sigma_T^{AZ}(0)}{M_Z^2} , & \delta Z_{AZ} &= -2\,\mathrm{Re}\,\frac{\Sigma_T^{AZ}(M_Z^2)}{M_Z^2} , \\
\delta Z_{AA} &= -\mathrm{Re}\,\frac{\partial\Sigma_T^{AA}(k^2)}{\partial k^2}\bigg|_{k^2=0} , & \delta Z_H &= -\mathrm{Re}\,\frac{\partial\Sigma^{HH}(k^2)}{\partial k^2}\bigg|_{k^2=M_H^2} ,
\end{aligned} \tag{2.125}$$

[18]Note that at one-loop order the condition $\Sigma_T^{AA}(0) = 0$ is guaranteed by the STIs and gives no constraint on the counterterms.

and those of the fermionic fields read

$$\begin{aligned}
\delta Z_{ij}^{f,L} &= \frac{2}{m_f^{i\,2} - m_f^{j\,2}} \widetilde{\mathrm{Re}} \left[m_f^{j\,2} \Sigma_{ij}^{f,L}(m_f^{j\,2}) + m_f^i m_f^j \Sigma_{ij}^{f,R}(m_f^{j\,2}) \right. \\
&\qquad \left. + \left(m_f^{i\,2} + m_f^{j\,2}\right) \Sigma_{ij}^{f,S}(m_f^{j\,2}) \right], \qquad i \neq j\,, \\
\delta Z_{ij}^{f,R} &= \frac{2}{m_f^{i\,2} - m_f^{j\,2}} \widetilde{\mathrm{Re}} \left[m_f^{j\,2} \Sigma_{ij}^{f,R}(m_f^{j\,2}) + m_f^i m_f^j \Sigma_{ij}^{f,L}(m_f^{j\,2}) \right. \\
&\qquad \left. + 2 m_f^i m_f^j \Sigma_{ij}^{f,S}(m_f^{j\,2}) \right], \qquad i \neq j\,, \\
\delta Z_{ii}^{f,L} &= -\widetilde{\mathrm{Re}}\, \Sigma_{ii}^{f,L}(m_f^{i\,2}) - m_f^{i\,2} \frac{\partial}{\partial k^2} \widetilde{\mathrm{Re}} \left(\Sigma_{ii}^{f,L}(k^2) + \Sigma_{ii}^{f,R}(k^2) + 2\Sigma_{ii}^{f,S}(k^2) \right) \Big|_{k^2 = m_f^{i\,2}}\,, \\
\delta Z_{ii}^{f,R} &= -\widetilde{\mathrm{Re}}\, \Sigma_{ii}^{f,R}(m_f^{i\,2}) - m_f^{i\,2} \frac{\partial}{\partial k^2} \widetilde{\mathrm{Re}} \left(\Sigma_{ii}^{f,L}(k^2) + \Sigma_{ii}^{f,R}(k^2) + 2\Sigma_{ii}^{f,S}(k^2) \right) \Big|_{k^2 = m_f^{i\,2}}\,.
\end{aligned} \tag{2.126}$$

The renormalization constants for the elements of the quark mixing matrix are determined from the renormalization prescription (2.112). Taking into account that $V_{ij} = V_{0,ij}$ at lowest order, we get

$$\begin{aligned}
\delta V_{ij} = \sum_{k=1}^{3} \widetilde{\mathrm{Re}} \Bigg[& \frac{1}{m_u^{i\,2} - m_u^{k\,2}} \left(\frac{1}{2} \left(m_u^{k\,2} + m_u^{i\,2}\right) \Sigma_{ik}^{u,L}(0) + m_u^k m_u^i \Sigma_{ik}^{u,R}(0) \right. \\
& \left. + \left(m_u^{k\,2} + m_u^{i\,2}\right) \Sigma_{ik}^{u,S}(0) \right) V_{kj} \\
& - V_{ik} \frac{1}{m_d^{k\,2} - m_d^{j\,2}} \left(\frac{1}{2} \left(m_d^{k\,2} + m_d^{j\,2}\right) \Sigma_{kj}^{d,L}(0) + m_d^k m_d^j \Sigma_{kj}^{d,R}(0) \right. \\
& \left. + \left(m_d^{k\,2} + m_d^{j\,2}\right) \Sigma_{kj}^{d,S}(0) \right) \Bigg]\,.
\end{aligned} \tag{2.127}$$

Clearly, if one chooses to set the right-handed off-diagonal wave function renormalization constants $\delta \bar{Z}^{u,R}$ and $\delta \bar{Z}^{d,R}$ to zero, the terms involving $\Sigma^{R,u}$ and $\Sigma^{R,d}$ have to be omitted.

In the on-shell renormalization scheme the weak mixing angle is a derived quantity. Following the standard approach [163, 176, 177] we define it by

$$s_W^2 = 1 - \frac{M_W^2}{M_Z^2}\,, \tag{2.128}$$

where M_W and M_Z are the physical masses of the $W^\pm$ and Z bosons. This definition is independent of a specific process and valid to all orders in perturbation theory. Recall, however, that the weak mixing angle is not a directly measurable quantity and beyond tree level could be defined in ways different from the choice adopted above.

Since the auxiliary parameters s_W and c_W frequently appear, it is useful to introduce the corresponding counterterms

$$s_{W,0} = s_W + \delta s_W\,, \qquad c_{W,0} = c_W + \delta c_W\,. \tag{2.129}$$

According to the definition (2.128) these are directly related to the gauge boson masses. To one-loop order one obtains

$$\begin{aligned}\delta s_W &= \frac{c_W^2}{2s_W}\left(\frac{\delta M_Z^2}{M_Z^2} - \frac{\delta M_W^2}{M_W^2}\right) = \frac{c_W^2}{2s_W}\,\widetilde{\mathrm{Re}}\left(\frac{\Sigma_T^{ZZ}(M_Z^2)}{M_Z^2} - \frac{\Sigma_T^{WW}(M_W^2)}{M_W^2}\right),\\ \delta c_W &= -\frac{s_W}{c_W}\delta s_W = -\frac{c_W}{2}\,\widetilde{\mathrm{Re}}\left(\frac{\Sigma_T^{ZZ}(M_Z^2)}{M_Z^2} - \frac{\Sigma_T^{WW}(M_W^2)}{M_W^2}\right).\end{aligned} \tag{2.130}$$

Finally, we have to determine the counterterm for the electric charge. In the electroweak SM charge renormalization looks formally pretty much the same as in pure Quantum Electrodynamics (QED). However, there is one big difference: Unlike in QED the electromagnetic current is not strictly conserved in the non-abelian case. More precisely, the divergence of this current acts as the null operator only on physical states, because it is the BRST transform of another operator. Therefore the simple proof of charge universality in QED, which relies on the Ward-Takahashi identity (WTI) [178,179] is not valid in such theories as the SM. In these cases a proof has to be based on the underlying BRST symmetry in the conventional Faddeev-Popov approach. Following references [147,148], we start from the invariance of the Green's function $\langle T\bar{u}_A(x)f^i(y)\bar{f}^i(z)\rangle$ under the action of the BRST operator s. After transforming to momentum space and amputating the external legs of the fermion-fermion-photon vertex function by multiplying with the appropriate inverse propagators we obtain the following identity for on-shell fermions:

$$\hat{\Gamma}_{A_\mu f^i \bar{f}^i}(p,p)\Big|_{p^2=m_f^{i\,2}} = -e_0 Q_f\left(Z_{AA}^{1/2} + \frac{s_{W,0}}{c_{W,0}}Z_{ZA}^{1/2}\right)\frac{\partial}{\partial p^\mu}\hat{\Gamma}_{f^i\bar{f}^i}(p)\Big|_{p^2=m_f^{i\,2}}. \tag{2.131}$$

Sandwiching this between the two spinors $\bar{u}_f(p)$ and $u_f(p)$ and using the on-shell condition for the fermion fields (2.106), and the analogue of the charge renormalization condition (2.113) for arbitrary fermions f^i this results in

$$Z_e = \left(Z_{AA}^{1/2} + \frac{s_W + \delta s_W}{c_W + \delta c_W}Z_{ZA}^{1/2}\right)^{-1}, \tag{2.132}$$

which is valid in all orders of perturbation theory. Thus, just as in QED, the on-shell definition of the electric charge together with the $U(1)_Q$ rigid invariance of the broken $SU(2)_L \times U(1)_Y$ symmetry automatically guarantees that the coupling of the photon to the charged particles is independent of the fermion species, reflecting charge universality in the minimal SM. Expanding the general formula (2.132) up to first order in the electromagnetic fine structure constant yields:

$$\delta Z_e = -\frac{1}{2}\left(\delta Z_{AA} + \frac{s_W}{c_W}\delta Z_{ZA}\right) = -\frac{1}{2}\left.\frac{\Sigma_T^{AA}(k^2)}{k^2}\right|_{k^2=0} - \frac{s_W}{c_W}\frac{\Sigma_T^{AZ}(0)}{M_Z^2}. \tag{2.133}$$

We have now determined all renormalization constants of the physical fields and parameters in terms of unrenormalized self-energies at the one-loop level. The explicit expressions for a abridged set of unrenormalized self-energies needed for the calculations performed in this thesis will be given in Chapter 4.4.

Part II

Radiative B Decays in the Standard Model

Chapter 3

Anatomy of the $B \to X_s\gamma$ Decay

In this chapter we review the status of the theoretical prediction of the weak radiative $B \to X_s\gamma$ decay in the SM, following largely the analysis of reference [180]. Radiative B decays represent one of the most important probes of new physics and a major testing ground for the SM. They already place severe constraints on many new physics scenarios. The present experimental accuracy for the branching ratio of $B \to X_s\gamma$ is around 12% and is expected to improve significantly in the near future. On the theoretical side, since precise predictions in the SM are particularly important, the subject has reached a high degree of technical sophistication. Indeed, perturbative QCD corrections are very sizeable [181,182] and give the dominant contribution. They are best implemented in the framework of an effective theory obtained by integrating out the heavy degrees of freedom characterized by a mass scale $M \geq M_W$. At lowest order in this approach the FCNC processes $B \to X_s\gamma$ and $B \to X_s g$ proceed through helicity violating amplitudes induced by magnetic type operators. Besides leading logarithmic (LO) $\mathcal{O}(\alpha_s^n L^n)$ and next-to-leading logarithmic (NLO) $\mathcal{O}(\alpha_s^n L^{n-1})$ QCD corrections [183–206], with $n = 0, 1, 2, \ldots$ and $L = \ln m_b^2/M_W^2$, and non-perturbative Heavy Quark Effective Theory (HQET) contributions [207–213], electroweak effects are known to play a non-negligible role [214–219].

3.1 Effective Off-Shell Hamiltonian

Before discussing in some detail the principle steps leading to the theoretical prediction of the branching ratio for the inclusive radiative decay $B \to X_s\gamma$, we briefly have to recall the general formalism on which it is based. We work in the framework of an effective low-energy theory with five quarks, obtained by integrating out the heavy degrees of freedom characterized by a mass scale $M \geq M_W$. In the leading order of the operator product expansion (OPE) the effective off-shell Hamiltonian relevant for the $b \to s\gamma$ and $b \to sg$ transition at a scale μ is given by

$$\mathcal{H}_{\text{eff}} = -\frac{G_F}{\sqrt{2}} V_{ts}^* V_{tb} \left(\sum_{i=1}^{16} C_i(\mu) Q_i + C_7^\gamma(\mu) Q_7^\gamma + C_8^g(\mu) Q_8^g \right) , \tag{3.1}$$

where V_{ts}^* and V_{tb} are the relevant elements of the CKM matrix, while $C_i(\mu)$, $C_7^\gamma(\mu)$ and $C_8^g(\mu)$ denote the Wilson coefficients of the following set of gauge-invariant local

operators [186, 187, 217, 220–226] built out of the light fields present in the SM[1]

$$
\begin{aligned}
Q_1 &= (\bar{s}_L\gamma_\mu T^a c_L)(\bar{c}_L\gamma^\mu T^a b_L)\,,\\
Q_2 &= (\bar{s}_L\gamma_\mu c_L)(\bar{c}_L\gamma^\mu b_L)\,,\\
Q_3 &= (\bar{s}_L\gamma_\mu b_L)\sum\nolimits_q(\bar{q}\gamma^\mu q)\,,\\
Q_4 &= (\bar{s}_L\gamma_\mu T^a b_L)\sum\nolimits_q(\bar{q}\gamma^\mu T^a q)\,,\\
Q_5 &= (\bar{s}_L\gamma_\mu\gamma_\nu\gamma_\lambda b_L)\sum\nolimits_q(\bar{q}\gamma^\mu\gamma^\nu\gamma^\lambda q)\,,\\
Q_6 &= (\bar{s}_L\gamma_\mu\gamma_\nu\gamma_\lambda T^a b_L)\sum\nolimits_q(\bar{q}\gamma^\mu\gamma^\nu\gamma^\lambda T^a q)\,,\\
Q_7 &= (\bar{s}_L\gamma_\mu b_L)\sum\nolimits_q Q_q(\bar{q}\gamma^\mu q)\,,\\
Q_8 &= (\bar{s}_L\gamma_\mu T^a b_L)\sum\nolimits_q Q_q(\bar{q}\gamma^\mu T^a q)\,,\\
Q_9 &= (\bar{s}_L\gamma_\mu\gamma_\nu\gamma_\lambda b_L)\sum\nolimits_q Q_q(\bar{q}\gamma^\mu\gamma^\nu\gamma^\lambda q)\,,\\
Q_{10} &= (\bar{s}_L\gamma_\mu\gamma_\nu\gamma_\lambda T^a b_L)\sum\nolimits_q Q_q(\bar{q}\gamma^\mu\gamma^\nu\gamma^\lambda T^a q)\,,\\
Q_7^\gamma &= \frac{e}{16\pi^2}m_b(\bar{s}_L\sigma^{\mu\nu}b_R)F_{\mu\nu}\,,\\
Q_8^g &= \frac{g_s}{16\pi^2}m_b(\bar{s}_L\sigma^{\mu\nu}T^a b_R)G^a_{\mu\nu}\,,\\
Q_{11} &= \frac{1}{e}\bar{s}_L\gamma^\mu b_L\partial^\nu F_{\mu\nu} + Q_7\,,\\
Q_{12} &= \frac{1}{g_s}\bar{s}_L\gamma^\mu T^a b_L D^\nu G^a_{\mu\nu} + Q_4\,,\\
Q_{13} &= \frac{ie}{16\pi^2}\left(\bar{s}_L\overleftarrow{\not{D}}\,\sigma^{\mu\nu}b_L F_{\mu\nu} - F_{\mu\nu}\bar{s}_L\sigma^{\mu\nu}\not{D}b_L\right) + Q_7^\gamma\,,\\
Q_{14} &= \frac{ig_s}{16\pi^2}\left(\bar{s}_L\overleftarrow{\not{D}}\,\sigma^{\mu\nu}T^a b_L G^a_{\mu\nu} - G^a_{\mu\nu}\bar{s}_L T^a\sigma^{\mu\nu}\not{D}b_L\right) + Q_8^g\,,\\
Q_{15} &= \frac{i}{16\pi^2}m_b\bar{s}_L\not{D}\not{D}b_R\,,\\
Q_{16} &= \frac{1}{16\pi^2}\bar{s}_L\not{D}\not{D}\not{D}b_L\,,
\end{aligned}
\tag{3.2}
$$

where $\sigma_{\mu\nu} = i\,[\gamma_\mu,\gamma_\nu]\,/2$ and the summation runs over $q = u, d, s, c, b$. Notice that in view of $m_s \ll m_b$ contributions stemming from the mass insertions on the external s-quark line are neglected here and in the following.

The above set of operators closes off-shell[2] under QCD and QED renormalization, up to non-physical so-called evanescent operators that vanish in four dimensions [187, 220]. It consists of the current-current operators Q_1–Q_2, the QCD penguin operators Q_3–Q_6,

[1] Notice that the CKM suppressed analogues of Q_1 and Q_2 involving the u-quark instead of the c-quark are present in the effective theory, too. Their effects will be included in the phenomenological analysis in the following sections.

[2] In an off-shell calculation it is important to use a background field version of the R_ξ gauges in order to maintain explicit gauge invariance at the level of off-shell Green's functions. A detailed discussion on the subtleties linked to the presence of non-physical operators which arise in the calculation of the $\mathcal{O}(\alpha)$ matching conditions for radiative B decays will be given in Chapter 4.2.

the electroweak penguin operators Q_7–Q_{10} and the magnetic moment type operators Q_7^γ and Q_8^g. It is the QED renormalization that forces us to introduce the operators Q_7–Q_{10}, in which the sum of the quark flavors is weighted by the electric charges Q_q. The remaining six operators Q_{11}–Q_{16}, characteristic of the processes $b \to s\gamma$ and $b \to sg$, were chosen in such a way that they vanish on-shell up to total derivatives. Only operators of dimension five or six are retained. Higher dimension operators are suppressed by at least one power of m_b^2/M_W^2, while those of lower dimensionality can be removed by choosing suitable renormalization conditions in the full theory [227, 228]. In the present case this is achieved by requiring that all flavor off-diagonal quark two-point functions which appear at the one-loop level in the full theory vanish when the equations of motion (EOM) are applied, that is, by using LSZ on-shell conditions on the external quark lines. Otherwise, these off-diagonal mass terms give rise to additional operators of dimension three and four [186, 225] which must be considered in the effective theory.

3.2 Renormalization Group Evolution

Let us start this section by recalling that at LO in QCD, only the tree level matrix elements of Q_7^γ and the one-loop matrix elements of Q_1–Q_6 that are of order α_s have to be included in the calculation of the branching ratio for the inclusive decay $B \to X_s\gamma$. The latter matrix elements vanish for an on-shell photon in any four-dimensional regularization scheme as well as in the 't Hooft-Veltman (HV) scheme [79, 229–231], while in the naive dimensional regularization (NDR) scheme with fully anticommuting γ_5 [232] the one-loop $b \to s\gamma$ and $b \to sg$ matrix elements of some of the four quark operators are proportional to the tree level matrix element of Q_7^γ and Q_8^g, respectively. The regularization scheme dependence of the LO QCD matrix elements is a peculiar feature of radiative B decays. It can arise because the one-loop mixing between the four quark operators Q_1–Q_6 and the magnetic moment type operators Q_7^γ and Q_8^g vanishes. In consequence, what usually would be a NLO QCD effect is only a LO one, and what would usually be NNLO in QCD, like for example the three-loop mixing of Q_1–Q_6 into Q_7^γ and Q_8^g to be discussed in Appendix A, is only NLO.

This peculiarity causes, that it is convenient to introduce the so-called effective coefficients [217, 233] for the magnetic moment type operators Q_7^γ and Q_8^g. In our case the two relevant combinations are

$$\begin{aligned} C_7^{\gamma,\mathrm{eff}}(\mu) &= C_7^\gamma(\mu) + \sum_{i=1}^{10} y_i C_i(\mu)\,, \\ C_8^{g,\mathrm{eff}}(\mu) &= C_8^g(\mu) + \sum_{i=1}^{10} z_i C_i(\mu)\,, \end{aligned} \tag{3.3}$$

where the numbers y_i and z_i are the coefficients relating the on-shell one-loop $b \to s\gamma$ and $b \to sg$ matrix elements of Q_1–Q_{10} to the tree level matrix elements of Q_7^γ and Q_8^g:

$$\begin{aligned} \langle s\gamma|Q_i(\mu)|b\rangle_{\mathrm{one-loop}} &= y_i \,\langle s\gamma|Q_7^\gamma(\mu)|b\rangle_{\mathrm{tree}}\,, \\ \langle sg|Q_i(\mu)|b\rangle_{\mathrm{one-loop}} &= z_i \,\langle sg|Q_8^g(\mu)|b\rangle_{\mathrm{tree}}\,, \end{aligned} \tag{3.4}$$

for $i = 1, \ldots, 10$. This, however, implies that the one-loop $b \to s\gamma$ and $b \to sg$ matrix elements of the effective Hamiltonian (3.1) can be expressed up to higher orders in terms

of the tree level matrix elements of Q_7^γ and Q_8^g in the following way

$$\begin{aligned}\langle s\gamma|\mathcal{H}_{\rm eff}|b\rangle_{\rm one-loop} &= -\frac{G_F}{\sqrt{2}}V_{ts}^*V_{tb}C_7^{\gamma,\rm eff}(\mu)\,\langle s\gamma|Q_7^\gamma(\mu)|b\rangle_{\rm tree}\,,\\ \langle sg|\mathcal{H}_{\rm eff}|b\rangle_{\rm one-loop} &= -\frac{G_F}{\sqrt{2}}V_{ts}^*V_{tb}C_8^{g,\rm eff}(\mu)\,\langle sg|Q_8^g(\mu)|b\rangle_{\rm tree}\,.\end{aligned} \tag{3.5}$$

In any four-dimensional regularization scheme and in the HV scheme the numbers y_i and z_i vanish, while in the NDR scheme we have[3]

$$\begin{aligned}\vec{y}^{\,T} &= \left(0,0,-\tfrac{1}{3},-\tfrac{4}{9},-\tfrac{20}{3},-\tfrac{80}{9},\tfrac{1}{9},\tfrac{4}{27},\tfrac{20}{9},\tfrac{80}{27}\right)\,,\\ \vec{z}^{\,T} &= \left(0,0,1,-\tfrac{1}{6},20,-\tfrac{10}{3},-\tfrac{1}{3},\tfrac{1}{18},-\tfrac{20}{3},-\tfrac{10}{9}\right)\,.\end{aligned} \tag{3.6}$$

This regularization scheme dependence is canceled by the corresponding scheme dependence in the LO anomalous dimension matrix, as has been first demonstrated in references [234,235]. Consequently, the quantities $C_7^{\gamma,\rm eff}(\mu)$ and $C_8^{g,\rm eff}(\mu)$ are regularization and renormalization scheme independent at LO, which would not be the case for the original coefficients $C_7^\gamma(\mu)$ and $C_8^g(\mu)$. Furthermore, it should be stressed that the vectors $\vec{y}$ and $\vec{z}$ come from divergent, that is, purely short-distance parts of the one-loop integrals. So no reference to any model for the matrix elements $\langle Q_i(\mu)\rangle$ is necessary here. This is why one is allowed to treat the expressions (3.5) as the proper effective Hamiltonian that has to be inserted in between hadronic states in a calculation of radiative B decays.

Although on-shell matrix elements of the effective Hamiltonian (3.1) are physical and therefore regularization and renormalization scale invariant quantities, the separate renormalization scale dependence of the Wilson coefficients $C_i(\mu)$ and the matrix elements $\langle Q_i(\mu)\rangle$ reflects the factorization of short- and long-distance physics. The effective coefficients evolve from the initial scale μ_0 down to the renormalization scale μ according to their renormalization group evolution (RGE). Restricting to the physical on-shell operators present in our operator basis (3.2) and using the scheme-independent vector

$$\vec{C}^{\,\rm eff\;T}(\mu) = \left(C_1(\mu),\ldots,C_{10}(\mu),C_7^{\gamma,\rm eff}(\mu),C_8^{g,\rm eff}(\mu)\right)\,, \tag{3.7}$$

it can be written as

$$\mu\frac{d}{d\mu}\vec{C}^{\,\rm eff}(\mu) = \hat{\gamma}^{\rm eff\;T}(\alpha_s,\alpha)\vec{C}^{\,\rm eff}(\mu)\,, \tag{3.8}$$

where $\hat{\gamma}^{\rm eff}(\alpha_s,\alpha)$ is the 12×12 anomalous dimension matrix governing the evolution of the effective coefficients. Neglecting the running of the electromagnetic coupling constant[4] the general solution of this equation reads

$$\vec{C}^{\,\rm eff}(\mu) = \hat{U}(\mu,\mu_0)\vec{C}^{\,\rm eff}(\mu_0)\,, \tag{3.9}$$

where

$$\hat{U}(\mu,\mu_0) = T_{g_s}\exp\int_{g_s(\mu_0)}^{g_s(\mu)} dg_s'\frac{\hat{\gamma}^{\rm eff\;T}(g_s'^2,\alpha)}{\beta(g_s')}\,. \tag{3.10}$$

[3]Notice that these numbers are different from those given in reference [233] because we use a different basis of four quark operators here.

[4]This is a very good approximation because only scales $m_b \le \mu \le M_W$ are involved in the following analysis.

Here $\vec{C}^{\,\text{eff}}(\mu_0)$ are the initial conditions of the evolution and T_{g_s} denotes ordering of the coupling constants $g_s(\mu)$ in such a way that their value increase from right to left. The T_{g_s} ordering is necessary, because in general $\left[\hat{\gamma}^{\text{eff}\,T}(\alpha_s(\mu_1),\alpha),\hat{\gamma}^{\text{eff}\,T}(\alpha_s(\mu_2),\alpha)\right] \neq 0$ for two different scales μ_1 and μ_2. $\beta(g_s)$ is the QCD beta function

$$\beta(g_s) = -\frac{g_s^3}{16\pi^2}\beta_s^{(0)} - \frac{g_s^5}{(16\pi^2)^2}\beta_s^{(1)} - \frac{e^2 g_s^3}{(16\pi^2)^2}\beta_{se}^{(1)}\,, \tag{3.11}$$

with

$$\begin{aligned}
\beta_s^{(0)} &= \frac{11}{3}C_A - \frac{2}{3}N_f\,,\\
\beta_s^{(1)} &= \frac{34}{3}C_A^2 - \frac{10}{3}C_A N_f - 2C_F N_f\,,\\
\beta_{se}^{(1)} &= -2N_u Q_u^2 - 2N_d Q_d^2\,,
\end{aligned} \tag{3.12}$$

where $N_f = N_u + N_d$ denotes the number of active flavors, while N_u and N_d are the numbers of up- and down-type flavors, respectively. Notice that from a conceptual point of view a resummation of $\mathcal{O}(\alpha\alpha_s^n L^n)$ terms requires the inclusion of the third term in the last but one equation. We will come back to this point in a moment.

By expanding the evolution matrix, which includes gluon and photon corrections, we obtain up to first order

$$\hat{U}(\mu,\mu_0) = \hat{U}_s^{(0)}(\mu,\mu_0) + \hat{U}_s^{(1)}(\mu,\mu_0) + \hat{U}_e^{(0)}(\mu,\mu_0) + \hat{U}_e^{(1)}(\mu,\mu_0)\,, \tag{3.13}$$

where the first two terms describe the pure QCD evolution, while the remaining ones are responsible for the additional running of the coefficient functions due to the presence of electromagnetic interactions. From the point of view of the expansion in α_s and α in the renormalization group improved perturbation theory, the evolution matrices $\hat{U}_s^{(0)}$ and $\hat{U}_s^{(1)}$ are $\mathcal{O}(1)$ and $\mathcal{O}(\alpha_s)$, while $\hat{U}_e^{(0)}$ and $\hat{U}_e^{(1)}$ are $\mathcal{O}(\alpha/\alpha_s)$ and $\mathcal{O}(\alpha)$, respectively. For completeness, let us now recall the formula for these matrices.

For this purpose we first have to expand the anomalous dimension matrix $\hat{\gamma}^{\text{eff}}(\alpha_s,\alpha)$ in α_s and α. Keeping terms up to second order in the coupling constants we find

$$\hat{\gamma}^{\text{eff}}(\alpha_s,\alpha) = \frac{\alpha_s(\mu)}{4\pi}\hat{\gamma}_s^{\text{eff}\,(0)} + \frac{\alpha_s^2(\mu)}{(4\pi)^2}\hat{\gamma}_s^{\text{eff}\,(1)} + \frac{\alpha}{4\pi}\hat{\gamma}_e^{\text{eff}\,(0)} + \frac{\alpha\alpha_s(\mu)}{(4\pi)^2}\hat{\gamma}_{se}^{\text{eff}\,(1)}\,. \tag{3.14}$$

Notice that the definition of the effective coefficients (3.3) guarantees that the LO matrices $\hat{\gamma}_s^{\text{eff}\,(0)}$ and $\hat{\gamma}_e^{\text{eff}\,(0)}$ are regularization and renormalization scheme independent, while this is not the case for the LO matrices governing the evolution of the original coefficients $\vec{C}(\mu)$. Explicit expressions for $\hat{\gamma}_s^{\text{eff}\,(0)}$ and $\hat{\gamma}_s^{\text{eff}\,(1)}$ as well as for $\hat{\gamma}_e^{\text{eff}\,(0)}$ will be given in Appendix A. $\hat{\gamma}_{se}^{\text{eff}\,(1)}$ is presently unknown as it requires the calculation of the two- and three-loop $\mathcal{O}(\alpha\alpha_s)$ mixing of the complete set of on-shell operators present in our operator basis.[5]

[5] In the operator basis of references [236, 237] the 10×10 submatrix for the mixing of Q_1–Q_{10} at $\mathcal{O}(\alpha\alpha_s)$ has been calculated nearly a decade ago [238]. To the best of our knowledge, nobody, however, tried to use these results to derive the anomalous dimension matrix for the choice of four quark operators adopted here.

Now keeping only the first terms in the expansions (3.11) and (3.14) of the beta function and of the anomalous dimension matrix the LO QCD evolution matrix can be written in the following way

$$\hat{U}_s^{(0)}(\mu,\mu_0) = \hat{V}\,\mathrm{diag}\left[\left(\frac{\alpha_s(\mu_0)}{\alpha_s(\mu)}\right)^{\vec{a}}\right]\hat{V}^{-1}\,, \tag{3.15}$$

with $\hat{V}$ and $\vec{a}$ defined by

$$\mathrm{diag}\left(\hat{\gamma}_s^{\mathrm{eff}\,(0)}\right) = \hat{V}^{-1}\hat{\gamma}_s^{\mathrm{eff}\,(0)\,T}\hat{V}\,, \qquad \vec{a} = \frac{\vec{\gamma}_s^{\,\mathrm{eff}\,(0)}}{2\beta_s^{(0)}}\,. \tag{3.16}$$

Here $\mathrm{diag}(\hat{\gamma}_s^{\mathrm{eff}\,(0)})$ denotes a diagonal matrix whose diagonal elements are the components of the vector $\vec{\gamma}_s^{\,\mathrm{eff}\,(0)}$.

Beyond leading order in α_s we have to keep the first two terms in the perturbative expansion of $\beta(g_s)$ and $\hat{\gamma}^{\mathrm{eff}}(\alpha_s,\alpha)$. As shown in references [190,193], the matrix $\hat{U}_s^{(1)}(\mu,\mu_0)$ can then nicely be written as follows

$$\hat{U}_s^{(1)}(\mu,\mu_0) = \frac{\alpha_s(\mu)}{4\pi}\hat{J}_s\hat{U}_s^{(0)}(\mu,\mu_0) - \frac{\alpha_s(\mu_0)}{4\pi}\hat{U}_s^{(0)}(\mu,\mu_0)\hat{J}_s\,. \tag{3.17}$$

Here $\hat{J}_s$ summarizes the additional running due to NLO QCD corrections. It is given by

$$\hat{J}_s = \hat{V}\hat{H}_s\hat{V}^{-1}\,. \tag{3.18}$$

where $\hat{H}_s$ is defined as the matrix whose elements are

$$(\hat{H}_s)_{ij} = \frac{\beta_s^{(1)}}{\beta_s^{(0)}}\delta_{ij}a_i - \frac{(\hat{G}_s)_{ij}}{2\beta_s^{(0)}\,(1+a_i-a_j)}\,, \tag{3.19}$$

with a_i being the components of $\vec{a}$ and $(\hat{G}_s)_{ij}$ denoting the elements of

$$\hat{G}_s = \hat{V}^{-1}\hat{\gamma}_s^{\mathrm{eff}\,(1)\,T}\hat{V}\,. \tag{3.20}$$

Notice that although $(\hat{H}_s)_{ij}$ can develop singularities for certain combinations of the coefficients a_i, the physically relevant evolution matrix (3.17) always remains finite after proper combination of relevant terms.

The QCD evolution from μ_0 to μ in the presence of the $\mathcal{O}(\alpha)$ term of the anomalous dimension matrix (3.14) requires beside $\hat{U}_s^{(0)}(\mu,\mu_0)$ and $\hat{U}_s^{(1)}(\mu,\mu_0)$ the additional evolution operator

$$\hat{U}_e^{(0)}(\mu,\mu_0) = \frac{\alpha}{\alpha_s(\mu)}\hat{J}_e\hat{U}_s^{(0)}(\mu,\mu_0) - \frac{\alpha}{\alpha_s(\mu_0)}\hat{U}_s^{(0)}(\mu,\mu_0)\hat{J}_e\,, \tag{3.21}$$

where the matrix $\hat{J}_e$ is found to be

$$\hat{J}_e = \hat{V}\hat{H}_e\hat{V}^{-1}\,, \tag{3.22}$$

with the elements of the matrix kernel $\hat{H}_e$ defined as

$$(\hat{H}_e)_{ij} = \frac{(\hat{G}_e)_{ij}}{2\beta_s^{(0)}\,(1+a_j-a_i)}\,, \tag{3.23}$$

which is precisely the result found in references [190, 193, 239]. Moreover, $(\hat{G}_e)_{ij}$ denotes the elements of the matrix

$$\hat{G}_e = \hat{V}^{-1}\hat{\gamma}_e^{\text{eff}\,(0)\,T}\hat{V}\,. \tag{3.24}$$

The next order QED corrections are represented by the matrix $\hat{U}_e^{(1)}(\mu,\mu_0)$. Following the standard approach [190, 193, 240] it can be written in the following way

$$\begin{aligned}\hat{U}_e^{(1)}(\mu,\mu_0) = {}& \frac{\alpha}{4\pi}\hat{J}_s\hat{J}_e\hat{U}_s^{(0)}(\mu,\mu_0) + \frac{\alpha}{4\pi}\hat{J}_{se}\hat{U}_s^{(0)}(\mu,\mu_0) - \frac{\alpha}{4\pi}\frac{\alpha_s(\mu)}{\alpha_s(\mu_0)}\hat{J}_s\hat{U}_s^{(0)}(\mu,\mu_0)\hat{J}_e \\ & - \frac{\alpha}{4\pi}\hat{U}_s^{(0)}(\mu,\mu_0)\hat{J}_e\hat{J}_s - \frac{\alpha}{4\pi}\hat{U}_s^{(0)}(\mu,\mu_0)\hat{J}_{se} - \frac{\alpha}{4\pi}\frac{\alpha_s(\mu_0)}{\alpha_s(\mu)}\hat{J}_e\hat{U}_s^{(0)}(\mu,\mu_0)\hat{J}_s \\ & + \frac{\alpha}{4\pi}\hat{U}_{se}^{(1)}(\mu,\mu_0)\,,\end{aligned} \tag{3.25}$$

with

$$\hat{J}_{se} = \hat{V}\hat{H}_{se}\hat{V}^{-1}\,, \tag{3.26}$$

and the elements of $(\hat{H}_{se})_{ij}$ given by

$$(\hat{H}_{se})_{ij} = \frac{(\hat{G}_{se})_{ij}}{2\beta_s^{(0)}\,(a_j - a_i)}\,. \tag{3.27}$$

The expression for $\hat{G}_{se}$ is quite complicated [190]. In terms of the relevant coefficients of the QCD beta function (3.11) and of the anomalous dimension matrix (3.14) it reads

$$\hat{G}_{se} = \hat{V}^{-1}\left(-\frac{\beta_s^{(1)}}{\beta_s^{(0)}}\hat{\gamma}_e^{\text{eff}\,(0)\,T} + \left[\hat{\gamma}_e^{\text{eff}\,(0)\,T},\hat{J}_s\right] + \hat{\gamma}_{se}^{\text{eff}\,(1)\,T}\right)\hat{V}\,, \tag{3.28}$$

We note that both matrices $\hat{H}_e$ and $\hat{H}_{se}$ can develop singularities for certain combinations of coefficients a_i and a_j. However, these singularities cancel in the final expression for $\hat{U}(\mu,\mu_0)$ when all contributing terms are combined.

Finally, $\hat{U}_{se}^{(1)}(\mu,\mu_0)$ denotes the QCD evolution due to the $\mathcal{O}(\alpha\alpha_s)$ correction to the beta function (3.11), which has been neglected in the literature throughout. From the conceptual point of view of the expansion in α_s and α in the renormalization group improved perturbation theory, however, one has to take into account this term. For completeness we will thus include it here, although its contribution to the coefficient functions turns out to be negligible small in the case of $\Delta S = 1$ transitions [190]. By straightforward integration and expansion in the electromagnetic coupling constant we find

$$\hat{U}_{se}^{(1)}(\mu,\mu_0) = \frac{\beta_{se}^{(1)}}{\beta_s^{(0)}}\ln\left(\frac{\alpha_s(\mu_0)}{\alpha_s(\mu)}\right)\hat{V}\,\text{diag}\left[\vec{a}\left(\frac{\alpha_s(\mu_0)}{\alpha_s(\mu)}\right)^{\vec{a}}\right]\hat{V}^{-1}\,. \tag{3.29}$$

With the evolution matrices (3.15), (3.17), (3.21) and (3.25) at hand, we are now able to discuss the structure of the coefficient functions $\vec{C}^{\,\text{eff}}(\mu)$. Let us define

$$\vec{C}^{\,\text{eff}}(\mu) = \vec{C}^{\,\text{eff}\,(0)}(\mu) + \frac{\alpha_s(\mu)}{4\pi}\vec{C}_s^{\,\text{eff}\,(1)}(\mu) + \frac{\alpha}{4\pi}\vec{C}_e^{\,\text{eff}\,(1)}(\mu)\,. \tag{3.30}$$

Inserting the expansion (3.13) into the solution of the RGE (3.9), we obtain for the coefficients at a scale μ in terms of the coefficients at the initial scale μ_0

$$\begin{aligned}
\vec{C}^{\text{eff}\,(0)}(\mu) &= \hat{U}_s^{(0)}(\mu,\mu_0)\vec{C}^{\text{eff}\,(0)}(\mu_0)\,,\\
\vec{C}_s^{\text{eff}\,(1)}(\mu) &= \frac{4\pi}{\alpha_s(\mu)}\left(\frac{\alpha_s(\mu_0)}{4\pi}\hat{U}^{(0)}(\mu,\mu_0)\vec{C}_s^{\text{eff}\,(1)}(\mu_0) + \hat{U}^{(1)}(\mu,\mu_0)\vec{C}^{\text{eff}\,(0)}(\mu_0)\right)\,,\\
\vec{C}_e^{\text{eff}\,(1)}(\mu) &= \frac{4\pi}{\alpha}\Bigg(\hat{U}_s^{(0)}(\mu,\mu_0)\vec{C}_e^{\text{eff}\,(1)}(\mu_0) + \hat{U}_e^{(0)}(\mu,\mu_0)\vec{C}^{\text{eff}\,(0)}(\mu_0)\\
&\qquad + \frac{\alpha_s(\mu_0)}{4\pi}\hat{U}_e^{(0)}(\mu,\mu_0)\vec{C}_s^{\text{eff}\,(1)}(\mu_0) + \hat{U}_e^{(1)}(\mu,\mu_0)\vec{C}^{\text{eff}\,(0)}(\mu_0)\Bigg)\,.
\end{aligned} \tag{3.31}$$

Here the first two equations result from pure QCD evolution. The last equation mixes QED, electroweak and QCD effects. Notice that, after the calculation of the two missing elements of $\vec{C}_e^{\text{eff}\,(1)}(\mu_0)$ to be presented in Chapter 4.2, the only unknown $\mathcal{O}(\alpha)$ contribution to the coefficient functions relevant for radiative B decays is the last term in $\vec{C}_e^{\text{eff}\,(1)}(\mu)$.

3.3 Magnetic Penguin Coefficients

In order to calculate the Wilson coefficients of the magnetic moment type operators, one has to match a suitable amplitude computed both in the full and the effective theory between the same external states at the matching scale $\mu_W = \mathcal{O}(M_W)$. Since the Wilson coefficients are independent of the external states in the matrix elements, the initial conditions may be determined by considering the decay process at the quark level. Therefore the off-shell amplitude is first to be calculated in the full theory which contains the full particle spectrum of the SM. In the background field version of the R_ξ gauges [154, 241]

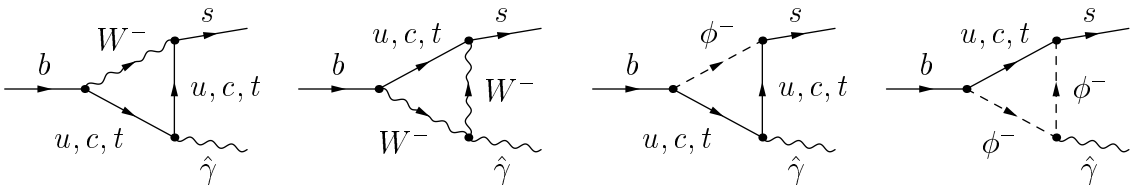

Figure 3.1: The one-loop diagrams contributing to $b \to s\gamma$ in the SM. Note that there is no $W^\pm\phi^\mp\hat{\gamma}$ coupling for a background photon $\hat{\gamma}$.

this amounts to compute the four 1PI electroweak diagrams shown in Fig. 3.1. Expanding up to the second order in the external momenta and m_b, the contributions from the internal quark with different flavor in those diagrams can be separately matched onto the gauge-invariant operators present in the effective Hamiltonian (3.1). For the magnetic type operators Q_7^γ and Q_8^g, each quark flavor yields a UV finite contribution that neither depends on the renormalization scheme nor on the gauge-fixing parameters.

When such a separation of flavor is made and the CKM suppressed u-quark contribution is neglected the effective Wilson coefficient $C_7^{\gamma,\text{eff}\,(0)}(\mu_b)$ at a low-energy scale

i	1	2	3	4	5	6	7	8
a_i	$\frac{14}{23}$	$\frac{16}{23}$	$\frac{6}{23}$	$-\frac{12}{23}$	0.4046	−0.4230	−0.8994	0.1456
h_i	$\frac{626126}{272277}$	$-\frac{56281}{51730}$	$-\frac{3}{7}$	$-\frac{1}{14}$	−0.6494	−0.0380	−0.0185	−0.0057
$\bar{h}_i$	$\frac{313063}{363036}$	0	0	0	−0.9135	−0.0873	−0.0571	−0.0209

Table 3.1: Magic numbers entering the LO expressions of the effective magnetic penguin coefficients.

$\mu_b = \mathcal{O}(m_b)$ can be decomposed into a contribution including only top and charm loops, respectively

$$C_7^{\gamma,\mathrm{eff}\,(0)}(\mu_b) = C_{7,t}^{\gamma,\mathrm{eff}\,(0)}(\mu_b) - C_{7,c}^{\gamma,\mathrm{eff}\,(0)}(\mu_b)\,. \tag{3.32}$$

In the NDR scheme the t-quark contribution is given by

$$C_{7,t}^{\gamma,\mathrm{eff}\,(0)}(\mu_b) = -\frac{1}{2}\eta^{\frac{16}{23}} A_0^t(x_t) - \frac{4}{3}\left(\eta^{\frac{14}{23}} - \eta^{\frac{16}{23}}\right) F_0^t(x_t)\,, \tag{3.33}$$

and the c-quark one reads

$$C_{7,c}^{\gamma,\mathrm{eff}\,(0)}(\mu_b) = \frac{23}{36}\eta^{\frac{16}{23}} + \frac{8}{9}\left(\eta^{\frac{14}{23}} - \eta^{\frac{16}{23}}\right) - \sum_{i=1}^{8} h_i \eta^{a_i}\,, \tag{3.34}$$

where $A_0^t(x_t)$ and $F_0^t(x_t)$ are the so-called Inami-Lim [187, 242] functions

$$\begin{aligned} A_0^t(x_t) &= \frac{46 - 159x_t + 153x_t^2 - 22x_t^3}{36(x_t-1)^3} + \frac{x_t^2(2-3x_t)}{2(x_t-1)^4}\ln x_t\,, \\ F_0^t(x_t) &= \frac{8 - 30x_t + 9x_t^2 - 5x_t^3}{12(x_t-1)^3} + \frac{3x_t^2}{2(x_t-1)^4}\ln x_t\,. \end{aligned} \tag{3.35}$$

Here $\eta = \alpha_s(\mu_W)/\alpha_s(\mu_b)$ and $x_t = m_t^2/M_W^2$ denotes the ratio of the t-quark mass divided by the $W^\pm$ boson mass squared. The numerical values of the magic numbers a_i and h_i entering the above expressions are collected in Tab. 3.1.

In order to see whether the top or the charm contribution is responsible for the substantially enhancement of the $B \to X_s\gamma$ rate due to short-distance QCD effects [181, 182], let us investigate the η-dependence of them separately. As illustrated in Fig. 3.2 the charm contribution $C_{7,c}^{\gamma,\mathrm{eff}\,(0)}(\mu_b)$ is a function of η that varies very slowly in the physically interesting region $0.4 \le \eta \le 1$. Moreover, looking at the individual contributions one observes that the second term in the expression (3.34) is numerically small, while there is a strong cancellation of the renormalization scale dependence between the first and the third component. However, these pieces are not separately physical in any conceivable limit, so the cancellation cannot be considered accidental.

Since the charm contribution is practically renormalization scale independent, the top contribution $C_{7,t}^{\gamma,\mathrm{eff}\,(0)}(\mu_b)$ must be the origin of the enormous QCD enhancement of the $B \to X_s\gamma$ branching ratio. This is indeed the case, because all the powers of η in the expression (3.33) are positive and quite large. As can be seen from Fig. 3.2, the top contribution decreases from 0.450 to 0.325, when η changes from unity to 0.566, corresponding to the scales $\mu = M_W$ and $\mu = 5\,\mathrm{GeV}$. At the same time, the charm

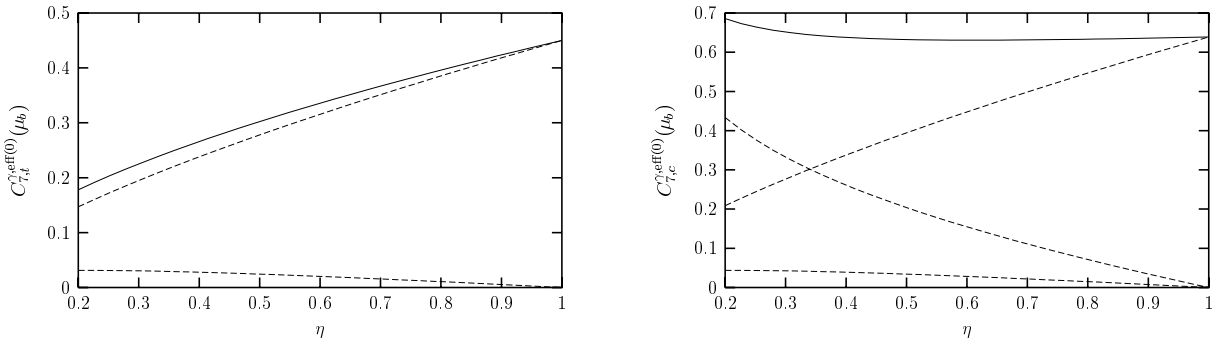

Figure 3.2: $C_{7,t}^{\gamma,\mathrm{eff}(0)}(\mu_b)$ and $C_{7,c}^{\gamma,\mathrm{eff}(0)}(\mu_b)$ as a function of η. The solid lines represent the complete corrections to the Wilson coefficients, the dashed lines the individual components.

contribution changes by only 0.008, from 0.639 to 0.631. In consequence, $|C_7^{\gamma,\mathrm{eff}(0)}(\mu_b)|^2$ increases from 0.036 to 0.094, which leads to a enhancement of the $B \to X_s\gamma$ branching ratio by a factor of 2.6.

The reason for the strong η-dependence of $C_{7,t}^{\gamma,\mathrm{eff}(0)}(\mu_b)$ is easy to identify [180]. It is the large anomalous dimension of the mass operator $m_b(\mu)$ that multiplies the magnetic type operator Q_7^γ. The anomalous dimension of the mass operator, $\gamma_{s,m}^{(0)} = 6C_F$, is responsible for 12/23 out of 16/23 in the power of η that multiplies the numerically dominant Inami-Lim function $A_0^t(x_t)$ in the expression for $C_{7,t}^{\gamma,\mathrm{eff}(0)}(\mu_b)$. Thus the logarithmic QCD effects in the $b \to s\gamma$ transition can be approximately taken into account by simply keeping $m_b(\mu_W)$ renormalized at the electroweak scale $\mu_W = \mathcal{O}(M_W)$.

It would be interesting to understand the physics behind the different optimal normalizations of $m_b(\mu)$ in the top and charm contributions. In this respect, the following observation may be useful. At the matching scale the $b \to s\gamma$ and $b \to sg$ diagrams mediated by charm loops give rise only to the following two dimension six off-shell operators

$$\begin{aligned} Q_{17} &= \frac{ie}{16\pi^2}\left(\bar{s}_L \overleftarrow{\not{D}}\, \sigma^{\mu\nu} b_L F_{\mu\nu} - F_{\mu\nu}\bar{s}_L\sigma^{\mu\nu}\not{D} b_L\right) , \\ Q_{18} &= \frac{ig_s}{16\pi^2}\left(\bar{s}_L \overleftarrow{\not{D}}\, \sigma^{\mu\nu} T^a b_L G^a_{\mu\nu} - G^a_{\mu\nu}\bar{s}_L T^a\sigma^{\mu\nu}\not{D} b_L\right) . \end{aligned} \tag{3.36}$$

The basis of physical operators in the off-shell effective theory for the charm sector can then be chosen to be Q_1–Q_6, Q_{17} and Q_{18}. It is important to note that the particular choice of the physical basis is a matter of convenience. The standard approach, as adopted in Eq. (3.2), is to keep Q_7^γ and Q_8^g as the physical operators, while Q_{17} and Q_{18} are combined with Q_7^γ and Q_8^g to form EOM-vanishing operators. However, one may choose another convention, and do the opposite. The latter choice seems more natural in the charm sector, where non-vanishing off-shell matching arises precisely for Q_{17} and Q_{18}. In consequence, the running of $C_{17,c}^{(0)}(\mu)$ agrees with the one of the charm contribution to the effective Wilson coefficient of Q_7^γ, as given in Eq. (3.34). Evolving the Wilson coefficient of Q_{17} down to μ_b and using the EOM, the off-shell operator Q_{17} reduces to Q_7^γ that contains an overall factor m_b. The b-quark mass associated with the charm loops is therefore a low

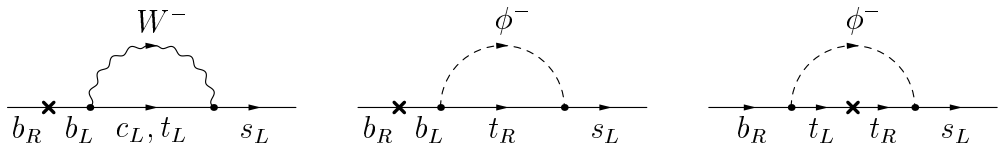

(a) (b) (c)

Figure 3.3: Chirality flow in the diagrams contributing to the Wilson coefficient of the magnetic operator Q_7^γ. The emitted photon can be attached to any of the internal lines.

energy, low virtuality mass $m_b(\mu_b)$.

On the other hand, in the top loops, m_b appears in two different ways: Either through the same mechanism as in the charm loops depicted in Fig. 3.3 (a) and (b), or via the bottom Yukawa coupling $y_b = g\, m_b/(2M_W)$ of a right handed b-quark with a left-handed t-quark, as shown Fig. 3.3 (c). In the first case the RGE running of $C_{17,t}^{(0)}(\mu)$ is much faster than in the charm sector. Such a fast running can be compensated to a large extent by using $m_b(\mu_W)$ in the EOM at the low-energy scale. In the second case it is not necessary to use the EOM to project on the on-shell operator Q_7^γ. The natural normalization scale of the Yukawa coupling $y_b(\mu)$ is given by the heavy masses that are involved in the diagram. Consequently, the b-quark mass associated with the Yukawa contributions is a high-energy mass $m_b(\mu_W)$. This reasoning leads us to the conclusion that the appropriate normalization scale of the t-quark contribution is $m_b(\mu_W)$.

Let us also investigate the η-dependence of the coefficient function of the chromomagnetic operator Q_8^g. Decomposing the effective Wilson coefficient $C_8^{g,\mathrm{eff}\,(0)}(\mu_b)$ as follows

$$C_8^{g,\mathrm{eff}\,(0)}(\mu_b) = C_{8,t}^{g,\mathrm{eff}\,(0)}(\mu_b) - C_{8,c}^{g,\mathrm{eff}\,(0)}(\mu_b)\,, \tag{3.37}$$

the t-quark contribution can be written as

$$C_{8,t}^{g,\mathrm{eff}\,(0)}(\mu_b) = -\frac{1}{2}\eta^{\frac{14}{23}} F_0^t(x_t)\,, \tag{3.38}$$

and the c-quark contribution takes the following form

$$C_{8,c}^{g,\mathrm{eff}\,(0)}(\mu_b) = \frac{1}{3}\eta^{\frac{14}{23}} - \sum_{i=1}^{8} \bar{h}_i \eta^{a_i}\,, \tag{3.39}$$

with $A_0^t(x_t)$ and $F_0^t(x_t)$ given in Eq. (3.35). The numerical values of the powers a_i and the coefficients $\bar{h}_i$ can be found in Tab. 3.1.

The η-dependence of the LO contribution to the effective coefficient of Q_8^g including only top and charm loops is very similar to scale dependence that we have observed in the case of $C_{7,c}^{\gamma,\mathrm{eff}\,(0)}(\mu_b)$ and $C_{7,t}^{\gamma,\mathrm{eff}\,(0)}(\mu_b)$: As can be seen from Fig. 3.4, the t-quark contribution decreases from 0.238 to 0.168 when η changes from unity to 0.566, while the c-quark contribution changes only little from 0.333 to 0.315. The reason for the strong η-dependence of the t-quark contribution to the Wilson coefficient is again the large anomalous dimension of the b-quark mass that multiplies the chromomagnetic operator Q_8^g. In consequence, the logarithmic QCD effects in $b \to sg$ can be approximately taken into account by simply keeping $m_b(\mu)$ renormalized at μ_W and μ_b in the top and charm

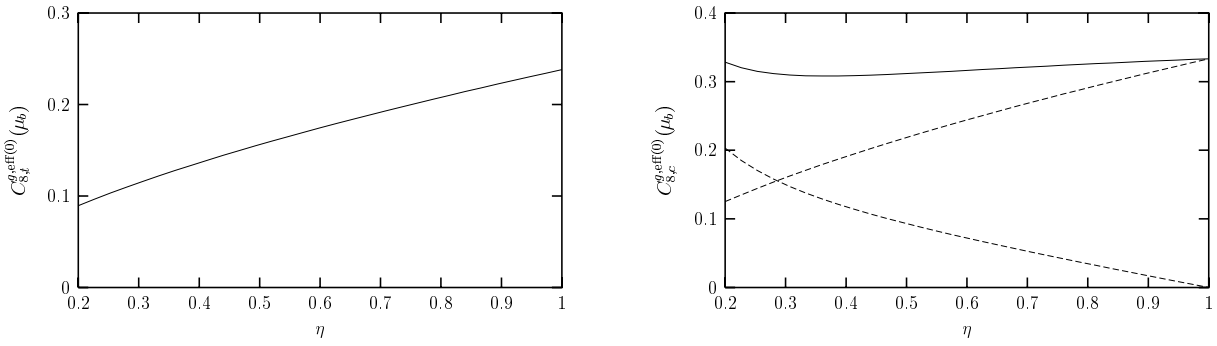

Figure 3.4: $C_{8,t}^{g,\mathrm{eff}\,(0)}(\mu_b)$ and $C_{8,c}^{g,\mathrm{eff}\,(0)}(\mu_b)$ as a function of η. The solid lines represent the complete corrections to the Wilson coefficients, the dashed lines the individual components.

contributions to the decay amplitude. The physical origin behind the different optimal normalizations of the b-quark mass has already been discussed, and thus will not be repeated here.

We have seen in the preceding paragraphs that most of the leading QCD logarithms can be taken into account by keeping the top and charm contribution separated, and by renormalizing $m_b(\mu)$ in Q_7^γ and Q_8^g at μ_W and μ_b in the top and charm contributions to the LO coefficients of the magnetic type operators, respectively. Motivated by this observation we will now rewrite the known $\mathcal{O}(\alpha_s)$ corrections to the Wilson coefficients Q_7^γ and Q_8^g in an analogous manner. Using the separate charm sector and top sector matching conditions for the relevant operators presented in reference [187], we obtain the following expressions for the t- and c-quark contribution to the effective coefficient of the magnetic penguin operator:

$$C_{7,t}^{\gamma,\mathrm{eff}\,(1)}(\mu_b) = -\frac{1}{2}\eta^{\frac{39}{23}}A_1^t(x_t) + \frac{4}{3}\left(\eta^{\frac{39}{23}} - \eta^{\frac{37}{23}}\right)F_1^t(x_t) + \frac{18604}{4761}\left(\eta^{\frac{16}{23}} - \eta^{\frac{39}{23}}\right)A_0^t(x_t) \quad (3.40)$$
$$+ \left(\frac{3582208}{357075}\eta^{\frac{14}{23}} - \frac{148832}{14283}\eta^{\frac{16}{23}} - \frac{128434}{14283}\eta^{\frac{37}{23}} + \frac{3349442}{357075}\eta^{\frac{39}{23}}\right)F_0^t(x_t) + \sum_{i=1}^{8} e_i\eta^{a_i+1}E_0^t(x_t)\,,$$

$$C_{7,c}^{\gamma,\mathrm{eff}\,(1)}(\mu_b) = -\sum_{i=1}^{8}\left(f_i + g_i\eta + l_i\eta\ln\frac{\mu_W^2}{M_W^2}\right)\eta^{a_i}\,. \quad (3.41)$$

In the case of the chromomagnetic penguin operator the $\mathcal{O}(\alpha_s)$ corrections to the effective coefficients including only top and charm loops can be written as[6]

$$C_{8,t}^{g,\mathrm{eff}\,(1)}(\mu_b) = -\frac{1}{2}\eta^{\frac{37}{23}}F_1^t(x_t) + \frac{64217}{19044}\left(\eta^{\frac{14}{23}} - \eta^{\frac{37}{23}}\right)F_0^t(x_t) + \sum_{i=1}^{8}\bar{e}_i\eta^{a_i+1}E_0^t(x_t)\,, \quad (3.42)$$

$$C_{8,c}^{g,\mathrm{eff}\,(1)}(\mu_b) = -\sum_{i=1}^{8}\left(\bar{f}_i + \bar{g}_i\eta + \bar{l}_i\eta\ln\frac{\mu_W^2}{M_W^2}\right)\eta^{a_i}\,. \quad (3.43)$$

[6]Notice that as far as the NLO analysis of $B \to X_s\gamma$ is concerned, only the LO contribution to $C_8^{g,\mathrm{eff}}(\mu_b)$ is needed. However, for completeness we decided to report also the expression for the $\mathcal{O}(\alpha_s)$ correction to the Wilson coefficient of Q_8^g here.

i	1	2	3	4	5	6	7	8
e_i	$\frac{4298158}{816831}$	$-\frac{8516}{2217}$	0	0	−1.9043	−0.1008	0.1216	0.0183
f_i	$-\frac{4246707584}{400095925}$	$-\frac{89606166}{13682585}$	$\frac{45043984}{9898119}$	$\frac{34505657}{45891279}$	2.0040	0.7476	−0.5385	0.0914
g_i	$\frac{3344583818789933}{360615755431797}$	$-\frac{90790555261878016}{13088650734603675}$	$-\frac{6473}{7406}$	$\frac{9371}{22218}$	−2.7231	0.4083	0.1465	0.0205
l_i	$\frac{199164}{30253}$	$-\frac{115596}{25865}$	$-\frac{6}{7}$	$\frac{2}{7}$	−2.0343	0.1232	0.1279	−0.0064
$\bar{e}_i$	$\frac{2149079}{1089108}$	$-\frac{8516}{2217}$	0	0	−2.6788	0.2318	0.3741	−0.0670
$\bar{f}_i$	$-\frac{456775521}{128030696}$	0	$\frac{12757}{9072}$	$-\frac{15511}{3888}$	3.2850	3.6851	−0.1424	0.6492
$\bar{g}_i$	$\frac{3344583818789933}{961642014484792}$	0	0	0	−3.8308	−0.9387	0.4508	−0.0747
$\bar{l}_i$	$\frac{149373}{60506}$	0	0	0	−2.8617	−0.2832	0.3936	0.0233

Table 3.2: Magic numbers entering the $\mathcal{O}(\alpha_s)$ corrections to the effective magnetic penguin coefficients. In their evaluation the three-loop anomalous dimensions computed in references [196, 197] have been used.

The Inami-Lim functions $A_0^t(x_t)$ and $F_0^t(x_t)$ have already been given in Eq. (3.35), and the one-loop function characterizing the effective off-shell vertex involving a gluon reads

$$E_0^t(x_t) = -\frac{4+42x_t-21x_t^2-7x_t^3}{36\,(x_t-1)^3} - \frac{4-16x_t+9x_t^2}{6\,(x_t-1)^4}\ln x_t\,. \tag{3.44}$$

The remaining two-loop functions $A_1^t(x_t)$ and $F_1^t(x_t)$ take the following form

$$\begin{aligned}
A_1^t(x_t) &= \frac{2006-9113x_t+20682x_t^2-18665x_t^3-94x_t^4}{243\,(x_t-1)^4} \\
&\quad - \frac{464-2968x_t+6788x_t^2-4632x_t^3-1176x_t^4-204x_t^5}{81\,(x_t-1)^5}\ln x_t \\
&\quad - \frac{x_t\,(8-256x_t+478x_t^2-70x_t^3-16x_t^4)}{9\,(x_t-1)^5}\ln^2 x_t \\
&\quad - \frac{x_t\,(16-160x_t+244x_t^2+32x_t^3)}{9\,(x_t-1)^4}\mathrm{Li}_2\,(1-x_t) \\
&\quad - \left(\frac{152-794x_t+804x_t^2+202x_t^3+68x_t^4}{27\,(x_t-1)^4} + \frac{x_t^2\,(56-92x_t-12x_t^2)}{3\,(x_t-1)^5}\ln x_t\right)\ln\frac{\mu_W^2}{M_W^2}\,, \\
F_1^t(x_t) &= \frac{1016-2966x_t+31779x_t^2+11890x_t^3-247x_t^4}{648\,(x_t-1)^4} \\
&\quad - \frac{304-2114x_t+3007x_t^2+4839x_t^3+1086x_t^4-210x_t^5}{108\,(x_t-1)^5}\ln x_t \\
&\quad + \frac{x_t\,(1+226x_t+101x_t^2-44x_t^3+4x_t^4)}{6\,(x_t-1)^5}\ln^2 x_t \\
&\quad + \frac{x_t\,(1+41x_t+40x_t^2-4x_t^3)}{3\,(x_t-1)^4}\mathrm{Li}_2\,(1-x_t)
\end{aligned}$$

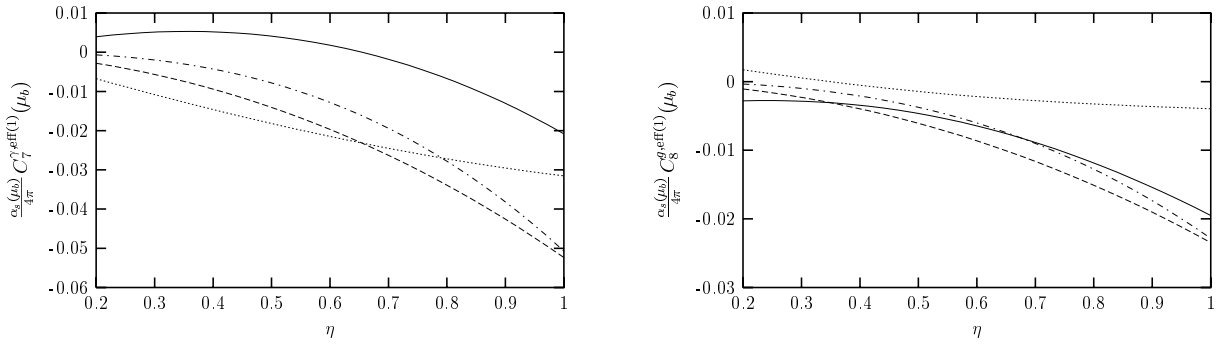

Figure 3.5: The complete $\mathcal{O}(\alpha_s)$ corrections to the magnetic penguin coefficients as a function of η, and their individual components, as explained in the text.

$$-\left(\frac{56-338x_t-447x_t^2-170x_t^3+35x_t^4}{18\,(x_t-1)^4}+\frac{x_t^2\,(31+17x_t)}{(x_t-1)^5}\ln x_t\right)\ln\frac{\mu_W^2}{M_W^2}\,, \qquad (3.45)$$

where $\mathrm{Li}_2(x) = -\int_0^x dt\,\ln(1-t)/t$ denotes the dilogarithmic or Spence function. The magic numbers necessary to calculate the $\mathcal{O}(\alpha_s)$ corrections to the effective coefficients of Q_7^γ and Q_8^g are summarized in Tab. 3.2.

The η-dependence of the $\mathcal{O}(\alpha_s)$ contributions to the effective Wilson coefficients of the magnetic type operators is illustrated in Fig. 3.5. From these figures we read off, that the top loop contribution to the $\mathcal{O}(\alpha_s)$ correction of $C_7^{\gamma,\mathrm{eff}}(\mu_b)$ represented by a dashed line, increases from -0.052 to -0.018 when η changes from unity to 0.566, while the charm loop contribution represented by a dotted line, changes only in a minor way from -0.032 to -0.020. The corresponding changes in the case of $C_8^{g,\mathrm{eff}}(\mu_b)$ are -0.023 to -0.008 and -0.004 to -0.002, respectively. Furthermore, in both cases the t-quark contribution can relatively well be approximated by the first term in the expressions for the $\mathcal{O}(\alpha_s)$ corrections to the effective Wilson coefficients of the magnetic type operators. This important aspect is illustrated by the dash-dotted lines in Fig. 3.5. Including only the first term of Eq. (3.40) and Eq. (3.42) in the effective coefficients of Q_7^γ and Q_8^g, we find that the $\mathcal{O}(\alpha_s)$ correction to $C_7^{\gamma,\mathrm{eff}}(\mu_b)$ increases from -0.051 to -0.011, while the $\mathcal{O}(\alpha_s)$ correction to $C_8^{g,\mathrm{eff}}(\mu_b)$ changes from -0.023 to -0.005, when η is varied between the ranges given above. As the large anomalous dimension of the b-quark mass is responsible for most of the power of η that multiplies the numerically dominant functions $A_1^t(x_t)$ and $F_1^t(x_t)$ in Eqs. (3.40) and (3.42), the features observed at LO carry on at the NLO level, lending support to the idea that they are not due to a numerical coincidence, and remain valid at the NNLO, too.

3.4 Non-Perturbative Corrections

In order to calculate the final rate we have to pass from the calculated b-quark decay rate to the B-meson decay rate. Going beyond leading order in the $1/m_b$ expansion the first subleading corrections are of order $1/m_b^2$. If one neglects perturbative QCD corrections and assumes that the decay $B \to X_s\gamma$ is due to the operator Q_7^γ only, the calculation of

these subleading contributions amounts to work out the imaginary part of the forward scattering amplitude

$$T_{7\gamma,7\gamma}(k) = i \int d^4x \, \langle B|T\{Q_7^{\gamma\dagger}(x), Q_7^{\gamma}(0)\}|B\rangle \, e^{ik\cdot x} \,. \tag{3.46}$$

Using the OPE for $T\{Q_7^{\gamma\dagger}(x), Q_7^{\gamma}(0)\}$ and HQET methods, the corresponding decay width reads

$$\Gamma_{7\gamma,7\gamma}(B \to X_s\gamma) = \frac{\alpha}{32\pi^4} G_F^2 m_b^5 \, |V_{ts}^* V_{tb}|^2 \, \left|C_7^{\gamma,\mathrm{eff}}(m_b)\right|^2 \left(1 + \frac{\delta_{m_b}^{\mathrm{NP}}}{m_b^2}\right) \,, \tag{3.47}$$

modulo higher terms in the $1/m_b$ expansion. Here $\delta_{m_b}^{\mathrm{NP}}$ parameterizes non-perturbative corrections to the radiative B-meson decay rate. Following references [207, 208] it can be expressed in terms of the HQET parameters λ_1 and λ_2 as

$$\delta_{m_b}^{\mathrm{NP}} = \frac{1}{2}\lambda_1 - \frac{9}{2}\lambda_2 \,. \tag{3.48}$$

The non-perturbative correction (3.47) is around 4% in magnitude. The discussion of non-perturbative effects becomes much more complex if we take into account operators other than Q_7^{γ}. In this case it is no longer possible to apply the OPE in analogy to $B \to X_u e\bar{\nu}_e$, because the b-quark annihilation and the photon emission may now be separated in space-time by more than $1/\Lambda_{\mathrm{QCD}}$ with Λ_{QCD} being the QCD scale parameter. The contribution of Q_8^g to the branching ratio of $B \to X_s\gamma$ has been analyzed in reference [243] with the help of fragmentation functions. Important non-perturbative effects have been found for photons with energies below 1 GeV, which are practically unobservable at the inclusive level, because of the overwhelming $b \to c$ background. For the current experimental cut-off of 2.0 GeV [30] a reliable approximation is thus given by the perturbative contribution to the b-quark decay rate from the matrix elements of Q_8^g. The accuracy of this approximation does not need to be known precisely, because the perturbative contribution of Q_8^g is less than 3%. Due to the smallness of the Wilson coefficients $C_3(m_b)$–$C_6(m_b)$ similar conclusions can be drawn for the QCD penguin operators. Perturbative effects for their matrix elements are even smaller than that of Q_8^g. As far as non-perturbative effects are concerned, one might worry about the production of virtual vector mesons that convert into a real photon. However, the creation of such tranverse mesons is impossible in the factorization approximation, because Q_3–Q_6 contain no magnetic type currents. In addition, deviations from the factorization approximation are either suppressed by α_s or by $\Lambda_{\mathrm{QCD}}/m_b$, as has been shown in references [244, 245]. Therefore its seems reasonable to conclude that the total non-perturbative $1/m_b^2$ correction to the branching ratio of the $B \to X_s\gamma$ decay is well below 10%, that is, it is smaller than the inaccuracy of the perturbative calculation.

There are also non-perturbative corrections that scale with $1/m_c^2$ which are induced by the interference of the four quark operator Q_1–Q_6 with the magnetic operator Q_7^{γ}. A particular non-perturbative contribution comes from the diagrams shown in Fig. 3.6. It arises when the gluon is soft and interacts with the spectator cloud of the b-quark inside the B-meson. This is the effect first pointed out in reference [209] and further discussed by several authors [210–213]. Staying with the quark picture, one may evaluate the vertex diagram depicted in Fig. 3.6 (a) directly. To first order in the gluon momentum k, one finds, that the vertex function is proportional to the following local operator

$$Q_{\gamma g} = \frac{e g_s Q_c}{24\pi^2 m_c^2} \, (\bar{s}_L \gamma_\mu T^a b_R) \, \epsilon^{\mu\nu\lambda\rho} G^a_{\nu\sigma} \partial^\sigma F_{\lambda\rho} \,, \tag{3.49}$$

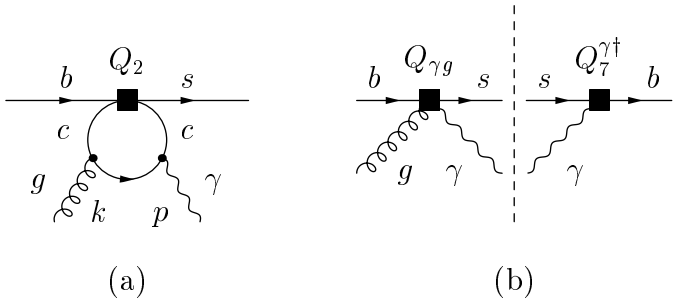

Figure 3.6: (a) Feynman diagram from which the operator $Q_{\gamma g}$ arises. The second diagram with the photon and gluon interchanged is omitted. (b) Relevant cut-diagram for the interference of Q_2 and Q_7^γ. Analogous diagrams with more gluons give effects suppressed by additional powers of $1/m_c$.

where our sign convention is such that $\epsilon^{0123} = +1$. Then working out the cut-diagram shown in Fig. 3.6 (b), one obtains the non-perturbative contribution $\Gamma_{2,7\gamma}(B \to X_s\gamma)$ to the decay width, which is due to the interference of Q_2 and Q_7^γ. Ignoring the small terms in the unitarity relation of the CKM matrix associated with the u-quark, one can write $V_{cs}^* V_{cb} = -V_{ts}^* V_{tb}$, and finally obtains

$$\Gamma_{2,7\gamma}(B \to X_s\gamma) = \frac{\alpha}{32\pi^4} G_F^2 m_b^5 \left|V_{ts}^* V_{tb}\right|^2 \left|C_7^{\gamma,\mathrm{eff}}(m_b)\right|^2 \frac{\delta_{m_c}^{\mathrm{NP}}}{m_c^2}\,, \tag{3.50}$$

with the $1/m_c^2$ correction to the radiative B decay rate given by

$$\delta_{m_c}^{\mathrm{NP}} = -\frac{1}{9}\lambda_2 \frac{C_2(m_b)}{C_7^{\gamma,\mathrm{eff}}(m_b)}\,. \tag{3.51}$$

This result corresponds to the leading term in an expansion in the ratio $t = k \cdot p/2m_c^2$, where p denotes the momentum of the photon. As the expansion parameter is approximately $m_b\Lambda_{\mathrm{QCD}}/2m_c^2 \approx 0.3$ rather than $\Lambda_{\mathrm{QCD}}^2/m_c^2 \approx 0.03$, it is a priori not clear whether formally higher order terms in the $1/m_c$ expansion are numerically suppressed. Although the presence of unknown matrix elements in these contributions does not allow a definite estimate of their actual size, the detailed investigations [211–213] have shown that these contributions are weighted by very small Wilson coefficients. Consequently, these higher order contributions are expected to be substantially smaller than the leading order term (3.50), and the 3% enhancement from $1/m_c^2$ corrections found in reference [213] appears to be a good estimate of the long-distance contributions to the $B \to X_s\gamma$ decay rate, stemming from the interference of Q_2 and Q_7^γ.

Notice that the corresponding long-distance contributions from u-quark loops are CKM suppressed in the $B \to X_s\gamma$ case, but this does not hold in the case of $B \to X_d\gamma$. Naively, one could expect that the corresponding contributions from u-quarks scale with $1/m_u^2$. However, following the approach [213], it is easy to see that the general $\bar{s}b\gamma g$ vertex function cannot be expanded in the parameter t in this case. Yet an expansion in inverse powers of t is reasonable. The leading term in this expansion scales like $1/t \sim m_u^2/k \cdot p$ and therefore cancels the artificial $1/m_u^2$ divergence present in the prefactor of the analogue of $Q_{\gamma g}$ involving a u-quark [213]. Thus, although the expansion in inverse powers

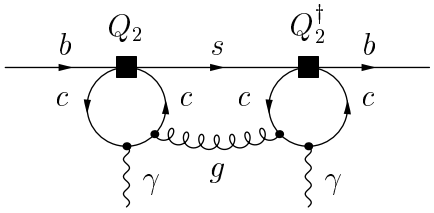

Figure 3.7: Diagram contributing to the forward scattering amplitude of Q_2 at $\mathcal{O}(\alpha_s)$.

of t induces non-local operators, whose matrix elements cannot be estimated reliably, one expects from naive dimensional counting, that the leading term scales with $\Lambda_{\rm QCD}/m_b$.

Finally, let us emphasize that a systematic analysis of non-perturbative effects in the matrix elements of Q_1 and Q_2 at first order in α_s is still missing [246]. Such an analysis would require to calculate the forward scattering amplitude induced by diagrams like the one presented in Fig. 3.7. In this case rigorous techniques such as the OPE do not seem to be applicable, and no sufficiently precise argument can be given that these contributions are either suppressed by $\Lambda_{\rm QCD}/m_b$ or $\Lambda_{\rm QCD}/m_c$, or small for any other reason [246].

3.5 Branching Ratio of the $B \to X_s\gamma$ Decay

At this point, we are ready to use the calculated coefficients of the magnetic penguin operators Q_7^γ and Q_8^g at μ_b as an input to determine the NLO expression for the $B \to X_s\gamma$ branching ratio. Making an explicit lower cut on the photon energy $E_\gamma > (1-\delta)E_\gamma^{\rm max} = (1-\delta)\, m_b/2$ in the B-meson rest frame the branching ratio of the $B \to X_s\gamma$ decay can be written in the following compact form:

$$\mathrm{BR}(B \to X_s\gamma)_{E_\gamma > (1-\delta)E_\gamma^{\rm max}} = \mathrm{BR}(B \to X_c e\bar\nu_e)_{\rm exp} \left|\frac{V_{ts}^* V_{tb}}{V_{cb}}\right|^2 \frac{6\alpha}{\pi C}\big(P(\delta) + N(\delta)\big)\,, \qquad (3.52)$$

where the electromagnetic coupling $\alpha = 1/137.036$ is the fine structure constant renormalized at $k^2 = 0$, as is appropriate for real photon emission [214]. The function $P(\delta)$ is given by the perturbative ratio

$$\left|\frac{V_{ub}}{V_{cb}}\right|^2 \frac{\Gamma(b \to X_s\gamma)_{E_\gamma > (1-\delta)E_\gamma^{\rm max}}}{\Gamma(b \to X_u e\bar\nu_e)} = \left|\frac{V_{ts}^* V_{tb}}{V_{cb}}\right|^2 \frac{6\alpha}{\pi} P(\delta)\,, \qquad (3.53)$$

and $N(\delta)$ denotes the non-perturbative correction. Notice that contrary to the standard approach [186, 196, 216, 218, 247], we have chosen the charmless semileptonic decay rate

$$\Gamma(b \to X_u e\bar\nu_e) = \frac{G_F^2 m_{b,\rm pole}^5}{192\pi^3} |V_{ub}|^2 \left[1 + \frac{\alpha_s(\mu_b)}{4\pi}\left(\frac{50}{3} - \frac{8}{3}\pi^2\right)\right] + \mathcal{O}(\alpha_s^2)\,, \qquad (3.54)$$

corrected for the appropriate CKM angles to be the normalization factor in the definition of $P(\delta)$. This particular choice of normalization introduced in reference [180] is motivated by the need for separating the problem of the determination of the c-quark mass from

the problem of convergence of the perturbation series in the partonic decay $b \to s\gamma$. This modification is offset by the factor

$$C = \left|\frac{V_{ub}}{V_{cb}}\right|^2 \frac{\Gamma(B \to X_c e \bar{\nu}_e)}{\Gamma(B \to X_u e \bar{\nu}_e)}\,, \tag{3.55}$$

in the expression (3.52). Notice that C can either be measured or calculated. A determination along the lines of the upsilon expansion [248,249] of this so-called non-perturbative semileptonic phase-space factor leads to $C = 0.575 \pm 0.02$ at NNLO [180], which will be our input in the numerical analysis of the branching ratio of $B \to X_s\gamma$ presented at the end of the next chapter.

The perturbative quantity $P(\delta)$ is given by

$$P(\delta) = \left|\left(1 + \frac{\alpha_s(\mu_W)}{4\pi}\ln\frac{\mu_W^2}{m_t^2}\right) r(\mu_W) K_t + K_c + \varepsilon_{\rm ew}\right|^2 + B(\delta)\,, \tag{3.56}$$

where K_t denotes the contribution to the $b \to s\gamma$ amplitude stemming from top loops. K_c summarizes the contributions from the light quark loops, among which the charm loops are by far dominant. The electroweak correction to the $b \to s\gamma$ amplitude that will be discussed in Chapter 4 is denoted by $\varepsilon_{\rm ew}$. Realize that the mass ratio $r(\mu_W) = m_{b,\overline{\rm MS}}(\mu_W)/m_{b,1S}$ appears in Eq. (3.56) because we keep the $\overline{\rm MS}$ mass $m_{b,\overline{\rm MS}}(\mu_W)$ renormalized at μ_W in the t-quark contribution to the Wilson coefficient of Q_7^γ, while all the kinematical factors of m_b are expressed in terms of the so-called bottom $1S$ mass $m_{b,1S}$, which is defined as half of the perturbative contribution to the Υ-meson [248, 249]. As argued in those articles, expressing the kinematical factor of m_b in inclusive B-meson decay rates in terms of the bottom $1S$ mass improves the behavior of the QCD perturbative series with respect to what would be obtained using the pole mass $m_{b,\rm pole}$ or $m_{b,\overline{\rm MS}}(m_b)$. At NLO the mass ratio $r(\mu_W)$ reads

$$r(\mu_W) = \eta^{\frac{12}{23}}\left[1 + \frac{\alpha_s(\mu_b)}{4\pi}\left(\frac{7462}{1587}\eta - \frac{15926}{1587} + \frac{12}{23}\beta_s^{(0)}\ln\frac{m_b^2}{\mu_b^2}\right) + \frac{2}{9}\alpha_s(m_b)^2\right]\,, \tag{3.57}$$

with $\beta_s^{(0)}$ given in Eq. (3.12). Following reference [180] the $\mathcal{O}(\alpha_s^2)$ term in the above equation has been included along the lines of the upsilon expansion. Its effect on $r(\mu_W)$ is at the level of 1% only, and it is canceled by an analogous term in the t-quark contribution K_t, as we will see in a moment.

The bremsstrahlungs function $B(\delta)$ arises from the $b \to s\gamma g$ and the $b \to s\gamma\bar{q}q$ transitions with $q = u, d, s$. It is the only δ-dependent part of the perturbative function $P(\delta)$ and will be given in Appendix C. We recall that the theoretical prediction for the branching ratio diverges in the limit $\delta \to 1$, because of a logarithmic singularity in $B(\delta)$, which reflects the soft-photon divergence of the $b \to s\gamma g$ subprocess. On the other hand, the $\mathcal{O}(\alpha_s)$ to the contribution to $B(\delta)$ changes the $B \to X_s\gamma$ branching ratio by less than 4% if the cut-off energy E_γ is varied between 1 GeV and 2 GeV. Therefore we do not split the top and charm contributions to this function, as it would not improve the overall accuracy at all, but would make the formulae unnecessarily complicated.

Before giving the explicit expressions for K_t and K_c, it is worthwhile to remember that the $B \to X_s\gamma$ decay rate is proportional to $m_{b,\rm pole}^3$ present in the two body phase space and to $m_{b,\overline{\rm MS}}(m_b)^2$ coming from the normalization of the magnetic type operator Q_7^γ. On

the other hand, the semileptonic decay rate (3.54) is proportional to $m^5_{b,\mathrm{pole}}$ present in the three body phase space. Thus the m_b^5 factors present in both rates differ by a $\mathcal{O}(\alpha_s)$ correction which is easily obtained from

$$\frac{m_{b,\mathrm{pole}}}{m_{b,\overline{\mathrm{MS}}}(\mu_b)} = 1 + \frac{\alpha_s(\mu_b)}{4\pi}\left(\frac{16}{3} - 4\ln\frac{m_b^2}{\mu_b^2}\right) + \mathcal{O}(\alpha_s^2)\,, \tag{3.58}$$

and has to be included in order to find the explicit result for the perturbative quantity $P(\delta)$ beyond LO approximation.

Finally we have to recall that as far as the NLO analysis of the $B \to X_s\gamma$ branching ratio is concerned, only the LO contributions of the Wilson coefficients of the QCD penguin operators Q_1–Q_6 are needed. The coefficient functions $C_1^{(0)}(\mu_b)$–$C_6^{(0)}(\mu_b)$ are equal to those found in reference [196]. They read

$$\begin{aligned}
C_1^{(0)}(\mu_b) &= \eta^{a_3} - \eta^{a_4}\,,\\
C_2^{(0)}(\mu_b) &= \frac{2}{3}\eta^{a_3} + \frac{1}{3}\eta^{a_4}\,,\\
C_3^{(0)}(\mu_b) &= \frac{2}{63}\eta^{a_3} - \frac{1}{27}\eta^{a_4} - 0.0659\eta^{a_5} + 0.0595\eta^{a_6} - 0.0218\eta^{a_7} + 0.00355\eta^{a_8}\,,\\
C_4^{(0)}(\mu_b) &= \frac{1}{21}\eta^{a_3} + \frac{1}{9}\eta^{a_4} + 0.0237\eta^{a_5} - 0.0173\eta^{a_6} - 0.1336\eta^{a_7} - 0.0316\eta^{a_8}\,,\\
C_5^{(0)}(\mu_b) &= -\frac{1}{126}\eta^{a_3} + \frac{1}{108}\eta^{a_4} + 0.0094\eta^{a_5} - 0.0100\eta^{a_6} + 0.0010\eta^{a_7} - 0.0017\eta^{a_8}\,,\\
C_6^{(0)}(\mu_b) &= -\frac{1}{84}\eta^{a_3} - \frac{1}{36}\eta^{a_4} + 0.0108\eta^{a_5} + 0.0163\eta^{a_6} + 0.0103\eta^{a_7} + 0.0023\eta^{a_8}\,.
\end{aligned} \tag{3.59}$$

Bearing all this in mind, we are now able to write down the NLO expressions for the functions K_t and K_c entering the perturbative quantity $P(\delta)$. Our result for the t-quark contribution K_t reads

$$\begin{aligned}
K_t = {} & \left(1 - \frac{2}{9}\alpha_s(m_b)^2\right)\left[-\frac{1}{2}\eta^{\frac{4}{23}}A_0^t(x_t) + \frac{4}{3}\left(\eta^{\frac{4}{23}} - \eta^{\frac{2}{23}}\right)F_0^t(x_t)\right]\\
& + \frac{\alpha_s(\mu_b)}{4\pi}\Bigg\{E_0^t(x_t)\sum_{k=1}^{8} e_k\eta^{a_k+\frac{11}{23}} - \eta^{\frac{4}{23}}\Bigg(\frac{1}{2}\eta A_1^t(x_t) - \Bigg[\frac{12523}{3174} - \frac{7411}{4761}\eta - \frac{2}{9}\pi^2\\
& - \frac{2}{3}\left(\ln\frac{m_b^2}{\mu_b^2} - \frac{3}{4}\eta\ln\frac{\mu_W^2}{m_t^2}\right)\Bigg]A_0^t(x_t) - \frac{4}{3}\eta F_1^t(x_t) + \Bigg[\frac{50092}{4761} - \frac{1110842}{357075}\eta - \frac{16}{27}\pi^2\\
& - \frac{16}{9}\left(\ln\frac{m_b^2}{\mu_b^2} - \frac{3}{4}\eta\ln\frac{\mu_W^2}{m_t^2}\right)\Bigg]F_0^t(x_t)\Bigg) - \eta^{\frac{2}{23}}\Bigg(\frac{4}{3}\eta F_1^t(x_t) - \Bigg[\frac{2745458}{357075} - \frac{38890}{14283}\eta\\
& - \frac{4}{9}\pi\,(\pi + i) - \frac{8}{9}\left(\ln\frac{m_b^2}{\mu_b^2} - \frac{3}{4}\eta\ln\frac{\mu_W^2}{m_t^2}\right)\Bigg]F_0^t(x_t)\Bigg)\Bigg\}\,,
\end{aligned} \tag{3.60}$$

and agrees with the expression for K_t given in reference [180].[7] Notice that the $\mathcal{O}(\alpha_s^2)$ term in the above equation has been included along the lines of the upsilon expansion. Its effect on K_t is at the level of 1% only, and it is compensated by an analogous term in the ratio $r(\mu_W)$, as has already been mentioned.

[7] Note that the terms proportional to $\ln\mu_W^2/m_t^2$ in Eq. (3.60) differ from the analogous ones in reference [180], because our definition of the two-loop functions $A_1^t(x_t)$ and $F_1^t(x_t)$ is different from the one used in that paper.

k	1	2	3	4	5	6	7	8
d_k	1.4107	−0.8380	−0.4286	−0.0714	−0.6494	−0.0380	0.0185	−0.0057
$\tilde{d}_k$	−17.6507	11.3460	2.4692	−0.8056	4.8898	−0.2308	−0.5290	0.1994
$\tilde{d}_k^\eta$	9.2746	−6.9366	−0.8740	0.4218	−2.7231	0.4083	0.1465	0.0205
$\tilde{d}_k^a$	0	0	0.8571	0.6667	0.1298	0.1951	0.1236	0.0276
$\tilde{d}_k^b$	0	0	0.8571	0.6667	0.2637	0.2906	−0.0611	−0.0171
$\tilde{d}_k^{i\pi}$	0.4702	0	−0.4268	−0.2222	−0.9042	−0.1150	−0.0975	0.0115

Table 3.3: Magic numbers entering the expression for K_c.

The NLO expression for the light quark contribution K_c is given by

$$K_c = \sum_{k=1}^{8} \eta^{a_k} \left\{ d_k + \frac{\alpha_s(\mu_b)}{4\pi} \left[\beta_s^{(0)} a_k d_k \left(\ln \frac{m_b^2}{\mu_b^2} + \eta \ln \frac{\mu_W^2}{M_W^2} \right) \right.\right. \tag{3.61}$$
$$\left.\left. + \tilde{d}_k + \tilde{d}_k^\eta \eta + \tilde{d}_k^a a(z) + \tilde{d}_k^b b(z) + \tilde{d}_k^{i\pi} i\pi \right] \right\} + \frac{V_{us}^* V_{ub}}{V_{ts}^* V_{tb}} \frac{\alpha_s(\mu_b)}{4\pi} \left(\eta^{a_3} + \eta^{a_4}\right) \big(a(z) + b(z)\big) \,,$$

where $z = m_c^2/m_b^2$ and $\beta_s^{(0)}$ has been reported in Eq. (3.12). The functions $a(z)$ and $b(z)$ originate from the two-loop $b \to s\gamma$ matrix elements of the four quark operators Q_1 and Q_2, which were calculated independently by two groups [203–205], and will be given in Appendix E. The relevant diagrams are shown in Fig. 3.8. The magic numbers $\tilde{d}_k$, $\tilde{d}_k^\eta$, $\tilde{d}_k^a$, $\tilde{d}_k^b$ and $\tilde{d}_k^{i\pi}$ necessary to compute K_c can be found in Tab. 3.3. In their evaluation all relevant two- and one-loop matrix elements, namely

$$\begin{aligned}
r_{1,s} &= \frac{833}{729} - \frac{a(z)}{3} - \frac{b(z)}{3} + \frac{40}{243} i\pi \,, \\
r_{2,s} &= -\frac{1666}{243} + 2a(z) + 2b(z) - \frac{80}{81} i\pi \,, \\
r_{3,s} &= \frac{2392}{243} + \frac{8\pi}{3\sqrt{3}} + \frac{32}{9} X_b - a(1) + 2b(1) + \frac{56}{81} i\pi \,, \\
r_{4,s} &= -\frac{761}{729} - \frac{4\pi}{9\sqrt{3}} - \frac{16}{27} X_b + \frac{a(1)}{6} + \frac{5}{3} b(1) + 2b(z) - \frac{148}{243} i\pi \,, \\
r_{5,s} &= \frac{56680}{243} + \frac{32\pi}{3\sqrt{3}} + \frac{128}{9} X_b - 16a(1) + 32b(1) + \frac{896}{81} i\pi \,, \\
r_{6,s} &= \frac{5710}{729} - \frac{16\pi}{9\sqrt{3}} - \frac{64}{27} X_b - \frac{10}{3} a(1) + \frac{44}{3} b(1) + 12a(z) + 20b(z) - \frac{2296}{243} i\pi \,, \\
r_{7\gamma,s} &= \frac{32}{9} - \frac{8}{9}\pi^2 \,, \\
r_{8g,s} &= \frac{44}{9} - \frac{8}{27}\pi^2 + \frac{8}{9} i\pi \,,
\end{aligned} \tag{3.62}$$

have been taken into account. Consequently, our results for the magic numbers $\tilde{d}_k$, $\tilde{d}_k^\eta$, $\tilde{d}_k^a$, $\tilde{d}_k^b$ and $\tilde{d}_k^{i\pi}$ agree with those presented in reference [206]. The constants X_b, $a(1)$

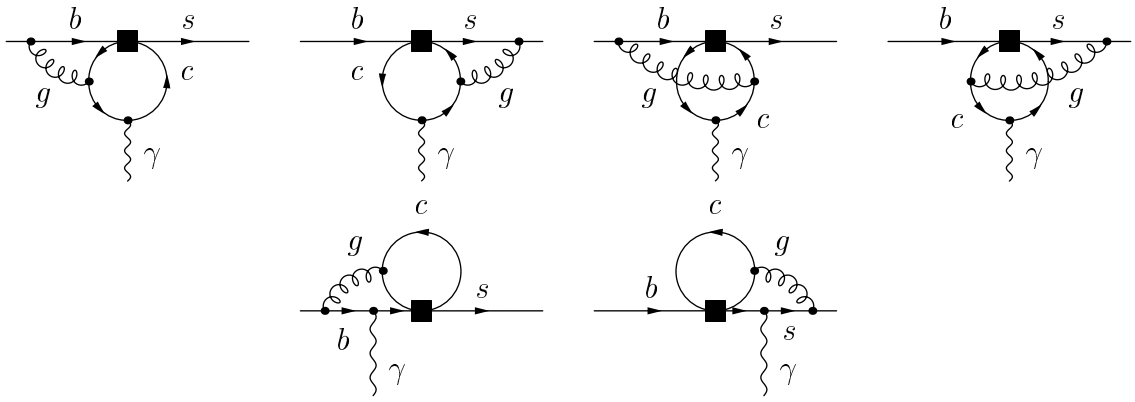

Figure 3.8: Charm loop contributions to the matrix element of the four quark operators.

and $b(1)$ entering the matrix elements of the QCD penguin operators Q_3–Q_6 are given in Appendix E. Although the inclusion of the two-loop matrix elements of the four quark operators Q_3–Q_6 calculated by Buras et al. [206] is necessary in order to complete the NLO QCD calculation of $B \to X_s\gamma$, their effect on the branching ratio is small: It leads to a reduction of around 1%. Notice that, such a small effect of the non-zero values of $r_{3,s}$–$r_{6,s}$ is due to the smallness of the Wilson coefficients of the corresponding operators.

As discussed in Section 3.4, the non-perturbative corrections to the branching ratio of the $B \to X_s\gamma$ decay are only partly known. Neglecting higher order terms in the HQE, as well as non-perturbative effects due to higher intermediate $\bar{c}c$ states, to light quark loops and to the motion of the b-quark inside the B-meson we find that the non-perturbative quantity $N(\delta)$ entering Eq. (3.52) is given by

$$N(\delta) = -\frac{1}{18}\left(\eta^{-\frac{12}{23}} + \eta^{\frac{6}{23}}\right)\left(r(\mu_W)K_t^{(0)} + K_c^{(0)}\right)\frac{\lambda_2}{m_c^2}\,, \tag{3.63}$$

where $K_t^{(0)}$ and $K_c^{(0)}$ denote the LO contributions to K_t and K_c, which are obtained from Eqs. (3.60) and (3.61) by neglecting the $\mathcal{O}(\alpha_s)$ as well as the $\mathcal{O}(\alpha_s^2)$ terms. Realize that in the above expression for $N(\delta)$ the calculable $\Lambda_{\rm QCD}^2/m_c^2$ corrections stemming from the interference between the current-current operators Q_1, Q_2 and the magnetic photon penguin operator Q_7^γ are taken into account, while the calculable $\Lambda_{\rm QCD}^2/m_b^2$ corrections to the semileptonic and the radiative B decay have canceled out because of our normalization to the charmless semileptonic decay rate.

Chapter 4

Electroweak Effects in Radiative B Decays

This chapter is devoted to the analysis of electroweak effects in the total branching ratio of $B \to X_s\gamma$. We compute the complete $\mathcal{O}(\alpha)$ Wilson coefficients relevant for radiative decays of the B-meson in the SM. This is a necessary step in the calculation of the $\mathcal{O}(\alpha\alpha_s^n L^n)$ corrections and improves on existing analyses [214–219]. The main difference and technical hurdle with respect to reference [218] is due to the presence of virtual photons in the two-loop diagrams. The resulting IR divergences are removed in the matching with the effective low-energy theory of quarks, photons and gluons. Several subtleties arise in the calculation, mostly linked to the presence of unphysical operators. We show that the leading term of a HTE of our result differs from the one obtained in the gaugeless approximation [215] where only the top Yukawa couplings are considered. Subsequently we discuss the origin of the discrepancy and provide a criterion for the validity of the gaugeless approximation. As a byproduct of the calculation we also obtain the $\mathcal{O}(\alpha)$ correction to the Wilson coefficient of the current-current operator Q_2. Moreover, we deal with the RGE of the Wilson coefficient functions and illustrate how $\mathcal{O}(\alpha\alpha_s^n L^n)$ effects should be taken into account in the calculation of the integrated branching ratio. We also include all relevant $\mathcal{O}(\alpha)$ matrix elements and conclude reconsidering the SM prediction of the $B \to X_s\gamma$ branching ratio.

4.1 Introduction and Motivation

Although generally small, two-loop purely electroweak effects are sometimes very important: An example is provided by the precision observables of the SM, like the effective sine measured on the Z pole and the $W^\pm$ mass, where radiative corrections up to $\mathcal{O}(g^4 m_t^2/M_W^2)$ [250, 251] are now routinely included in the analysis with important consequences in the electroweak fits [1–3]. Moreover, by fixing the normalization of the electroweak coupling, two-loop effects reduce the electroweak scheme dependence of the SM prediction, which can be quite large also for FCNC processes [252].

The study of electroweak corrections in the $B \to X_s\gamma$ decay began with a work by Czarnecki and Marciano [214], who pointed out that large logarithm of the form $\ln(m_e^2/m_b^2)$ are absent when the fine structure constant $\alpha = 1/137.036$ renormalized at $k^2 = 0$ is used in the overall normalization of the partonic decay rate. This reduces the

branching ratio by roughly 5%. Another type of large logarithm that might enhance some of the electroweak corrections is $\ln(m_b^2/M_W^2)$, that is, the same logarithm that is responsible for the huge QCD enhancement of the $b \to s\gamma$ amplitude. The leading logarithms of QED origin are formally of order $\mathcal{O}(\alpha/\alpha_s)$, so it might be numerically relevant, given the accuracy of Eq. (1.2). However, it has been demonstrated in references [214, 216, 217] by performing explicit calculations, that this effect is negligible, as it amounts to a reduction of only 0.7%. As heavy weak bosons decouple, genuine electroweak corrections affect only the initial conditions of the Wilson coefficient functions. They are not logarithmically enhanced, but can be more important than purely QED effect. Unfortunately, our knowledge of genuine electroweak effects in $b \to s\gamma$ was limited to the subset of two-loop fermion loop corrections computed in reference [214] and to the leading term in the HTE computed by Strumia [215]. In fact, the two results are numerically quite different as they amount to a reduction of about 2.2% and of less than 0.7%, respectively, on the Wilson coefficient of Q_7^γ evaluated at the electroweak scale. The leading term of the HTE was calculated in the article [215] using the gaugeless limit of the SM, that is, in a Yukawa theory where the heavy top couples to the Higgs doublet, setting $M_W = 0$ and keeping the Higgs mass M_H finite and arbitrary. In the presence of external gauge bosons, these can be considered as background sources. This approach presents a few limitations that motivated our calculation presented here:

- The lowest order contribution to the Wilson coefficient of Q_7^γ is a function of the top mass whose HTE converges very slowly. Using $x_t \approx 4.7$ and writing explicitly the numerical values of the successive $\mathcal{O}(1/x_t^n)$ terms, it reads

$$C_7^{\gamma(0)}(M_W) = -0.333 - 0.010 + 0.070 + 0.046 + 0.021 + \ldots = -0.195\,, \qquad (4.1)$$

  where the ellipses represent contributions of $\mathcal{O}(1/x_t^5)$ or higher. The leading HTE is therefore unlikely to provide anything more than an order of magnitude estimate of the two-loop electroweak contribution. In this respect, the similar case of $B^0 - \bar{B}^0$ mixing [252] is very instructive: For realistic values of the top mass the complete two-loop electroweak correction is not well approximated even by the first three terms of the HTE and the leading HTE term is numerically far from the complete result.

- Even assuming the leading HTE term to be representative, it should not be expected to give an accurate result for a light Higgs mass, $M_H = \mathcal{O}(M_W)$, because it is obtained by setting $M_W = 0$ [253]. On the other hand, present electroweak fits show a decisive preference for a light Higgs boson, $M_H < 193\,\text{GeV}$ at 95% confidence level [3].

- The gaugeless limit has often been used to compute the leading HTE term, but it is known [254] that in some cases it does not reproduce the correct result. In the following we explain why it fails for radiative B decays and provide a general criterion for its use.

A complete calculation of all electroweak effects in radiative B decays in the framework of effective Hamiltonians is a very complex enterprise which involves all physical operators introduced in Eq. (3.2). Ideally, one would like to have all $\mathcal{O}(\alpha\alpha_s^n L^n)$ corrections under control. The procedure is summarized, for instance in reference [240]. Its necessary steps would be:

(i) The calculation of the two-loop $\mathcal{O}(\alpha)$ matching conditions for the magnetic operators Q_7^γ and Q_8^g at a scale $\mathcal{O}(M_W)$ as well as the $\mathcal{O}(\alpha)$ contributions to the coefficients of various four quark operators.

(ii) The QCD and QED evolution of the Wilson coefficients down to the B-meson mass scale, including the calculation of the two- and three-loop $\mathcal{O}(\alpha\alpha_s)$ anomalous dimension matrix.

(iii) The calculation of the one-loop $\mathcal{O}(\alpha)$ matrix elements of the magnetic type operators Q_7^γ and Q_8^g, and the computation of the two-loop $\mathcal{O}(\alpha)$ matrix elements of the four quark operators Q_1–Q_6.

(iv) The computation of the $\mathcal{O}(\alpha)$ bremsstrahlungs corrections arising from the $b \to s\gamma g$ and the $b \to s\bar{q}q$ transitions with $q = u, d, s$.

Our analysis in reference [218] was based on the simplifying assumption that terms vanishing in the limit $s_W \to 0$ can be neglected, unless they are enhanced by powers of the top mass m_t. In this case, introducing $\alpha_W = g^2/(4\pi)$, all electroweak corrections are in fact $\mathcal{O}(\alpha_W \alpha_s^n L^n)$ or $\mathcal{O}(\alpha\, m_t^2/M_W^2 \alpha_s^n L^n)$ and are included by step (i) only. Moreover, as all light virtual degrees of freedom are removed the calculation of the Wilson coefficients simplifies considerably. In particular, all the diagrams with virtual photons and all IR divergences drop out of the two-loop calculation in a gauge-invariant way. Although reasonable, the assumption made in the latter article should be verified. In particular, Z boson corrections to the one-loop $b \to s\gamma$ magnetic penguin diagrams give rise to $\mathcal{O}(s_W^2)$ terms which are not formally suppressed by an electric charge factor $Q_d^2 = 1/9$ or $Q_u|Q_d| = 2/9$, unlike the purely QED corrections of steps (ii) and (iii). This happens, for instance, because of the mass difference between $W^\pm$ and Z bosons. Such $\mathcal{O}(s_W^2)$ terms originate at the electroweak scale and affect only step (i). In a recent article [219] we therefore extend our subsequent calculation and computed the full $\mathcal{O}(\alpha)$ contribution to the Wilson coefficients of the $b \to s$ magnetic operators, thus completing step (i). In what follows we will summarize the progress made in the papers mentioned above, extending them by calculating the two-loop matrix elements of the QCD penguin operators Q_3–Q_6, that is, the last missing element of step (iii). Thus the only electroweak $\mathcal{O}(\alpha)$ corrections that remain unknown at present are the two- and three-loop $\mathcal{O}(\alpha\alpha_s)$ anomalous dimension matrix and the $\mathcal{O}(\alpha)$ bremsstrahlungs corrections. As these corrections are enhanced neither by leading large logarithms nor by s_W, we can practically be certain about their irrelevance.

4.2 Two-Loop Matching for the Magnetic Penguins

In order to obtain the Wilson coefficients of the magnetic operator Q_7^γ, we calculate the off-shell amplitude $b \to s\gamma$ in the full SM and in the effective theory at $\mathcal{O}(\alpha)$ and match the two results. Retaining only the leading terms in $1/M_W^2$ the off-shell amplitude in the full theory can be written in the following form[1]

$$\mathcal{A}_{\text{full}}(\mu) = -\frac{G_F}{\sqrt{2}} V_{ts}^* V_{tb} \sum_i A_i(\mu) \left\langle s\gamma \left| Q_i(\mu) \right| b \right\rangle^{(0)} , \tag{4.2}$$

[1] In Eqs. (4.2) and (4.5), the sum runs over Q_1–Q_{16}, Q_7^γ, Q_8^g and, as we will explain later on, some evanescent operators.

where $\langle s\gamma\,|Q_i(\mu)|\,b\rangle^{(0)}$ are the tree level matrix elements of the operators in Eq. (3.2). The perturbative expansion of the coefficients $A_i(\mu)$ reads

$$A_i(\mu) = A_i^{(0)}(\mu) + \frac{\alpha}{4\pi} A_{i,e}^{(1)}(\mu)\,. \tag{4.3}$$

Realize that all UV divergences in $A_{i,e}^{(1)}(\mu)$ are removed by electroweak renormalization. The actual procedure we have adopted follows closely the simple framework presented in references [218, 219, 252] and will be illustrated in great detail in Section 4.4. After electroweak renormalization, the complete corrections to the amplitudes are of course UV finite, but some of the diagrams containing a photon develop a IR pole. In order to regularize these IR divergences, we have adopted two different methods and found identical results for the Wilson coefficients. In the first method the IR divergences are regulated by quark masses [186], while the second method consists in using dimensional regularization for both UV and IR divergences [187].

A second step involves the calculation of the off-shell amplitude in the QED effective theory. Since we calculate the two-loop amplitudes in the background field gauge we apparently need effective vertices with both background and quantum photons. Interestingly, the latter introduce some gauge-variant operators at $\mathcal{O}(\alpha)$. In fact, on the full theory side there are heavy particle subdiagrams that are coupled to quantum photons and contribute to gauge-variant operators not included in the operator basis of Eq. (3.2). Two examples of such Feynman graphs are shown in Fig. 4.1. The appearance of gauge-variant operators is due to the R_ξ gauge coupling of the quantum photon with the $W^\pm$ and the would-be Goldstone boson $\phi^\mp$ and is different from what happens in the case of the off-shell $\mathcal{O}(\alpha_s)$ matching [186, 187]. Indeed, at $\mathcal{O}(\alpha_s)$ only quark-gluon couplings and trilinear quantum-quantum-background gluon couplings are relevant and no gauge-variant operator is induced.

We have explicitly verified that it is not necessary to take any gauge-variant operator into account on the effective theory side. This follows from well-known theorems[2] [257–266] on the renormalization of gauge-invariant operators: One is that gauge-variant operators that mix with gauge-invariant operators can be chosen so that they are all BRST-exact, that is, they can be written as the BRST-variation of some other operators, modulo terms vanishing by the EOM. Therefore, while gauge-invariant operators generally mix into gauge-variant operators[3], the opposite is not true. Next, physical matrix elements of BRST-exact operators are zero. Since we are eventually interested in the matrix elements of physical operators only, we thus do not need to include gauge-variant effective operators in our basis. Of course this holds only as long as the regularization respects the symmetries, like it is in our case.

In a similar way and because of the same theorems, the operators that vanish by the EOM in our operator basis (3.2) do not mix into the physical operators of the same basis, and the renormalization mixing matrix is block triangular. This property drastically simplifies the computation at hand, as we will see in a moment. In particular, the renormalization mixing matrix $\hat{Z}$ is such that $Z_{ij} = 0$ when Q_i is EOM-vanishing and Q_j is a physical operator.

[2] The theorems apply to Yang-Mills theories, but extend to the full SM after imposing the antighost equation [255, 256].

[3] At $\mathcal{O}(\alpha)$ the operators in our basis do not actually mix into gauge-variant operators, as we have checked by explicit calculation.

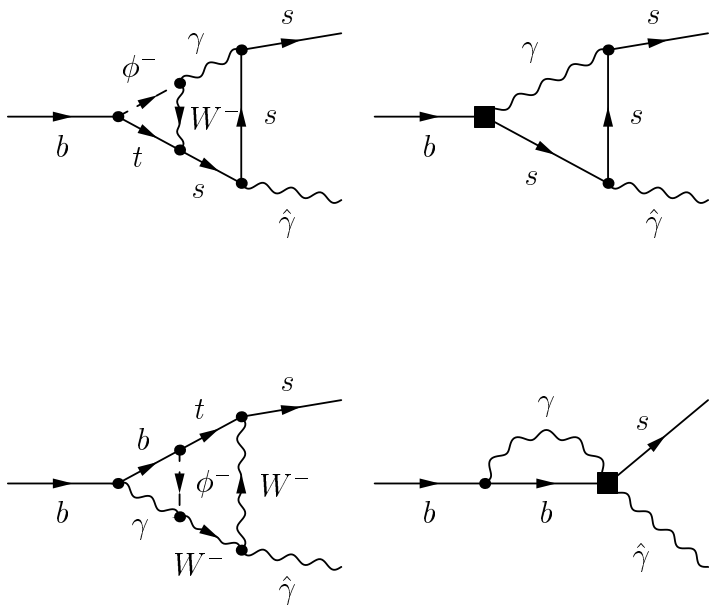

Figure 4.1: Subdiagrams involving the coupling of a quantum photon γ to the $W^{\pm}$ and its corresponding would-be Goldstone boson $\phi^{\pm}$ contribute to gauge-variant operators, as explained in the text.

We have seen that effective vertices involving quantum photons are induced in the calculation. Even though contributions to gauge-variant operators turn out to be irrelevant, the distinction is important in the case that the calculation is performed using quark masses to regularize IR divergences. For example, it turns out that the gauge-invariant part of the off-shell $b \to s\gamma$ effective vertex depends on whether the external photon is quantum or background.[4] This can be explained by noting that the operators involving only background fields are combinations of truly gauge-invariant operators and of operators containing also quantum gauge fields. This follows, for example from a decomposition of the kind $\hat{\not{D}} = \not{D} + ieQ_q \not{Q}$, where we used a hat to denote the covariant background derivative and Q_μ for the quantum photon field. The operators containing quantum gauge bosons eventually decouple from the calculation, as they are not gauge-invariant. Because of the above decomposition, the coefficients of the operators involving only background fields are related to the coefficients of the operators in Eq. (3.2), as can be seen using STIs of the kind used in reference [267].

The effective theory calculation depends crucially on the IR regularization. The first method mentioned above, that is, quark masses as an IR regulator, can be applied at the diagrammatic level [186]. The effective theory diagrams are obtained by replacing hard subdiagrams involving only heavy masses in the two-loop SM amplitudes with their Taylor expansions with respect to their external momenta. In principle, this method does not require a discussion of the effective operators. On the other hand, it is relatively complicated to implement. Here we limit our discussion to the second method only, following reference [187]. In order to get the renormalized off-shell amplitude on the

[4] The one-loop matching for $b \to s\hat{\gamma}$ and $b \to s\gamma$ will be performed in Appendix B.

effective theory side, we need to reexpress the Hamiltonian (3.1) in terms of renormalized quantities. The relations between the bare and the QED renormalized quantities are as follows

$$e_0 = Z_e e\,, \quad m_{b,0} = Z_{m_b} m_b\,, \quad A_0^\mu = Z_e^{-1} A^\mu\,, \quad q_0 = Z_q^{1/2} q\,, \quad C_{i,0}(\mu) = \sum_j C_j(\mu) Z_{ji}\,, \tag{4.4}$$

with Z_e, Z_{m_b}, Z_q and Z_{ij} being the renormalization constant of the charge, the b-quark mass, the quark fields and the Wilson coefficients, respectively. Notice that the relation between the renormalization of the gauge field and of the electric charge is a direct consequence of the QED WTI.

After renormalization the off-shell amplitude in the effective theory is given by

$$\mathcal{A}_{\text{eff}}(\mu) = -\frac{G_F}{\sqrt{2}} V_{ts}^* V_{tb} \sum_{i,j} C_j(\mu) Z_{ji} \widetilde{Z}_i \left\langle s\gamma \left| Q_i(\mu) \right| b \right\rangle\,, \tag{4.5}$$

where $\widetilde{Z}_i$ denotes a product of Z_e, Z_m and Z_q depending on the particular structure of the operator Q_i and the Wilson coefficients may be expanded in powers of α as follows

$$C_i(\mu) = C_i^{(0)}(\mu) + \frac{\alpha}{4\pi} C_{i,e}^{(1)}(\mu)\,. \tag{4.6}$$

As long as we are only interested in the Wilson coefficient of the magnetic photon penguin operator, it is sufficient to keep only terms proportional to $\langle s\gamma | Q_7^\gamma(\mu) | b \rangle$ in Eq. (4.5). Using the short hand notation $\langle Q_7^\gamma \rangle \equiv \langle s\gamma | Q_7^\gamma(\mu) | b \rangle$, the part of the off-shell amplitude in the effective theory needed for the matching of $C_7^\gamma(\mu)$ is then written as

$$\mathcal{A}_{\text{eff}} \sim -\frac{G_F}{\sqrt{2}} V_{ts}^* V_{tb} \left[Z_q Z_{m_b} \sum_j C_j Z_{j,7\gamma} + Z_q \left(Z_{m_b} - 1\right) \sum_j C_j Z_{j,13} \right] \langle Q_7^\gamma \rangle\,, \tag{4.7}$$

where all coefficients are understood at the scale μ. Notice that the second term in the above equation proportional to $Z_{j,13}$ originates from the renormalization of the EOM-vanishing operator Q_{13}:

$$Q_{13,0} = Q_{17,0} + Q_{7,0}^\gamma = Z_q Q_{17} + Z_q Z_{m_b} Q_7^\gamma = Z_q \Big[Q_{13} + \left(Z_{m_b} - 1\right) Q_7^\gamma \Big]\,. \tag{4.8}$$

Realize that the QED quark field renormalization on the effective side can be avoided as it cancels in the matching against the photon contribution to the corresponding term in the SM. The same applies to the renormalization of the b-quark mass, which is retained only up to linear terms. Consequently, after checking the cancellation of the UV divergences in Eq. (4.3) we have omitted the photon contributions in the left- and right-handed down quark wave function renormalization constants $\delta Z_{ij}^{d,L}$ and $\delta Z_{ij}^{d,R}$ as well as in the b-quark on-shell mass counterterm δZ_{m_b} and simultaneously set Z_{m_b} and Z_q to unity in the effective theory. This simplifies the following considerations.

Adopting the $\overline{\text{MS}}$ scheme for the operator renormalization the corresponding renormalization constants can be written as

$$Z_{ij} = \delta_{ij} + \left(Z_{ij}^{(0),01} + \frac{1}{\epsilon} Z_{ij}^{(0),11} \right) + \frac{\alpha}{4\pi} \left(Z_{ij}^{(1),02} + \frac{1}{\epsilon} Z_{ij}^{(1),12} + \frac{1}{\epsilon^2} Z_{ij}^{(1),22} \right)\,, \tag{4.9}$$

where the coefficients are labeled $Z_{ij}^{(k),lm}$, with k being the order in α, l denoting the order in the $1/\epsilon$ expansion and m standing for the number of loops involved in the calculation.

Apparently, the terms $Z_{ij}^{(k),0m}$ in Eq. (4.9) imply a finite renormalization of Q_i. Indeed, in situations where evanescent operators are present, the standard practice is to extend the $\overline{\text{MS}}$ scheme and to allow for a finite operator renormalization. The finite terms $Z_{ij}^{(k),0m}$ differ from zero when Q_i is an evanescent operator and Q_j is not, and their values are fixed by requiring that renormalized matrix elements of evanescent operators vanish in four dimensions [189, 268–271]. This requirement also ensures that evanescent operators do not mix into physical ones [189, 268, 269]. Furthermore, in the case of the $b \to s\gamma$ calculation, it is well-known [234, 272] that some four quark operators can mix into the magnetic operators through one-loop diagrams at zeroth order in α_s and α. Thus, not only we have finite terms in Eq. (4.9), but they appear at the lowest order in the coupling constant.

The renormalization constants $Z_{ij}^{(k),lm}$ are found by calculating the UV divergent parts of Feynman diagrams in the effective theory. Within the scope of this computation, it is essential to carefully distinguish UV from IR singularities. As explained in reference [273], this can be done most easily by introducing a common mass parameter into all the propagator denominators including the photon ones. Apart from the finite terms $Z_{ij}^{(k),0m}$ all renormalization constants in the effective theory up to two loops are known from previous anomalous dimension calculations [216, 217]. As we shall see later on, only five entries of the anomalous dimension matrix mixing physical operators are relevant in the present computation and we have recalculated these elements to check the results mentioned above. Our results are in full agreement with references [216, 217] and we will give the numerical values of the required renormalization constants in Eqs. (4.13), (4.15), (4.19) and (4.20).

The computation of the necessary matrix elements on the effective side is trivial, as we can set all the light particles masses to zero.[5] Accordingly, all loop diagrams on the effective side vanish in dimensional regularization, because of the cancellation between UV and IR divergences. Therefore only the tree level matrix elements $\langle Q_i \rangle^{(0)}$ are different from zero and higher order matrix elements do not play any role in the matching. Notice that due to the cancellation of UV and IR singularities the UV counterterms present in the tree level matrix elements reproduce precisely the IR divergences in the effective theory. Furthermore, the IR divergence on the effective side has to be equal to the IR singularity on the SM side, to guarantee that the final results of the Wilson coefficients are free of IR poles. Eventually, all $1/\epsilon$ poles cancel out in $C_7^\gamma(\mu)$, if the full and the effective theory are matched in the correct way.

Bearing all this in mind, we are now able to extract from Eq. (4.7) those terms which are actually needed to calculate the $\mathcal{O}(\alpha)$ correction to the Wilson coefficient of the magnetic operator. First of all, we have to perform the tree level matching by computing the relevant diagrams for the various operator insertions. At the electroweak scale only $C_2(\mu)$, $C_7^\gamma(\mu)$, $C_8^g(\mu)$ and $C_{11}(\mu)$–$C_{16}(\mu)$ are found to be non-vanishing at leading order. However, due to the triangularity of the mixing matrix the coefficients $C_{11}(\mu)$–$C_{16}(\mu)$ do not contribute to the first term in Eq. (4.7) and therefore will not affect the matching conditions at the next order. Furthermore, as we set Z_{m_b} equal to one also the term

[5] We include only terms that are linear in the b-quark mass. These originate solely from the use of the EOM.

proportional to $(Z_{m_b}-1)$ in Eq. (4.7) does not contribute to $C_7^\gamma(\mu)$ at $\mathcal{O}(\alpha)$. Using $Z_q=1$ we thus obtain

$$\mathcal{A}_{\rm eff} \sim -\frac{G_F}{\sqrt{2}}V_{ts}^*V_{tb}\Bigg\{C_7^{\gamma(0)}+\frac{\alpha}{4\pi}\Bigg[C_{7,e}^{\gamma(1)}+\frac{1}{\epsilon}\left(Z_{2,7\gamma}^{(1),12}C_2^{(0)}+Z_{7\gamma,7\gamma}^{(1),11}C_7^{\gamma(0)}\right) + \frac{1}{\epsilon^2}Z_{2,7\gamma}^{(1),22}C_2^{(0)}+\sum_{i=1}^{3}\left(Z_{E_i,7\gamma}^{(0),01}+\frac{1}{\epsilon}Z_{E_i,7\gamma}^{(0),11}\right)C_{i,e}^{E,(1)}\Bigg]\Bigg\}\langle Q_7^\gamma\rangle^{(0)}\,. \quad (4.10)$$

It is quite remarkable that, with the exception of the last term, only physical operators play a role in this expression, even though the calculation has been performed off-shell.

The matching procedure between the full and the effective theory establishes the initial conditions for the Wilson coefficients at a scale $\mu_W=\mathcal{O}(M_W)$. Comparing Eqs. (4.2), (4.3) and (4.10), the matching condition $\mathcal{A}_{\rm full}(\mu_W)=\mathcal{A}_{\rm eff}(\mu_W)$ translates into the following identities

$$C_7^{\gamma(0)}(\mu_W)=A_7^{\gamma(0)}(\mu_W)\,, \quad (4.11)$$

$$C_{7,e}^{\gamma(1)}(\mu_W)=A_{7,e}^{\gamma(1)}(\mu_W)-\frac{1}{\epsilon}\left(Z_{2,7\gamma}^{(1),12}C_2^{(0)}(\mu_W)+Z_{7\gamma,7\gamma}^{(1),11}C_7^{\gamma(0)}(\mu_W)\right) - \frac{1}{\epsilon^2}Z_{2,7\gamma}^{(1),22}C_2^{(0)}(\mu_W)-\sum_{i=1}^{3}\left(Z_{E_i,7\gamma}^{(0),01}+\frac{1}{\epsilon}Z_{E_i,7\gamma}^{(0),11}\right)C_{i,e}^{E(1)}(\mu_W)\,, \quad (4.12)$$

from which the Wilson coefficient of the magnetic operator up to first order in α can be calculated. The leading order initial condition for the Wilson coefficient of Q_2 is simply $C_2^{(0)}(\mu_W)=1$ and the elements of the mixing matrix relating physical operators needed for the next leading order matching of $C_7^\gamma(\mu_W)$ are given by

$$Z_{2,7\gamma}^{(1),12}=-\frac{58}{243}\,,\qquad Z_{2,7\gamma}^{(1),22}=0\,,\qquad Z_{7\gamma,7\gamma}^{(1),11}=\frac{8}{9}\,. \quad (4.13)$$

Note that the first two renormalization constants, related to the mixing of the operators Q_2 and Q_7^γ, are obtained from a two-loop calculation, as opposed to $Z_{7\gamma,7\gamma}^{(1),11}$ which only involves a one-loop calculation. Whereas the one-loop renormalization constant is regularization and renormalization scheme independent, the two-loop element $Z_{2,7\gamma}^{(1),12}$ is scheme dependent. The value given above corresponds to the NDR scheme.

For what concerns the last term in Eq. (4.12), it is necessary to introduce the following evanescent operators

$$\begin{aligned}
Q_1^E&=(\bar s_L\gamma_\mu b_L)\sum\nolimits_q(\bar q_L\gamma^\mu q_L)+(1+a_1\epsilon)\left(\frac{1}{3}Q_3-\frac{1}{12}Q_5\right)\,,\\
Q_2^E&=(\bar s_L\gamma_\mu b_L)\sum\nolimits_q Q_q(\bar q_L\gamma^\mu q_L)+(1+a_2\epsilon)\left(\frac{1}{3}Q_7-\frac{1}{12}Q_9\right)\,,\\
Q_3^E&=(\bar s_L\gamma_\mu b_L)\sum\nolimits_q Q_q(\bar q_R\gamma^\mu q_R)-(1+a_3\epsilon)\left(\frac{4}{3}Q_7-\frac{1}{12}Q_9\right)\,,
\end{aligned} \quad (4.14)$$

where a_i are arbitrary constants. In the NDR scheme inserting these operators into the one-loop photon penguin diagrams yields

$$\begin{aligned}
&Z_{E_1,7\gamma}^{(0),01}=\frac{4}{9}\,, && Z_{E_2,7\gamma}^{(0),01}=-\frac{4}{27}\,, && Z_{E_3,7\gamma}^{(0),01}=\frac{4}{27}\,,\\
&Z_{E_1,7\gamma}^{(0),11}=0\,, && Z_{E_2,7\gamma}^{(0),11}=0\,, && Z_{E_3,7\gamma}^{(0),11}=0\,.
\end{aligned} \quad (4.15)$$

Realize that the last term in Eq. (4.12) does not depend on the special choice of evanescent operators adopted above, but it does depend on the choice of physical operators. For instance, in the operator basis of references [236,237], all evanescent operators that project on Q_7^γ have vanishing Wilson coefficients, both at $\mathcal{O}(\alpha_s)$ and $\mathcal{O}(\alpha)$. Therefore, in this basis evanescent operators do not affect the matching equations and it is not necessary to introduce them in Eq. (4.9). Curiously, in the operators basis of Eq. (3.2) the same holds only at $\mathcal{O}(\alpha_s)$.

Let us now turn to the matching for the Wilson coefficient of the chromomagnetic penguin operator Q_8^g. The calculation for the $b \to sg$ off-shell amplitude proceeds in the same way as above. Adopting the notation $\langle Q_8^g \rangle \equiv \langle sg\,|Q_8^g(\mu)|\,b\rangle$, we see that the analogue of Eq. (4.10) is

$$\mathcal{A}_{\text{eff}} \sim -\frac{G_F}{\sqrt{2}} V_{ts}^* V_{tb} \Bigg\{ C_8^{g(0)} + \frac{\alpha}{4\pi} \Bigg[C_{8,e}^{g(1)} + \frac{1}{\epsilon} \left(Z_{2,8g}^{(1),11} C_2^{(0)} + Z_{7\gamma,8g}^{(1),11} C_7^{\gamma(0)} + Z_{8g,8g}^{(1),11} C_8^{g(0)} \right) + \frac{1}{\epsilon^2} Z_{2,8g}^{(1),22} C_2^{(0)} + \sum_{i=1}^{3} \left(Z_{E_i,8g}^{(0),01} + \frac{1}{\epsilon} Z_{E_i,8g}^{(0),11} \right) C_{i,e}^{E(1)} \Bigg] \Bigg\} \langle Q_8^g \rangle^{(0)} \,, \tag{4.16}$$

from which we obtain

$$C_8^{g(0)}(\mu_W) = A_8^{g(0)}(\mu_W)\,, \tag{4.17}$$

$$C_{8,e}^{g(1)}(\mu_W) = A_{8,e}^{g(1)}(\mu_W) - \frac{1}{\epsilon} \left(Z_{2,8g}^{(1),11} C_2^{(0)}(\mu_W) + Z_{7\gamma,8g}^{(1),11} C_7^{\gamma(0)}(\mu_W) + Z_{8g,8g}^{(1),11} C_8^{g(0)}(\mu_W) \right) - \frac{1}{\epsilon^2} Z_{2,8g}^{(1),22} C_2^{(0)}(\mu_W) - \sum_{i=1}^{3} \left(Z_{E_i,8g}^{(0),01} + \frac{1}{\epsilon} Z_{E_i,8g}^{(0),11} \right) C_{i,e}^{E(1)}(\mu_W)\,. \tag{4.18}$$

In the NDR scheme the renormalization constants which describe the mixing of physical operators into physical ones read

$$Z_{2,8g}^{(1),12} = -\frac{23}{81}\,, \qquad Z_{2,8g}^{(1),22} = 0\,, \qquad Z_{7\gamma,8g}^{(1),11} = -\frac{4}{3}\,, \qquad Z_{8g,8g}^{(1),11} = \frac{4}{9}\,, \tag{4.19}$$

and those relating evanescent and physical operators are given by

$$\begin{aligned} Z_{E_1,8g}^{(0),01} &= -\frac{4}{3}\,, & Z_{E_2,8g}^{(0),01} &= \frac{4}{9}\,, & Z_{E_3,8g}^{(0),01} &= -\frac{4}{9}\,, \\ Z_{E_1,8g}^{(0),11} &= 0\,, & Z_{E_2,8g}^{(0),11} &= 0\,, & Z_{E_3,8g}^{(0),11} &= 0\,. \end{aligned} \tag{4.20}$$

From the next leading order matching relations (4.12) and (4.18) one observes that the $\mathcal{O}(\epsilon)$ terms of the leading order Wilson coefficients $C_7^{\gamma(0)}(\mu_W)$ and $C_8^{g(0)}(\mu_W)$ yield a finite contribution when being combined with the $1/\epsilon$ poles proportional to the $\mathcal{O}(\alpha)$ terms of the renormalization constants. The initial conditions $C_{7,e}^{\gamma(1)}(\mu_W)$ and $C_{8,e}^{g(1)}(\mu_W)$ are therefore obtained from the next leading order relations (4.12) and (4.18), but they require the leading order matching to be performed up to $\mathcal{O}(\epsilon)$. Decomposing the leading order Wilson coefficients accordingly,

$$C_i^{(0)}(\mu_W) = C_{i,0}^{(0)}(\mu_W) + \epsilon\, C_{i,\epsilon}^{(0)}(\mu_W)\,, \tag{4.21}$$

the results for the $\mathcal{O}(1)$ terms of $C_7^{\gamma(0)}(\mu_W)$ and $C_8^{g(0)}(\mu_W)$ obtained from the leading order matching relations read

$$\begin{aligned} C_{7,0}^{\gamma(0)}(\mu_W) &= \frac{x_t(7-5x_t-8x_t^3)}{24(x_t-1)^3} - \frac{x_t^2(2-3x_t)}{4(x_t-1)^4}\ln x_t\,, \\ C_{8,0}^{g(0)}(\mu_W) &= \frac{x_t(2+5x_t-x_t^2)}{8(x_t-1)^3} - \frac{3x_t^2}{4(x_t-1)^4}\ln x_t\,. \end{aligned} \tag{4.22}$$

For the $\mathcal{O}(\epsilon)$ terms we get

$$\begin{aligned} C_{7,\epsilon}^{\gamma(0)}(\mu_W) &= \frac{x_t(35-21x_t-56x_t^2)}{144(x_t-1)^3} + \frac{x_t(48-162x_t+157x_t^2-22x_t^3)}{72(x_t-1)^4}\ln x_t \\ &\quad + \frac{x_t^2(2-3x_t)}{8(x_t-1)^4}\ln^2 x_t + C_{7,0}^{\gamma(0)}(\mu_W)\ln\frac{\mu_W^2}{M_W^2}\,, \\ C_{8,\epsilon}^{g(0)}(\mu_W) &= -\frac{x_t(26-93x_t+25x_t^2)}{48(x_t-1)^3} + \frac{x_t(24-54x_t+14x_t^2-5x_t^3)}{24(x_t-1)^4}\ln x_t \\ &\quad + \frac{3x_t^2}{8(x_t-1)^4}\ln^2 x_t + C_{8,0}^{g(0)}(\mu_W)\ln\frac{\mu_W^2}{M_W^2}\,, \end{aligned} \tag{4.23}$$

which is in full agreement with the explicit formulas for the $\mathcal{O}(\epsilon)$ terms of the leading order initial conditions of the Wilson coefficients of Q_7^γ and Q_8^g given in the literature [184,185].

The last ingredient needed to complete the electroweak two-loop matching procedure for the magnetic penguin operators Q_7^γ and Q_8^g are the $\mathcal{O}(\alpha)$ contributions to the Wilson coefficients of the evanescent operators. Calculating the usual one-loop electroweak box and penguin diagrams one obtains in the NDR scheme

$$\begin{aligned} C_{1,e}^{E(1)}(\mu_W) &= \frac{1}{s_W}\left(\frac{4}{3}B_0(x_t) + \frac{2}{3}C_0(x_t)\right)\,, \\ C_{2,e}^{E(1)}(\mu_W) &= 4C_0(x_t) + D_0(x_t) + \frac{1}{s_W}\Big(10B_0(x_t) - 4C_0(x_t)\Big)\,, \\ C_{3,e}^{E(1)}(\mu_W) &= 4C_0(x_t) + D_0(x_t)\,, \end{aligned} \tag{4.24}$$

where $B_0(x_t)$, $C_0(x_t)$ and $D_0(x_t)$ denote well-known Inami-Lim functions. They are explicitly given by

$$\begin{aligned} B_0(x_t) &= -\frac{x_t}{4(x_t-1)} + \frac{x_t}{4(x_t-1)^2}\ln x_t\,, \\ C_0(x_t) &= -\frac{x_t(6-x_t)}{8(x_t-1)} + \frac{x_t(2+3x_t)}{8(x_t-1)^2}\ln x_t\,, \\ D_0(x_t) &= \frac{16-48x_t+73x_t^2-35x_t^3}{36(x_t-1)^3} - \frac{8-32x_t+54x_t^2-30x_t^3+3x_t^4}{18(x_t-1)^4}\ln x_t\,. \end{aligned} \tag{4.25}$$

Now it is straightforward to verify that all the IR poles cancel in the next leading order matching relations (4.12) and (4.18), and that the final results for the $\mathcal{O}(\alpha)$ corrections to the Wilson coefficients $C_7^\gamma(\mu_W)$ and $C_8^g(\mu_W)$ obtained in this way coincide with those obtained using quark masses for the IR regularization. In the latter case evanescent operators do not play any role in the matching, as their contribution to the matrix elements cancels against a corresponding term stemming from the finite renormalization in Eqs. (4.15) and (4.20).

4.3 Technical Details of the Calculation

As far as the two-loop diagrams contributing to the off-shell amplitude $b \to s\gamma$ and $b \to sg$ are concerned, we need to consider all the topologies shown in Fig. 4.2, which correspond to a few thousand diagrams. In view of this very large number of Feynman graphs we decided to use the MATHEMATICA [274] package *FeynArts* 2.2 [275, 276] to generate automatically all the two-loop amplitudes. The corresponding unrenormalized amputated Green's function are calculated in the background field version of the 't Hooft-Feynman gauge. After setting to zero all light fermion masses but the b-quark mass, the number of diagrams is significantly reduced by the following simple observation: For a given topology, one can consider equivalence classes of Feynman graphs characterized by the number of massless fermion propagators they contain and by the lines to which those fermions are assigned. Since all light fermions but the b-quark are treated as massless, diagrams within such subsets differ solely by the CKM factor, and can be grouped together, reducing the total number of diagrams to be actually computed. Using the unitarity of the quark mixing matrix, the overall factor turns out to be always proportional to $V_{ts}^* V_{tb}$, as expected from hard GIM cancellation.

In order to extract the coefficients $A_{7,e}^{\gamma}(\mu_W)$ and $A_{8,e}^{g}(\mu_W)$ of the magnetic type operators Q_7^{γ} and Q_8^{g} we recall that off-shell the most general three-point vertex function involving two fermions and a vector field can be decomposed into $2 \cdot 12 = 24$ different form factors, where the factor 2 stems from the two possible chiralities, while the factor 12 takes into account all possible combinations of one Lorentz index and two momenta, namely

$$\{S_i\} = \{k_\mu, p_\mu, \gamma_\mu, k_\mu \not{k}, k_\mu \not{p}, p_\mu \not{k}, p_\mu \not{p}, \gamma_\mu \not{k}, \gamma_\mu \not{p}, k_\mu \not{k} \not{p}, p_\mu \not{p} \not{k}, \gamma_\mu \not{p} \not{k}\}\,, \tag{4.26}$$

with k and p being linear independent. To construct projectors for each of those 24 objects we first introduce a generalized scalar product $(,)$ defined by

$$(S_i, S_j) = \mathrm{tr}\,[S_i S_j]\ . \tag{4.27}$$

The projector on the i-th component of the 24 different Dirac structures

$$P_i = \sum_{j=1}^{24} c_{ij} S_j\,, \tag{4.28}$$

is then determined by requiring that it should fulfill the following orthogonality condition

$$(P_i, S_j) = \delta_{ij}\,, \tag{4.29}$$

for all $j = 1, \ldots, 24$. After some simple algebra one finds that the unknown coefficients c_{ij} defining the projector P_i are given by

$$c_{ij} = (\hat{M}^{-1})_{ij}\,, \tag{4.30}$$

where $\hat{M}$ denotes the matrix whose elements are

$$(\hat{M})_{ij} = (S_i, S_j)\ . \tag{4.31}$$

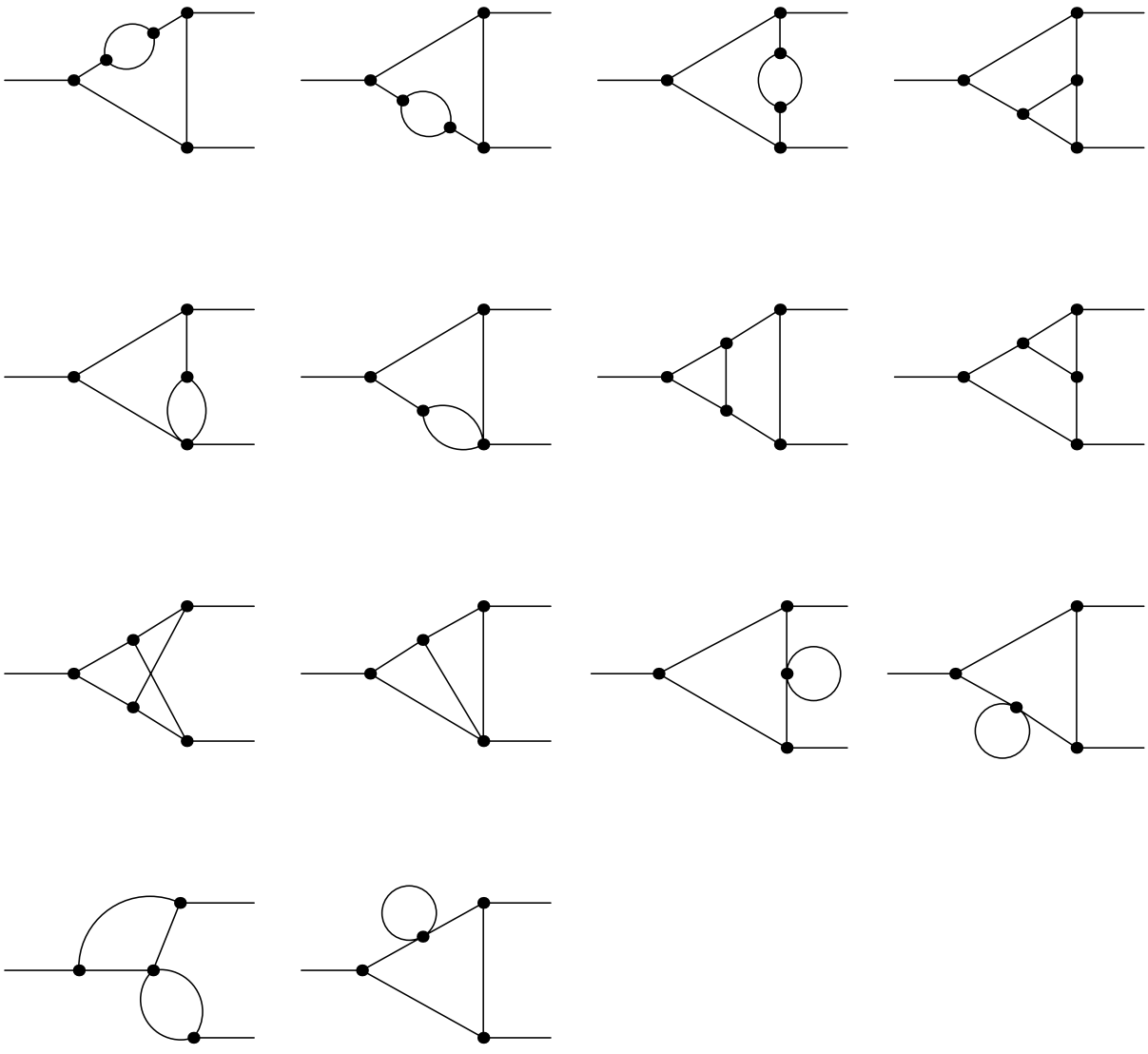

Figure 4.2: The 14 two-loop topologies contributing to $b \to s\gamma$ and $b \to sg$ at $\mathcal{O}(\alpha^2)$.

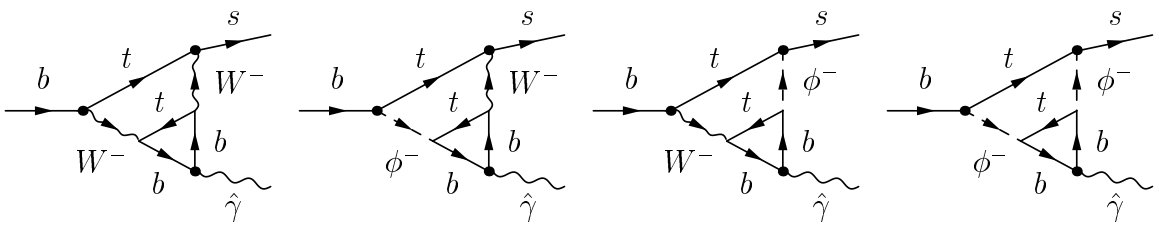

Figure 4.3: Examples of diagrams containing a anomalous fermionic triangle as a subgraph.

After having constructed the projectors for each of the 24 different objects one then has to take the appropriate combination of them which, after the use of the EOM and the Gordon identity, contributes to the on-shell magnetic type operators Q_7^γ and Q_8^g. Apparently, these projectors depend on the kinematical configuration assumed for the external particles. In order to attain the maximal simplicity we decided to follow reference [186] and work in a scaled configuration defined by $p^2 = 0$ and $k \cdot p = k^2/2$, where k and p are the momenta carried by the incoming b-quark and the outgoing vector field, respectively. In this configuration the projector for the tensor part of the on-shell magnetic type operators is explicitly given by

$$\begin{aligned} P_\sigma = \frac{1}{2k^4\,(n-2)} \big(& -2k^2 k_\mu + n m_b p_\mu \not{k} - n m_b p_\mu \not{p} + k^2 \gamma_\mu \not{k} \\ & - k^2 \gamma_\mu \not{p} + 2 k_\mu \not{k} \not{p} + n p_\mu \not{p} \not{k} - m_b \gamma_\mu \not{p} \not{k} \big) P_R \,, \end{aligned} \tag{4.32}$$

and works by contracting it with the amplitudes and taking the trace in n dimensions. Notice that P_σ contains terms proportional to inverse powers of the b-quark momentum k. However, because of the assumption $k^2 \ll m_s^2$ and $k^2 \ll m_b^2$, we can perform a ordinary Taylor expansion in k and p to eliminate the unphysical poles when $k^2 \to 0$. Consequently, the complete result for the unrenormalized two-loop amplitudes can be written in terms of massive two-loop vacuum diagrams. Explicit results of this kind of integrals which admit a relatively compact representation in terms of logarithms and dilogarithms of the internal masses are well-known [277–282].

A peculiarity of the two-loop calculation for the $b \to s\gamma$ and $b \to sg$ transitions is the presence of diagrams containing anomalous fermionic loops like the one shown in Fig. 4.3. It is well-known that the naive definition of anticommuting γ_5 in n dimensions that we employ in the rest of the calculation fails for these diagrams because it leads to algebraical ambiguities and cannot reproduce the axial anomaly. Our solution consists in calculating Dirac structures containing an odd number of γ_5 matrices, that is, those leading to the anomalous term, using an anticommuting γ_5 in strictly four dimensions, which is possible because of their apparent UV convergence. The anomaly cancellation then guarantees the absence of both anomalous and ambiguous terms in the sum of all diagrams [283]. We have also checked our results for these specific terms using the HV definition of γ_5 in n dimensions. From a formal point of view, the equivalence of the two methods follows from the absence of non-invariant counterterms for the odd γ_5 part in the HV case [283], as can be also seen in full generality using the powerful formalism of reference [267].

All necessary steps of the calculation, namely, the projection on the magnetic operators, the Dirac algebra, the reduction of scalar integrals to a set of master integrals, and the substitution of the master integrals have been implemented in two independent and completely automatic codes that involve various combinations of the MATHEMATICA packages *Tracer* [284], *Coltrane* [285] and *ProcessDiagram* [286], and of FORM [287]. Although the final expression for the two-loop diagrams can be expressed in terms of logarithms and dilogarithms, it is rather lengthy due to the presence of four different heavy masses, and thus we have decided to provide only approximate formulas that allow the reader to reproduce our numerical results with high accuracy. On the other hand, we feel that it may be more useful to explain in some detail the renormalization procedure that we have adopted. This will be done in the next section, where we stress the importance of keeping it as simple as possible in order to reduce the number of terms we have to deal with.

4.4 Electroweak Renormalization

In renormalizing the two-loop amplitudes our aim is to attain the maximal simplicity. Therefore we follow closely the procedure outlined in references [218, 219, 252]: We avoid the wave function renormalization of the internal lines whenever possible, and choose a particularly simple procedure for the unphysical sector. All masses are defined on-shell and for the electroweak coupling we use the $\overline{\rm MS}$ scheme, although we explain in detail the connection to other schemes.

In the following we will give explicit expressions for the various counterterms. They are written in terms of logarithms and of a single function $B_0(x,y)$ which is defined through the one-loop scalar self-energy integral

$$\begin{aligned}\mathrm{Im}\,\mu^{2\epsilon}\int\frac{d^np}{(2\pi)^n}\frac{1}{[p^2-m_1^2][(p-k)^2-m_2^2]} = \\ \frac{1}{16\pi^2}\left(\frac{\overline{\mu}^2}{k^2}\right)^{\epsilon}\left[\frac{1}{\epsilon}+B_0\left(\frac{m_1^2}{k^2},\frac{m_2^2}{k^2}\right)+\mathcal{O}(\epsilon)\right],\end{aligned} \tag{4.33}$$

whose analytical form is well-known. Here $\overline{\mu}^2 = 4\pi e^{-\gamma_E}\mu^2$ with γ_E denoting the Euler constant and $n = 4-2\epsilon$. The $\mathcal{O}(\epsilon)$ part of the counterterms is not needed at the two-loop level. For convenience we report here the explicit expression of $B_0(x,y)$ for the two special cases that are needed in our calculation:

$$\begin{aligned}B_0(0,x) &= 2 - x\ln x - (1-x)\ln|1-x|\,,\\ B_0(1,x) &= 2 - \frac{x}{2}\ln x - \frac{1}{2}a(x)\,,\end{aligned} \tag{4.34}$$

where the function $a(x)$ is given by

$$a(x) = \begin{cases} 2\sqrt{x(4-x)}\,\arctan\sqrt{\frac{4}{x}-1}\,, & \text{for } 0<x\le 4\,,\\ \sqrt{x(x-4)}\,\ln\frac{1-\sqrt{1-\frac{4}{x}}}{1+\sqrt{1-\frac{4}{x}}}\,, & \text{for } x>4\,.\end{cases} \tag{4.35}$$

Tadpole Renormalization

To start with, let us give the explicit expression for the tadpole counterterm [148, 288]. In the 't Hooft-Feynman gauge calculating the sum of the one-loop tadpole diagrams one obtains

$$\delta t = \frac{g}{16\pi^2} M_W^3 \left(\frac{\overline{\mu}^2}{m_t^2}\right)^{\epsilon} \left(\frac{1}{\epsilon} E_t + F_t\right) , \tag{4.36}$$

with

$$\begin{aligned} E_t &= \frac{12 + 2x_t h_t - 24 x_t^2 - 3 x_t^2 h_t^2}{4} + \frac{x_t h_t}{4 c_W^2} + \frac{3}{2 c_W^4} , \\ F_t &= E_t + \frac{6 + x_t h_t}{2} \ln x_t - \frac{1}{c_W^2}\left(\frac{x_t h_t}{4} + \frac{3}{2 c_W^2}\right) \ln z_t - \frac{3 x_t^2 h_t^2}{4} \ln h_t - 2 - \frac{1}{c_W^4} , \end{aligned} \tag{4.37}$$

where $z_t = M_Z^2/m_t^2$ and $h_t = M_H^2/m_t^2$ denotes the ratio of the Z and the Higgs boson mass divided by the t-quark mass squared, respectively.

Top Quark Mass Renormalization

The complete on-shell top mass counterterm is gauge-independent only after inclusion of the tadpole counterterm, whose explicit expression has been given in the last subsection. Here we report only the two-point function contribution to δm_t in the 't Hooft-Feynman gauge [148]. It can be written as

$$\frac{\delta m_t}{m_t} = \frac{g^2}{16\pi^2} \left(\frac{\overline{\mu}^2}{m_t^2}\right)^{\epsilon} \left\{ -\frac{3}{8\epsilon} \left[x_t + \frac{1}{c_W^2}\left(1 - \frac{14}{9} s_W^2\right)\right] + F_{m_t} + \mathcal{O}(\epsilon) \right\} , \tag{4.38}$$

where the function F_{m_t} is given by

$$\begin{aligned} F_{m_t} = &-\frac{2 - x_t - x_t^2 + x_t^2 h_t}{8 x_t} + \frac{1}{c_W^2}\left(\frac{1 + z_t - z_t^2}{8 z_t} - \frac{z_t}{3} s_W^2 + \frac{4 z_t}{9} s_W^4\right) - \frac{2 + x_t}{8 x_t} \ln x_t \\ &+ \frac{1}{c_W^2}\left(\frac{1 + z_t}{8} - \frac{z_t}{3} s_W^2 + \frac{4 z_t}{9} s_W^4\right) \ln z_t + \frac{x_t h_t}{8} \ln h_t + \frac{2 - x_t - x_t^2}{8 x_t} B_0\left(0, \frac{1}{x_t}\right) \\ &- \frac{x_t (4 - h_t)}{8} B_0(1, h_t) - \frac{1}{c_W^2}\left(\frac{1 - z_t}{8} + \frac{2 + z_t}{3} s_W^2 - \frac{8 + 4 z_t}{9} s_W^4\right) B_0(1, z_t) + \frac{16}{9} s_W^2 , \end{aligned} \tag{4.39}$$

Replacing m_t by $m_t - \delta m_t$ in the leading order result for the Wilson coefficient of the magnetic type operator Q_7^γ one finds the following top mass counterterm contribution to be added to the unrenormalized two-loop magnetic photon penguin amplitude[6]

$$\Delta_{m_t}^{\rm ct} = \left(\frac{\overline{\mu}^2}{m_t^2}\right)^{\epsilon} \left\{ -\frac{3}{8\epsilon} \left[x_t + \frac{1}{c_W^2}\left(1 - \frac{14}{9} s_W^2\right)\right] + F_{m_t} \right\} \left(2 x_t \frac{\partial}{\partial x_t} C_7^{\gamma(0)}(\mu) \right) , \tag{4.40}$$

where the $\mathcal{O}(1)$ and $\mathcal{O}(\epsilon)$ part of the coefficient function $C_7^{\gamma(0)}(\mu)$ has been given in Eq. (4.22) and Eq. (4.23), respectively. Obviously, the t-quark mass counterterm term

[6] Notice that the Eqs. (4.40), (4.43), (4.50), (4.51), (4.61), (4.63) and (4.66) contain some $\mathcal{O}(\epsilon)$ terms which vanish after renormalization of the magnetic penguin amplitudes in $n = 4$ dimensions.

needed for the renormalization of the chromomagnetic penguin amplitude is obtained from the above expression by replacing $C_7^{\gamma(0)}(\mu)$ with $C_8^{g(0)}(\mu)$.

The top mass is thus renormalized on-shell as far as electroweak effects are concerned, while we use an $\overline{\rm MS}$ definition at a scale μ_t for the QCD renormalization, in accordance to the standard convention [236, 237]. Although the choice of the scale μ_t for the $\overline{\rm MS}$ top mass is a matter of convention, the NLO QCD corrections depend sensitively on μ_t. For convenience, we follow reference [180] and set $\mu_t = m_t$. Using the pole mass value $m_{t,\rm pole} = (174.3 \pm 5.1)$ GeV [2], we therefore find $m_{t,\overline{\rm MS}}(m_{t,\overline{\rm MS}}) = (165 \pm 5)$ GeV, which will be our input in the following.

Bottom Quark Mass Renormalization

The renormalization of the b-quark mass is also performed on-shell. In the 't Hooft-Feynman gauge the corresponding bottom mass counterterm reads

$$\frac{\delta m_b}{m_b} = \frac{g^2}{16\pi^2}\left(\frac{\overline{\mu}^2}{m_t^2}\right)^\epsilon \left\{-\frac{1}{8\epsilon}\left[(2-3x_t) + \frac{1}{c_W^2}\left(1 + 4s_W^2 - \frac{8}{3}s_W^4\right)\right] + F_{m_b} + \mathcal{O}(\epsilon)\right\}\,, \quad (4.41)$$

where the finite part F_{m_b} is given by

$$\begin{aligned} F_{m_b} = &-\frac{2+9x_t-5x_t^2}{16(x_t-1)} - \frac{2-7x_t+2x_t^2}{8(x_t-1)^2}\ln x_t \\ &+ \frac{1}{c_W^2}\left(\frac{1}{8} + \frac{s_W^2}{2} - \frac{s_W^4}{3}\right)\ln z_t + \frac{1}{c_W^2}\left(\frac{1}{16} - \frac{5}{12}s_W^2 + \frac{5}{18}s_W^4\right)\,. \end{aligned} \quad (4.42)$$

Notice that the above counterterm does not include the photon contribution, for a reason that should be clear from the discussion on the QED renormalization of the b-quark mass on the effective side given in Section 4.2.

In renormalizing the bottom mass, one has to keep in mind that the m_b factors in the operators (3.2) originate either from the b-quark Yukawa coupling to the would-be Goldstone boson $\phi^\pm$ or from the use of the EOM. In the latter case, m_b should not be renormalized as it is on-shell by definition. Indeed, besides the on-shell magnetic type operators, there are additional off-shell operators, namely Q_{17} and Q_{18}, that project on Q_7^γ and Q_8^g when the external momenta are set on-shell. Consequently, the m_b renormalization only refers to the parts of the Wilson coefficients of Q_7^γ and Q_g^8 stemming from diagrams involving b-quark Yukawa couplings, which are given by the differences of the Wilson coefficients of the on-shell magnetic operator Q_7^γ and Q_8^g, and the coefficient functions of the corresponding off-shell operator Q_{17} and Q_{18}, respectively. Replacing m_b by $m_b - \delta m_b$ in the b-quark Yukawa couplings of the one-loop diagrams contributing to $C_7^\gamma(\mu)$ we find

$$\Delta_{m_b}^{\rm ct} = \left(\frac{\overline{\mu}^2}{m_t^2}\right)^\epsilon \left\{-\frac{1}{8\epsilon}\left[(2-3x_t) + \frac{1}{c_W^2}\left(1 + 4s_W^2 - \frac{8}{3}s_W^4\right)\right] + F_{m_b}\right\}\left(C_7^{\gamma,(0)}(\mu) - C_{17}^{(0)}(\mu)\right)\,. \quad (4.43)$$

Here $C_7^{\gamma,(0)}(\mu)$ and $C_{17}^{(0)}(\mu)$ denotes the leading order Wilson coefficient of Q_7^γ and Q_{17}, respectively. The expression needed to renormalize the chromomagnetic penguin amplitude is obtained from the one given above by replacing the on-shell magnetic penguin coefficient by the chromomagnetic one and simultaneously substituting $C_{17}^{(0)}(\mu)$ with $C_{18}^{(0)}(\mu)$.

For completeness let us also give the explicit expressions for the leading order Wilson coefficients of the off-shell operators Q_{17} and Q_{18}, which are needed to determine the

bottom mass counterterm contributions. Using the decomposition (4.21) we find in the 't Hooft-Feynman gauge for the $\mathcal{O}(1)$ terms

$$\begin{aligned} C_{17,0}^{(0)}(\mu) &= -\frac{x_t(1+11x_t-18x_t^2)}{24(x_t-1)^3} - \frac{x_t(4-16x_t+15x_t^2)}{12(x_t-1)^4}\ln x_t\,, \\ C_{18,0}^{(0)}(\mu) &= \frac{x_t(4-13x_t+3x_t^2)}{8(x_t-1)^3} - \frac{x_t(2-5x_t)}{4(x_t-1)^4}\ln x_t\,, \end{aligned} \tag{4.44}$$

and for the $\mathcal{O}(\epsilon)$ parts

$$\begin{aligned} C_{17,\epsilon}^{(0)}(\mu) &= -\frac{x_t(5+75x_t-122x_t^2)}{144(x_t-1)^3} - \frac{x_t(48-150x_t+115x_t^2+8x_t^3)}{72(x_t-1)^4}\ln x_t \\ &\quad + \frac{x_t(4-16x_t+15x_t^2)}{24(x_t-1)^4}\ln^2 x_t + C_{17,0}^{(0)}(\mu)\ln\frac{\mu^2}{M_W^2}\,, \\ C_{18,\epsilon}^{(0)}(\mu) &= \frac{x_t(68-141x_t+31x_t^2)}{48(x_t-1)^3} - \frac{x_t(24-30x_t-16x_t^2+x_t^3)}{24(x_t-1)^4}\ln x_t \\ &\quad + \frac{x_t(2-5x_t)}{8(x_t-1)^4}\ln^2 x_t + C_{18,0}^{(0)}(\mu)\ln\frac{\mu^2}{M_W^2}\,, \end{aligned} \tag{4.45}$$

respectively. The leading order initial condition of the off-shell operators Q_{17} and Q_{18} are obtained by calculating the usual one-loop magnetic penguin diagrams including terms of $\mathcal{O}(\epsilon)$. These functions have already been computed in references [186, 226]. We have repeated this calculation and confirmed the findings of Cella et al. and Ciuchini et al. except for the $\mathcal{O}(\epsilon)$ parts, which have not been given in the articles mentioned above.

Renormalization of the Unphysical Sector

Before discussing the renormalization of the $W^\pm$ boson mass it is necessary to explain the procedure which we have followed to renormalize the unphysical scalar fields. As already noted in Chapter 2.4, the renormalization of the unphysical sector is not independent from the way the physical sector is treated. In fact, as long as the regularization and renormalization procedure respects the symmetry of the underlying theory, it is governed by the STIs. According to the organization of the calculation, it is possible to use different procedures that respect the STIs and are particularly convenient in order, for instance, to minimize the number of counterterms to be considered. Of course, physical amplitudes must be independent of the chosen procedure, and this can be used as an additional check of the computation. Obviously, for the problem at hand the discussion can be kept at the one-loop level.

Following references [147,148], the STI relating the longitudinal part of the $W^\pm$ boson self-energy Σ^{WW}, the $W^\pm$ would-be Goldstone boson mixing two-point function $\Sigma^{W\phi}$ and the would-be Goldstone boson self-energy $\Sigma^{\phi\phi}$ can easily be derived from the identity $\langle TF^+(x)F^-(y)\rangle = -i\delta^{(4)}(x-y)$, with F^+ and F^- given in Eq. (2.74). Writing the propagators as the inverse of the truncated 1PI irreducible two-point functions and expanding up to first order we find in the 't Hooft-Feynman gauge

$$k^2\left(\Sigma_L^{WW}(k^2) + 2M_W\Sigma^{W\phi}(k^2)\right) - M_W^2\,\Sigma^{\phi\phi}(k^2) + \frac{gM_W}{2}\Gamma_H(0) = 0\,. \tag{4.46}$$

At $k^2 = 0$ the first two terms vanish and the STI implies the cancellation between the would-be Goldstone boson contribution proportional to $\Sigma^{\phi\phi}(0)$ and the one of the Higgs boson proportional to the one-point function $\Gamma_H(0)$. This uncovers the connection between the renormalization of the would-be Goldstone mass and the one of the tadpole. As anticipated, the counterterm contributions to the various terms in the above equation must also respect the STI. In our calculation we employ the usual tadpole renormalization that minimizes the effective potential and consists in removing all tadpole diagrams. This choice implies the subtraction of $\Sigma^{\phi\phi}(0)$ from the two-point function of the would-be Goldstone boson.[7] Since we will use the physical masses to define the masses of the vector bosons, it is convenient to renormalize the longitudinal component of the two-point function of the $W^\pm$ boson in the same way as the transverse, using the first relation given in Eq. (2.124). For the other unphysical two-point functions different choices are possible, which however should all respect the STI (4.46). Apparently, these choices are equivalent at the level of physical amplitudes, as they correspond to different ways of renormalizing the gauge-fixing parameters.

A first convenient option consists in assigning no counterterm to the $W^\pm$ boson would-be Goldstone boson transition. This decreases the number of counterterms and simplifies their implementation. In fact, in the 't Hooft-Feynman gauge it corresponds to renormalize the masses of the electroweak gauge bosons and of the associated scalar bosons in the same way. This procedure goes by the name of bare gauge-fixing. Of course, the masses of the would-be Goldstone bosons still need a supplementary subtraction at $k^2 = 0$ corresponding to the tadpole contribution, that we have discussed above. It therefore amounts to fix the would-be Goldstone boson mass counterterm in the following way

$$\delta M_\phi^2 = \delta M_W^2 - \frac{g}{2M_W}\delta t\,, \tag{4.47}$$

and is the closet to the naive parameter renormalization. Apparently, this possibility satisfies the STI (4.46) at $k^2 = M_W^2$. In addition it leaves room for a further arbitrary wave function renormalization of the $W^\pm$ boson field, which we avoid altogether, since the $W^\pm$ boson appears only inside loops.

Another possibility would consist in the subtraction of the first two terms of the Taylor expansion around $k^2 = M_W^2$ of the individual two-point functions in the external momentum. Obviously, this method would respect the STI (4.46), as well as the unrenormalized self-energies do. In this case a counterterm for the $W^\pm$ boson would-be Goldstone boson transition is needed. However, it is easy to verify that all choices of renormalization that satisfy Eq. (4.46) lead to the same physical amplitudes.

$W^\pm$ Boson Mass Renormalization

Following the strategy outlined in the preceding subsection, we use the same counterterm to renormalize the $W^\pm$ and the would-be Goldstone boson mass terms. In the 't Hooft-Feynman gauge, one finds [148, 176] for the $W^\pm$ boson mass counterterm:

$$\frac{\delta M_W^2}{M_W^2} = \frac{g^2}{16\pi^2}\left(\frac{\overline{\mu}^2}{m_t^2}\right)^\epsilon \left[\frac{1}{\epsilon}\left(\frac{3}{2}x_t + \frac{7}{6} - \frac{1}{c_W^2}\right) + F_{M_W} + \mathcal{O}(\epsilon)\right], \tag{4.48}$$

[7] This point is nicely explained in the textbook of Taylor [152].

where the finite part F_{M_W} reads

$$\begin{aligned} F_{M_W} &= \frac{106 - 6x_t h_t - 18x_t^2 + 3x_t^2 h_t^2}{36} + \left(\frac{14 + 6x_t + 3x_t h_t + 6x_t^2 - x_t^2 h_t^2}{12} - \frac{1}{c_W^2}\right) \ln x_t \\ &+ \frac{x_t h_t \left(3 - x_t h_t\right)}{12} \ln h_t - \frac{18 - 43 s_W^2 + 24 s_W^4}{6 c_W^4} \ln c_W - \frac{2 - x_t - x_t^2}{2} B_0\left(0, x_t\right) \\ &+ \frac{99 - 264 s_W^2 + 212 s_W^4 - 48 s_W^6}{12 c_W^4} B_0\left(1, x_t z_t\right) - \frac{12 - 4 x_t h_t + x_t^2 h_t^2}{12} B_0\left(1, x_t h_t\right) \\ &- \frac{89 - 282 s_W^2 + 288 s_W^4 - 96 s_W^6}{12 c_W^4} \,. \end{aligned} \tag{4.49}$$

Replacing M_W^2 by $M_W^2 - \delta M_W^2$ in the leading order result for the Wilson coefficient $C_7^\gamma(\mu)$, one obtains the following $W^\pm$ boson mass counterterm contribution

$$\Delta_{M_W}^{\rm ct} = \left(\frac{\overline{\mu}^2}{m_t^2}\right)^\epsilon \left[\frac{1}{\epsilon}\left(\frac{3}{2} x_t + \frac{7}{6} - \frac{1}{c_W^2}\right) + F_{M_W}\right] \left(C_7^{\gamma(0)}(\mu) + x_t \frac{\partial}{\partial x_t} C_7^{\gamma(0)}(\mu)\right) \,. \tag{4.50}$$

Here again $C_7^{\gamma(0)}(\mu)$ denotes the leading order contribution including $\mathcal{O}(\epsilon)$ terms, which has been given explicitly in Eqs. (4.22) and (4.23). An analogue expression applies to the case of the chromomagnetic penguin transition.

In our analysis the $W^\pm$ boson mass is treated a fundamental input parameter, whose value is taken directly from experiment: $M_W = (80.451 \pm 0.033)$ GeV [2]. Although the indirect determination of M_W from M_Z, G_F and α is presently more precise than the experimental one after including all theoretical uncertainties [1, 289], this is certainly sufficient for our purpose.

Would-be Goldstone Boson Mass Renormalization

In the 't Hooft-Feynman gauge the renormalization of the would-be Goldstone boson mass term can be performed in the same way as the one of the $W^\pm$ boson mass, apart from the additional tadpole contribution, whose physical origin has been already discussed. In practice, this means that the one-loop diagrams containing scalars induce a further counterterm contribution that can easily be computed from the one-loop tadpole counterterm (4.36) and from the one-loop amplitudes containing only scalar fields. For simplicity we will give only the final result for this additional contribution in the following. Using the counterterm (4.36) and the relation (4.47) we obtain in the 't Hooft-Feynman gauge

$$\Delta_{M_\phi}^{\rm ct} = \left(\frac{\overline{\mu}^2}{m_t^2}\right)^\epsilon \left(\frac{1}{\epsilon} E_t + F_t\right) \left(t_0 + \epsilon\, t_\epsilon\right) , \tag{4.51}$$

where the functions t_0 and t_ϵ read

$$\begin{aligned} t_0 &= \frac{x_t \left(49 - 104 x_t + 31 x_t^2\right)}{72 \left(x_t - 1\right)^4} - \frac{x_t \left(4 - 4 x_t - 7 x_t^2 + 3 x_t^3\right)}{12 \left(x_t - 1\right)^5} \ln x_t \,, \\ t_\epsilon &= \frac{x_t \left(299 - 700 x_t + 137 x_t^2\right)}{432 \left(x_t - 1\right)^4} - \frac{x_t^2 \left(48 - 123 x_t + 31 x_t^2\right)}{72 \left(x_t - 1\right)^5} \ln x_t \\ &+ \frac{x_t \left(4 - 4 x_t - 7 x_t^2 + 3 x_t^3\right)}{24 \left(x_t - 1\right)^5} \ln^2 x_t + t_0 \ln \frac{\mu^2}{M_W^2} \,, \end{aligned} \tag{4.52}$$

and E_t and F_t have been given in Eq. (4.37).

Wave Function Renormalization

The external quark fields of the down-type are renormalized according to Eq. (2.101). Since the magnetic type operators Q_7^γ and Q_8^g flip the helicity of the external fermion fields, it is clear that we need the left- as well as the right-handed down quark wave function renormalization constant. These renormalization constants can be determined from Eq. (2.126). In the limiting case of vanishing masses of the down-type quarks[8] these prescriptions imply the customary relations

$$\delta Z_{ij}^{d,L} = -\Sigma_{ij}^L(0)\,, \qquad \delta Z_{ij}^{d,R} = -\Sigma_{ij}^R(0)\,. \tag{4.53}$$

By calculating the relevant one-loop diagrams, we obtain in this way for the left-handed wave function renormalization constant

$$\delta Z_{ij}^{d,L} = \frac{g^2}{16\pi^2}\left(\frac{\overline{\mu}^2}{m_t^2}\right)^\epsilon \Big(\delta_{ij} A_L + V_{tj}^* V_{ti} B_L + \mathcal{O}(\epsilon)\Big)\,, \tag{4.54}$$

where

$$\begin{aligned} A_L &= -\frac{1}{\epsilon}\left[\frac{1}{c_W^2}\left(\frac{3}{4} - \frac{5}{6}s_W^2 + \frac{s_W^4}{9}\right)\right] - \frac{1}{2}\ln x_t + \frac{1}{c_W^2}\left(\frac{1}{4} - \frac{s_W^2}{3} + \frac{s_W^4}{9}\right)\ln z_t \\ &\quad + \frac{1}{c_W^2}\left(\frac{3}{8} - \frac{5}{12}s_W^2 + \frac{s_W^4}{18}\right)\,, \\ B_L &= -\frac{x_t}{4\epsilon} + \frac{3x_t\,(1+x_t)}{8\,(x_t-1)} + \frac{x_t^2\,(2+x_t)}{4\,(x_t-1)^2}\ln x_t\,. \end{aligned} \tag{4.55}$$

The right-handed down quark wave function renormalization constant reads

$$\delta Z_{ij}^{d,R} = \frac{g^2}{16\pi^2}\left(\frac{\overline{\mu}^2}{m_t^2}\right)^\epsilon \Big(\delta_{ij} A_R + \mathcal{O}(\epsilon)\Big)\,, \tag{4.56}$$

with the flavor diagonal part A_R given by

$$A_R = \frac{s_W^4}{9c_W^2}\left(\frac{1}{\epsilon} - \frac{1}{2} - \ln z_t\right)\,. \tag{4.57}$$

Realize that A_L and A_R again do not include the contribution stemming from the one-loop two-point functions involving the exchange of a virtual photon.

Bearing all this in mind, we can now discuss the wave function renormalization of the external s-quark. The corresponding counterterm contribution $\Delta_s^{\rm ct}$ is obtained as follows. First we need to know the amputated amplitude for the magnetic penguin transition $b_R \to k_L\gamma$ with $k = d, s, b$. At the one-loop level we have

$$\mathcal{A}_{7,k}^{\gamma(0)}(\mu) = -\frac{G_F}{\sqrt{2}}\sum_{i=u,c,t} V_{ik}^* V_{ib} C_{7,i}^{\gamma(0)}(\mu)\,\big\langle Q_{7,k}^\gamma\big\rangle^{(0)}\,, \tag{4.58}$$

where $\langle Q_{7,k}^\gamma\rangle^{(0)}$ denotes the tree level matrix element of the relevant magnetic operator. Using the unitarity of the CKM matrix this can be rewritten in the following way

$$\mathcal{A}_{7,k}^{\gamma(0)}(\mu) = -\frac{G_F}{\sqrt{2}}\Big[V_{tk}^* V_{tb}\Big(C_{7,t}^{\gamma(0)}(\mu) - C_{7,c}^{\gamma(0)}(\mu)\Big) + \delta_{ks} C_{7,c}^{\gamma(0)}(\mu)\Big]\big\langle Q_{7,k}^\gamma\big\rangle^{(0)}\,. \tag{4.59}$$

[8] Recall that m_b is actually treated as an external scalar field.

Here the second term originates in the unitarity relation $V_{uk}^* V_{us} + V_{ck}^* V_{cs} + V_{tk}^* V_{ts} = \delta_{ks}$. Now the counterterm contribution due to the wave function renormalization of the external s-quark field takes the form

$$\Delta_s^{\rm ct} = \frac{1}{2} \sum_{k=d,s,b} \delta Z_{sk}^{d,L*} \mathcal{A}_{7,k}^{\gamma(0)}(\mu) \,. \tag{4.60}$$

Combining Eqs. (4.54) and (4.59) we thus obtain

$$\Delta_s^{\rm ct} = \frac{1}{2} \left(\frac{\overline{\mu}^2}{m_t^2} \right)^{\epsilon} \left[(A_L + B_L)\, C_7^{\gamma(0)}(\mu) + B_L C_{7,c}^{\gamma(0)}(\mu) \right] , \tag{4.61}$$

with $C_7^{\gamma(0)}(\mu)$ as given in Eqs. (4.22) and (4.23). The c-quark contributions to the Wilson coefficients of the magnetic type operators Q_7^γ and Q_8^g read

$$\begin{aligned} C_{7,c}^{\gamma(0)}(\mu) &= \frac{23}{36} + \epsilon \left(\frac{145}{216} + \frac{23}{36} \ln \frac{\mu^2}{M_W^2} \right) , \\ C_{8,c}^{g(0)}(\mu) &= \frac{1}{3} + \epsilon \left(\frac{11}{18} + \frac{1}{3} \ln \frac{\mu^2}{M_W^2} \right) . \end{aligned} \tag{4.62}$$

In correcting the external b-quark fields, one has to keep in mind that the chirality of the b-quark is different in the on-shell operators Q_7^γ and Q_8^g, and in the off-shell ones Q_{17} and Q_{18}. Accordingly, one needs to consider the amputated amplitudes for the magnetic penguin transitions $k_R \to s_L \gamma$ and $k_L \to s_L \gamma$ with $k = d, s, b$. Aside from this the calculation of the counterterm contribution stemming from the external leg correction of the b-quark field proceeds in the same way as described above. Combining the expressions for the wave function renormalization of the left- and right-handed b-quark field we find

$$\Delta_b^{\rm ct} = \frac{1}{2} \left(\frac{\overline{\mu}^2}{m_t^2} \right)^{\epsilon} \left[(A_L + B_L)\, C_{17}^{(0)}(\mu) + B_L C_{17,c}^{(0)}(\mu) + A_R \left(C_7^{\gamma(0)}(\mu) - C_{17}^{(0)}(\mu) \right) \right] , \tag{4.63}$$

with $C_7^{\gamma(0)}(\mu)$ and $C_{17}^{(0)}(\mu)$ given in Eqs. (4.22) and (4.23), and Eqs. (4.44) and (4.45), respectively. The contributions to the Wilson coefficients of the off-shell operators Q_{17} and Q_{18} including only charm loops are given by

$$\begin{aligned} C_{17,c}^{(0)}(\mu) &= \frac{23}{36} + \epsilon \left(\frac{145}{216} + \frac{23}{36} \ln \frac{\mu^2}{M_W^2} \right) , \\ C_{18,c}^{(0)}(\mu) &= \frac{1}{3} + \epsilon \left(\frac{11}{18} + \frac{1}{3} \ln \frac{\mu^2}{M_W^2} \right) . \end{aligned} \tag{4.64}$$

As it should be the c-quark contributions to the coefficient functions of the off-shell operators Q_{17} and Q_{18} coincide with those of the magnetic type operators Q_7^γ and Q_8^g.

Unfortunately, some of the UV divergences related to the exchange of would-be Goldstone bosons persist after inclusion of the external leg corrections. In a calculation of physical on-shell amplitudes, this would not be the case. However, the IR regularization we have adopted prevents the cancellation among the off-diagonal wave function renormalization of the internal quarks, which is a prerequisite for this procedure. We are then forced to renormalize the set of diagrams in which the wave function renormalization of

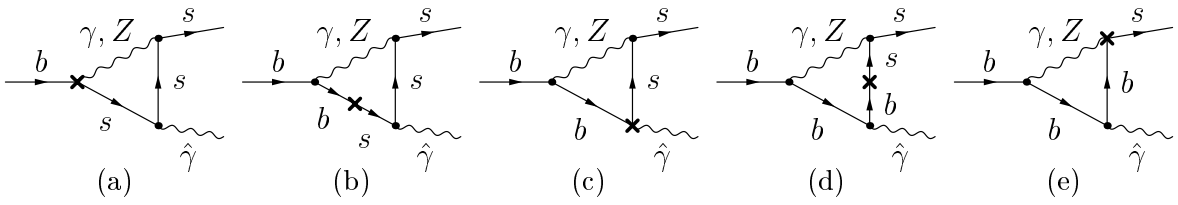

Figure 4.4: Counterterm diagrams involving a wave function renormalization of the internal quark fields, as explained in the text.

the internal quarks does not vanish after summation of all contributions at the diagrammatic level. Following reference [240] we do that by zero momentum subtraction of the one-loop subdivergences. Specifically, writing the unrenormalized quark self-energy for the $b \to s$ transition as

$$\Sigma_{bs}(k^2) = \not{k}\, P_L \Sigma_{bs}^L(k^2) + \not{k}\, P_R \Sigma_{bs}^R(k^2) + (m_b P_L + m_s P_R)\, \Sigma_{bs}^S(k^2)\,, \tag{4.65}$$

the subtraction involves $\Sigma_{bs}^L(0)$ and $\Sigma_{bs}^S(0)$. The right-handed part of the unrenormalized quark self-energy is proportional to $m_s m_b$ and thus can be neglected. This subtraction procedure removes the spurious IR sensitivity of the two-loop diagrams corresponding to the counterterm graphs (b) and (d) shown in Fig. 4.4. The case of the vertex counterterm diagrams (a), (c) and (e) is easier because the associated two-loop graphs are less IR sensitive. In this case one can neglect all terms proportional to m_s and m_b in Eq. (4.65). In consequence the subtraction involves only the left-handed part $\Sigma_{bs}^L(0)$ of the quark self-energy for the $b \to s$ transition.

For simplicity we just give the final result for this additional contribution stemming from the wave function renormalization of the internal quark fields here. Using dimensional regularization for both UV and IR divergencies one obtains in the 't Hooft-Feynman gauge

$$\Delta_{bs}^{\rm ct} = \left(\frac{\overline{\mu}^2}{m_t^2}\right)^{\epsilon} \left[\frac{(3-2s_W^2)^2}{648 s_W^2}\left(\frac{x_t}{\epsilon} - \frac{x_t\,(1-10x_t)}{3\,(x_t-1)} - \frac{x_t^2\,(1+2x_t^2)}{(x_t-1)^2}\ln x_t - x_t \ln z_t\right)\right]. \tag{4.66}$$

Notice that in dimensional regularization only the counterterm diagrams involving a Z boson exchange will give a non-vanishing contribution to $\Delta_{bs}^{\rm ct}$. On the other hand, if the IR divergences are regulated by quark masses also the Feynman graphs containing a photon have to be considered.

Finally, it is worth mentioning that the external leg corrections (4.61) and (4.63) together with the additional contribution stemming from the renormalization of the internal quark fields (4.66) correspond to the correct LSZ factors and implement the renormalization of the CKM matrix according to reference [167] within our approximations. We recall that this gauge-invariant definition of the CKM matrix is the most appropriate to the present low-energy measurements because, unlike an $\overline{\rm MS}$ renormalization, it avoids $\mathcal{O}(g^2)$ corrections not suppressed by GIM and proportional to $(m_q^{i\,2} + m_q^{j\,2})/(m_q^{i\,2} - m_q^{j\,2})$, where m_q^i and m_q^j are light quark masses [167].

Coupling Constant Renormalization

The counterterm for the renormalization of the $SU(2)_L$ coupling constant in the electroweak $\overline{\rm MS}$ scheme is well-known. It reads

$$\frac{\delta\hat{g}}{\hat{g}} = \frac{g^2}{16\pi^2}\frac{19}{12}\left(\frac{1}{\epsilon} - \gamma_E + \ln 4\pi\right) . \tag{4.67}$$

where a hat has been used to indicate $\overline{\rm MS}$ scheme quantities. Performing the renormalization, by replacing $\hat{g}$ with $\hat{g} - \delta\hat{g}$ in the leading order result for the Wilson coefficient $C_7^\gamma(\mu)$, we obtain the following counterterm contribution to be added to the unrenormalized two-loop magnetic photon penguin amplitude

$$\Delta_g^{\rm ct} = -\frac{19}{6\epsilon}C_7^{\gamma(0)}(\mu) . \tag{4.68}$$

In the $\overline{\rm MS}$ scheme the electroweak coupling constant can be calculated from $\hat{\alpha}(M_Z) = 1/127.934$ [290] and $\sin^2\hat{\theta}_W(M_Z) = 0.23113$ [2], which leads to $\hat{g}^2(M_Z) = 0.424943$. This is the value that we will use in the following numerical analysis.

However, beside the $\overline{\rm MS}$ scheme there are a number of other popular schemes leading to values for $\alpha(M_Z)$ and $\sin^2\theta_W$ which differ by small factors depending on m_t and M_H. In any other renormalization scheme different from $\overline{\rm MS}$ the counterterm would have a finite part, namely

$$\frac{\delta g}{g} = \frac{g^2}{16\pi^2}\left(\frac{\mu^2}{M_Z^2}\right)^\epsilon\frac{19}{12}\left(\frac{1}{\epsilon} - \gamma_E + \ln 4\pi\right) + F_g , \tag{4.69}$$

so that the difference between the result in the scheme characterized by F_g and the result in the $\overline{\rm MS}$ scheme at the scale $\mu = M_Z$ is just given by

$$\delta\Delta_g^{\rm ct} = -2C_{7,0}^{\gamma,(0)}(\mu)F_g . \tag{4.70}$$

It is well-known that the use of the electromagnetic fine structure constant $\alpha = 1/137.036$ to normalize the electroweak coupling would introduce large and uncompensated mass singularities [163] in the two-loop results. Therefore, it is indispensable to normalize g at a short distance scale. The most obvious choice in the present situation is to use $G_F = 1.16637\times10^{-5}\,{\rm GeV}^{-2}$ [2] and M_W to define the electroweak coupling constant as $g^2 = 4\sqrt{2}\,G_F\,M_W^2$. In this case the finite part of the counterterm reads

$$F_g^{G_F} = \frac{1}{2}\left(\Delta\hat{r}_W + 2\frac{\delta e}{e}\bigg|_{\overline{\rm MS}}\right) , \tag{4.71}$$

where $\Delta\hat{r}_W$ is a function of the $W^\pm$, Z, top and Higgs masses, as well as of the couplings, which summarizes the electroweak corrections to the muon decay in the $\overline{\rm MS}$ scheme and can be found for example in references [291,292]. The second term in parenthesis, instead, represents the finite part of the conventional electric charge counterterm [163], evaluated in the $\overline{\rm MS}$ scheme. The function $F_g^{G_F}$ has only a mild dependence on both m_t and M_H, because shifts in M_W are absorbed into the observed G_F. Numerically it is very small, as can be seen comparing the value of g^2 obtained from the relation $g^2 = 4\sqrt{2}\,G_F\,M_W^2$ with the value of $\hat{g}^2(M_Z)$ given above, which differ by only 0.5%.

Another possibility to define g is to use the relation $g^2 = 4\pi\hat{\alpha}(M_Z)/s_W^2$. Thereby, $\hat{\alpha}(M_Z)$ stands for the running electromagnetic coupling constant at the $\overline{\rm MS}$ scale $\mu = M_Z$,

and we have adopted the on-shell definition (2.128) of the weak mixing angle leading to $s_W^2 = 0.2228$ [2]. In this case the finite part of the counterterm takes the form

$$F_g^{\rm OS} = \frac{c_W^2}{2s_W^2}\Delta\hat{\rho}\,, \tag{4.72}$$

where $\Delta\hat{\rho}$ is another function depending on all the heavy masses [291, 292]. Unlike $\Delta\hat{r}_W$, however, $\Delta\hat{\rho}$ is very sensitive to the top mass, as it depends quadratic on m_t. In fact, the $\overline{\rm MS}$ and the on-shell definitions of $\sin^2\theta_W$, and so g^2, differ by almost 4%. One can therefore anticipate that the latter normalization will introduce large two-loop corrections when compared to the $\overline{\rm MS}$ scheme. Moreover, as the origin of the large counterterm contribution has nothing to do with the process at hand, one can also expect this choice to give unnaturally large two-loop corrections.

4.5 Results and Discussion

Before giving the final results for the $\mathcal{O}(\alpha)$ corrections to the Wilson coefficients of the magnetic type operators Q_7^γ and Q_8^g in an approximated form, we recall that the regularization scheme independent quantity entering the calculation of the branching ratio for $B \to X_s\gamma$ is not $C_7^\gamma(\mu)$ but the effective Wilson coefficient $C_7^{\gamma,\rm eff}(\mu)$, as given in Eq. (3.3). Since the effective Wilson coefficients of Q_7^γ and Q_8^g are combinations of $C_7^\gamma(\mu)$ and $C_8^g(\mu)$, and of the coefficients of the four quark operators present in our operator basis (3.2), we also need to know the $\mathcal{O}(\alpha)$ contributions to the coefficient functions of the latter one in order to find the complete electroweak corrections to $C_7^{\gamma,\rm eff}(\mu)$ and $C_8^{g,\rm eff}(\mu)$. In the NDR scheme the non-vanishing $\mathcal{O}(\alpha)$ contributions to the Wilson coefficients of the four quark operators at $\mu_W = M_W$ are given by[9]

$$\begin{aligned}
C_{2,e}^{(1)}(M_W) &= -\frac{7}{3} + \frac{4}{3}\ln\frac{M_Z^2}{M_W^2}\,,\\
C_{3,e}^{(1)}(M_W) &= -\frac{1}{s_W}\left(\frac{4}{9}B_0(x_t) + \frac{2}{9}C_0(x_t)\right)\,,\\
C_{5,e}^{(1)}(M_W) &= \frac{1}{s_W}\left(\frac{1}{9}B_0(x_t) + \frac{1}{18}C_0(x_t)\right)\,,\\
C_{7,e}^{(1)}(M_W) &= 4C_0(x_t) + D_0(x_t) - \frac{1}{s_W}\left(\frac{10}{3}B_0(x_t) - \frac{4}{3}C_0(x_t)\right)\,,\\
C_{9,e}^{(1)}(M_W) &= \frac{1}{s_W}\left(\frac{5}{6}B_0(x_t) - \frac{1}{3}C_0(x_t)\right)\,,
\end{aligned} \tag{4.73}$$

where $B_0(x_t)$, $C_0(x_t)$ and $D_0(x_t)$ can be found in Eq. (4.25). Notice that the result for the Wilson coefficient function of the four quark operator Q_2 given above differs from the one reported in reference [218] by a term 1/9. Recalling that the $\mathcal{O}(\alpha)$ correction to $C_2(M_W)$ was obtained in the latter article in the standard operator basis [236, 237], it should be clear that this difference stems from a change of basis. As we will explain later on, the

[9] These $\mathcal{O}(\alpha)$ contributions can be found either by calculating the usual one-loop box and penguin diagrams or from those in the operator basis of references [236, 237] after a basis transformation in four dimensions. All ingredients necessary to perform this transformation will be given in Appendix D.

extra term present in $C_{2,e}^{(1)}(M_W)$ introduces a scheme dependence into our final result. Although relevant from a conceptual point of view, its effect on the branching ratio of the $B \to X_s\gamma$ decay is numerically very small.

Approximate Formulas

The final results for $C_{7,e}^{\gamma,\mathrm{eff}\,(1)}(\mu_W)$ and $C_{8,e}^{g,\mathrm{eff}\,(1)}(\mu_W)$ are quite lengthy and hence not suitable for a simple implementation in numerical analyses. Instead let us give two accurate approximate formulas for the $\mathcal{O}(\alpha)$ contributions to $C_7^{\gamma,\mathrm{eff}}(\mu_W)$ and $C_8^{g,\mathrm{eff}}(\mu_W)$, which are valid when the effective Hamiltonian is normalized in terms of G_F as has been done in Eq. (3.1). We find

$$\begin{aligned}
C_{7,e}^{\gamma,\mathrm{eff}\,(1)}(\mu_W) &= \frac{1}{s_W^2}\left[1.11 - 1.15\left(1 - \frac{m_{t,\overline{\mathrm{MS}}}^2}{170^2}\right) - 0.444\ln\frac{M_H}{100} - 0.21\ln^2\frac{M_H}{100}\right.\\
&\quad \left. -0.513\ln\frac{M_H}{100}\,\ln\frac{m_{t,\overline{\mathrm{MS}}}}{170}\right] + \left(\frac{8}{9}C_7^{\gamma\,(0)}(M_W) - \frac{104}{243}\right)\ln\frac{\mu_W^2}{M_W^2}\,,\\
C_{8,e}^{g,\mathrm{eff}\,(1)}(\mu_W) &= \frac{1}{s_W^2}\left[-0.143 + 0.156\left(1 - \frac{m_{t,\overline{\mathrm{MS}}}^2}{170^2}\right) - 0.129\ln\frac{M_H}{100} - 0.0244\ln^2\frac{M_H}{100}\right.\\
&\quad \left. -0.037\ln\frac{M_H}{100}\,\ln\frac{m_{t,\overline{\mathrm{MS}}}}{170}\right] + \left(\frac{4}{9}C_8^{g\,(0)}(M_W) - \frac{4}{3}C_7^{\gamma\,(0)}(M_W) - \frac{58}{81}\right)\ln\frac{\mu_W^2}{M_W^2}\,,
\end{aligned} \tag{4.74}$$

where M_H is the Higgs boson mass expressed, like $m_{t,\overline{\mathrm{MS}}}$ in GeV. In the above formulas we use the coupling $\hat{\alpha}(M_Z) = 1/127.934$, while in general we employ $s_W^2 = 0.23$, corresponding to $g^2 = 4\sqrt{2}\,G_F\,M_W^2$, $M_W = 80.451\,\mathrm{GeV}$ and $M_Z = 91.1876\,\mathrm{GeV}$ [2]. The relations (4.74) reproduce accurately, within 1.5%, the analytic results in the ranges $80\,\mathrm{GeV} < M_H < 300\,\mathrm{GeV}$ and $160\,\mathrm{GeV} < m_{t,\overline{\mathrm{MS}}} < 180\,\mathrm{GeV}$. We stress that the above results are independent of the choice of the scale μ_t in the QCD top mass definition: It is sufficient to calculate $m_{t,\overline{\mathrm{MS}}}(\mu_t)$ and employ it in the approximate formulas (4.74). Different choices of μ_t lead to different NLO QCD corrections, but they are higher order effects as far as the present calculation is concerned. Realize that the renormalization scale dependence of the effective coefficients agrees with the results given in the literature [214, 216, 217].

The size of the electroweak corrections to $C_7^{\gamma,\mathrm{eff}}(M_W)$ and $C_8^{g,\mathrm{eff}}(M_W)$ relative to the one-loop results is shown in Fig. 4.5 for $m_{t,\overline{\mathrm{MS}}}(m_{t,\overline{\mathrm{MS}}}) = 165\,\mathrm{GeV}$: At $M_H = 100\,\mathrm{GeV}$ the Wilson coefficient of Q_7^γ is reduced by 1.5%, and diminishes with increasing Higgs boson mass. The electroweak corrections modify $C_8^{g,\mathrm{eff}}(M_W)$ only very little by about 0.4% for a light Higgs boson mass of around 100 GeV. If we consider only fermionic loops we reproduce the result of Czarnecki and Marciano [214], which leads to a 2.2% reduction of the effective Wilson coefficient $C_7^{\gamma,\mathrm{eff}}(M_W)$. Although purely accidental, the closeness of this fermion loop approximation to our complete result for a light Higgs boson is quite acceptable.

In order to compare directly the results in Eq. (4.74) with the approximate ones in reference [218], let us also display the size of the two-loop electroweak corrections to $C_7^{\gamma,\mathrm{eff}}(M_W)$ and $C_8^{g,\mathrm{eff}}(M_W)$ for $m_{t,\overline{\mathrm{MS}}}(M_W) = 175.5\,\mathrm{GeV}$ used in that paper. This is done in Fig. 4.6. First, notice that the Higgs mass dependence is identical, as should be expected since all the diagrams involving the Higgs boson also involve a charged boson. Therefore these diagrams are not sensitive to the $W^\pm$–Z boson mass difference or to $\mathcal{O}(s_W^2)$

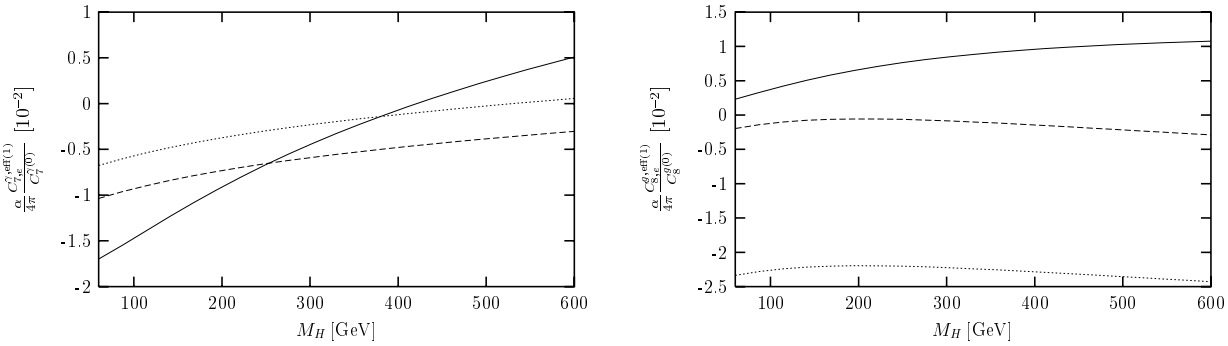

Figure 4.5: Electroweak corrections to the Wilson coefficients $C_7^{\gamma,\mathrm{eff}}(M_W)$ and $C_8^{g,\mathrm{eff}}(M_W)$ for $m_{t,\overline{\mathrm{MS}}}(m_{t,\overline{\mathrm{MS}}}) = 165\,\mathrm{GeV}$. The solid lines represent the results of the complete corrections to the Wilson coefficients at M_W, the dashed lines their leading HTE, and the dotted lines the results of the gaugeless approximation.

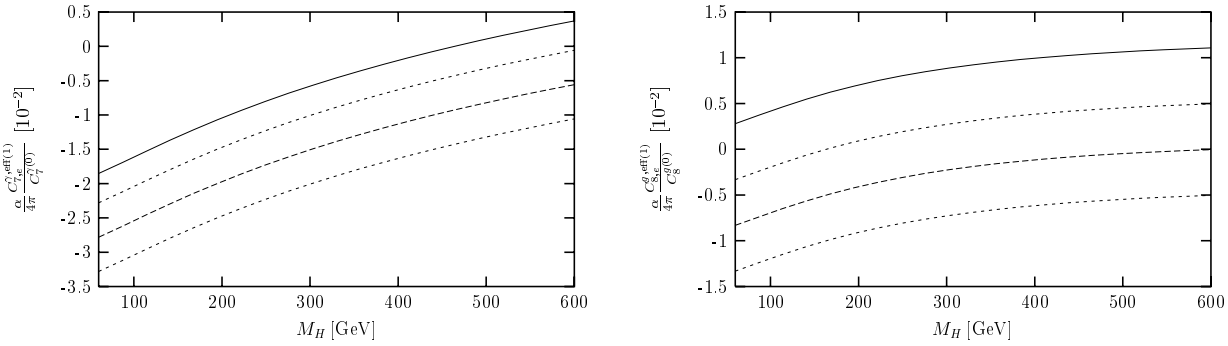

Figure 4.6: Electroweak corrections to the Wilson coefficients $C_7^{\gamma,\mathrm{eff}}(M_W)$ and $C_8^{g,\mathrm{eff}}(M_W)$ for $m_{t,\overline{\mathrm{MS}}}(M_W) = 175.5\,\mathrm{GeV}$. The dashed lines represent the results of reference [218] with their error estimates, the solid lines the complete corrections to the Wilson coefficients.

couplings. Numerically, we see that the difference is larger than estimated in the article mentioned above, in which the difference between the complete electroweak correction to the muon decay and its $s_W \to 0$ limit has been used as a measure of the uncertainty due to the expansion around $s_W = 0$. Although an expansion of the results in powers of s_W^2 converges quickly, it turns out that its second term of $\mathcal{O}(s_W^2)$ is larger than naively expected, and that the two-loop correction is very sensitive to the M_W–M_Z difference.

Heavy Top Expansion

Let us now consider the HTE of our results and see how it compares with existing analyses. Expanding the complete result for the $\mathcal{O}(\alpha)$ correction to the Wilson coefficient of the magnetic operator Q_7^γ and Q_8^g in powers of x_t, we find that at $\mu_W = M_W$ the leading term

in a HTE is given by

$$C_{7,e}^{\gamma,\mathrm{eff}\,(1)}(M_W) = \frac{g^2}{16\pi^2}\, x_t \Bigg[-\frac{16-55h_t+11h_t^2+26h_t^3}{288h_t} + \frac{8-17h_t-2h_t^2-14h_t^3}{144h_t}\ln h_t$$
$$- \frac{h_t^2\,(74-45h_t+2h_t^2)}{576}\ln^2 h_t + \frac{16-2h_t+36h_t^2-74h_t^4+45h_t^5-2h_t^6}{1728h_t^2}\,\pi^2$$
$$- \frac{8-h_t-6h_t^2-52h_t^2+85h_t^4-33h_t^5+2h_t^6}{144h_t^2}\,\mathrm{Li}_2\,(1-h_t)$$
$$- \frac{80+68h_t-262h_t^2+134h_t^3-25h_t^4+2h_t^5}{576h_t}\,\phi\left(\frac{h_t}{4}\right) + \frac{s_W^2}{27}\Bigg] + \mathcal{O}\left(x_t^0\right)\,, \qquad (4.75)$$

and

$$C_{8,e}^{g,\mathrm{eff}\,(1)}(M_W) = \frac{g^2}{16\pi^2}\, x_t \Bigg[\frac{32-83h_t-23h_t^2+16h_t^2}{192h_t} - \frac{8+h_t+7h_t^2-5h_t^3}{48h_t}\ln h_t$$
$$+ \frac{h_t^2\,(1-9h_t+h_t^2)}{96}\ln^2 h_t - \frac{8-h_t-18h_t^2-h_t^4+9h_t^5-h_t^6}{288h_t^2}\,\pi^2$$
$$+ \frac{16-2h_t-12h_t^2+40h_t^3-h_t^4-30h_t^5+4h_t^6}{96h_t^2}\,\mathrm{Li}_2\,(1-h_t)$$
$$+ \frac{8-58h_t+62h_t^2+17h_t^3-16h_t^4+2h_t^5}{192h_t}\,\phi\left(\frac{h_t}{4}\right) - \frac{s_W^2}{18}\Bigg] + \mathcal{O}\left(x_t^0\right)\,, \qquad (4.76)$$

respectively. Here we have introduced

$$\phi(x) = \begin{cases} 4\sqrt{\frac{x}{1-x}}\,\mathrm{Cl}_2\left(2\arcsin\sqrt{x}\right)\,, & \text{for } 0 < x \leq 1\,, \\ \frac{1}{\lambda}\left[-4\,\mathrm{Li}_2\left(\frac{1-\lambda}{2}\right) + 2\ln^2\left(\frac{1-\lambda}{2}\right) - \ln^2(4x) + \frac{\pi^2}{3}\right]\,, & \text{for } x > 1\,, \end{cases} \qquad (4.77)$$

where $\lambda = \sqrt{1-1/x}$ and $\mathrm{Cl}_2(x) = \mathrm{Im}\,\mathrm{Li}_2(e^{ix})$ denotes the Clausen function. As can be seen in Fig. 4.5, the leading HTE term approximates our full result very poorly, especially for a light Higgs. We have also studied the convergence of the HTE, calculating its first three terms, and found that for realistic m_t values they do not converge, in a way very similar to what has been observed in the case of $B^0 - \bar{B}^0$ mixing [252]. It is therefore quite different from what happens in the case of the calculation of precision observables [250, 251, 293], where the top contributions originate from two-point functions. The HTE for the latter seems to work remarkably well up to two-loops [294, 295] and has been checked even at the three-loop level in the case of the mixed $\mathcal{O}(\alpha\alpha_s^2)$ corrections [293].

Finally, it is important to mention that Eq. (4.75) differs from the analogous one presented in reference [215] by a term

$$\delta C_{7,e}^{\gamma,\mathrm{eff}\,(1)}(M_W) = \frac{g^2}{16\pi^2}\, x_t \left[\frac{1}{9}\left(\frac{1}{2} - \frac{s_W^2}{3}\right) + \frac{s_W^2}{18}\right] + \mathcal{O}\left(x_t^0\right)\,. \qquad (4.78)$$

On the other hand, we agree with the findings of Strumia [215] if we perform the calculation in the so-called gaugeless limit. This is not surprising because it is known [254]

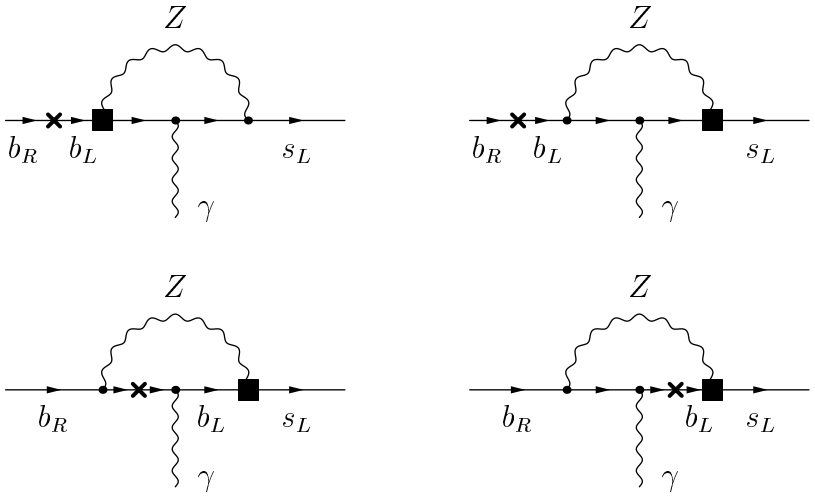

Figure 4.7: Possible insertions of an effective Z penguin vertex into a one-loop diagram.

that the gaugeless approximation does not always include all leading m_t^2 contributions. To understand better this point, notice that for a asymptotically heavy top both the top Yukawa coupling y_t, and the loop integration can provide powers of the top mass. In the case at hand, the one-loop integrals are convergent, so that the one-loop contributions scale at most like $y_t^2/m_t^2 \sim g^2/M_W^2$. At the two-loop level, the gaugeless contributions scale as $y_t^4/m_t^2 \sim y_t^2\, g^2/M_W^2 \sim g^4 m_t^2/M_W^2$, but the same heavy top behavior can be obtained by inserting a dimension four operator[10] proportional to y_t^2 in a topless loop. In general, the effective Lagrangian obtained after integrating out the heavy top tells us exactly which the relevant operators are [296, 297]. In our case, only the diagrams in Fig. 4.7 contribute to the leading HTE through the insertion of a flavor changing dimension four Z boson penguin operator. The diagrams with a mass insertion on the internal b-quark line depend on the regularization scheme — they vanish if IR divergences are regulated dimensionally — and in the schemes where they do not vanish they are canceled in the matching by a contribution from the electroweak penguin operator Q_7. In both cases, however, their contributions is reintroduced in the quantity $C_7^{\gamma,\mathrm{eff}}(M_W)$ and $C_8^{g,\mathrm{eff}}(M_W)$ by $C_7(M_W)$. In the limit of a heavy top the effective vertex has the form

$$\Gamma_{Z_\mu b\bar{s}} = \frac{g^3}{16\pi^2}\frac{V_{ts}^* V_{tb}}{c_W}\frac{x_t}{4}\,\bar{s}_L\gamma_\mu b_L + \mathcal{O}\left(x_t^0\right) . \tag{4.79}$$

Inserting this gauge-independent effective coupling in the one-loop diagrams of Fig. 4.7, and keeping in mind that the tree level couplings of the Z boson with b_L proportional to $1/2 - s_W^2/3$, and with b_R proportional to $-s_W^2/3$, we obtain the difference between the HTE of our result and the gaugeless limit. The argument is completely analogous for $C_8^{g,\mathrm{eff}}(M_W)$, whose HTE also differs from the gaugeless approximation:

$$\delta C_{8,e}^{g,\mathrm{eff}\,(1)}(M_W) = -\frac{g^2}{16\pi^2}\,x_t\left[\frac{1}{3}\left(\frac{1}{2}-\frac{s_W^2}{3}\right)+\frac{s_W^2}{6}\right] + \mathcal{O}\left(x_t^0\right) . \tag{4.80}$$

[10] Dimension two insertions are removed by our choice of renormalization in the unphysical sector.

	$B \to X_s\gamma$	$H\gamma\gamma$, Hgg [254, 298]	HZZ, $K \to \pi\nu\bar{\nu}$, $\Delta\rho$, R_b [254, 299–302]	$B^0 - \bar{B}^0$ [252]
One-loop	$\frac{y_t^2}{m_t^2} \sim \frac{g^2}{M_W^2}$	$\frac{(e^2,g_s^2)\, v\, y_t\, m_t}{m_t^2} \sim (e^2, g_s^2)$	$\frac{g^2 m_t^2}{M_W^2}$ or y_t^2	$\frac{y_t^4}{m_t^2}$
Two-loop	$\frac{y_t^4}{m_t^2} \sim \frac{g^2 y_t^2}{M_W^2}$	$\frac{(e^2,g_s^2)\, v\, y_t^3\, m_t}{m_t^2} \sim (e^2, g_s^2) y_t^2$	$\frac{g^2 y_t^2 m_t^2}{M_W^2}$ or y_t^4	$\frac{y_t^6}{m_t^2}$

Table 4.1: Leading HTE contributions to different processes. Following the criterion given in the text, the gaugeless limit fails in the first two cases.

So when does the gaugeless limit potentially fails at two-loop? Whenever at the one-loop level the t-quark diagrams in the limit of a heavy top scale like a constant, namely in the same way as the topless contributions. Indeed, in this case we know that there are some dimension four effective operators proportional to y_t^2 that can be inserted in one-loop diagrams not containing the top and give contributions of the same order, in the limit of a heavy top, of those belonging to the two-loop gaugeless approximation.

In Tab. 4.5 we summarize the situation for the processes considered in the literature at the two-loop level. It should be clear that the gaugeless limit works safely only when the asymptotic expansion in m_t has maximal power, that is, m_t^2 at the one-loop, and m_t^4 at the two-loop level. Of course, there might be exceptions. Indeed, whether the $\mathcal{O}(y_t^2)$ dimension four operators are relevant or not depends on the process under consideration. For instance, in the Hgg effective vertex [298] — relevant for gluon-gluon fusion production and hadronic decays of the SM Higgs boson — they are not because the gluons have no electroweak interaction. This is in contrast to the similar case of the $H\gamma\gamma$ effective vertex [254], where the gaugeless approximation does not give the correct result. Similar considerations apply to the heavy Higgs limit, although the leading term in the heavy Higgs expansion, subject to other constraints, is not always what is expected from dimensional analysis.

Effect on the Branching Ratio

Let us now examine in some detail the effect of our calculation on the $B \to X_s\gamma$ branching ratio. As a first step we calculate the $\mathcal{O}(\alpha)$ corrections to the Wilson coefficients of the magnetic type operators Q_7^γ and Q_8^g. It is well known that the large mixing between the current-current operator Q_2 and the magnetic photon penguin operator Q_7^γ induces additive terms in the running of the coefficient functions from the $W^\pm$ to the b-quark mass scale which are numerically very important. Thereby, our aim should be to resum all contributions of $\mathcal{O}(\alpha\alpha_s^n L^n)$. As already mentioned in Section 4.1, these terms either originate in logarithmically enhanced contributions due to gluonic or photonic interactions or in genuine electroweak corrections involving $W^\pm$ and Z bosons, which enter only the determination of the Wilson coefficient functions at the electroweak scale.

Turning to the particular case of $C_7^{\gamma,\mathrm{eff}}(\mu_b)$ and neglecting the last term in $\vec{C}_e^{\,\mathrm{eff}\,(1)}(\mu_b)$ which is presently unknown, we see from Eq. (3.31) that the $\mathcal{O}(\alpha)$ terms are given by

$$C_{7,e}^{\gamma,\mathrm{eff}\,(1)}(\mu_b) = C_{7,e}^{\gamma,U_s}(\mu_b) + C_{7,e}^{\gamma,U_e}(\mu_b) + C_{7,e}^{\gamma,U_e'}(\mu_b)\,, \tag{4.81}$$

i	1	2	3	4
k_i	$\frac{2199454}{272277}$	$-\frac{19501}{3695}$	0	0
m_i	$\frac{55245280}{272277}$	$-\frac{110456}{739}$	0	0
n_i	$-\frac{129771266}{170717679}$	$\frac{1265317}{1008735}$	$-\frac{6}{7}$	$\frac{1}{7}$
o_i	$-\frac{2346358688}{170717679}$	$\frac{20453476}{1008735}$	$-\frac{96}{7}$	$\frac{16}{7}$
p_i	$\frac{50090080}{131509791}$	$-\frac{107668}{646625}$	$-\frac{3254504085930274}{23167509579260865}$	$\frac{34705151}{143124975}$
q_i	$\frac{10974039505456}{21104973066375}$	$-\frac{13056852574}{29922509799}$	$-\frac{718812}{6954395}$	$-\frac{154428730}{12196819523}$
r_i	$\frac{34030521610456}{63314919199125}$	$-\frac{3263300223796}{10323265880655}$	$\frac{776628}{6954395}$	$-\frac{20986276}{36590458569}$
s_i	$\frac{37795840}{394529373}$	$-\frac{2677664}{44617125}$	$-\frac{3254504085930274}{69502528737782595}$	$-\frac{69410302}{429374925}$
t_i	$-\frac{9399750637096}{12662983839825}$	$\frac{1054439887036}{794097375435}$	$-\frac{24928}{60473}$	$-\frac{440752}{38802183}$
u_i	$\frac{372895520}{394529373}$	$-\frac{749408}{1274775}$	0	0

Table 4.2: First part of the magic numbers entering the $\mathcal{O}(\alpha)$ correction to the effective Wilson coefficient of the magnetic operator Q_7^γ.

where the first term on the right-hand side corresponds to the term proportional to $\hat{U}_s^{(0)}(\mu_b, M_W)\vec{C}^{\,\mathrm{eff}\,(0)}(M_W)$ in Eq. (3.31). After substituting the explicit anomalous dimension matrices and the initial conditions we find[11]

$$\begin{aligned} C_{7,e}^{\gamma,U_s}(\mu_b) &= \eta^{\frac{16}{23}} C_{7,e}^{\gamma,\mathrm{eff}\,(1)}(M_W) + \frac{8}{3}\left(\eta^{\frac{14}{23}} - \eta^{\frac{16}{23}}\right) C_{8,e}^{g,\mathrm{eff}\,(1)}(M_W) \\ &\quad + \sum_{i=1}^{8}\left(h_i\eta^{a_i} C_{2,e}^{(1)}(M_W) + k_i\eta^{a_i} C_{3,e}^{(1)}(M_W) + m_i\eta^{a_i} C_{5,e}^{(1)}(M_W)\right) \\ &\quad + \left(\frac{167}{1425}\eta^{-\frac{24}{23}} - \frac{40}{143}\eta^{\frac{3}{23}} + \sum_{i=1}^{8} n_i\eta^{a_i}\right) C_{7,e}^{(1)}(M_W) \\ &\quad + \left(\frac{668}{1425}\eta^{-\frac{24}{23}} - \frac{160}{143}\eta^{\frac{3}{23}} + \sum_{i=1}^{8} o_i\eta^{a_i}\right) C_{9,e}^{(1)}(M_W)\,, \end{aligned} \tag{4.82}$$

with $\eta = \alpha_s(M_W)/\alpha_s(\mu_b)$. The $\mathcal{O}(\alpha)$ corrections to the Wilson coefficients of Q_7^γ and Q_8^g are given in Eqs. (4.73) and (4.74), while the magic numbers k_i, m_i, n_i and o_i entering the above expression can be found in Tabs. 4.2 and 4.3.

The second term in Eq. (4.81) corresponds to the term proportional to $\hat{U}_e^{(0)}(\mu_b, M_W)$ $\vec{C}^{\,\mathrm{eff}\,(0)}(M_W)$ in Eq. (3.31) and reads

$$\begin{aligned} C_{7,e}^{\gamma,U_e}(\mu_b) &= \frac{4\pi}{\alpha_s(\mu_b)}\Bigg[\left(\frac{32}{75}\eta^{-\frac{9}{23}} - \frac{40}{69}\eta^{-\frac{7}{23}} + \frac{88}{575}\eta^{\frac{16}{23}}\right) C_7^{\gamma,\mathrm{eff}\,(0)}(M_W) \\ &\quad - \left(\frac{32}{575}\eta^{-\frac{9}{23}} - \frac{32}{1449}\eta^{-\frac{2}{23}} - \frac{640}{1449}\eta^{\frac{14}{23}} + \frac{704}{1725}\eta^{\frac{16}{23}}\right) C_8^{g,\mathrm{eff}\,(0)}(M_W) \end{aligned}$$

[11] Let us note that in contrast to reference [218] the cofactors of all Wilson coefficients are given analytically in Eqs. (4.82) and (4.85).

i	5	6	7	8
k_i	−2.8536	0.1281	0.1495	−0.2244
m_i	−55.2813	2.6494	0.7191	−1.5213
n_i	0.3292	0.0389	0.0248	−0.0104
o_i	4.6264	0.6629	0.2854	−0.0282
p_i	−0.2502	0.1063	−0.0525	0.0213
q_i	−0.1374	−0.0078	−0.0023	−0.0001
r_i	−0.0700	0.0033	−0.0001	0.0003
s_i	−0.0491	−0.0888	0.0221	0.0115
t_i	0.0445	−0.0032	−0.0029	−0.0064
u_i	−0.7338	0.2821	0.3440	−0.0682

Table 4.3: Second part of the magic numbers entering the $\mathcal{O}(\alpha)$ correction to the effective Wilson coefficient of the magnetic operator Q_7^γ.

$$- \frac{526074716}{4417066408125}\eta^{-\frac{47}{23}} + \frac{65590}{1686113}\eta^{-\frac{20}{23}} + \sum_{i=1}^{8}\left(k_i\eta^{a_i} + m_i\eta^{a_i-1}\right)\Bigg]\,. \tag{4.83}$$

The LO expressions for the effective coefficients of Q_7^γ and Q_8^g are given in terms of the one-loop functions $A_0^t(x_t)$ and $F_0^t(x_t)$ by

$$\begin{aligned} C_7^{\gamma,\text{eff}\,(0)}(M_W) &= -\frac{23}{36} - \frac{1}{2}A_0^t(x_t)\,, \\ C_8^{g,\text{eff}\,(0)}(M_W) &= -\frac{1}{3} - \frac{1}{2}F_0^t(x_t)\,, \end{aligned} \tag{4.84}$$

while the values p_i and q_i can be found in Tabs. 4.2 and 4.3. Our analytic result for $C_{7,e}^{\gamma,U_e}(\mu_b)$ agrees with the one presented by Baranowski and Misiak [217], while it differs from the analogous expression found by Kagan and Neubert [216], who used a truncated operator basis in order to compute this $\mathcal{O}(\alpha\alpha_s^{n-1}L^n)$ correction. For realistic values of η, however, the two formulae are numerically very close. Hence, truncating the operator basis is a correct approximation in the present case.

The third term in Eq. (4.81) stemming from the term proportional to $\hat{U}_e^{(0)}(\mu_b, M_W)$ $\vec{C}_s^{\,\text{eff}\,(1)}(M_W)$ in Eq. (3.31) can be written as

$$\begin{aligned} C_{7,e}^{\gamma,U_e'}(\mu_b) = &\left(\frac{32}{75}\eta^{\frac{14}{23}} - \frac{40}{69}\eta^{\frac{16}{23}} + \frac{88}{575}\eta^{\frac{39}{23}}\right) C_{7,s}^{\gamma,\text{eff}\,(1)}(M_W) \\ &- \left(\frac{32}{575}\eta^{\frac{14}{23}} - \frac{32}{1449}\eta^{\frac{16}{23}} - \frac{640}{1449}\eta^{\frac{37}{23}} + \frac{704}{1725}\eta^{\frac{39}{23}}\right) C_{8,s}^{g,\text{eff}\,(1)}(M_W) \\ &- \left[\frac{70164078728}{13251199224375}\eta^{-\frac{24}{23}} - \frac{81580}{5058339}\eta^{\frac{3}{23}} - \sum_{i=1}^{8}\left(r_i\eta^{a_i} + s_i\eta^{a_i+1}\right)\right] C_{1,s}^{(1)}(M_W) \\ &- \left[\frac{197699944}{7143503625}\eta^{-\frac{24}{23}} + \frac{135280}{389103}\eta^{\frac{3}{23}} - \sum_{i=1}^{8}\left(t_i\eta^{a_i} + u_i\eta^{a_i+1}\right)\right] C_{4,s}^{(1)}(M_W)\,, \end{aligned} \tag{4.85}$$

i	1	2	3	4	5	6	7	8
$\bar{k}_i$	$\frac{1099727}{363036}$	0	0	0	−4.0143	−0.2945	0.4600	0.8196
$\bar{m}_i$	$\frac{6905660}{90759}$	0	0	0	−77.7679	−6.0904	2.2128	5.5576
$\bar{n}_i$	$-\frac{64885633}{227623572}$	0	0	0	0.4632	−0.0895	0.0763	0.0379
$\bar{o}_i$	$-\frac{293294836}{56905893}$	0	0	0	6.5082	−1.5238	0.8782	0.1030
$\bar{p}_i$	$-\frac{2191441}{6262371}$	$\frac{112562}{646625}$	$-\frac{24851322767}{629945606745}$	$\frac{1241}{829710}$	0.0848	0.1098	−0.0201	0.0008
$\bar{q}_i$	$\frac{1371754938182}{7034991022125}$	0	0	0	−0.1932	0.0180	−0.0070	0.0004
$\bar{r}_i$	$\frac{4253815201307}{21104973066375}$	0	0	0	−0.0982	−0.0076	−0.0004	−0.0012
$\bar{s}_i$	$-\frac{1653568}{18787113}$	$\frac{121712}{1939875}$	$-\frac{24851322767}{1889836820235}$	$-\frac{1241}{1244565}$	0.0166	−0.0917	0.0084	0.0004
$\bar{t}_i$	$-\frac{1174968829637}{4220994613275}$	0	0	0	0.0626	0.0073	−0.0090	0.0233
$\bar{u}_i$	$-\frac{16314179}{18787113}$	$\frac{34064}{55425}$	0	0	0.2486	0.2914	0.1314	−0.0026

Table 4.4: Magic numbers entering the $\mathcal{O}(\alpha)$ correction to the effective Wilson coefficient of the chromomagnetic operator Q_8^g.

where the non-vanishing $\mathcal{O}(\alpha_s)$ corrections to the initial conditions of the Wilson coefficients take the following form in the NDR scheme

$$\begin{aligned} C_{1,s}^{(1)}(M_W) &= 15\,, \\ C_{4,s}^{(1)}(M_W) &= -\frac{7}{9} + E_0^t(x_t)\,, \\ C_{7,s}^{\gamma,\mathrm{eff}\,(1)}(M_W) &= \frac{797}{243} - \frac{4}{9}E_0^t(x_t) - \frac{1}{2}A_1^t(x_t)\,, \\ C_{8,s}^{g,\mathrm{eff}\,(1)}(M_W) &= \frac{133}{324} - \frac{1}{6}E_0^t(x_t) - \frac{1}{2}F_1^t(x_t)\,, \end{aligned} \tag{4.86}$$

with the Inami-Lim functions $E_0^t(x_t)$, $A_1^t(x_t)$ and $F_1^t(x_t)$ given in Eqs. (3.44) and (3.45). The values of the magic numbers r_i, s_i, t_i and u_i are summarized in Tabs. 4.2 and 4.3.

Now let us also give the results for the $\mathcal{O}(\alpha)$ corrections to $C_8^{g,\mathrm{eff}}(\mu_b)$. Neglecting again the unknown terms in the last relation of Eq. (3.31) and using the decomposition

$$C_{8,e}^{g,\mathrm{eff}\,(1)}(\mu_b) = C_{8,e}^{g,U_s}(\mu_b) + C_{8,e}^{g,U_e}(\mu_b) + C_{8,e}^{g,U_e'}(\mu_b)\,, \tag{4.87}$$

we find for the first term on the right-hand side of the above equation

$$\begin{aligned} C_{8,e}^{g,U_s}(\mu_b) &= \eta^{\frac{14}{23}} C_{8,e}^{g,\mathrm{eff}\,(1)}(M_W) \\ &\quad + \sum_{i=1}^{8} \left(\bar{h}_i \eta^{a_i} C_{2,e}^{(1)}(M_W) + \bar{k}_i \eta^{a_i} C_{3,e}^{(1)}(M_W) + \bar{m}_i \eta^{a_i} C_{5,e}^{(1)}(M_W) \right) \\ &\quad - \left(\frac{2}{95}\eta^{-\frac{24}{23}} + \frac{2}{11}\eta^{\frac{3}{23}} - \sum_{i=1}^{8} \bar{n}_i \eta^{a_i} \right) C_{7,e}^{(1)}(M_W) \\ &\quad - \left(\frac{8}{95}\eta^{-\frac{24}{23}} - \frac{8}{11}\eta^{\frac{3}{23}} + \sum_{i=1}^{8} \bar{o}_i \eta^{a_i} \right) C_{9,e}^{(1)}(M_W)\,. \end{aligned} \tag{4.88}$$

The $\mathcal{O}(\alpha)$ corrections to the coefficient functions are given in Eqs. (4.73) and (4.74), and the values of the magic numbers $\bar{k}_i$, $\bar{m}_i$, $\bar{n}_i$ and $\bar{o}_i$ can be read of from Tab. 4.4.

The second term on the right-hand side of Eq. (4.87) reads in analytic form

$$\begin{aligned} C_{8,e}^{g,U_e}(\mu_b) = \frac{4\pi}{\alpha_s(\mu_b)} \Bigg[& \frac{4}{25}\left(\eta^{-\frac{9}{23}} - \eta^{\frac{16}{23}}\right) C_7^{\gamma,\text{eff}\,(0)}(M_W) \\ & - \left(\frac{12}{575}\eta^{-\frac{9}{23}} + \frac{28}{69}\eta^{\frac{14}{23}} - \frac{32}{75}\eta^{\frac{16}{23}}\right) C_8^{g,\text{eff}\,(0)}(M_W) \\ & + \frac{6300296}{294471093875}\eta^{-\frac{47}{23}} + \frac{6559}{259402}\eta^{-\frac{20}{23}} + \sum_{i=1}^{8}\left(\bar{p}_i\eta^{a_i} + \bar{q}_i\eta^{a_i-1}\right)\Bigg], \end{aligned} \tag{4.89}$$

with the LO expressions of the magnetic type operators Q_7^γ and Q_8^g given in Eq. (4.84), and $\bar{p}_i$ and $\bar{q}_i$ presented in Tab. 4.4.

The third term on the right-hand side of Eq. (4.87) can be written as

$$\begin{aligned} C_{8,e}^{g,U_e'}(\mu_b) = & \frac{4}{25}\left(\eta^{\frac{14}{23}} - \eta^{\frac{39}{23}}\right) C_{7,s}^{\gamma,\text{eff}\,(1)}(M_W) \\ & - \left(\frac{12}{575}\eta^{\frac{14}{23}} + \frac{28}{69}\eta^{\frac{37}{23}} - \frac{39}{75}\eta^{\frac{16}{23}}\right) C_{8,s}^{g,\text{eff}\,(1)}(M_W) \\ & + \left[\frac{840288368}{883413281625}\eta^{-\frac{24}{23}} + \frac{4079}{389103}\eta^{\frac{3}{23}} + \sum_{i=1}^{8}\left(\bar{r}_i\eta^{a_i} + \bar{s}_i\eta^{a_i+1}\right)\right] C_{1,s}^{(1)}(M_W) \\ & + \left[\frac{2367664}{476233575}\eta^{-\frac{24}{23}} - \frac{6764}{29931}\eta^{\frac{3}{23}} + \sum_{i=1}^{8}\left(\bar{t}_i\eta^{a_i} + \bar{u}_i\eta^{a_i+1}\right)\right] C_{4,s}^{(1)}(M_W)\,, \end{aligned} \tag{4.90}$$

where the non-vanishing $\mathcal{O}(\alpha_s)$ corrections to the initial conditions of the Wilson coefficients have already been given in Eq. (4.86). The values of the magic numbers $\bar{r}_i$, $\bar{s}_i$, $\bar{t}_i$ and $\bar{u}_i$ can be found in Tab. 4.4. Notice that the results presented in Eqs. (4.88), (4.89) and (4.90) are given for the first time.

We are now ready to give numerical values for the $\mathcal{O}(\alpha)$ corrections to the effective coefficients of Q_7^γ and Q_8^g. Using $\mu_b = 4.69\,\text{GeV}$ and renormalizing the t-quark mass at $\mu_t = 165\,\text{GeV}$, we find

$$\begin{aligned} C_{7,e}^{\gamma,\text{eff}\,(1)}(\mu_b) &= 4.085 - 1.286\ln\frac{M_H}{100} - 0.614\ln^2\frac{M_H}{100} + 1.865 + 0.511\,, \\ C_{8,e}^{g,\text{eff}\,(1)}(\mu_b) &= -1.494 - 0.388\ln\frac{M_H}{100} - 0.074\ln^2\frac{M_H}{100} + 1.906 - 0.148\,. \end{aligned} \tag{4.91}$$

Here the first three terms correspond to the $\mathcal{O}(\alpha)$ corrections labeled by U_s, the fourth to the $\mathcal{O}(\alpha)$ corrections with an index U_e, and the last one to the $\mathcal{O}(\alpha)$ corrections characterized by U_e'. Notice that in the case of the $\mathcal{O}(\alpha)$ correction to the effective coefficient of Q_7^γ the first three terms, formally $\mathcal{O}(\alpha\alpha_s^n L^n)$, are twice the sum of the fourth and the fifth term, formally $\mathcal{O}(\alpha\alpha_s^{n-1}L^n)$, for a light Higgs of around 100 GeV. We interpret this as an evidence that genuine electroweak effects involving $W^\pm$ and Z bosons in the electroweak correction to the $b \to s\gamma$ amplitude are dominant with respect to logarithmically enhanced contributions due to gluonic or photonic interactions. From Eq. (4.91) we see that $C_7^{\gamma,\text{eff}}(\mu_b)$ is increased by only 1.3% for $M_H = 100\,\text{GeV}$ due to the

electroweak corrections that we have calculated. The effect is less pronounced for larger Higgs masses. In a similar way, we find that for $C_8^{g,\text{eff}}(\mu_b)$ the numerical impact on the last two terms in Eq. (4.91) is more important than that of the two-loop correction. Due to the cancellation of the individual contributions, electroweak effects increase $C_8^{g,\text{eff}}(\mu_b)$ by less than 0.1% for a light Higgs.

In order to see how electroweak corrections affect the calculation of the branching ratio of $B \to X_s\gamma$ it is sufficient to remember the structure of the perturbative QCD corrections. Once we keep this in mind, it is easy to see that the electroweak correction ε_{ew} to the perturbative quantity $P(\delta)$ introduced in Eq. (3.56) is given by

$$\begin{aligned}\varepsilon_{\text{ew}} = \frac{\alpha}{4\pi}\Bigg[&C_{7,e}^{\gamma,\text{eff}\,(1)}(\mu_b) + \sum_{i=1}^{8} C_i^{\text{eff}\,(0)}(\mu_b)\left(r_{i,e} + \frac{1}{2}\left(\hat{\gamma}_e^{\text{eff}\,(0)}\right)_{i,7\gamma}\ln\frac{m_b^2}{\mu_b^2}\right)\\ &-2C_7^{\gamma,\text{eff}\,(0)}(\mu_b)\ln\frac{M_Z^2}{\mu_b^2}\Bigg]\,.\end{aligned} \tag{4.92}$$

where the sum runs over the operators Q_1–Q_6, Q_7^γ and Q_8^g. The final correction in Eq. (4.92) stems from short-distance photonic corrections to $\Gamma(b \to X_u e\bar{\nu}_e)$. That type of correction is generic to semileptonic charged current decays [303]. It is generally factored out of semileptonic B decays before the extraction of $|V_{ub}|$ and $|V_{cb}|$, and hence must be included here. The quantities $r_{i,e}$ originate from the two-loop $\mathcal{O}(\alpha)$ matrix elements of the four quark operators Q_1–Q_6 and the one-loop matrix elements of the magnetic type operators Q_7^γ and Q_8^g. The calculation of the $\overline{\text{MS}}$-renormalized on-shell $b \to s\gamma$ amplitude at $\mathcal{O}(\alpha)$ from which the coefficients $r_{i,e}$ can determine will be presented in Appendix E. For Q_1 and Q_2, and for Q_7^γ and Q_8^g we confirm the findings of reference [219]. For the QCD penguin operators Q_3–Q_6 our results are new. Altogether they read

$$\begin{aligned}
r_{1,e} &= \frac{3332}{2187} - \frac{4}{9}a(z) - \frac{4}{9}b(z) + \frac{160}{729}i\pi\,,\\
r_{2,e} &= \frac{833}{729} - \frac{a(z)}{3} - \frac{b(z)}{3} + \frac{40}{243}i\pi\,,\\
r_{3,e} &= \frac{748}{729} + \frac{2\pi}{9\sqrt{3}} - \frac{2}{81}\pi^2 + \frac{8}{27}X_b - \frac{a(1)}{12} + \frac{7}{6}b(1) - 2b(z) + \frac{26}{243}i\pi\,,\\
r_{4,e} &= \frac{2680}{2187} + \frac{8\pi}{27\sqrt{3}} - \frac{8}{243}\pi^2 + \frac{32}{81}X_b - \frac{a(1)}{9} + \frac{2}{9}b(1) + \frac{56}{729}i\pi\,,\\
r_{5,e} &= \frac{78301}{729} + \frac{8\pi}{9\sqrt{3}} - \frac{40}{81}\pi^2 + \frac{32}{27}X_b - \frac{13}{3}a(1) + \frac{38}{3}b(1) - 12a(z) - 20b(z) + \frac{3908}{243}i\pi\,,\\
r_{6,e} &= \frac{62440}{2187} + \frac{32\pi}{27\sqrt{3}} - \frac{160}{243}\pi^2 + \frac{128}{81}X_b - \frac{16}{9}a(1) + \frac{32}{9}b(1) + \frac{896}{729}i\pi\,,\\
r_{7\gamma,e} &= -\frac{25}{27} - \frac{2}{9}i\pi\,,\\
r_{8g,e} &= 0\,,
\end{aligned} \tag{4.93}$$

with $z = m_c^2/m_b^2$. Similar ratios for the light u-, d- and s-quarks have been set to zero. The functions $a(z)$ and $b(z)$ as well as the constants X_b, $a(1)$ and $b(1)$ entering the $\mathcal{O}(\alpha)$ matrix elements are given in Appendix E. The numerical values of $r_{i,e}$ for two different values of m_c/m_b are presented in Tab. 4.5. From that table we observe that the real parts

	$m_c/m_b = 0.22$		$m_c/m_b = 0.29$	
	$\mathrm{Re}\, r_{i,e}$	$\mathrm{Im}\, r_{i,e}$	$\mathrm{Re}\, r_{i,e}$	$\mathrm{Im}\, r_{i,e}$
$r_{1,e}$	1.1079	0.1997	0.9095	0.1000
$r_{2,e}$	0.8309	0.1498	0.6821	0.0750
$r_{3,e}$	0.9044	0.2196	0.8809	0.1518
$r_{4,e}$	0.9244	0.1207	0.9244	0.1207
$r_{5,e}$	75.7092	32.4895	70.2601	29.5256
$r_{6,e}$	16.7843	1.9306	16.7843	1.9306
$r_{7\gamma,e}$	−0.9259	−0.6981	−0.9259	−0.6981
$r_{8g,e}$	0	0	0	0

Table 4.5: Real and imaginary parts of $r_{i,e}$ for two different values of m_c/m_b.

of $r_{5,e}$ and $r_{6,e}$ are considerably larger than the remaining ones. However, since the Wilson coefficients of the QCD penguin operators are small in the SM, the $\mathcal{O}(\alpha)$ matrix elements of these operators affect the branching ratio of $B \to X_s\gamma$ in a negligible way. Nevertheless, we will include all relevant QED matrix elements in our numerical analysis.

We stress that, as we neglect the term $\vec{C}_e^{\,\mathrm{eff}\,(1)}(\mu_b)$ in Eq. (3.31), our evaluation of $\mathcal{O}(\alpha\alpha_s^n L^n)$ effects in $B \to X_s\gamma$ is incomplete, although we are confident that it should provide a good approximation. Our numerical result is valid in the NDR scheme supplemented by the definition of evanescent operators of references [196, 273]. An analysis of the way the scheme dependent terms recombine can be found in the NNLO study [240]. The scheme dependence of our result is introduced in Eq. (4.73) and in the $\mathcal{O}(\alpha)$ matrix elements $r_{i,e}$. The one from Eq. (4.73) is numerically negligible, as it affects the $B \to X_s\gamma$ branching ratio by less than 0.01%. All the residual scheme dependent pieces would be canceled by corresponding terms in the anomalous dimension matrix at $\mathcal{O}(\alpha\alpha_s)$, if it were available.

Neglecting the last term in $\vec{C}_e^{\,\mathrm{eff}\,(1)}(\mu_b)$ and using the reference value $M_H = 115\,\mathrm{GeV}$ and $m_c/m_b = 0.22$ as in the study [180], we see from Eq. (4.92) that for $\mu_b = m_b$ the $\mathcal{O}(\alpha)$ contribution to the $B \to X_s\gamma$ branching ratio under absolute value is given by

$$\begin{aligned} \varepsilon_{\mathrm{ew}} &= 0.0024 + 0.0012 + 0.0003 + (0.0004 + 0.0002\,i) + 0.0028 \\ &= 0.0071 + 0.0002\,i\,, \end{aligned} \tag{4.94}$$

which updates the result given in reference [219]. Here the first, second and third term corresponds to the U_s, U_e and U_e' component of the $\mathcal{O}(\alpha)$ correction to the effective coefficient of Q_7^γ, respectively. The fourth term derives from the QED matrix elements and was partly included in the paper mentioned above. The last term is due to the QED corrections to the semileptonic decay amplitude and is the same as in reference [180]. Notice that the first term, although formally suppressed with respect to the second and third, is larger, as it incorporates all purely electroweak contributions. The total effect of the QED and electroweak corrections in $\varepsilon_{\mathrm{ew}}$ on the branching ratio is a 3.6%

reduction while the $\mathcal{O}(\alpha\alpha_s^n L^n)$ contributions alone lead to a 1.6% reduction. As different contributions accidentally compensate each other, $\varepsilon_{\rm ew}$ is almost exactly the same that was used in the analyses [180, 218, 219].

Numerical Analysis of the $B \to X_s\gamma$ Branching Ratio

In the present subsection, we shall calculate the branching ratio of the $B \to X_s\gamma$ decay using the NLO QCD formulae collected in Chapter 3, including all known higher order effects as well as our new results. We also update the input parameters and introduce some minor refinements in the NLO analysis. For instance, with respect to the detailed analyses [186, 196, 216, 247], we adopt a new value of the ratio of the CKM angles standing in front of $P(\delta)$. This CKM cofactor can be expressed in terms of the so-called Wolfenstein parameters [304, 305] as follows

$$\begin{aligned}\left|\frac{V_{ts}^* V_{tb}}{V_{cb}}\right|^2 &= 1 + (2\bar\rho - 1)\,\lambda^2 + \left(\bar\rho^2 + \bar\eta^2 - A^2\right)\lambda^4 + \mathcal{O}\left(\lambda^6\right) \\ &\approx 0.971 + 0.10\,(\bar\rho - 0.224) = 0.971 \pm 0.004\,,\end{aligned} \tag{4.95}$$

where $\lambda = 0.2237$, $A = 0.819$, $\bar\rho = 0.224 \pm 0.038$ and $\bar\eta = 0.317$ [4] have been used. The only relevant source of uncertainty is the error in $\bar\rho$. Even if this error were enlarged by a factor of 2, the influence of $|V_{ts}^* V_{tb}/V_{cb}|^2$ on the overall uncertainty in $B \to X_s\gamma$ would remain negligible. Notice that the central value of Eq. (4.95) is also consistent with the analysis of reference [5]. We also use $M_Z = 91.1876\,\text{GeV}$, $M_W = 80.451\,\text{GeV}$, $\alpha_s(M_Z) = 0.1185 \pm 0.0020$, $m_{c,\overline{\rm MS}}(m_{c,\overline{\rm MS}}) = (1.25 \pm 0.10)$ GeV and $\text{BR}\,(B \to X_c e\bar\nu_e) = 0.1045 \pm 0.0021$ [2]. For the b-quark in the so-called $1S$-scheme, we use $m_{b,1S} = (4.69 \pm 0.03)$ GeV [306]. As far as the t-quark mass is concerned, $m_{t,\overline{\rm MS}}(m_{t,\overline{\rm MS}}) = (165 \pm 5)$ GeV is used, which corresponds to $m_{t,\rm pole} = (174.3 \pm 5.1)$ GeV [2].

The mass ratio $r(\mu_W)$ and the phase-space factor C entering the NLO prediction for the branching ratio of $B \to X_s\gamma$ given in Eq. (3.52) have been determined in reference [180] along the lines of the upsilon expansion. The final results obtained there read

$$r\left(m_{t,\overline{\rm MS}}(m_{t,\overline{\rm MS}})\right) = 0.578 \pm 0.002\,, \qquad C = 0.575 \pm 0.02\,. \tag{4.96}$$

The main uncertainty in the perturbative ratio on the right-hand side of Eq. (3.53) originates from the two-loop diagrams with c-quarks presented in Fig. 3.8. Such 1PI diagrams which where calculated nearly a decade ago by Greub et al. [203, 204] and recently by Buras et al. [205] are the only source of m_c/m_b dependence of the $b \to s\gamma$ amplitude. Since the dependence of these matrix elements on m_c/m_b is quite strong, we should ask what renormalization scheme should be used for the quark masses. Should we use $m_{c,\rm pole}/m_{b,\rm pole} = 0.29 \pm 0.02$ or, perhaps, $m_{c,\overline{\rm MS}}(\mu)/m_{b,\rm pole} = 0.22 \pm 0.02$ with μ chosen between m_c and m_b? In principle, such a question is a NNLO issue that can be resolved only after calculating three-loop corrections to the diagrams depicted in Fig. 3.8. However, it is numerically very important, because changing m_c/m_b from 0.29 to 0.22 in the considered matrix elements causes an enhancement of the $B \to X_s\gamma$ branching ratio by 11% [180], that is, by as much as the present experimental and theoretical uncertainties.

Since calculating finite parts of three-loop corrections to the diagrams shown in Fig. 3.8 would be a very difficult task at present, one has to guess the optimal choice for m_c and m_b, on the basis of our experience from other calculations. As argued in reference [180], the

uncertainty in the branching ratio of $B \to X_s\gamma$ stemming from this scheme-dependence can be accounted for setting $m_c/m_b = m_{c,\overline{\rm MS}}(\mu)/m_{b,1S}$ in the two-loop diagrams, and varying the scale μ between m_c and m_b. This particular choice of scheme can be understood if one bears in mind that all the factors of m_c in the considered diagrams originate from explicit mass factors in the c-quark propagators. In the real part of the associated amplitudes, those c-quarks are dominantly off-shell, with momentum scale μ set by m_b or some seizable fraction of it. Therefore, it seems reasonable [180] to vary μ between m_c and m_b, and use $m_{c,\overline{\rm MS}}(\mu)$ in the ratio m_c/m_b.

As far as the factors of m_b are concerned, they originate either from the overall momentum release in $b \to s\gamma$ or from the explicit appearance of m_b in the b-quark propagators. In the first case, the appropriate choice of m_b is a low-virtuality mass. In the latter case, there is no intuitive argument that could tell us whether $m_{b,\rm pole}$ or $m_{b,\overline{\rm MS}}(m_{b,\overline{\rm MS}})$ should be used. However, as long as the NNLO QCD corrections remain unknown, setting all m_b factors equal to $m_{b,1S}$ seems to be a good choice [180]. The distinction between $m_{b,1S}$ and $m_{b,\rm pole}$, which differ numerically by only 1% at one-loop, as well as the IR sensitivity of the pole mass can be ignored here, because the uncertainties due to $m_{c,\overline{\rm MS}}(\mu)$ are very large.

It remains to determine the numerical value of $m_{c,\overline{\rm MS}}(\mu)/m_{b,1S}$. Using the c-quark mass given above the authors of reference [180] find

$$\frac{m_{c,\overline{\rm MS}}(\mu)}{m_{b,1S}} = 0.22 \pm 0.04\,, \tag{4.97}$$

which implies

$$\begin{aligned} a(z) &= (0.97 \pm 0.27) + (1.01 \pm 0.15)\,i\,, \\ b(z) &= (-0.04 \pm 0.01) + (0.09 \pm 0.02)\,i\,, \end{aligned} \tag{4.98}$$

where the uncertainties correspond to varying μ between m_c and m_b. The uncertainty in $m_{c,\overline{\rm MS}}(m_{c,\overline{\rm MS}})$ is practically irrelevant here, when compared to the error originating from the variation of the renormalization scale. We also note that the central value of Eq. (4.97), is very close to the renormalization group invariant $\overline{\rm MS}$ ratio $m_{c,\overline{\rm MS}}(\mu)/m_{b,\overline{\rm MS}}(\mu) = 0.215$.

The numerical value of the electroweak correction $\varepsilon_{\rm ew}$ has already been given in Eq. (4.94), and the one of the non-perturbative correction $N(\delta)$ introduced in Eq. (3.63) reads

$$N(\delta) = 0.0036 \pm 0.0006\,, \tag{4.99}$$

where $\lambda_2 = 0.12\,\text{GeV}^2$ and the value of the c-quark mass given above have been used. The indicated uncertainty is due to the c-quark mass only. Numerically, one find that the non-perturbative contributions parameterized by $N(\delta)$ increase the $B \to X_s\gamma$ branching ratio by about 2.5%.

Last but not least, we also have to give the numerical values for the quantities K_t, K_c and $B(\delta)$. For a cut on the photon energy of $E_\gamma = 1.6\,\text{GeV}$ we find at the NLO level

$$\begin{aligned} K_t &= (0.397 \pm 0.003) + (0.011 \pm 0.002)\,i\,, \\ K_c &= (-0.611 \pm 0.002) + (-0.032 \pm 0.008)\,i\,, \\ B(\delta) &= (3.1 \pm 1.0) \times 10^{-3}\,, \end{aligned} \tag{4.100}$$

in agreement with reference [180]. Here the quoted uncertainties are due to variation of the low-energy scale μ_b between $m_b/2$ and $2m_b$ only. We recall that in the NLO QCD

μ_b	μ_W	m_c/m_b	$m_{b,1S}$	m_t	$\alpha_s(M_Z)$	C	BR $(B \to X_c e \bar{\nu}_e)$
$\pm 1.4\%$	$\pm 0.8\%$	$\pm 5.5\%$	$\pm 0.2\%$	$\pm 1.0\%$	$\pm 2.3\%$	$\pm 3.6\%$	$\pm 2.0\%$

Table 4.6: Uncertainties in the branching ratio of $B \to X_s\gamma$ due to various sources.

computation, the imaginary parts of the quantities K_t and K_c are irrelevant, because all the $\mathcal{O}(\alpha_s^2)$ terms on the right-hand side of Eq. (3.53) are set to zero after taking the square. If one does not set the imaginary parts of K_t and K_c to zero, they affect the perturbative quantity $P(\delta)$ by only 0.5%. Furthermore, it is important to remember that a complete analysis of electroweak $\mathcal{O}(\alpha)$ effects in $B \to X_s\gamma$ would require to know the $\mathcal{O}(\alpha)$ corrections to the $b \to s\gamma g$ and $b \to s\gamma\bar{q}q$ transitions with $q = u, d, s$ as well. Unfortunately, these bremsstrahlungs corrections are unknown at present. Hence, we have neglected them in $B(\delta)$. The resulting error will be absorbed in the NNLO uncertainty below. This is mandatory because the $\mathcal{O}(\alpha_s)$ contribution to $B(\delta)$ changes the branching ratio of $B \to X_s\gamma$ by at most 4% if the cut-off energy E_γ is varied between 1 GeV and 2 GeV, and there are good reasons to expect that the corresponding $\mathcal{O}(\alpha)$ corrections are numerically even less important.

From Eq. (4.100) one can see that the residual μ_b-dependence of the real parts of K_t and K_c is very weak at the NLO level. Such a weak μ_b-dependence is not caused by any accidental cancellations among strongly μ_b-dependent terms. This is contrary to what has been observed in many previous calculations [186, 196, 216, 218, 247]. In the present approach, there is no indication that the unknown NNLO corrections[12] could be much larger than $(\alpha_s(m_b)/\pi)^2 \approx 0.5\%$ times a factor of order unity. Thus, it seems safe to assume a value of $\pm 4\%$ for the theoretical error due to higher-order QCD and QED effects. Realize that this is almost twice the combined scale dependence of the result obtained by scanning μ_b and μ_W between one half and twice their central value, which amounts to $\pm 2.2\%$. Consequently, our estimate of the overall uncertainty in the final prediction for the $B \to X_s\gamma$ branching ratio is not larger than in the previous analyses [186, 196, 216, 218, 247], despite taking into account a error of $\pm 5.5\%$ related to the value for m_c/m_b.

Incorporating all perturbative and non-perturbative corrections, including all errors, and adding them in quadrature, one obtains[13]

$$\text{BR}\,(B \to X_s\gamma)_{E_\gamma > 1.6\,\text{GeV}} = (3.58 \pm 0.30) \times 10^{-4}\,, \tag{4.101}$$

very close to the findings of reference [206]. The relative importance of various uncertainties is shown in Tab. 4.6. The sensitivity of our final result Eq. (4.101) to M_H is very weak: We find a reduction of only 0.3% when the Higgs mass M_H is changed from 115 GeV to 200 GeV.

In view of the fact that many of the published results have been calculated for $E_\gamma = m_b/20$, corresponding to a cut-off parameter $\delta = 0.9$, it interesting to check what Eq. (3.52) gives in this case. We find

$$\text{BR}\,(B \to X_s\gamma)_{E_\gamma > m_b/20} = (3.70 \pm 0.30) \times 10^{-4}\,. \tag{4.102}$$

[12] Except those related to the ratio m_c/m_b that has been discussed above.

[13] At this point, we would like to thank Dr. P. Gambino for providing us with the Fortran code that was used to calculate the branching ratio of $B \to X_s\gamma$ in the recent analysis [180].

It is the above result that should be compared [216] with the experimental world average (1.2) for the total branching ratio. The difference between theory and experiment is at the level of $1\,\sigma$. However, one should remember that the theoretical errors have no statistical interpretation, which implies that the value of $1\,\sigma$ has only an illustrative character.

Notice that the choice $\delta = 0.9$ for the cut-off parameter made in Eq. (4.102) corresponds to the unrealistic case of an almost fully inclusive measurement, whereas the choice $\delta = 0.3$ made in Eq. (4.101) corresponds to the restriction to the high-energy part of the photon spectrum, which in practice is required for experimental reasons. For higher values of the cut-off parameter of around $\delta = 0.15$, non-perturbative uncertainties are much larger because the B-meson shape function are unknown. Models for the shape functions considered in references [207, 216] suggest that $E_\gamma = 1.6\,\text{GeV}$ used in Eq. (4.101) might already be low enough to make those uncertainties negligible. On the other hand, the experimental measurement of is based on a much stronger cut, $E_\gamma = 2.0\,\text{GeV}$ [30], but needs to be extrapolated to a more inclusive branching fraction [216]. For this purpose an approximation formula for the central value of the integrated branching ratio as a function of δ might be useful. Performing a fit to our result in the region $0.15 < \delta < 0.55$ we obtain

$$\text{BR}\,(B \to X_s\gamma)_{E_\gamma > (1-\delta)E_\gamma^{\max}} = \left(3.25 + 1.93\,\delta - 3.57\,\delta^2 + 2.51\,\delta^3\right) \times 10^{-4}\,, \tag{4.103}$$

which exhibits a mild, almost linear dependence on the cut-off in a large region of δ, and reproduces the exact result within $\pm 0.1\%$. Outside the considered region of δ, our formulae from Chapter 3 are not expected to work well. On the low-energy side, this is due to the fact that we have not included the non-perturbative contributions stemming from Q_8^g which has been analyzed in reference [243] with the help of fragmentation functions. As far as the high-energy side is concerned, the growth of the uncertainties with E_γ can roughly estimated by using the plots showing the theoretical predictions for the integrated $B \to X_s\gamma$ branching given in references [207, 216]. However, translating those plots into quantitative estimates is rather difficult, because of the model dependence resulting from the inclusion of the Fermi motion involved. In our opinion, a further study of this issue will be necessary for a precise comparison of theory and experiment in the $B \to X_s\gamma$ decay.

Finally, let us mention that if we had used $m_c/m_b = 0.29$ instead of $m_c/m_b = 0.22$ in our analysis, we would have found

$$\text{BR}\,(B \to X_s\gamma)_{E_\gamma > m_b/20} = (3.33 \pm 0.30) \times 10^{-4}\,, \tag{4.104}$$

for the integrated branching ratio. The latter result is very close to the ones obtained in many previous analyses [186, 196, 216, 218, 247]. Thus, the replacement of $m_{c,\text{pole}}/m_{b,\text{pole}}$ by the more appropriate $m_{c,\overline{\text{MS}}}(\mu)/m_{b,1S}$ in the two-loop matrix element of the current-current operator Q_2 is the main reason why our result is significantly higher than the previously published ones.

Part III

Conclusions

Chapter 5

Conclusions and Outlook

In the present thesis, we have summarized the existing calculations of perturbative and non-perturbative contributions to the inclusive radiative B decays, paying special attention to the electroweak effects in the $B \to X_s\gamma$ and $B \to X_s g$ decays. In particular, we have computed the complete two-loop $\mathcal{O}(\alpha)$ Wilson coefficients relevant for the radiative weak decays of the B-meson. Several subtleties arise in the calculation, mostly linked to the presence of unphysical operators. In order to clarify these subtleties we have adopted two different methods to regulate IR divergences. In contrast to the off-shell $\mathcal{O}(\alpha_s)$ calculation [186, 187], evanescent operators turn out to play a crucial role in the $\mathcal{O}(\alpha)$ computation. In addition, we have explained the relevance of gauge-variant operators in our calculation. As a byproduct of our calculation we have presented the complete $\mathcal{O}(\alpha)$ corrections to the Wilson coefficient of the current-current operator Q_2. Our results improve upon existing calculations [214, 215, 218] and put genuine electroweak corrections to $B \to X_s\gamma$ on a firmer basis. We have also accurately discussed the interplay between electroweak and QCD corrections, and explained the implementation of $\mathcal{O}(\alpha\alpha_s^n L^n)$ effects in detail, including all relevant QED matrix elements. Still, not all $\mathcal{O}(\alpha\alpha_s^n L^n)$ contributions to radiative decays of the B-meson are under control. We have pointed out that the uncalculated corrections are related to the two- and three-loop $\mathcal{O}(\alpha\alpha_s)$ anomalous dimension matrix and to the $\mathcal{O}(\alpha)$ bremsstrahlungs corrections, which are both unknown at present. The incompleteness of our calculation makes it scheme-dependent, but as we have noted, the scheme dependence is remarkable small. On the other hand, the calculation of the missing contributions would require a significant effort.

Finally, we have updated the SM prediction for the $B \to X_s\gamma$ branching ratio following closely the analysis [180]. We have pointed out that the charm loop contribution to $B \to X_s\gamma$ is numerically dominant and very stable under logarithmic QCD corrections. The strong enhancement of the branching ratio appears to be almost entirely due to the t-quark sector, and can be attributed to the large anomalous dimension of the b-quark mass. These observations allow one to achieve better control over the residual scale-dependences at the NLO level. Furthermore, we have discussed the main uncertainties in the present-day SM prediction for the branching ratio of $B \to X_s\gamma$. In particular, we have stressed that replacing $m_{c,\text{pole}}/m_{b,\text{pole}}$ in the two-loop matrix elements of the QCD penguin operators by the more appropriate $m_{c,\overline{\text{MS}}}(\mu)/m_{b,1S}$ with μ chosen between m_c and m_b causes an increase of the branching ratio of $B \to X_s\gamma$ by around 11%. After inclusion of all NLO QCD contributions, of non-perturbative corrections and of all known QED and electroweak effects, we find $\text{BR}\,(B \to X_s\gamma) = (3.58 \pm 0.30) \times 10^{-4}$, for a cut-off energy of

$E_\gamma > 1.6\,\text{GeV}$ in the B-meson rest frame. The total effect of the QED and electroweak corrections on the branching ratio is a 3.6% reduction, while the $\mathcal{O}(\alpha\alpha_s^n L^n)$ contributions alone lead to a 1.6% reduction for a light Higgs mass M_H of around 100 GeV, and decreases slowly for larger values of M_H. In view of the fact, that the leading $\mathcal{O}(\alpha\alpha_s^{n-1}L^n)$ corrections decrease the branching ratio of $B \to X_s\gamma$ only in a minor way, by about 0.7%, and the effect of the QED matrix elements are very small, although formally of the same order as the matching conditions, we expect the subleading QED effects to be eventually small.

Removing the perturbative uncertainty due to the m_c-dependence would be a extremely tedious task, as it requires the calculation of three-loop penguin diagrams with an insertion of Q_1–Q_6. UV-divergent parts of such diagrams have been already computed in the process of calculating the anomalous dimension matrix at NLO [196, 197]. Evaluating the finite parts would be extremely difficult, though not impossible, if numerical integration was applied. In view of the fact, that fully automatized analytic methods are now available [307–310], finding the remaining NNLO corrections would be relatively simpler. However, before undertaking such a ambitious task, one should make sure that all the non-perturbative effects are really under control. In this connection, the most worrisome effects have their origin in the fact that non-local c-quark contributions might be particularly large [246]. These kind of contributions are related to the two-loop penguin diagrams with c-quark loops shown in Fig. 3.8. The corresponding non-perturbative effects are expected to be suppressed by both $\alpha_s(m_b)$ and Λ_{QCD}/m_b or Λ_{QCD}/m_c. Thus, at first glance, they seem to be irrelevant. However, it remains an open question whether their suppression is numerically sufficient. No quantitative estimates of this kind of non-perturbative effects have been performed so far. The numerical importance of the non-local parts of the latter diagrams can be illustrated by the fact that the right-hand side of Eq. (4.101) changes by about 35% when m_c is changed form the original value $m_c = 0.22\,m_b$ to the threshold for charm pair production $m_c = m_b/2$. Consequently, a Λ_{QCD}/m_b suppressed non-perturbative effect on top of such a large perturbative contribution might not be negligible. Unfortunately, no systematic methods have yet been developed to calculate this kind of non-perturbative corrections.

The present agreement at the 10% level between the experimental (1.2) and the theoretical (4.101) determinations of the $B \to X_s\gamma$ branching ratio implies that clear signatures of new physics in this observable are not likely to be found in the foreseeable future. The importance of improving the accuracy on both the experimental and theoretical side follows from the need for strengthening the $b \to s\gamma$ constraints on theories beyond the SM. Such constraints are likely to be crucial in identifying the origin of new physics effect that we expect to encounter in the LHC era.

Part IV

Appendices

Appendix A

Anomalous Dimension Matrices

In this appendix we report the preliminary results of a new calculation of the anomalous dimension matrices $\hat{\gamma}_s^{\mathrm{eff}\,(0)}$, $\hat{\gamma}_e^{\mathrm{eff}\,(0)}$ and $\hat{\gamma}_s^{\mathrm{eff}\,(1)}$. However, before presenting the final results, we shall spend some words on the algorithm that is used to evaluate the one-, two- and three-loop anomalous dimensions of the effective operators mediating the inclusive $B \to X_s\gamma$ decay. Further details on this subject as well as a comprehensive discussion of the classification of physical and non-physical operators of dimension five and six arising in the renormalization of the effective theory at two- and three-loop level will be given in a forthcoming publication [197].

In the renormalization of QCD and QED at higher loop order the standard method of extracting the UV divergence structure of a Feynman integral with respect to the regularization, such as dimensional regularization, is to perform the calculation with massless propagators. However, if one uses massless propagators to compute three point or higher Green's functions one might generate spurious IR infinities which, in dimensional regularization, cannot be distinguished from the UV divergences one seeks. These can occur when one reduces the class of Feynman integrals to vacuum integrals by expanding them in powers of the external momenta. The classical method to circumvent this potential problem is called IR rearrangement [311,312], which uses the property that within dimensional regularization the overall UV divergences are polynomial in external momenta[1] and masses [313]. It is a recursive subtraction scheme where the UV divergences are removed from the Feynman integrals in a way compatible to adding local counterterms to the Lagrangian. In practice it amounts to adding artificial masses or external momenta in certain propagators of a given Feynman diagram before the expansion in the true external momenta is performed. The artificial external momenta have to be introduced in such a way that all spurious IR divergences are regulated, and the resulting Feynman integrals are calculable. Unfortunately, satisfying these two requirements is rather difficult in practical multiloop calculations. Moreover, the condition that no IR infinities may be introduced is quite restrictive and makes the application of the IR rearrangement very tedious. Often one has to remain with Feynman integrals which are not as simple as one would like them to have. Hence, it was not clear until recently how one could develop the method for an application in an automatic computer algebra program.

In our approach, the IR arrangement is performed by introducing an artificial mass

[1] In any meaningful renormalization prescription, counterterms are polynomial in the external momenta, but not necessarily in the masses.

rather than artificial external momenta. For the calculation of the renormalization constants this means, that we can safely apply Taylor expansions in all the particle masses and the external momenta after introducing a non-zero auxiliary mass M for each internal propagators, including those of the massless vector particles. Following references [195, 273], the starting point of our procedure is the following exact decomposition of propagators:

$$\frac{1}{(k+p)^2 - m^2} = \frac{1}{k^2 - M^2} - \frac{p^2 + 2k \cdot p - m^2 + M^2}{k^2 - M^2} \frac{1}{(k+p)^2 - m^2} \,. \tag{A.1}$$

Here k is a linear combination of the integration momenta, p stands for a linear combination of the external momenta, and m denotes the mass of the propagating particle. If we assume that the theory we are considering is given by an effective Hamiltonian which does not contain non-negligible operators of arbitrarily high dimension, we can always perform so many steps in the propagator decomposition given above, that the overall degree of divergence of any diagram in the corresponding Green's function would become negative if any of its propagators was replaced by the last term in the decomposition. We are then allowed to drop the last term in the propagator decomposition, as it does not affect the UV divergent part of the Green's function after subtraction of all subdivergences. In consequence, this general technique reduces the calculation of the counterterms to the direct calculation of massive tadpole integrals, that is, massive integrals with no external momenta. Provided that all the tadpole diagrams are computable at the considered loop order this algorithm provides a procedure that is well suited for the automatic evaluation of larger numbers of Feynman diagrams.

A further simplification can be achieved by noticing that terms containing powers of the auxiliary mass squared in the numerators contribute only to such UV divergent terms that are proportional to those powers of M^2. These terms are local after the subtraction of all subdivergences, and must precisely cancel similar terms originating from integrals with no auxiliary mass in the numerators. Since using Eq. (A.1) the propagators are decomposed exactly, no dependence on M^2 can remain after performing the whole calculation. This observation allows one to avoid calculating integrals that contain an artificial mass in the numerator. Instead of calculating them, one can just replace them by local counterterms proportional to M^2 which cancel the corresponding subdivergences in the integrals with no M^2 in the propagator numerators. Nevertheless, the final result for the UV divergent parts of the Green's functions are precisely the same as if the full propagators were used.

However, counterterms proportional to M^2 will in general not preserve the symmetry of the underlying theory. Fortunately, the number of these counterterms is usually rather small, because their dimension must be at least twice smaller than the maximal dimension of the operators belonging to the effective theory. For instance, in QCD only a single possible gauge-variant operator exists that fulfills the above requirement. It looks like a gluon mass counterterm[2], and cancels gauge-variant pieces of integrals with no M^2 in the numerators. To ensure that our renormalization procedure with such a gauge violating counterterm is valid, we have checked explicitly the full $\overline{\text{MS}}$ renormalization of QCD and QED up to the three-loop level using the exact decomposition (A.1). This is important since the operators we are interested in are composite and therefore each field present

[2] A ghost mass counterterm does not arise, due to the structure of the ghost two-point function.

in the operators will be renormalized requiring a wave function renormalization. For example,

$$Q^g_{8,0} = Z_q Z_{m_b} Z_g Z_G^{1/2} \sum_i Z_{8g,i} Q_i \,, \tag{A.2}$$

where the sum runs over all possible operators and the subscript 0 denotes bare quantities. In this expression Z_q, Z_g and Z_G are the usual gauge-dependent renormalization constants of the quark field, the coupling constant and the gluon field, respectively, and $Z_{8g,i}$ is related to the gauge-independent anomalous dimension of the particular operator. Therefore, by using an arbitrary covariant gauge with a gauge parameter ξ for the massless vector fields, we can explicitly check that the operator renormalization constants that emerge are gauge-independent. Further, by first renormalizing QCD and QED, this allows us to check that the Feynman rules we are using are consistent. This is important since in order to find the anomalous dimension matrix at $\mathcal{O}(\alpha_s^2)$ one has to evaluate more than 10000 Feynman diagrams, which makes an automatic treatment absolutely mandatory.

The procedure of renormalization with an auxiliary mass works well for individual diagrams. However, the introduction of the mass M in the massless vector field propagators spoils the multiplicative renormalizability of the Green's functions. Here we use an intermediate approach to renormalization in order to get the three-loop counterterms for the sum of the diagrams. We compute the UV poles of the corresponding three-loop massive diagrams. But we do not renormalize each diagram separately. The subtraction of subdivergences is done for the whole sum of the three-loop diagrams. This is done by means of adding to the sum of the three-loop diagrams the sum of the necessary bare diagrams of one- and two-loop with all the vertices replaced by effective vertices and all propagators replaced by effective propagators. The effective vertices contain the necessary vertex renormalization constants up to the appropriate order in the coupling constant and similarly, the effective propagators contain the necessary propagator counterterms. Furthermore, counterterms have to be introduced which correspond to the renormalization of the gluon and photon mass. They are contained in the effective vector field propagators that are needed for the cancellation of subdivergences.

The large number of diagrams which occurs if one considers higher loop orders makes it necessary to generate the diagrams automatically. For the evaluation of the anomalous dimension matrices presented in this appendix all diagrams have been generated with the MATHEMATICA [274] package *FeynArts* 2.2 [275, 276], which provides the possibility to implement own models in a simple way. Furthermore it is quite fast, as it generates several thousand diagrams in a few minutes. In a next step a MATHEMATICA program is used to convert the output into a format recognizable by the language FORM [287]. The group theory for each graph is performed before the integrals are evaluated. The very computation of the integrals is done with the program package `MATAD` [310], which is able to deal with vacuum diagrams at one-, two- and three-loop order where several of the internal lines may have a common mass. The basic idea for the calculation of the tadpole integrals is based on the so-called integration-by-parts technique [314, 315]. It can be used for the derivation of recurrence relations which relate vacuum integrals with different denominator structures. The proper use of the recurrence relations allows the reduction of an arbitrary integral to simpler ones, which can be solved using one- and two-loop formulae, and a linear combination of a small set of so-called master integrals. Only for them a hard calculation is necessary. At the end of the computation the results of the individual diagrams are summed and the bare results are stored. Moreover, a

convenient environment is provided which, for example, makes sure that all result files are up-to-date. Thus processes involving a larger number of diagrams can be treated automatically without taking care of each individual result.

Having summarized the general formalism and our method, we will now record our results. The regularization- and renormalization-scheme independent anomalous dimension matrices $\hat{\gamma}_s^{\mathrm{eff}\,(0)}$ and $\hat{\gamma}_e^{\mathrm{eff}\,(0)}$ is given by

$$\hat{\gamma}_s^{\mathrm{eff}\,(0)} = \begin{pmatrix}
-4 & \frac{8}{3} & 0 & -\frac{2}{9} & 0 & 0 & 0 & 0 & 0 & 0 & -\frac{208}{243} & \frac{173}{162} \\
12 & 0 & 0 & \frac{4}{3} & 0 & 0 & 0 & 0 & 0 & 0 & \frac{416}{81} & \frac{70}{27} \\
0 & 0 & 0 & -\frac{52}{3} & 0 & 2 & 0 & 0 & 0 & 0 & -\frac{176}{81} & \frac{14}{27} \\
0 & 0 & -\frac{40}{9} & -\frac{100}{9} & \frac{4}{9} & \frac{5}{6} & 0 & 0 & 0 & 0 & -\frac{152}{243} & -\frac{587}{126} \\
0 & 0 & 0 & -\frac{256}{3} & 0 & 20 & 0 & 0 & 0 & 0 & -\frac{6272}{81} & \frac{6596}{27} \\
0 & 0 & -\frac{256}{9} & \frac{56}{9} & \frac{40}{9} & -\frac{2}{3} & 0 & 0 & 0 & 0 & \frac{4624}{243} & \frac{4772}{81} \\
0 & 0 & 0 & -\frac{8}{9} & 0 & 0 & 0 & -20 & 0 & 2 & \frac{176}{243} & -\frac{14}{81} \\
0 & 0 & 0 & \frac{16}{27} & 0 & 0 & -\frac{40}{9} & -\frac{52}{3} & \frac{4}{9} & \frac{5}{6} & -\frac{136}{729} & -\frac{295}{486} \\
0 & 0 & 0 & -\frac{128}{9} & 0 & 0 & 0 & -128 & 0 & 20 & \frac{6272}{243} & -\frac{764}{81} \\
0 & 0 & 0 & \frac{184}{27} & 0 & 0 & -\frac{256}{9} & -\frac{160}{3} & \frac{40}{9} & -\frac{2}{3} & \frac{39152}{729} & -\frac{1892}{243} \\
0 & 0 & 0 & 0 & 0 & 0 & 0 & 0 & 0 & 0 & \frac{32}{3} & 0 \\
0 & 0 & 0 & 0 & 0 & 0 & 0 & 0 & 0 & 0 & -\frac{32}{9} & \frac{28}{3}
\end{pmatrix}, \qquad \text{(A.3)}$$

and

$$\hat{\gamma}_e^{\mathrm{eff}\,(0)} = \begin{pmatrix}
-\frac{8}{3} & 0 & 0 & 0 & 0 & 0 & \frac{32}{27} & 0 & 0 & 0 & -\frac{832}{729} & \frac{22}{243} \\
0 & -\frac{8}{3} & 0 & 0 & 0 & 0 & \frac{8}{9} & 0 & 0 & 0 & -\frac{208}{243} & -\frac{116}{81} \\
0 & 0 & 0 & 0 & 0 & 0 & \frac{76}{9} & 0 & -\frac{2}{3} & 0 & -\frac{20}{243} & \frac{20}{81} \\
0 & 0 & 0 & 0 & 0 & 0 & -\frac{32}{27} & \frac{20}{3} & 0 & -\frac{2}{3} & -\frac{176}{729} & \frac{14}{243} \\
0 & 0 & 0 & 0 & 0 & 0 & \frac{496}{9} & 0 & -\frac{20}{3} & 0 & -\frac{22712}{243} & \frac{1328}{81} \\
0 & 0 & 0 & 0 & 0 & 0 & -\frac{512}{27} & \frac{128}{3} & 0 & -\frac{20}{3} & -\frac{6272}{729} & -\frac{1180}{243} \\
0 & 0 & \frac{40}{27} & 0 & -\frac{4}{27} & 0 & \frac{332}{27} & \frac{20}{9} & 0 & -\frac{2}{9} & -\frac{544}{729} & \frac{544}{243} \\
0 & 0 & 0 & \frac{40}{27} & 0 & -\frac{4}{27} & \frac{32}{81} & \frac{20}{9} & 0 & -\frac{2}{9} & \frac{80}{2187} & \frac{962}{2187} \\
0 & 0 & \frac{256}{27} & 0 & -\frac{40}{27} & 0 & \frac{3152}{27} & 0 & -\frac{20}{9} & 0 & -\frac{21064}{729} & -\frac{4208}{243} \\
0 & 0 & 0 & \frac{256}{27} & 0 & -\frac{40}{27} & \frac{512}{81} & \frac{128}{9} & 0 & -\frac{20}{9} & \frac{27200}{2187} & \frac{20648}{2187} \\
0 & 0 & 0 & 0 & 0 & 0 & 0 & 0 & 0 & 0 & \frac{16}{9} & -\frac{8}{3} \\
0 & 0 & 0 & 0 & 0 & 0 & 0 & 0 & 0 & 0 & 0 & \frac{8}{9}
\end{pmatrix}, \qquad \text{(A.4)}$$

respectively. In the above matrices, the $\mathcal{O}(\alpha)$ mixing of the electroweak penguin operators Q_7–Q_{10} into Q_7^γ and Q_8^g is given for the first time. As far as the remaining entries are concerned, our results agree with the old ones of reference [217] and those of references [216,238,239]. However, in order to perform a comparison with the latter results, one needs to make a linear transformation[3] of our operator basis to the standard basis [236, 237] of the four quark operators used in those articles. Notice that the rows corresponding to Q_7–Q_{10} in the matrix $\hat{\gamma}_e^{\mathrm{eff}\,(0)}$ would affect the branching ratio of $B \to X_s\gamma$ only at higher orders in α, since the Wilson coefficient function of the electroweak penguin operators start at first order in α. Yet they are needed in any analysis of non-leptonic weak decays which goes beyond the leading logarithmic approximation.

[3] These linear transformations read $\hat{\gamma}_s^{\mathrm{eff}\,(0)} = \hat{R}\,\hat{\gamma}_s'^{\mathrm{eff}\,(0)}\,\hat{R}^{-1}$ and $\hat{\gamma}_e^{\mathrm{eff}\,(0)} = \hat{R}\,\hat{\gamma}_e'^{\mathrm{eff}\,(0)}\,\hat{R}^{-1}$ where $\hat{\gamma}_s'^{\mathrm{eff}\,(0)}$ and $\hat{\gamma}_s'^{\mathrm{eff}\,(0)}$ denote the anomalous dimension matrices in the basis of references [236, 237] and $\hat{R}$ can be found in Eq. (D.3).

While the matrices $\hat{\gamma}_s^{\mathrm{eff}\,(0)}$ and $\hat{\gamma}_e^{\mathrm{eff}\,(0)}$ are renormalization-scheme independent, $\hat{\gamma}_s^{\mathrm{eff}\,(1)}$ is not. In the $\overline{\mathrm{MS}}$ scheme with fully anticommuting γ_5 supplemented by the definition of evanescent operators of references [196, 273] we obtain

$$\hat{\gamma}_s^{\mathrm{eff}\,(1)} = \begin{pmatrix}
-\frac{355}{9} & -\frac{502}{27} & -\frac{1412}{243} & -\frac{1369}{243} & \frac{134}{243} & -\frac{35}{162} & 0 & 0 & 0 & 0 & -\frac{818}{243} & \frac{3779}{324} \\
-\frac{35}{3} & -\frac{28}{3} & -\frac{416}{81} & \frac{1280}{81} & \frac{56}{81} & \frac{35}{27} & 0 & 0 & 0 & 0 & \frac{508}{81} & \frac{1841}{108} \\
0 & 0 & -\frac{4468}{81} & -\frac{31469}{81} & \frac{400}{81} & \frac{3373}{108} & 0 & 0 & 0 & 0 & \frac{22348}{243} & \frac{10178}{81} \\
0 & 0 & -\frac{8158}{243} & -\frac{59399}{243} & \frac{269}{486} & \frac{12899}{648} & 0 & 0 & 0 & 0 & -\frac{17584}{243} & -\frac{172471}{648} \\
0 & 0 & -\frac{251680}{81} & -\frac{128648}{81} & \frac{23836}{81} & \frac{6106}{27} & 0 & 0 & 0 & 0 & \frac{1183696}{729} & \frac{2901296}{243} \\
0 & 0 & \frac{58640}{243} & -\frac{26348}{243} & -\frac{14324}{243} & -\frac{2551}{162} & 0 & 0 & 0 & 0 & \frac{2480344}{2187} & -\frac{3296257}{729} \\
0 & 0 & 0 & -\frac{5074}{243} & 0 & 0 & -\frac{4468}{81} & -\frac{9589}{27} & \frac{400}{81} & \frac{3373}{108} & ? & ? \\
0 & 0 & 0 & \frac{5117}{729} & 0 & 0 & -\frac{8158}{243} & -\frac{20986}{81} & \frac{269}{486} & \frac{12899}{648} & ? & ? \\
0 & 0 & 0 & -\frac{92872}{243} & 0 & 0 & -\frac{251680}{81} & -\frac{49216}{27} & \frac{23836}{81} & \frac{6106}{27} & ? & ? \\
0 & 0 & 0 & \frac{97238}{729} & 0 & 0 & \frac{58640}{243} & -\frac{48814}{81} & -\frac{14324}{243} & -\frac{2551}{162} & ? & ? \\
0 & 0 & 0 & 0 & 0 & 0 & 0 & 0 & 0 & 0 & \frac{4688}{27} & 0 \\
0 & 0 & 0 & 0 & 0 & 0 & 0 & 0 & 0 & 0 & -\frac{2192}{81} & \frac{4063}{27}
\end{pmatrix} . \quad \text{(A.5)}$$

where question marks denote unknown entries. The two-loop mixing involving the QCD penguin operators Q_1–Q_6 and the electroweak penguin operators Q_7–Q_{10} were found in the standard operator basis [236, 237] in references [189, 190] and in references [193], respectively. In the article [194] the results for the two-loop mixing in the Q_1–Q_6 sector have been calculated in the new operator basis (3.2). The authors of the latter publication also showed how their results for the mixing in the Q_1–Q_6 sector can be transformed to the previously used renormalization scheme, finding agreement with the original calculations. Our results for the mixing between Q_1–Q_6 in the anomalous dimension matrix $\hat{\gamma}_s^{\mathrm{eff}\,(1)}$ are in full conformity with the findings presented in reference [194]. The entries describing the mixing of the remaining four quark operators Q_7–Q_{10} are given for the first time in the operator basis (3.2). However, it is quite non-trivial [194] to verify whether they agree with the previous calculations [193]. Such a comparison is essential because of the phenomenological relevance of the considered quantities. Therefore we will devote a sizable part of a forthcoming article [197] to show how this verification is performed. The two-loop mixing in the sector of the magnetic penguin operators Q_7^γ and Q_8^g was calculated in reference [195]. We have confirmed these results and will give the details of the computation in a subsequent publication [197]. The three-loop mixing between the set Q_1–Q_6 and the operators Q_7^γ and Q_8^g has been completed six years ago [196, 273]. It is currently verified by us [197]. In the latter article we will give the details of this new three-loop calculation as well as the results of the remaining unknown entries in $\hat{\gamma}_s^{\mathrm{eff}\,(1)}$ describing the mixing of the electroweak penguin operators Q_7–Q_{10} into the sector of the magnetic type operators Q_7^γ and Q_8^g. Finally, let us recall that the rows corresponding to Q_7–Q_{10} are irrelevant as far as $\mathcal{O}(\alpha_s^n L^{n-1})$ and $\mathcal{O}(\alpha\alpha_s^n L^n)$ corrections to the radiative B decays are concerned, because the coefficients of these operators start at $\mathcal{O}(\alpha)$. However, it should be emphasized that the $\mathcal{O}(\alpha_s^2)$ mixing of the complete set of four quark operators Q_1–Q_{10} is needed in any NLO analysis of non-leptonic weak decays.

Appendix B

One-Loop Matching for $b \to s\gamma$

In the appendix at hand, we will explicitly show that the gauge-invariant part of the one-loop off-shell $b \to s\gamma$ effective vertex depends on whether the external photon is quantum or background. At first, let us as consider the $b \to s\gamma$ transition in the background field version of the 't Hooft-Feynman gauge.[1] In this case, the calculation of the off-shell amplitude amounts to compute the four 1PI electroweak diagrams shown in Fig. 3.1. Expanding up to the second order in the external momenta and m_b, and requiring equality of our result to the similar off-shell 1PI Green's function in the effective theory described by the effective Hamiltonian (3.1), we obtain the following non-zero coefficients at the matching scale $\mu_W = M_W$:

$$\begin{aligned}
C_7^{\gamma(0)}(M_W) &= \frac{x_t\,(7-5x_t-8x_t^3)}{24\,(x_t-1)^3} - \frac{x_t^2\,(2-3x_t)}{4\,(x_t-1)^4}\ln x_t\,,\\
C_{11}^{(0)}(M_W) &= -\frac{16-48x_t+73x_t^2-35x_t^3}{36\,(x_t-1)^3} + \frac{8-32x_t+54x_t^2-30x_t^3+3x_t^4}{18\,(x_t-1)^4}\ln x_t\,,\\
C_{13}^{(0)}(M_W) &= -\frac{x_t\,(1+11x_t-18x_t^2)}{24\,(x_t-1)^3} - \frac{x_t\,(4-16x_t+15x_t^2)}{12\,(x_t-1)^4}\ln x_t\,,\\
C_{15}^{(0)}(M_W) &= -\frac{x_t\,(1+x_t)}{6\,(x_t-1)^2} + \frac{x_t^2}{3\,(x_t-1)^3}\ln x_t\,,\\
C_{16}^{(0)}(M_W) &= \frac{x_t\,(1+5x_t)}{6\,(x_t-1)^3} - \frac{x_t^2\,(2+x_t)}{3\,(x_t-1)^4}\ln x_t\,.
\end{aligned} \tag{B.1}$$

Let us mention that the LO matching of the off-shell effective Hamiltonian (3.1) has already been performed in reference [226]. We have repeated the calculation and confirmed the findings of the latter article.

Next, let us turn to the case of the $b \to s\gamma$ transition in the usual 't Hooft-Feynman gauge. The diagrams that we have to consider now, consist of those presented in Fig. 3.1 and two additional ones containing a $W^\pm\phi^\mp\gamma$ coupling. Interestingly, the latter diagrams introduce some gauge-variant operators, as they do not maintain explicit gauge invariance at the level of off-shell Green's functions. At the one-loop level the following two gauge-

[1] While the coefficient functions of Q_7^γ and Q_8^g do not depend on the gauge-fixing parameter, this is not the case for the Wilson coefficients of the EOM-vanishing operators Q_{11}-Q_{16}.

variant operators are generated

$$\begin{aligned} Q_{19} &= \frac{e}{16\pi^2}\left[\bar{s}_L\left(\overleftarrow{\not{D}}\overleftarrow{\not{D}}\not{Q} + \not{Q}\not{D}\not{D}\right)b_L + im_b\bar{s}_L\not{Q}\not{D}b_R\right], \\ Q_{20} &= \frac{e}{16\pi^2}\left[\bar{s}_L\left(\overleftarrow{\not{D}} + \not{D}\right)b_L + im_b\bar{s}_L b_R\right]\partial^\mu Q_\mu\,, \end{aligned} \tag{B.2}$$

where Q_μ denotes the quantum photon field. Notice that Q_{19} and Q_{20} are chosen in such a way that the vanish on-shell up to total derivatives, that is, they are EOM-vanishing.

After including these two new operators in the off-shell effective theory, the initial conditions of the Wilson coefficients are found by requiring equality of the off-shell 1PI Green's function on the full and the effective side. In this way we immediately find that the non-vanishing coefficient functions at $\mu_W = M_W$ are given by

$$\begin{aligned} C_7^{\gamma(0)}(M_W) &= \frac{x_t\,(7-5x_t-8x_t^3)}{24\,(x_t-1)^3} - \frac{x_t^2\,(2-3x_t)}{4\,(x_t-1)^4}\ln x_t\,, \\ C_{11}^{(0)}(M_W) &= -\frac{16-48x_t+73x_t^2-35x_t^3}{36\,(x_t-1)^3} + \frac{8-32x_t+54x_t^2-30x_t^3+3x_t^4}{18\,(x_t-1)^4}\ln x_t\,, \\ C_{13}^{(0)}(M_W) &= \frac{x_t\,(2-11x_t+15x_t^2)}{24\,(x_t-1)^3} - \frac{x_t\,(4-13x_t+12x_t^2)}{12\,(x_t-1)^4}\ln x_t\,, \\ C_{15}^{(0)}(M_W) &= -\frac{x_t\,(1+x_t)}{6\,(x_t-1)^2} + \frac{x_t^2}{3\,(x_t-1)^3}\ln x_t\,, \\ C_{16}^{(0)}(M_W) &= \frac{x_t\,(1+5x_t)}{6\,(x_t-1)^3} - \frac{x_t^2\,(2+x_t)}{3\,(x_t-1)^4}\ln x_t\,, \\ C_{19}^{(0)}(M_W) &= \frac{x_t\,(1+x_t)}{2\,(x_t-1)^2} - \frac{x_t^2}{(x_t-1)^3}\ln x_t\,, \\ C_{20}^{(0)}(M_W) &= -\frac{x_t\,(1+x_t)}{4\,(x_t-1)^2} + \frac{x_t^2}{2\,(x_t-1)^3}\ln x_t\,. \end{aligned} \tag{B.3}$$

Comparing Eqs. (B.1) and (B.3) we see that the Wilson coefficients of the operators Q_7^γ, Q_{11}, Q_{15} and Q_{16} do not depend on the gauge chosen for the photon field. It is easy to understand that this must be the case: The Wilson coefficients of the operators Q_7^γ and Q_{11} must be regarded as physical[2], whereas the Wilson coefficients of the EOM-vanishing operators Q_{15} and Q_{16} are determined by the $b \to s$ transition already. In contrast, the Wilson coefficient of Q_{13} does depend on whether a covariant or a background gauge for the photon field is used. Even though contributions to gauge-variant operators arise at the one-loop level due to diagrams containing a $W^\pm\phi^\mp\gamma$ coupling, it is easy to show that these operators are irrelevant in the two-loop calculation presented in Chapter 4, as long as dimensional regularization for both IR and UV divergences is used. This can be either done by explicit calculation, as we did, or by applying the results from the well-developed, formal theory of local operator mixing which is based upon the constraint of the BRST invariance of quantized Yang-Mills field theories [257–266], which tells us that gauge-variant operators do not contribute to physical matrix elements and thus can be disregarded in practical calculations.

[2]Notice that $C_{11}(M_W)$ agrees with the Wilson coefficient of the electroweak penguin operator Q_7 up to $\mathcal{O}(\alpha^2)$ terms.

Appendix C

Bremsstrahlungs Corrections

In this appendix we give all the relevant functions necessary for the calculation of the bremsstrahlungs function $B(\delta)$ introduced in Eq. (3.53). At $\mathcal{O}(\alpha_s)$ the bremsstrahlungs function $B(\delta)$ arising from the $b \to s\gamma g$ and $b \to s\bar{q}q$ transitions with $q = u, d, s$ is given by[1]

$$B(\delta) = \frac{\alpha_s(\mu_b)}{4\pi} \sum_{\substack{i,j=1 \\ i\leq j}}^{8} C_i^{\text{eff}\,(0)}(\mu_b) C_j^{\text{eff}\,(0)}(\mu_b) \phi_{ij}(\delta) + \varphi_{\bar{q}q}(\delta)\,. \tag{C.1}$$

The functions $\phi_{ij}(\delta)$ originate from the gluon bremsstrahlung $b \to s\gamma g$ and have been calculated by several authors [200–202]. For a cut-off energy of $E_\gamma = 1.6\,\text{GeV}$ the numerically dominant functions $\phi_{ij}(\delta)$ entering the bremsstrahlungs function $B(\delta)$ read

$$\begin{aligned}
\phi_{11}(\delta) &= \frac{1}{36}\phi_{22}(\delta)\,, \quad \phi_{12}(\delta) = -\frac{1}{3}\phi_{22}(\delta)\,, \quad \phi_{17}(\delta) = -\frac{1}{6}\phi_{27}(\delta)\,, \quad \phi_{18}(\delta) = \frac{1}{18}\phi_{27}(\delta)\,, \\
\phi_{22}(\delta) &= \frac{64z}{27}\left[\delta \int_0^{(1-\delta)/z} dt\ (1-zt)\left|\frac{G(t)}{t} + \frac{1}{2}\right|^2 + \int_{(1-\delta)/z}^{1/z} dt\ (1-zt)^2 \left|\frac{G(t)}{t} + \frac{1}{2}\right|^2\right]\,, \\
\phi_{27}(\delta) &= -\frac{32z^2}{9}\left[\delta \int_0^{(1-\delta)/z} dt\,\text{Re}\left(G(t) + \frac{t}{2}\right) + \int_{(1-\delta)/z}^{1/z} dt\ (1-zt)\,\text{Re}\left(G(t) + \frac{t}{2}\right)\right]\,, \\
\phi_{28}(\delta) &= -\frac{1}{3}\phi_{27}(\delta)\,, \\
\phi_{77}(\delta) &= -\frac{124}{9} + \frac{40}{3}\delta + \frac{4}{3}\delta^2 - \frac{8}{9}\delta^3 - \left(\frac{28}{3} + \frac{16}{3}\delta - \frac{4}{3}\delta^2\right)\ln\delta - \frac{8}{3}\ln^2\delta\,, \\
\phi_{78}(\delta) &= \frac{32}{9}\left[\frac{9}{4}\delta - \frac{1}{4}\delta^2 + \frac{1}{12}\delta^3 - \delta\ln\delta + \text{Li}_2\,(1-\delta) - \frac{\pi^2}{6}\right]\,, \\
\phi_{88}(\delta) &= \frac{4}{27}\left[7\delta + 3\delta^2 - \frac{2}{3}\delta^3 - \delta\,(2+\delta)\ln\delta + 8\ln\,(1-\delta)\right. \\
&\qquad \left. +4\text{Li}_2\,(1-\delta) - \frac{2}{3}\pi^2 - 2\big(\delta^2 + 2\delta + 4\ln\,(1-\delta)\,\big)\ln\frac{m_b}{m_s}\right]\,.
\end{aligned} \tag{C.2}$$

[1] Here the sum runs over the operators Q_1–Q_6, Q_7^γ and Q_8^g.

The function $G(t)$ in the integrand of $\phi_{22}(\delta)$ and $\phi_{27}(\delta)$ is given by

$$G(t) = \begin{cases} -2\arctan^2\sqrt{\frac{t}{4-t}}\,, & \text{for } t<4\,, \\ 2\ln^2\left(\frac{\sqrt{t}+\sqrt{t-4}}{2}\right) - 2i\pi\ln\left(\frac{\sqrt{t}+\sqrt{t-4}}{2}\right) - \frac{\pi^2}{2}\,, & \text{for } t\geq 4\,. \end{cases} \tag{C.3}$$

The above integrals can be performed analytically with the substitutions $t = 4\sin^2 y$ for $t < 4$ and $t = 4\cosh^2 y$ for $t \geq 4$. The resulting expressions are quite long and therefore we will not report them here. For practical purposes, the compact integral representations given above are however adequate. Notice that apart from a factor of 4 the functions given in Eq. (C.2) are identical to the functions $f_{ij}(\delta)$ used in many previous analyses of the $B \to X_s\gamma$ branching ratio [186, 196, 216, 218, 247], except for the case $\phi_{77}(\delta)$. The difference between $\phi_{77}(\delta)$ and $f_{77}(\delta)$ of reference [196] is due to the Sudakov logarithms $\ln\delta$ and $\ln\delta^2$ and the constant term, which is chosen in such a way that $\phi_{77}(\delta)$ vanishes in the limit $\delta \to 1$. For simplicity, we refrain from resumming the Sudakov logarithms here, because we are interested only in cut-off energies of $E_\gamma < 2.1\,\text{GeV}$, corresponding to $\delta > 0.1$. For such values of δ, the logarithmic divergence of $\phi_{77}(\delta)$ arising at the limit $\delta \to 0$ is not yet relevant. The function $\phi_{88}(\delta)$ is sensitive to collinear singularities regulated by the mass of the s-quark. The collinear singularities can be resummed to all orders of perturbation theory, leading to a collinear safe result [243]. Unless δ is chosen very close to one, the net effect of the resummation is a moderate increase in the result. Since the contribution proportional to $\phi_{88}(\delta)$ is very small, however, it is sufficient for all practical purposes to work with the leading order expression given above. Following reference [196], we take a rather large value for the quark mass ratio, $m_b/m_s = 50$, in order to mimic the effect of the resummation of the collinear logarithms.

The only functions $\phi_{ij}(\delta)$ which have not yet been given explicitly are the ones with at least one index corresponding to the QCD penguin operators Q_3–Q_6. These functions can easily be derived from the results of reference [201] by making a linear transformation of our operator basis to the standard basis [236, 237] of the four quark operators used in the latter article.[2] As these functions have only a 0.1% effect on the $B \to X_s\gamma$ branching ratio for $E_\gamma > 1.6\,\text{GeV}$, we shall not give them explicitly here. Instead, let us give the numerically values of the coefficients $\phi_{ij}(\delta)$ that were used in our numerical analysis of the branching ratio of $B \to X_s\gamma$ leading to the final predictions presented in Eq. (4.101) and Eq. (4.102). For $m_c/m_b = 0.22$ and a cut-off energy of $E_\gamma = 1.6\,\text{GeV}$ we find

$$\phi_{ij} = \begin{pmatrix} 0.0031 & -0.0371 & 0.0003 & -0.0001 & -0.0088 & -0.2217 & 0.0146 & -0.0049 \\ & 0.1113 & -0.0017 & 0.0003 & 0.0531 & 1.3300 & -0.0877 & 0.0292 \\ & & 0.0289 & -0.0096 & 0.6396 & -0.1277 & 0.1128 & -0.0376 \\ & & & 0.0288 & -0.1066 & 0.5807 & -0.0188 & 0.0063 \\ & & & & 3.5616 & -0.9955 & 1.5573 & -0.5191 \\ & & & & & 3.8713 & -0.8168 & 0.2723 \\ & & & & & & -0.5283 & 0.9258 \\ & & & & & & & 0.4550 \end{pmatrix}. \tag{C.4}$$

[2] The formula from which the coefficients $\phi_{ij}(\delta)$ can be obtained have been given in reference [196].

On the other hand, using $m_c/m_b = 0.22$ and a cut-off energy of $E_\gamma = m_b/20$ we obtain

$$\phi_{ij} = \begin{pmatrix} 0.0060 & -0.0724 & -0.0052 & 0.0009 & -0.0896 & -0.4198 & 0.0136 & -0.0045 \\ & 0.2172 & 0.0313 & -0.0052 & 0.5374 & 2.5187 & -0.0817 & 0.0272 \\ & & 0.0556 & -0.0185 & 1.2984 & -0.0470 & 0.1681 & -0.0561 \\ & & & 0.0559 & -0.2164 & 1.0955 & -0.0280 & 0.0093 \\ & & & & 7.6545 & 0.4497 & 2.3680 & -0.7893 \\ & & & & & 7.1087 & -0.9252 & 0.3084 \\ & & & & & & -0.0001 & 1.5494 \\ & & & & & & & 5.2697 \end{pmatrix} . \quad \text{(C.5)}$$

The term denoted by $\varphi_{\bar{q}q}(\delta)$ in Eq. (C.1) stands for the contributions from the $b \to s\bar{q}q$ transitions with $q = u, d, s$. Perturbatively, such effects to the partonic decay rate are suppressed either by the small Wilson coefficients of the QCD penguin operators Q_3–Q_6 or by the tiny CKM cofactor $V_{us}^* V_{ub}$ with respect to the leading terms. A further suppression occurs when we restrict ourselves to high-energy photons [202]. In the numerical analysis of the branching ratio of $B \to X_s\gamma$ presented at the end of Chapter 4, we have thus set $\varphi_{\bar{q}q}(\delta)$ to zero without including any additional uncertainty. At present we expect this to be acceptable for cut-off energies of $E_\gamma > 1.6\,\text{GeV}$.

Appendix D

Wilson Coefficients Transformations

Here we demonstrate how the $\mathcal{O}(\alpha)$ corrections to the Wilson coefficients of the four quark operators transform when passing from one operator basis to another. The $\mathcal{O}(\alpha)$ contributions to the coefficients of Q_1–Q_{10} in our operator basis (3.2) can be found from those in the operator basis of references [236, 237] after a basis transformation which in four dimensions is simply

$$\vec{C}(M_W) = \hat{R}^T \vec{C}'(M_W)\,, \tag{D.1}$$

where $\vec{C}'(M_W)$ are the Wilson coefficients in the basis of the latter reviews. In the NDR scheme the non-vanishing $\mathcal{O}(\alpha)$ corrections to their initial conditions are given by

$$\begin{aligned}
C'^{(1)}_{2,e}(M_W) &= -\frac{22}{9} + \frac{4}{3}\ln\frac{M_z^2}{M_W^2}\,,\\
C'^{(1)}_{3,e}(M_W) &= \frac{1}{s_W}\left(\frac{4}{3}B_0(x_t) + \frac{2}{3}C_0(x_t)\right)\,,\\
C'^{(1)}_{7,e}(M_W) &= \frac{1}{s_W}\left(\frac{8}{3}C_0(x_t) + \frac{2}{3}D_0(x_t)\right)\,,\\
C'^{(1)}_{9,e}(M_W) &= \frac{8}{3}C_0(x_t) + \frac{2}{3}D_0(x_t) + \frac{1}{s_W}\left(\frac{20}{3}B_0(x_t) - \frac{8}{3}C_0(x_t)\right)\,,
\end{aligned} \tag{D.2}$$

where $B_0(x_t)$, $C_0(x_t)$ and $D_0(x_t)$ can be found in Eq. (4.25). The matrix $\hat{R}$ is the extension of the same matrix of reference [194] and is needed only for the physical operators Q_1–Q_{10}, Q_7^γ and Q_8^g. It reads

$$\hat{R} = \begin{pmatrix}
2 & \frac{1}{3} & 0 & 0 & 0 & 0 & 0 & 0 & 0 & 0 & 0 & 0\\
0 & 1 & 0 & 0 & 0 & 0 & 0 & 0 & 0 & 0 & 0 & 0\\
0 & 0 & -\frac{1}{3} & 0 & \frac{1}{12} & 0 & 0 & 0 & 0 & 0 & 0 & 0\\
0 & 0 & -\frac{1}{9} & -\frac{2}{3} & \frac{1}{36} & \frac{1}{6} & 0 & 0 & 0 & 0 & 0 & 0\\
0 & 0 & \frac{4}{3} & 0 & -\frac{1}{12} & 0 & 0 & 0 & 0 & 0 & 0 & 0\\
0 & 0 & \frac{4}{9} & \frac{8}{3} & -\frac{1}{36} & -\frac{1}{6} & 0 & 0 & 0 & 0 & 0 & 0\\
0 & 0 & 0 & 0 & 0 & 0 & 2 & 0 & -\frac{1}{8} & 0 & 0 & 0\\
0 & 0 & 0 & 0 & 0 & 0 & \frac{2}{3} & 4 & -\frac{1}{24} & -\frac{1}{4} & 0 & 0\\
0 & 0 & 0 & 0 & 0 & 0 & -\frac{1}{2} & 0 & \frac{1}{8} & 0 & 0 & 0\\
0 & 0 & 0 & 0 & 0 & 0 & -\frac{1}{6} & -1 & \frac{1}{24} & \frac{1}{4} & 0 & 0\\
0 & 0 & 0 & 0 & 0 & 0 & 0 & 0 & 0 & 0 & 1 & 0\\
0 & 0 & 0 & 0 & 0 & 0 & 0 & 0 & 0 & 0 & 0 & 1
\end{pmatrix}\,. \tag{D.3}$$

In fact, beyond LO, the operator basis must be supplemented by a definition of the evanescent operators. This definition corresponds to a choice of scheme and it is different, for instance, in the standard basis of references [236, 237] and in the operator basis used throughout this thesis. On the other hand, a change of scheme can in general be accommodated by an additional non-linear term in the transformation (D.1), namely

$$\vec{C}(M_W) = \left(1 + \frac{\alpha}{4\pi}\Delta\hat{r}_e^T\right)\hat{R}^T\vec{C}'(M_W)\,, \tag{D.4}$$

where $\Delta\hat{r}_e$ is a matrix that depends on the way the projection on the space of physical operators is implemented in the effective theory calculation, which in turn corresponds to a definition of evanescent operators. At the order we are interested in, it affects only the coefficient function of the current-current operator Q_2.

The calculation of the entries of $\Delta\hat{r}_e$ that affect the $\mathcal{O}(\alpha)$ corrections to the matching conditions of Q_1–Q_{10} is straightforward. First, we note that

$$\hat{R}^T\vec{C}'^{(0)}(M_W) = \vec{C}'^{(0)}(M_W) = \left(0, C_2'^{(0)}(M_W), 0, \ldots, 0, C_7'^{\gamma(0)}(M_W), C_8'^{g(0)}(M_W)\right)^T\,, \tag{D.5}$$

which tells us that the only entries that might affect the coefficients of the four quark operators at $\mathcal{O}(\alpha)$ are those entering the second and the last two rows of $\Delta\hat{r}_e$. However, since the calculation of the LO Wilson coefficients of Q_7^γ and Q_8^g does not involve any evanescent operators it is obvious that the eleventh and the twelve row of $\Delta\hat{r}_e$ contain only zeros, and thus do not give a contribution to the left-hand side of Eq. (D.4).

In order to find the second row of $\Delta\hat{r}_e$, it is important to remember that the standard operator basis of references [236, 237] is supplemented with evanescent operators that differ from the ones used here by $\mathcal{O}(\epsilon)$ terms. In fact, it is easy to see, that the only one that matter to the present discussion are[1]

$$\begin{aligned} Q_E &= (\bar{s}_L\gamma_\mu\gamma_\nu\gamma_\lambda c_L)(\bar{c}_L\gamma^\mu\gamma^\nu\gamma^\lambda b_L) - 16Q_2\,, \\ Q'_E &= (\bar{s}_L\gamma_\mu\gamma_\nu\gamma_\lambda c_L)(\bar{c}_L\gamma^\mu\gamma^\nu\gamma^\lambda b_L) - (16-4\epsilon)Q_2\,, \end{aligned} \tag{D.6}$$

where as hitherto the prime indicates the evanescent operator belonging to the standard operator basis [236, 237]. In consequence, the last ingredient needed to find the entries of $\Delta\hat{r}_e$ that affect the $\mathcal{O}(\alpha)$ corrections to the matching conditions, is the calculation of the mixing of Q_2 into these evanescent operators. Computing the usual one-loop current-current diagrams one immediately finds

$$Z_{2,Q_E} = \frac{\alpha}{4\pi}\frac{(Q_u+Q_d)^2}{4\epsilon}\,, \qquad Z_{2,Q'_E} = \frac{\alpha}{4\pi}\frac{(Q_u+Q_d)^2}{4\epsilon}\,. \tag{D.7}$$

Combining Eqs. (D.6) and (D.7) we obtain

$$(\Delta\hat{r}_e)_{22} = \frac{1}{9}\,, \tag{D.8}$$

which is the only element of $\Delta\hat{r}_e$ that affects the quantities that we want to calculate. According to Eq. (D.4), finding the $\mathcal{O}(\alpha)$ corrections to the initial conditions of Q_1–Q_{10} in the basis (3.2) is now only a matter of simple matrix multiplication.

[1] The full set of evanescent operators of the standard operator basis [236, 237] and of the one used throughout this thesis can be found in reference [194].

Appendix E

Two-Loop Matrix Elements of the QCD Penguin Operators

In the present appendix, we shall describe how to evaluate the $\overline{\rm MS}$ renormalized on-shell $b \to s\gamma$ amplitude at $\mathcal{O}(\alpha)$, from which the two-loop matrix elements $r_{1,e}$–$r_{6,e}$ of the four quark operators can be determined. Thereby the framework outlined in reference [206] will be largely followed. In the effective theory the renormalized on-shell $b \to s\gamma$ amplitude is given by

$$\mathcal{A}_{\rm eff}(\mu) = -\frac{G_F}{\sqrt{2}} V_{ts}^* V_{tb} \Bigg\{ Z_q Z_{m_b} \Big[C_7^\gamma(\mu) \big(Z_{7\gamma,7\gamma} Q_7^\gamma + Z_{7\gamma,8g} Q_8^g \big) + C_8^g(\mu) \big(Z_{8g,7\gamma} Q_7^\gamma + Z_{8g,8g} Q_8^g \big) \Big] + \sum_{i=1}^{10} C_i(\mu) \left[Z_q^2 \left(\sum_{j=1}^{10} Z_{ij} Q_j + \sum_{j=1}^{2} Z_{i,E_j} E_j \right) + Z_q Z_{m_b} \big(Z_{i,7\gamma} Q_7^\gamma + Z_{i,8g} Q_8^g \big) \right] \Bigg\} + \ldots \,. \tag{E.1}$$

Here in addition to the physical operators introduced in Eq. (3.2) two evanescent operators, namely

$$\begin{aligned} E_1 &= (\bar{s}_L \gamma_\mu \gamma_\nu \gamma_\lambda \gamma_\rho \gamma_\sigma b_L) \sum\nolimits_q Q_q (\bar{q} \gamma^\mu \gamma^\nu \gamma^\lambda \gamma^\rho \gamma^\sigma q) + 64 Q_7 - 20 Q_9 \,, \\ E_2 &= (\bar{s}_L \gamma_\mu \gamma_\nu \gamma_\lambda \gamma_\rho \gamma_\sigma T^a b_L) \sum\nolimits_q Q_q (\bar{q} \gamma^\mu \gamma^\nu \gamma^\lambda \gamma^\rho \gamma^\sigma T^a q) + 64 Q_8 - 20 Q_{10} \,, \end{aligned} \tag{E.2}$$

need to be considered. The dots in Eq. (E.1) stand for other evanescent operators that do not affect the $\mathcal{O}(\alpha)$ matrix elements of Q_1–Q_6. They are relevant for the $\mathcal{O}(\alpha)$ anomalous dimension matrix though. As far as Z_q and Z_{m_b} are concerned, only the one-loop expressions

$$Z_q = 1 - \frac{\alpha}{4\pi} \frac{3 Q_d^2}{\epsilon} \,, \qquad Z_{m_b} = 1 - \frac{\alpha}{4\pi} \frac{Q_d^2}{\epsilon} \,, \tag{E.3}$$

are needed in the following. The $\mathcal{O}(\alpha)$ contributions to the renormalization constants Z_{i,E_1} and Z_{i,E_2} are found by a simple one-loop calculation. The only non-vanishing elements at that order are

$$Z_{5,E_1} = \frac{\alpha}{4\pi} \frac{Q_d}{\epsilon} \,, \qquad Z_{6,E_2} = \frac{\alpha}{4\pi} \frac{Q_d}{\epsilon} \,. \tag{E.4}$$

The renormalization constants Z_{ij} can be found from the anomalous dimension matrix $\hat{\gamma}_e^{\text{eff}\,(0)}$ given in Eq. (A.4). The relations connecting the renormalization constants Z_{ij} with the entries of the anomalous dimension matrices read

$$Z_{ij} = \frac{\alpha}{4\pi}\frac{\left(\hat{\gamma}_e^{(0)}\right)_{ij}}{4\epsilon} - \frac{1}{2}\sum_{j=1}^{2} Z_{i,E_j} y_{E_j}\,, \tag{E.5}$$

for all elements of the last two columns and

$$Z_{ij} = \delta_{ij} + \frac{\alpha}{4\pi}\frac{\left(\hat{\gamma}_e^{\text{eff}\,(0)}\right)_{ij}}{2\epsilon}\,, \tag{E.6}$$

otherwise. The entries of the anomalous dimension matrix $\hat{\gamma}_e^{(0)}$ are given in terms of those of $\hat{\gamma}_e^{\text{eff}\,(0)}$ by the following well-known [233] relation

$$\left(\hat{\gamma}_e^{\text{eff}}\right)_{ij} = \begin{cases} \left(\hat{\gamma}_e\right)_{i,7\gamma} + \sum_{k=1}^{10} y_k \left(\hat{\gamma}_e\right)_{ik} - y_i \left(\hat{\gamma}_e\right)_{7\gamma,7\gamma} - z_i \left(\hat{\gamma}_e\right)_{8g,7\gamma}\,, & i = 1,\ldots,10\,,\ \ j = 7\gamma\,, \\ \left(\hat{\gamma}_e\right)_{i,8g} + \sum_{k=1}^{10} z_k \left(\hat{\gamma}_e\right)_{ik} - y_i \left(\hat{\gamma}_e\right)_{7\gamma,8g} - z_i \left(\hat{\gamma}_e\right)_{8g,8g}\,, & i = 1,\ldots,10\,,\ \ j = 8g\,, \\ \left(\hat{\gamma}_e\right)_{ij}\,, & \text{otherwise}\,, \end{cases} \tag{E.7}$$

with y_i and z_i given in Eq. (3.6). At the one-loop level the unrenormalized on-shell $b \to s\gamma$ matrix elements of the four quark operators

$$\begin{aligned} \langle Q_i \rangle_{\text{one-loop}} &= \left(\frac{\mu}{m_b}\right)^{2\epsilon} \tilde{y}_i \,\langle Q_7^\gamma \rangle_{\text{tree}} + \mathcal{O}(\epsilon^2)\,, \qquad i = 1,\ldots,10\,, \\ \langle E_i \rangle_{\text{one-loop}} &= \left(\frac{\mu}{m_b}\right)^{2\epsilon} \tilde{y}_{E_i} \,\langle Q_7^\gamma \rangle_{\text{tree}} + \mathcal{O}(\epsilon^2)\,, \qquad i = 1,2\,, \end{aligned} \tag{E.8}$$

can be parameterized by the numbers $\tilde{y}_i$ and $\tilde{y}_{E_i}$, respectively. An easy one-loop calculation gives

$$\begin{aligned} &\tilde{y}_1 = 0\,, && \tilde{y}_2 = 0\,, && \tilde{y}_3 = Q_d\,, \\ &\tilde{y}_4 = Q_d C_F\,, && \tilde{y}_5 = (20-12\epsilon)\,Q_d\,, && \tilde{y}_6 = (20-12\epsilon)\,Q_d C_F\,, \\ &\tilde{y}_7 = Q_d^2\,, && \tilde{y}_8 = Q_d^2 C_F\,, && \tilde{y}_9 = (20-12\epsilon)\,Q_d^2\,, \\ &\tilde{y}_{10} = (20-12\epsilon)\,Q_d^2 C_F\,, && \tilde{y}_{E_1} = (64-400\epsilon)\,Q_d\,, && \tilde{y}_{E_2} = (64-400\epsilon)\,Q_d C_F\,. \end{aligned} \tag{E.9}$$

The unrenormalized one-loop matrix elements of Q_7^γ and Q_8^g read

$$\begin{aligned} \langle Q_7^\gamma \rangle_{\text{one-loop}} &= \left(\frac{\mu}{m_b}\right)^{2\epsilon} \left[-\left(Z_q Z_{m_b} Z_{7\gamma,7\gamma} - 1\right) + \frac{\alpha}{4\pi} r_{7\gamma,e}\right] \langle Q_7^\gamma \rangle_{\text{tree}} + \mathcal{O}(\alpha^2,\epsilon)\,, \\ \langle Q_8^g \rangle_{\text{one-loop}} &= 0\,, \end{aligned} \tag{E.10}$$

where $r_{7\gamma,e}$ has already been given in Eq. (4.93). Notice that for our purpose a explicit expression for the unrenormalized one-loop matrix elements of Q_7^γ is needed. This is due to the fact that $Z_q Z_{m_b} Z_{7\gamma,7\gamma} = 1 + \mathcal{O}(\alpha)$ and is different from what happens in the case of the $\mathcal{O}(\alpha_s)$ calculation of the matrix elements of the QCD penguin operators [206]. We also note that the unrenormalized one-loop matrix element of Q_7^γ contains an IR pole, which we assume to be regulated by a small photon mass.

In order to find the quantities $r_{1,e}$–$r_{6,e}$ it is easy to see [206] that one needs in addition two unrenormalized matrix elements of evanescent operators, namely

$$\begin{aligned}\left\langle Q_0 - \frac{1}{2}Q_2 + Q_4^{\bar{c}c} + \frac{1}{6}Q_3^{\bar{c}c}\right\rangle_{\text{two-loop}} &= \frac{\alpha}{4\pi}e_{e,4}\,\langle Q_7^\gamma\rangle_{\text{tree}} + \mathcal{O}(\epsilon)\,,\\ \left\langle 4Q_0 - 8Q_2 + Q_6^{\bar{c}c} + \frac{1}{6}Q_5^{\bar{c}c}\right\rangle_{\text{two-loop}} &= \frac{\alpha}{4\pi}e_{e,6}\,\langle Q_7^\gamma\rangle_{\text{tree}} + \mathcal{O}(\epsilon)\,,\end{aligned} \tag{E.11}$$

where $Q_0 = (\bar{s}_L c_R)(\bar{c}_L b_R)$, and $Q_3^{\bar{c}c}$, $Q_4^{\bar{c}c}$, $Q_5^{\bar{c}c}$ and $Q_6^{\bar{c}c}$ are just the $\bar{c}c$-parts of the QCD penguin operators. Notice that $\langle Q_4^{\bar{c}c}\rangle = \langle Q_6^{\bar{c}c}\rangle = 0$ due to the tracelessness of the color generators. For the quantities $e_{e,4}$ and $e_{e,6}$ parameterizing the unrenormalized matrix elements of the evanescent operators we find

$$e_{e,4} = \left(\frac{3}{4}Q_u - \frac{2}{9}Q_d\right)Q_d Q_u\,, \qquad e_{e,6} = \left(12Q_u - \frac{8}{9}Q_d\right)Q_d Q_u\,. \tag{E.12}$$

Since these results are independent of m_c, they hold, after proper replacement of quark charges, for any flavor running in the loop. In consequence, is it not necessary to calculate two-loop diagrams with an insertion of Q_3–Q_6 containing Dirac traces separately. Such an approach is very convenient, because the quantities $e_{e,4}$ and $e_{e,6}$ can be, and are in fact found by performing a Taylor expansion in the external momenta. More precisely, such an expansion is applied to diagrams with subtracted subdivergences, because subtracted matrix elements of evanescent operators must be local, that is, polynomial in the external momenta. Once they are found, we can add the one-loop subdivergences again, setting the external momenta on-shell. Then the only relevant subdivergence is proportional to $\langle Q_3^{\bar{c}c}\rangle_{\text{one-loop}}$ and $\langle Q_5^{\bar{c}c}\rangle_{\text{one-loop}}$, respectively. However, these divergences are known already. In consequence, the calculation of $e_{e,4}$ and $e_{e,6}$ can be performed using the algorithm described in Appendix A.

Now we are ready to calculate the unrenormalized two-loop matrix elements of Q_1–Q_6 at $\mathcal{O}(\alpha)$. Let us write them as follows

$$\langle Q_i\rangle_{\text{two-loop}} = \left(\frac{\mu}{m_b}\right)^{4\epsilon}\left(x_i + \langle Q_7^\gamma\rangle_{\text{one-loop}}\,\tilde{y}_i\right)\langle Q_7^\gamma\rangle_{\text{tree}} + \mathcal{O}(\epsilon)\,, \qquad i = 1,\ldots,6\,, \tag{E.13}$$

where the terms proportional to $\tilde{y}_i$ originate from the usual penguin diagrams with a photon joining the external quark lines. The evaluation of the quantities x_i amounts to forming appropriate linear combinations of the results given in reference [206], by taking into account the Dirac and flavor structure of the QCD penguin operator under consideration. Explicitly one finds[1]

$$\begin{aligned}x_1 &= \frac{184}{729\epsilon} + \frac{3332}{2187} - \frac{4}{9}a(z) - \frac{4}{9}b(z) + \frac{160}{729}i\pi\,,\\ x_2 &= \frac{46}{243\epsilon} + \frac{833}{729} - \frac{a(z)}{3} - \frac{b(z)}{3} + \frac{40}{243}i\pi\,,\\ x_3 &= \frac{38}{243\epsilon} + \frac{811}{729} + \frac{2\pi}{9\sqrt{3}} - \frac{2}{81}\pi^2 + \frac{8}{27}X_b - \frac{a(1)}{12} + \frac{7}{6}b(1) - 2b(z) + \frac{44}{243}i\pi\,,\end{aligned}$$

[1] We are grateful to Dr. J. Urban for providing us with the MATHEMATICA code that was used in the calculation of the NLO QCD matrix elements [206].

$$
\begin{aligned}
x_4 &= \frac{248}{729\epsilon} + \frac{2932}{2187} + \frac{8\pi}{27\sqrt{3}} - \frac{8}{243}\pi^2 + \frac{32}{81}X_b - \frac{a(1)}{9} + \frac{2}{9}b(1) + \frac{128}{729}i\pi\,, \\
x_5 &= \frac{6494}{243\epsilon} + \frac{73297}{729} + \frac{8\pi}{9\sqrt{3}} - \frac{40}{81}\pi^2 + \frac{32}{27}X_b - \frac{13}{3}a(1) + \frac{38}{3}b(1) - 12a(z) - 20b(z) + \frac{4268}{243}i\pi\,, \\
x_6 &= \frac{5552}{729\epsilon} + \frac{42424}{2187} + \frac{32\pi}{27\sqrt{3}} - \frac{160}{243}\pi^2 + \frac{128}{81}X_b - \frac{16}{9}a(1) + \frac{32}{9}b(1) + \frac{2336}{729}i\pi\,,
\end{aligned}
\tag{E.14}
$$

up to terms of $\mathcal{O}(\epsilon)$. Here the constant X_b, which has been calculated by Buras et al. [206], is given by

$$
X_b = \int_0^1 dx \int_0^1 dy \int_0^1 dv\, xy \ln\left[vx\,(1-x)\,(1-v)\,(1-v+vy)\right] \approx -0.1684\,. \tag{E.15}
$$

The exact expressions for the functions $a(z)$ and $b(z)$ can also be found in the latter paper:

$$
\begin{aligned}
a(z) &= \frac{8}{9}\int_0^1 dx \int_0^1 dy \int_0^1 dv \,\Big\{ \left[2 - v - xy\,(3-2v)\right] \ln\left[vz + x\,(1-x)\,(1-v)\,(1-v+vy)\right] \\
&\quad + \left[1 - v - xy\,(1-2v)\right] \ln\left[z - vxy\,(1-x) - i\epsilon\right] \Big\} + \frac{43}{9} + \frac{4}{9}i\pi\,, \\
b(z) &= \frac{8}{9}\int_0^1 dx \int_0^1 dy\, \frac{x\,(1-x)\,y^2\,(1-y^2) - (4-2y)\,u_1 \ln u_1 + (2-4y-4y^2)\,u_2 \ln u_2}{2\,(1-y)^2} \\
&\quad - \frac{92}{243} + \frac{224}{81}z + \frac{16}{27}z^2 + \frac{4}{81}\ln z + \frac{4 - 64z - 48z^2}{81}\sqrt{1-4z}\, f(z) \\
&\quad + \frac{z^2\,(24-16z)}{27} f(z)^2 + \frac{4}{81}i\pi\,,
\end{aligned}
\tag{E.16}
$$

with $u_i = x\,(1-x)\,y^i + (1-z)\,z$ and

$$
f(z) = \theta\,(1-4z)\left(\ln\frac{1+\sqrt{1-4z}}{1-\sqrt{1-4z}} - i\pi\right) - 2i\,\theta\,(-1+4z)\arctan\frac{1}{\sqrt{-1+4z}}\,, \tag{E.17}
$$

where $\theta(x)$ is the Heaviside function. Notice that additive constants in the functions $a(z)$ and $b(z)$ have been chosen in such a way that $a(0) = b(0) = 0$. According to reference [206], $a(1)$ and $b(1)$ are given by

$$
\begin{aligned}
a(1) &\approx 4.0859 + \frac{4}{9}i\pi\,, \\
b(1) &= \frac{320}{81} - \frac{4\pi}{3\sqrt{3}} + \frac{632}{1215}\pi^2 - \frac{8}{45}\left.\frac{d^2 \ln\Gamma(x)}{dx^2}\right|_{x=1/6} + \frac{4}{81}i\pi \approx 0.0316 + \frac{4}{81}i\pi\,,
\end{aligned}
\tag{E.18}
$$

where $\Gamma(x)$ is the Gamma function. For realistic values of $z = m_c^2/m_b^2 \approx 0.1$ there is no need to apply numerical integration in order to find $a(z)$ and $b(z)$, because both functions are then accurately given by their expansions in z

$$
\begin{aligned}
a(z) &= \frac{16}{9}\Bigg\{ \left[\frac{5}{2} - \frac{\pi^2}{3} - 3\zeta(3) + \left(\frac{5}{2} - \frac{3}{4}\pi^2\right)\ln z + \frac{1}{4}\ln^2 z + \frac{1}{12}\ln^3 z\right] z \\
&\quad + \left(\frac{7}{4} + \frac{2}{3}\pi^2 - \frac{\pi^2}{2}\ln z - \frac{1}{4}\ln^2 z + \frac{1}{12}\ln^3 z\right) z^2 - \left(\frac{7}{6} + \frac{\pi^2}{4} - 2\ln z + \frac{3}{4}\ln^2 z\right) z^3
\end{aligned}
$$

$$
\begin{aligned}
&+\left(\frac{457}{216}-\frac{5}{18}\pi^2-\frac{1}{72}\ln z-\frac{5}{6}\ln^2 z\right)+\left(\frac{35101}{8640}-\frac{35}{72}\pi^2-\frac{185}{144}\ln z-\frac{35}{24}\ln^2 z\right)z^5\\
&+\left(\frac{67801}{8000}-\frac{21}{20}\pi^2-\frac{3303}{800}\ln z-\frac{63}{20}\ln^2 z\right)z^6+\left[\left(2-\frac{\pi^2}{6}+\frac{1}{2}\ln z+\frac{1}{2}\ln^2 z\right)z\right.\\
&\left.+\left(\frac{1}{2}-\frac{\pi^2}{6}-\ln z+\frac{1}{2}\ln^2 z\right)z^2+z^3+\frac{5}{9}z^4+\frac{49}{72}z^5+\frac{231}{200}z^6\right]i\pi\Bigg\}+\mathcal{O}\left(z^7\ln^2 z\right)\,,\\
b(z)=\frac{8}{9}\Bigg\{&\left(3-\frac{\pi^2}{6}+\ln z\right)z-\frac{2}{3}\pi^2 z^{\frac{3}{2}}-\left(\frac{1}{2}+\pi^2-2\ln z-\frac{1}{2}\ln^2 z\right)z^2\\
&+\left(\frac{25}{12}+\frac{\pi^2}{9}+\frac{19}{18}\ln z-2\ln^2 z\right)z^3+\left(\frac{1376}{225}-\frac{2}{3}\pi^2-\frac{137}{30}\ln z-2\ln^2 z\right)z^4\\
&+\left(\frac{131317}{11760}-\frac{5}{3}\pi^2-\frac{887}{84}\ln z-5\ln^z\right)z^5+\left(\frac{2807617}{97200}-\frac{14}{3}\pi^2-\frac{16597}{540}\ln z-14\ln^2 z\right)z^6\\
&+\left[z-(1-2\ln z)\,z^2+\left(\frac{10}{9}-\frac{4}{3}\ln z\right)z^3-z^4-\frac{2}{3}z^5-\frac{7}{9}z^6\right]i\pi\Bigg\}+\mathcal{O}\left(z^7\ln^2 z\right)\,,
\end{aligned}
\tag{E.19}
$$

which have been calculated by Greub et al. [203, 204] up to $\mathcal{O}(z^3)$ terms. Recently, these results have been confirmed by the authors of reference [205] generalizing them to include terms up to $\mathcal{O}(z^6)$.

Once we have found the unrenormalized matrix elements of Q_1–Q_6 it is straightforward to calculate the renormalized ones. From Eq. (E.1) we read off that the $\overline{\text{MS}}$-renormalized amplitude for the $b\to s\gamma$ transition up to $\mathcal{O}(\alpha)$ terms is given by

$$
\begin{aligned}
\mathcal{A}_{\text{eff}}(\mu)=-\frac{G_F}{\sqrt{2}}V_{ts}^*V_{tb}\Bigg\{&Z_q Z_{m_b} Z_{7\gamma,7\gamma}\left(C_7^{\gamma(0)}(\mu)+\frac{\alpha}{4\pi}C_{7,e}^{\gamma(1)}(\mu)\right)\left(\langle Q_7^\gamma\rangle_{\text{tree}}+\langle Q_7^\gamma\rangle_{\text{one-loop}}\right)\\
&+\sum_{i=1}^{6}\left(C_i^{(0)}(\mu)+\frac{\alpha}{4\pi}C_{i,e}^{(1)}(\mu)\right)\Bigg[\sum_{j=1}^{10}\left[\left(Z_qZ_{ij}+(1-2\epsilon)\left(Z_{m_b}-1\right)\delta_{ij}\right]\langle Q_j\rangle_{\text{one-loop}}\right.\\
&\left.+\langle Q_i\rangle_{\text{two-loop}}+Z_{i,7\gamma}\langle Q_7^\gamma\rangle_{\text{tree}}+\sum_{j=1}^{2}Z_{i,E_j}\langle E_j\rangle_{\text{one-loop}}\Bigg]\Bigg\}+\ldots\,,
\end{aligned}
\tag{E.20}
$$

where the dots stand for terms that do not affect the matrix elements of Q_1–Q_6 at $\mathcal{O}(\alpha)$.

As explained in reference [206] the appearance of Z_q and Z_{m_b} in the above equation can be understood without calculating any diagram. In fact, it is enough to remember that the insertions of the wave function counterterms on internal quark lines always cancel with the $Z_q^{1/2}$ factors at the ends of those lines. Thus one is left with a single power of Z_q that corresponds to two external quark lines of the down-type. On the other hand, the term proportional to $(Z_{m_b}-1)$ is found from

$$
\langle Q_i\rangle_{\text{one-loop}}\Big|_{m_b\to Z_{m_b}m_b}-\langle Q_i\rangle_{\text{one-loop}}\,,
\tag{E.21}
$$

with $\langle Q_i\rangle_{\text{one-loop}}$ given in Eq. (E.8). Thereby, it is important to remember that $\langle Q_7^\gamma\rangle_{\text{tree}}$ is proportional to m_b.

Now it is easy to check, that if one substitutes all matrix elements and renormalization constants into Eq. (E.20), all UV poles cancel as they should. Moreover, if one replaces

the Wilson coefficients by their effective counterparts according to Eq. (3.3), all terms proportional to $\ln m_b/\mu$ are found to be multiplied by the elements of the next to last column of the anomalous dimension matrix $\hat{\gamma}_e^{\text{eff}\,(0)}$ given in Eq. (A.4). Thus the $b \to s\gamma$ transition amplitude $\mathcal{A}_{\text{eff}}(\mu)$ takes the following form

$$\mathcal{A}_{\text{eff}}(\mu) = -\frac{G_F}{\sqrt{2}} V_{ts}^* V_{tb} \Bigg[C_7^{\gamma,\text{eff}\,(0)}(\mu) + \frac{\alpha}{4\pi} C_{7,e}^{\gamma,\text{eff}\,(1)}(\mu) + \frac{\alpha}{4\pi} \sum_{i=1}^{8} C_i^{\text{eff}\,(0)}(\mu) \left(r_{i,e} + \frac{1}{2} \left(\hat{\gamma}_e^{\text{eff}\,(0)}\right)_{i,7\gamma} \ln \frac{m_b^2}{\mu^2} \right) \Bigg] \langle Q_7^\gamma \rangle_{\text{tree}} + \dots \,, \tag{E.22}$$

where again the sum runs over the operators Q_1–Q_6, Q_7^γ and Q_8^g. From the above expression, we have determined the results for the matrix elements $r_{1,e}$–$r_{6,e}$ that have already been given in Eq. (4.93).

Bibliography

[1] ALEPH, D. Abbaneo et al., (2001), hep-ex/0112021.

[2] Particle Data Group, K. Hagiwara et al., Phys. Rev. D66 (2002) 010001.

[3] LEP Electroweak Working Group, LEPEWWG/2002-01, May 2002, http://lepewwg.web.cern.ch/LEPEWWG/.

[4] M. Ciuchini et al., JHEP 07 (2001) 013, hep-ph/0012308.

[5] S. Mele, (2001), hep-ph/0103040.

[6] BABAR, B. Aubert et al., Nucl. Instrum. Meth. A479 (2002) 1, hep-ex/0105044.

[7] BELLE, S. Mori et al., Nucl. Instrum. Meth. A479 (2002) 117.

[8] CLEO, D. Andrews et al., Nucl. Instr. Meth. 211 (1983) 47.

[9] CLEO, Y. Kubota et al., Nucl. Instrum. Meth. A320 (1992) 66.

[10] ALEPH, D. Decamp et al., Nucl. Instrum. Meth. A294 (1990) 121, Erratum ibid. A303 (1991) 393.

[11] ALEPH, D. Buskulic et al., Nucl. Instrum. Meth. A360 (1995) 481.

[12] DELPHI, P.A. Aarnio et al., Nucl. Instrum. Meth. A303 (1991) 233.

[13] DELPHI, P. Abreu et al., Nucl. Instrum. Meth. A378 (1996) 57, Erratum ibid. A396 (1997) 281.

[14] L3, O. Adriani et al., Nucl. Instrum. Meth. A302 (1991) 53.

[15] L3 SMD, M. Acciarri et al., Nucl. Instrum. Meth. A351 (1994) 300.

[16] OPAL, K. Ahmet et al., Nucl. Instrum. Meth. A305 (1991) 275.

[17] OPAL, P.P. Allport et al., Nucl. Instrum. Meth. A324 (1993) 34.

[18] CDF, D. Amidei et al., Nucl. Instrum. Meth. A350 (1994) 73.

[19] CDF, F. Abe et al., Nucl. Instr. Meth. A271 (1988) 387.

[20] D0, S. Abachi et al., Nucl. Instrum. Meth. A338 (1994) 185.

[21] D. Axen et al., Nucl. Instrum. Meth. A328 (1993) 472.

[22] LHCb, S. Amato et al., CERN-LHCC-98-4.

[23] ATLAS, M.S. Alam et al., CERN-LHCC-98-13.

[24] CMS, G. Acquistapace et al., CERN-LHCC-97-10.

[25] LHCb, N. Harnew, Nucl. Instrum. Meth. A408 (1998) 137.

[26] BTeV, A. Kulyavtsev et al., (1998), hep-ph/9809557.

[27] BABAR, B. Aubert et al., Phys. Rev. Lett. 87 (2001) 091801, hep-ex/0107013.

[28] Belle, K. Abe et al., Phys. Rev. Lett. 87 (2001) 091802, hep-ex/0107061.

[29] CLEO, R. Ammar et al., Phys. Rev. Lett. 71 (1993) 674.

[30] CLEO, S. Chen et al., Phys. Rev. Lett. 87 (2001) 251807, hep-ex/0108032.

[31] Belle, K. Abe et al., Phys. Lett. B511 (2001) 151, hep-ex/0103042.

[32] BABAR, B. Aubert et al., Phys. Rev. Lett. 88 (2002) 101805, hep-ex/0110065.

[33] A. Ali and A.Y. Parkhomenko, Eur. Phys. J. C23 (2002) 89, hep-ph/0105302.

[34] M. Beneke, T. Feldmann and D. Seidel, Nucl. Phys. B612 (2001) 25, hep-ph/0106067.

[35] S.W. Bosch and G. Buchalla, Nucl. Phys. B621 (2002) 459, hep-ph/0106081.

[36] A.L. Kagan and M. Neubert, Phys. Lett. B539 (2002) 227, hep-ph/0110078.

[37] CLEO, M.S. Alam et al., Phys. Rev. Lett. 74 (1995) 2885.

[38] CLEO, S. Ahmed et al., (1999), hep-ex/9908022.

[39] BaBar, B. Aubert et al., (2002), hep-ex/0207076.

[40] ALEPH, R. Barate et al., Phys. Lett. B429 (1998) 169.

[41] M. Gell-Mann, Phys. Lett. 8 (1964) 214.

[42] O.W. Greenberg, Phys. Rev. Lett. 13 (1964) 598.

[43] G. Zweig, CERN-TH-412.

[44] M.Y. Han and Y. Nambu, Phys. Rev. 139 (1965) B1006.

[45] M. Gell-Mann, Acta Phys. Austriaca Suppl. 9 (1972) 733.

[46] H. Fritzsch, M. Gell-Mann and H. Leutwyler, Phys. Lett. B47 (1973) 365.

[47] S.L. Glashow, Nucl. Phys. 22 (1961) 579.

[48] S. Weinberg, Phys. Rev. Lett. 19 (1967) 1264.

[49] A. Salam, in N. Svartholm, Elementary Particle Theory, Proceedings of the Nobel Symposium held 1968 at Lerum, Stockholm 1968, 367.

[50] S.L. Glashow, J. Iliopoulos and L. Maiani, Phys. Rev. D2 (1970) 1285.

[51] D.J. Gross and F. Wilczek, Phys. Rev. D8 (1973) 3633.

[52] H.D. Politzer, Phys. Rev. Lett. 30 (1973) 1346.

[53] D.J. Gross and F. Wilczek, Phys. Rev. D9 (1974) 980.

[54] Kamiokande, Y. Fukuda et al., Phys. Rev. Lett. 77 (1996) 1683.

[55] Super-Kamiokande, Y. Fukuda et al., Phys. Rev. Lett. 81 (1998) 1562, hep-ex/9807003.

[56] SuperKamiokande, Y. Fukuda et al., Phys. Rev. Lett. 82 (1999) 2644, hep-ex/9812014.

[57] B.T. Cleveland et al., Astrophys. J. 496 (1998) 505.

[58] GALLEX, W. Hampel et al., Phys. Lett. B447 (1999) 127.

[59] SAGE, J.N. Abdurashitov et al., Phys. Rev. C60 (1999) 055801, astro-ph/9907113.

[60] GNO, M. Altmann et al., Phys. Lett. B490 (2000) 16, hep-ex/0006034.

[61] Super-Kamiokande, S. Fukuda et al., Phys. Rev. Lett. 85 (2000) 3999, hep-ex/0009001.

[62] SuperKamiokande, S. Fukuda et al., Phys. Rev. Lett. 86 (2001) 5651, hep-ex/0103032.

[63] SuperKamiokande, T. Toshito, (2001), hep-ex/0105023.

[64] SNO, Q.R. Ahmad et al., Phys. Rev. Lett. 87 (2001) 071301, nucl-ex/0106015.

[65] SuperKamiokande, M.B. Smy, (2001), hep-ex/0106064.

[66] P.W. Higgs, Phys. Lett. 12 (1964) 132.

[67] F. Englert and R. Brout, Phys. Rev. Lett. 13 (1964) 321.

[68] P.W. Higgs, Phys. Rev. Lett. 13 (1964) 508.

[69] G.S. Guralnik, C.R. Hagen and T.W.B. Kibble, Phys. Rev. Lett. 13 (1964) 585.

[70] P.W. Higgs, Phys. Rev. 145 (1966) 1156.

[71] T.W.B. Kibble, Phys. Rev. 155 (1967) 1554.

[72] C.H. Llewellyn Smith, Phys. Lett. B46 (1973) 233.

[73] J.M. Cornwall, D.N. Levin and G. Tiktopoulos, Phys. Rev. D10 (1974) 1145, Erratum ibid. D11 (1975) 927.

[74] J. Goldstone, Nuovo Cim. 19 (1961) 154.

[75] J. Goldstone, A. Salam and S. Weinberg, Phys. Rev. 127 (1962) 965.

[76] G. 't Hooft, Nucl. Phys. B33 (1971) 173.

[77] J.C. Taylor, Nucl. Phys. B33 (1971) 436.

[78] G. 't Hooft, Nucl. Phys. B35 (1971) 167.

[79] G. 't Hooft and M.J.G. Veltman, Nucl. Phys. B44 (1972) 189.

[80] G. Costa and M. Tonin, Riv. Nuovo Cim. 5 (1975) 29.

[81] N. Cabibbo, Phys. Rev. Lett. 10 (1963) 531.

[82] M. Kobayashi and T. Maskawa, Prog. Theor. Phys. 49 (1973) 652.

[83] M. Gell-Mann, P. Ramond and R. Slansky, Print-80-0576 (CERN).

[84] T. Yanagida, Prog. Theor. Phys. 64 (1980) 1103.

[85] T. Yanagida and M. Yoshimura, Phys. Lett. B97 (1980) 99.

[86] R.N. Mohapatra and G. Senjanovic, Phys. Rev. Lett. 44 (1980) 912.

[87] R.N. Mohapatra and G. Senjanovic, Phys. Rev. D23 (1981) 165.

[88] Z. Maki, M. Nakagawa and S. Sakata, Prog. Theor. Phys. 28 (1962) 870.

[89] J. Schechter and J.W.F. Valle, Phys. Rev. D21 (1980) 309.

[90] J. Schechter and J.W.F. Valle, Phys. Rev. D22 (1980) 2227.

[91] J.S. Schwinger, Phys. Rev. 82 (1951) 914.

[92] G. Lueders, Dan. Mat. Phys. Medd. 28 (1954) 5.

[93] J. Bell, Proc. Roy. Soc. Lond. A231 (1955) 479.

[94] W. Pauli, in W. Pauli, Niels Bohr and the Development of Physics, McGraw-Hill, New York 1955, 30.

[95] G. Lueders, Annals Phys. 2 (1957) 1.

[96] G. Lueders and B. Zuminio, Phys. Rev. 106 (1957) 385.

[97] NA31, R. Carosi et al., Phys. Lett. B237 (1990) 303.

[98] B. Schwingenheuer et al., Phys. Rev. Lett. 74 (1995) 4376.

[99] E731, L.K. Gibbons et al., Phys. Rev. D55 (1997) 6625.

[100] V.A. Kostelecky and R. Potting, Nucl. Phys. B359 (1991) 545.

[101] V.A. Kostelecky and R. Potting, Phys. Lett. B381 (1996) 89, hep-th/9605088.

[102] V.A. Kostelecky and S. Samuel, Phys. Rev. Lett. 63 (1989) 224.

[103] V.A. Kostelecky and S. Samuel, Phys. Rev. D39 (1989) 683.

[104] V.A. Kostelecky and S. Samuel, Phys. Rev. D40 (1989) 1886.

[105] V.A. Kostelecky and S. Samuel, Phys. Rev. Lett. 66 (1991) 1811.

[106] J.E. Kim, Phys. Rept. 150 (1987) 1.

[107] H.Y. Cheng, Phys. Rept. 158 (1988) 1.

[108] R.D. Peccei, in C. Jarlskog, CP Violation, World Scientific, Singapore 1989, 503.

[109] J. Bernabeu, G.C. Branco and M. Gronau, Phys. Lett. B169 (1986) 243.

[110] M. Gronau, A. Kfir and R. Loewy, Phys. Rev. Lett. 56 (1986) 1538.

[111] C. Jarlskog, Phys. Rev. Lett. 55 (1985) 1039.

[112] C. Jarlskog, Z. Phys. C29 (1985) 491.

[113] I. Dunietz, O.W. Greenberg and D.D. Wu, Phys. Rev. Lett. 55 (1985) 2935.

[114] C. Jarlskog and R. Stora, Phys. Lett. B208 (1988) 268.

[115] S.L. Adler, Phys. Rev. 177 (1969) 2426.

[116] J.S. Bell and R. Jackiw, Nuovo Cim. A60 (1969) 47.

[117] W.A. Bardeen, Phys. Rev. 184 (1969) 1848.

[118] J. Wess and B. Zumino, Phys. Lett. B37 (1971) 95.

[119] R.A. Bertlmann, Anomalies in Quantum Field Theories, Clarendon Press, Oxford 1996.

[120] A.A. Belavin et al., Phys. Lett. B59 (1975) 85.

[121] G. 't Hooft, Phys. Rev. Lett. 37 (1976) 8.

[122] G. 't Hooft, Phys. Rev. D14 (1976) 3432, Erratum ibid. D18 (1978) 2199.

[123] J.H. Lowenstein, Commun. Math. Phys. 24 (1971) 1.

[124] Y.M.P. Lam, Phys. Rev. D6 (1972) 2161.

[125] Y.M.P. Lam, Phys. Rev. D7 (1973) 2943.

[126] J.H. Lowenstein and B. Schroer, Phys. Rev. D7 (1973) 1929.

[127] M. Gomes, J.H. Lowenstein and W. Zimmermann, Commun. Math. Phys. 39 (1974) 81.

[128] L.D. Faddeev and V.N. Popov, Phys. Lett. B25 (1967) 29.

[129] G. 't Hooft and M.J.G. Veltman, Nucl. Phys. B50 (1972) 318.

[130] B.W. Lee and J. Zinn-Justin, Phys. Rev. D5 (1972) 3121.

[131] B.W. Lee and J. Zinn-Justin, Phys. Rev. D5 (1972) 3137.

[132] B.W. Lee and J. Zinn-Justin, Phys. Rev. D5 (1972) 3155.

[133] B.W. Lee and J. Zinn-Justin, Phys. Rev. D7 (1973) 1049.

[134] C. Becchi, A. Rouet and R. Stora, Phys. Lett. B52 (1974) 344.

[135] C. Becchi, A. Rouet and R. Stora, Commun. Math. Phys. 42 (1975) 127.

[136] I.V. Tyutin, LEBEDEV-75-39.

[137] N. Nakanishi, Prog. Theor. Phys. 35 (1966) 1111.

[138] B. Lautrup, Mat. Fys. Medd. Dan. Vid. Selsk. 35 (1967) No. 11.

[139] T. Kugo and I. Ojima, Phys. Lett. B73 (1978) 459.

[140] T. Kugo and I. Ojima, Prog. Theor. Phys. 60 (1978) 1869.

[141] T. Kugo and I. Ojima, Prog. Theor. Phys. 61 (1979) 294.

[142] T. Kugo and I. Ojima, Prog. Theor. Phys. 61 (1979) 644.

[143] T. Kugo and I. Ojima, Prog. Theor. Phys. Suppl. 66 (1979) 1.

[144] D.A. Ross and J.C. Taylor, Nucl. Phys. B51 (1973) 125,
Erratum ibid. B58 (1973) 643.

[145] W.E. Thirring, Phil. Mag. 41 (1950) 1193.

[146] S. Dittmaier, Phys. Lett. B409 (1997) 509, hep-ph/9704368.

[147] K.I. Aoki et al., Prog. Theor. Phys. Suppl. 73 (1982) 1.

[148] M. Böhm, H. Spiesberger and W. Hollik, Fortsch. Phys. 34 (1986) 687.

[149] A. Denner, Fortschr. Phys. 41 (1993) 307.

[150] A.A. Slavnov, Theor. Math. Phys. 10 (1972) 99.

[151] P. Gambino and P.A. Grassi, Phys. Rev. D62 (2000) 076002, hep-ph/9907254.

[152] J.C. Taylor, Gauge Theories of Weak Interactions, Cambridge University Press, Cambridge 1976.

[153] C. Itzykson and J.B. Zuber, Quantum Field Theory, McGraw-Hill, New York 1980.

[154] P.A. Grassi, Nucl. Phys. B560 (1999) 499, hep-th/9908188.

[155] A. Sirlin, Phys. Rev. Lett. 67 (1991) 2127.

[156] A. Sirlin, Phys. Lett. B267 (1991) 240.

[157] R.G. Stuart, Phys. Lett. B262 (1991) 113.

[158] R.G. Stuart, Phys. Rev. Lett. 70 (1993) 3193.

[159] M. Passera and A. Sirlin, Phys. Rev. D58 (1998) 113010, hep-ph/9804309.

[160] E. Kraus, Acta Phys. Polon. B29 (1998) 2647, hep-th/9807102.

[161] W.J. Marciano and A. Sirlin, Nucl. Phys. B93 (1975) 303.

[162] A. Denner and T. Sack, Nucl. Phys. B347 (1990) 203.

[163] A. Sirlin, Phys. Rev. D22 (1980) 971.

[164] H. Lehmann, K. Symanzik and W. Zimmermann, Nuovo Cim. 1 (1955) 205.

[165] W.A. Bardeen et al., Phys. Rev. D18 (1978) 3998.

[166] C.G. Bollini and J.J. Giambiagi, Phys. Lett. B40 (1972) 566.

[167] P. Gambino, P.A. Grassi and F. Madricardo, Phys. Lett. B454 (1999) 98, hep-ph/9811470.

[168] A. Barroso, L. Brücher and R. Santos, Phys. Rev. D62 (2000) 096003, hep-ph/0004136.

[169] B.A. Kniehl, F. Madricardo and M. Steinhauser, Phys. Rev. D62 (2000) 073010, hep-ph/0005060.

[170] A.O. Bouzas, Eur. Phys. J. C20 (2001) 238, hep-ph/0101101.

[171] Y. Yamada, Phys. Rev. D64 (2001) 036008, hep-ph/0103046.

[172] K.P.O. Diener and B.A. Kniehl, Nucl. Phys. B617 (2001) 291, hep-ph/0109110.

[173] A. Pilaftsis, (2002), hep-ph/0203210.

[174] D. Espriu, J. Manzano and P. Talavera, (2002), hep-ph/0204085.

[175] B.A. Kniehl and A. Pilaftsis, Nucl. Phys. B474 (1996) 286, hep-ph/9601390.

[176] W.J. Marciano and A. Sirlin, Phys. Rev. D22 (1980) 2695, Erratum ibid. D31 (1985) 213.

[177] A. Sirlin and W.J. Marciano, Nucl. Phys. B189 (1981) 442.

[178] J.C. Ward, Phys. Rev. 78 (1950) 182.

[179] Y. Takahashi, Nuovo Cim. 6 (1957) 371.

[180] P. Gambino and M. Misiak, Nucl. Phys. B611 (2001) 338, hep-ph/0104034.

[181] S. Bertolini, F. Borzumati and A. Masiero, Phys. Rev. Lett. 59 (1987) 180.

[182] N.G. Deshpande et al., Phys. Rev. Lett. 59 (1987) 183.

[183] K. Adel and Y.P. Yao, Phys. Rev. D49 (1994) 4945, hep-ph/9308349.

[184] C. Greub and T. Hurth, Phys. Rev. D56 (1997) 2934, hep-ph/9703349.

[185] A.J. Buras, A. Kwiatkowski and N. Pott, Nucl. Phys. B517 (1998) 353, hep-ph/9710336.

[186] M. Ciuchini et al., Nucl. Phys. B527 (1998) 21, hep-ph/9710335.

[187] C. Bobeth, M. Misiak and J. Urban, Nucl. Phys. B574 (2000) 291, hep-ph/9910220.

[188] G. Altarelli et al., Nucl. Phys. B187 (1981) 461.

[189] A.J. Buras and P.H. Weisz, Nucl. Phys. B333 (1990) 66.

[190] A.J. Buras et al., Nucl. Phys. B370 (1992) 69, Erratum ibid. B375 (1992) 501.

[191] A.J. Buras et al., Nucl. Phys. B400 (1993) 37, hep-ph/9211304.

[192] M. Ciuchini et al., Phys. Lett. B301 (1993) 263, hep-ph/9212203.

[193] M. Ciuchini et al., Nucl. Phys. B415 (1994) 403, hep-ph/9304257.

[194] K.G. Chetyrkin, M. Misiak and M. Münz, Nucl. Phys. B520 (1998) 279, hep-ph/9711280.

[195] M. Misiak and M. Münz, Phys. Lett. B344 (1995) 308, hep-ph/9409454.

[196] K.G. Chetyrkin, M. Misiak and M. Münz, Phys. Lett. B400 (1997) 206, Erratum ibid. B425 (1998) 414, hep-ph/9612313.

[197] P. Gambino, M. Gorbahn and U. Haisch, in preparation.

[198] A. Ali and C. Greub, Z. Phys. C49 (1991) 431.

[199] A. Ali and C. Greub, Phys. Lett. B259 (1991) 182.

[200] A. Ali and C. Greub, Phys. Lett. B361 (1995) 146, hep-ph/9506374.

[201] N. Pott, Phys. Rev. D54 (1996) 938, hep-ph/9512252.

[202] Z. Ligeti et al., Phys. Rev. D60 (1999) 034019, hep-ph/9903305.

[203] C. Greub, T. Hurth and D. Wyler, Phys. Lett. B380 (1996) 385, hep-ph/9602281.

[204] C. Greub, T. Hurth and D. Wyler, Phys. Rev. D54 (1996) 3350, hep-ph/9603404.

[205] A.J. Buras et al., Nucl. Phys. B611 (2001) 488, hep-ph/0105160.

[206] A.J. Buras et al., Nucl. Phys. B631 (2002) 219, hep-ph/0203135.

[207] A.F. Falk, M.E. Luke and M.J. Savage, Phys. Rev. D49 (1994) 3367, hep-ph/9308288.

[208] A. Ali et al., Phys. Rev. D55 (1997) 4105, hep-ph/9609449.

[209] M.B. Voloshin, Phys. Lett. B397 (1997) 275, hep-ph/9612483.

[210] A. Khodjamirian et al., Phys. Lett. B402 (1997) 167, hep-ph/9702318.

[211] Z. Ligeti, L. Randall and M.B. Wise, Phys. Lett. B402 (1997) 178, hep-ph/9702322.

[212] A.K. Grant et al., Phys. Rev. D56 (1997) 3151, hep-ph/9702380.

[213] G. Buchalla, G. Isidori and S.J. Rey, Nucl. Phys. B511 (1998) 594, hep-ph/9705253.

[214] A. Czarnecki and W.J. Marciano, Phys. Rev. Lett. 81 (1998) 277, hep-ph/9804252.

[215] A. Strumia, Nucl. Phys. B532 (1998) 28, hep-ph/9804274.

[216] A.L. Kagan and M. Neubert, Eur. Phys. J. C7 (1999) 5, hep-ph/9805303.

[217] K. Baranowski and M. Misiak, Phys. Lett. B483 (2000) 410, hep-ph/9907427.

[218] P. Gambino and U. Haisch, JHEP 09 (2000) 001, hep-ph/0007259.

[219] P. Gambino and U. Haisch, JHEP 10 (2001) 020, hep-ph/0109058.

[220] B. Grinstein and M.B. Wise, Phys. Lett. B201 (1988) 274.

[221] B. Grinstein, R. Springer and M.B. Wise, Phys. Lett. B202 (1988) 138.

[222] B. Grinstein, R. Springer and M.B. Wise, Nucl. Phys. B339 (1990) 269.

[223] R. Grigjanis et al., Phys. Lett. B213 (1988) 355, Erratum ibid. B286 (1992) 413.

[224] R. Grigjanis et al., Phys. Lett. B223 (1989) 239.

[225] H. Simma, Z. Phys. C61 (1994) 67, hep-ph/9307274.

[226] G. Cella et al., Nucl. Phys. B431 (1994) 417, hep-ph/9406203.

[227] G. Altarelli and L. Maiani, Phys. Lett. B52 (1974) 351.

[228] M.K. Gaillard and B.W. Lee, Phys. Rev. Lett. 33 (1974) 108.

[229] P. Breitenlohner and D. Maison, Commun. Math. Phys. 52 (1977) 11.

[230] P. Breitenlohner and D. Maison, Commun. Math. Phys. 52 (1977) 39.

[231] P. Breitenlohner and D. Maison, Commun. Math. Phys. 52 (1977) 55.

[232] M.S. Chanowitz, M. Furman and I. Hinchliffe, Nucl. Phys. B159 (1979) 225.

[233] A.J. Buras et al., Nucl. Phys. B424 (1994) 374, hep-ph/9311345.

[234] M. Ciuchini et al., Phys. Lett. B316 (1993) 127, hep-ph/9307364.

[235] M. Ciuchini et al., Nucl. Phys. B421 (1994) 41, hep-ph/9311357.

[236] G. Buchalla, A.J. Buras and M.E. Lautenbacher, Rev. Mod. Phys. 68 (1996) 1125, hep-ph/9512380.

[237] A.J. Buras, (1998), hep-ph/9806471.

[238] A.J. Buras, M. Jamin and M.E. Lautenbacher, Nucl. Phys. B400 (1993) 75, hep-ph/9211321.

[239] G. Buchalla, A.J. Buras and M.K. Harlander, Nucl. Phys. B337 (1990) 313.

[240] A.J. Buras, P. Gambino and U.A. Haisch, Nucl. Phys. B570 (2000) 117, hep-ph/9911250.

[241] A. Denner, G. Weiglein and S. Dittmaier, Nucl. Phys. B440 (1995) 95, hep-ph/9410338.

[242] T. Inami and C.S. Lim, Prog. Theor. Phys. 65 (1981) 297.

[243] A. Kapustin, Z. Ligeti and H.D. Politzer, Phys. Lett. B357 (1995) 653, hep-ph/9507248.

[244] M. Beneke et al., Phys. Rev. Lett. 83 (1999) 1914, hep-ph/9905312.

[245] M. Beneke et al., Nucl. Phys. B591 (2000) 313, hep-ph/0006124.

[246] M. Misiak, (2000), hep-ph/0002007.

[247] A.J. Buras, A. Kwiatkowski and N. Pott, Phys. Lett. B414 (1997) 157, Erratum ibid. B434 (1998) 459, hep-ph/9707482.

[248] A.H. Hoang, Z. Ligeti and A.V. Manohar, Phys. Rev. Lett. 82 (1999) 277, hep-ph/9809423.

[249] A.H. Hoang, Z. Ligeti and A.V. Manohar, Phys. Rev. D59 (1999) 074017, hep-ph/9811239.

[250] G. Degrassi, P. Gambino and A. Vicini, Phys. Lett. B383 (1996) 219, hep-ph/9603374.

[251] G. Degrassi, P. Gambino and A. Sirlin, Phys. Lett. B394 (1997) 188, hep-ph/9611363.

[252] P. Gambino, A. Kwiatkowski and N. Pott, Nucl. Phys. B544 (1999) 532, hep-ph/9810400.

[253] G. Degrassi and P. Gambino, Nucl. Phys. B567 (2000) 3, hep-ph/9905472.

[254] A. Djouadi, P. Gambino and B.A. Kniehl, Nucl. Phys. B523 (1998) 17, hep-ph/9712330.

[255] G. Bandelloni et al., Annales Poincare Phys. Theor. 28 (1978) 255.

[256] P.A. Grassi, Nucl. Phys. B537 (1999) 527, hep-th/9804013.

[257] J.A. Dixon and J.C. Taylor, Nucl. Phys. B78 (1974) 552.

[258] H. Kluberg-Stern and J.B. Zuber, Phys. Rev. D12 (1975) 467.

[259] H. Kluberg-Stern and J.B. Zuber, Phys. Rev. D12 (1975) 482.

[260] H. Kluberg-Stern and J.B. Zuber, Phys. Rev. D12 (1975) 3159.

[261] S.D. Joglekar and B.W. Lee, Ann. Phys. 97 (1976) 160.

[262] W.S. Deans and J.A. Dixon, Phys. Rev. D18 (1978) 1113.

[263] J.C. Collins, Renormalization, Cambridge University Press, Cambridge 1984.

[264] M. Henneaux, Phys. Lett. B313 (1993) 35, Erratum ibid. B316 (1993) 633, hep-th/9306101.

[265] G. Barnich and M. Henneaux, Phys. Rev. Lett. 72 (1994) 1588, hep-th/9312206.

[266] G. Barnich, F. Brandt and M. Henneaux, Phys. Rept. 338 (2000) 439, hep-th/0002245.

[267] P.A. Grassi, T. Hurth and M. Steinhauser, Annals Phys. 288 (2001) 197, hep-ph/9907426.

[268] M.J. Dugan and B. Grinstein, Phys. Lett. B256 (1991) 239.

[269] S. Herrlich and U. Nierste, Nucl. Phys. B455 (1995) 39, hep-ph/9412375.

[270] M. Misiak and J. Urban, Phys. Lett. B451 (1999) 161, hep-ph/9901278.

[271] G. Buchalla and A.J. Buras, Nucl. Phys. B548 (1999) 309, hep-ph/9901288.

[272] M. Misiak, Phys. Lett. B269 (1991) 161.

[273] K. Chetyrkin, M. Misiak and M. Münz, Nucl. Phys. B518 (1998) 473, hep-ph/9711266.

[274] S. Wolfram, The MATHEMATICA book, Fourth Edition, Wolfram Media/Cambridge University Press, Champaign/Melbourne 1999.

[275] J. Küblbeck, M. Böhm and A. Denner, Comput. Phys. Commun. 60 (1990) 165.

[276] T. Hahn, Comput. Phys. Commun. 140 (2001) 418, hep-ph/0012260.

[277] J. van der Bij and M.J.G. Veltman, Nucl. Phys. B231 (1984) 205.

[278] F. Hoogeveen, Nucl. Phys. B259 (1985) 19.

[279] L. Culumovic, D.G.C. McKeon and T.N. Sherry, Ann. Phys. 197 (1990) 94.

[280] C. Ford and D.R.T. Jones, Phys. Lett. B274 (1992) 409, Erratum ibid. B285 (1992) 399.

[281] C. Ford, I. Jack and D.R.T. Jones, Nucl. Phys. B387 (1992) 373, Erratum ibid. B504 (1997) 551, hep-ph/0111190.

[282] A.I. Davydychev and J.B. Tausk, Nucl. Phys. B397 (1993) 123.

[283] C.P. Martin and D. Sanchez-Ruiz, Nucl. Phys. B572 (2000) 387, hep-th/9905076.

[284] M. Jamin and M.E. Lautenbacher, Comput. Phys. Commun. 74 (1993) 265.

[285] U. Haisch, *Coltrane* a MATHEMATICA package for two-loop computations, unpublished.

[286] G. Degrassi, P. Gambino and S. Fanchiotti, *ProcessDiagram* a MATHEMATICA package for two-loop computations, unpublished.

[287] J.A.M. Vermaseren, Symbolic Manipulation with FORM, Tutorial and Reference Manual, CAN, 1991.

[288] G. Degrassi and A. Sirlin, Nucl. Phys. B383 (1992) 73.

[289] A. Ferroglia et al., Phys. Rev. D65 (2002) 113002, hep-ph/0203224.

[290] J. Erler, Phys. Rev. D59 (1999) 054008, hep-ph/9803453.

[291] A. Sirlin, Phys. Lett. B232 (1989) 123.

[292] G. Degrassi, S. Fanchiotti and A. Sirlin, Nucl. Phys. B351 (1991) 49.

[293] K.G. Chetyrkin, J.H. Kühn and M. Steinhauser, Phys. Rev. Lett. 75 (1995) 3394, hep-ph/9504413.

[294] S. Bauberger and G. Weiglein, Phys. Lett. B419 (1998) 333, hep-ph/9707510.

[295] P. Gambino, A. Sirlin and G. Weiglein, JHEP 04 (1999) 025, hep-ph/9903249.

[296] F. Feruglio, A. Masiero and L. Maiani, Nucl. Phys. B387 (1992) 523.

[297] F. Feruglio, Int. J. Mod. Phys. A8 (1993) 4937, hep-ph/9301281.

[298] A. Djouadi and P. Gambino, Phys. Rev. Lett. 73 (1994) 2528, hep-ph/9406432.

[299] G. Buchalla and A.J. Buras, Phys. Rev. D57 (1998) 216, hep-ph/9707243.

[300] R. Barbieri et al., Nucl. Phys. B409 (1993) 105.

[301] J. Fleischer, O.V. Tarasov and F. Jegerlehner, Phys. Rev. D51 (1995) 3820.

[302] G. Degrassi, S. Fanchiotti and P. Gambino, Int. J. Mod. Phys. A10 (1995) 1377, hep-ph/9403250.

[303] A. Sirlin, Nucl. Phys. B196 (1982) 83.

[304] L. Wolfenstein, Phys. Rev. Lett. 51 (1983) 1945.

[305] A.J. Buras, M.E. Lautenbacher and G. Ostermaier, Phys. Rev. D50 (1994) 3433, hep-ph/9403384.

[306] A.H. Hoang, (2000), hep-ph/0008102.

[307] K.G. Chetyrkin, Acta Phys. Polon. B28 (1997) 725, hep-ph/9610531.

[308] T. van Ritbergen, J.A.M. Vermaseren and S.A. Larin, Phys. Lett. B400 (1997) 379, hep-ph/9701390.

[309] J.A.M. Vermaseren, S.A. Larin and T. van Ritbergen, Phys. Lett. B405 (1997) 327, hep-ph/9703284.

[310] M. Steinhauser, Comput. Phys. Commun. 134 (2001) 335, hep-ph/0009029.

[311] A.A. Vladimirov, Teor. Mat. Fiz. 43 (1980) 210.

[312] K.G. Chetyrkin, A.L. Kataev and F.V. Tkachov, Nucl. Phys. B174 (1980) 345.

[313] J.C. Collins, Nucl. Phys. B92 (1975) 477.

[314] F.V. Tkachov, Phys. Lett. B100 (1981) 65.

[315] K.G. Chetyrkin and F.V. Tkachov, Nucl. Phys. B192 (1981) 159.

Acknowledgments

In the first place I would like to thank my advisor, Prof. Andrzej Buras, for guiding my way into the exciting field of rare weak decays. I highly value his fatherly advice and the permanent encouragement during my work. With all my ventures I always could rely on his quick and favorable support. I am also grateful to Andrzej for proofreading the manuscript. In my future places I will certainly miss the stimulating and creative atmosphere at his chair.

Next I would like to thank Dr. Paolo Gambino for his exclusive support. He suggested and very pedagogically introduced me to the subject of this work. At any time he was ready to discuss my questions and ideas. The collaboration with him has been very pleasant and certainly very fruitful. I also want to thank Paolo for the assistance in arranging my stay at the CERN Theory Division.

Moreover, I would to thank Prof. Gerhard Buchalla for his financial support during my time at CERN. I very much appreciate the kind hospitality of the CERN Theory Division during my stay.

To all friends and colleagues at the Max-Planck-Institut für Physik and at the Technischen Universität München I am grateful for stimulating discussions and creating a very pleasant social environment. In particular I would like to thank my collaborator Martin Gorbahn and my roommate Sebastian Jäger here. In addition I have enjoyed many helpful discussions on other fields of particle physics with many members of the chair of Andrzej, especially with Christoph Bobeth, Thorsten Ewerth, Dr. Frank Krüger and Dr. Jörg Urban and all other associated members of the $\overline{\text{MFV}}$ club, formally known as the large $\tan\beta$ club. Furthermore, I would like to mention that the lunch time conversations with Dr. Rouzbeh Allahverdi, Cyrille Barbot, Robert Buras, Prof. Manuel Drees, Benedikt Gaissmaier, Dr. Janusz Rosiek, Anton Poschenrieder, Michael Rauch, Michael Spranger and Andreas Weiler will stick lively in my mind.

Last but not least, a great thank you goes to my parents, my brother and all of my friends for all their unconditional support of any kind, the interest in my work, and for keeping me grounded.

Financial support of the Max-Planck-Gesellschaft is gratefully acknowledged.